

Fiscal Year 2016: Fourth Quarter

Progress Report
**Advanced Battery Materials
Research (BMR) Program**

Released December 2016
for the period of July – September 2016

Approved by

Tien Q. Duong, Advanced Battery Materials Research Program Manager
Vehicle Technologies Office, Energy Efficiency and Renewable Energy

TABLE OF CONTENTS

A Message from the Advanced Battery Materials Research Program Manager.....	1
Task 1 – Advanced Electrode Architectures	2
Task 1.1 – Higher Energy Density via Inactive Components and Processing Conditions (Vincent Battaglia, Lawrence Berkeley National Laboratory)	3
Task 1.2 – Electrode Architecture-Assembly of Battery Materials and Electrodes (Karim Zaghib, HydroQuebec).....	5
Task 1.3 – Design and Scalable Assembly of High-Density, Low-Tortuosity Electrodes (Yet-Ming Chiang, Massachusetts Institute of Technology)	7
Task 1.4 – Hierarchical Assembly of Inorganic/Organic Hybrid Silicon Negative Electrodes (Gao Liu, Lawrence Berkeley National Laboratory)	9
Task 2 – Silicon Anode Research.....	11
Task 2.1 – Development of Silicon-Based High-Capacity Anodes (Ji-Guang Zhang and Jun Liu, PNNL; Prashant Kumta, University of Pittsburgh)	12
Task 2.2 – Pre-Lithiation of Silicon Anode for High-Energy Lithium-Ion Batteries (Yi Cui, Stanford University) ...	15
Task 3 – High-Energy Density Cathodes for Advanced Lithium-Ion Batteries.....	18
Task 3.1 – Studies of High-Capacity Cathodes for Advanced Lithium-Ion Systems (Jagjit Nanda, Oak Ridge National Laboratory).....	19
Task 3.2 – High Energy Density Lithium Battery (Stanley Whittingham, SUNY Binghamton).....	22
Task 3.3 – Development of High-Energy Cathode Materials (Ji-Guang Zhang and Jianming Zheng, Pacific Northwest National Laboratory)	25
Task 3.4 – <i>In Situ</i> Solvothermal Synthesis of Novel High-Capacity Cathodes (Feng Wang and Jianming Bai, Brookhaven National Laboratory).....	28
Task 3.5 – Novel Cathode Materials and Processing Methods (Michael M. Thackeray and Jason R. Croy, Argonne National Laboratory)	31
Task 3.6 – Advanced Cathode Materials for High-Energy Lithium-Ion Batteries (Marca Doeff, Lawrence Berkeley National Laboratory)	34
Task 3.7 – Lithium Batteries with Higher Capacity and Voltage (John B. Goodenough, UT Austin).....	37
Task 3.8 – Exploiting Cobalt and Nickel Spinel in Structurally Integrated Composite Electrodes (Michael M. Thackeray and Jason R. Croy, Argonne National Laboratory)	39
Task 3.9 – Discovery of High-Energy Lithium-Ion Battery Materials (Wei Tong, Lawrence Berkeley National Laboratory)	42

Task 4 – Electrolytes for High-Voltage, High-Energy Lithium-Ion Batteries.....44

Note: This task is closed. Projects awarded from a recent BMR call in this area will start in FY 2017.

Task 5 – Diagnostics45

Task 5.1 – Design and Synthesis of Advanced High-Energy Cathode Materials (Guoying Chen, Lawrence Berkeley National Laboratory)	46
Task 5.2 – Interfacial Processes – Diagnostics (Robert Kostecki, Lawrence Berkeley National Laboratory).....	49
Task 5.3 – Advanced <i>In Situ</i> Diagnostic Techniques for Battery Materials (Xiao-Qing Yang and Xiqian Yu, Brookhaven National Laboratory)	52
Task 5.4 – NMR and Pulse Field Gradient Studies of SEI and Electrode Structure (Clare Grey, Cambridge University)	55
Task 5.5 – Optimization of Ion Transport in High-Energy Composite Cathodes (Shirley Meng, UC San Diego).....	58
Task 5.6 – Analysis of Film Formation Chemistry on Silicon Anodes by Advanced <i>In Situ</i> and <i>Operando</i> Vibrational Spectroscopy (Gabor Somorjai, UC Berkeley, and Phil Ross, Lawrence Berkeley National Laboratory)	61
Task 5.7 – Microscopy Investigation on the Fading Mechanism of Electrode Materials (Chongmin Wang, Pacific Northwest National Laboratory).....	64
Task 5.8 – Characterization and Computational Modeling of Structurally Integrated Electrodes (Michael M. Thackeray and Jason R. Croy, Argonne National Laboratory)	67

Task 6 – Modeling Advanced Electrode Materials69

Task 6.1 – Electrode Materials Design and Failure Prediction (Venkat Srinivasan, Lawrence Berkeley National Laboratory)	70
Task 6.2 – Predicting and Understanding Novel Electrode Materials from First Principles (Kristin Persson, Lawrence Berkeley National Laboratory).....	72
Task 6.3 – First Principles Calculations of Existing and Novel Electrode Materials (Gerbrand Ceder, Lawrence Berkeley National Laboratory).....	75
Task 6.4 – First Principles Modeling of SEI Formation on Bare and Surface/Additive Modified Silicon Anode (Perla Balbuena, Texas A&M University)	77
Task 6.5 – A Combined Experimental and Modeling Approach for the Design of High-Current Efficiency Silicon Electrodes (Xingcheng Xiao, General Motors, and Yue Qi, Michigan State University)	80
Task 6.6 – Predicting Microstructure and Performance for Optimal Cell Fabrication (Dean Wheeler and Brian Mazzeo, Brigham Young University)	83

Task 7 – Metallic Lithium and Solid Electrolytes	86
Task 7.1 – Mechanical Properties at the Protected Lithium Interface (Nancy Dudney, ORNL; Erik Herbert, Michigan Technological University; and Jeff Sakamoto, University of Michigan).....	88
Task 7.2 – Solid Electrolytes for Solid-State and Lithium–Sulfur Batteries (Jeff Sakamoto, University of Michigan)	91
Task 7.3 – Composite Electrolytes to Stabilize Metallic Lithium Anodes (Nancy Dudney and Frank Delnick, Oak Ridge National Laboratory).....	93
Task 7.4 – Overcoming Interfacial Impedance in Solid-State Batteries (Eric Wachsman, Liangbing Hu, and Yifei Mo, University of Maryland, College Park)	96
Task 7.5 – Nanoscale Interfacial Engineering for Stable Lithium-Metal Anodes (Yi Cui, Stanford University)	99
Task 7.6 – Lithium Dendrite Suppression for Lithium-Ion Batteries (Wu Xu and Ji-Guang Zhang, Pacific Northwest National Laboratory)	102
Task 8 – Lithium–Sulfur Batteries	105
Task 8.1 – New Lamination and Doping Concepts for Enhanced Lithium–Sulfur Battery Performance (Prashant N. Kumta, University of Pittsburgh).....	107
Task 8.2 – Simulations and X-Ray Spectroscopy of Lithium–Sulfur Chemistry (Nitash Balsara, Lawrence Berkeley National Laboratory)	110
Task 8.3 – Novel Chemistry: Lithium Sulfur and Sulfur Sulfur Couple (Khalil Amine, Argonne National Laboratory)	113
Task 8.4 – Multi-Functional Cathode Additives (MFCA) for Lithium-Sulfur Battery Technology (Hong Gan, Brookhaven National Laboratory, and Co-PI Esther Takeuchi, Brookhaven National Laboratory and Stony Brook University).....	115
Task 8.5 – Development of High-Energy Lithium–Sulfur Batteries (Jun Liu and Dongping Lu, Pacific Northwest National Laboratory)	118
Task 8.6 – Nanostructured Design of Sulfur Cathodes for High-Energy Lithium-Sulfur Batteries (Yi Cui, Stanford University).....	121
Task 8.7 – Addressing Internal “Shuttle” Effect: Electrolyte Design and Cathode Morphology Evolution in Lithium–Sulfur Batteries (Perla Balbuena, Texas A&M University)	123
Task 8.8 – Mechanistic Investigation for the Rechargeable Lithium–Sulfur Batteries (Deyang Qu, U Wisconsin - Milwaukee; Xiao-Qing Yang, BNL)	126
Task 8.9 – Statically and Dynamically Stable Lithium–Sulfur Batteries (Arumugam Manthiram, U Texas Austin).....	129
Task 9 – Li-Air Batteries	132
Task 9.1 – Rechargeable Lithium–Air Batteries (Ji-Guang Zhang and Wu Xu, PNNL)	133
Task 9.2 – Efficient Rechargeable Li/O ₂ Batteries Utilizing Stable Inorganic Molten Salt Electrolytes (Vincent Giordani, Liox)	136
Task 9.3 – Lithium–Air Batteries (Khalil Amine, ANL)	139
Task 10 – Sodium-Ion Batteries	142
Task 10.1 – Exploratory Studies of Novel Sodium-Ion Battery Systems (Xiao-Qing Yang and Xiqian Yu, Brookhaven National Laboratory)	143

LIST OF FIGURES

Figure 1. Power v Energy densities x 2 for laminates at different loadings and porosities.	4
Figure 2. C/3 energy density for different loadings.	4
Figure 3. Formation voltage profile of Si/C powder with different binders; (a) Alginate, (b) Acrylic Resins, (c) Polyimide, and (d) Acrylic Resin+Additive.	6
Figure 4. Cycle retention of (a) different binders in coin half-cell level test with low loading level electrode and (b) different electrolytes in full-cell tests.	6
Figure 5. (a) Areal capacity vs. C-rate plot for the low-tortuosity mesocarbon microbead (MCMB) anode in comparison with a high-tortuosity reference sample. (b) First cycle lithiation-delithiation voltage profile of the low-tortuosity MCMB anode tested at 1/20 C. (c) First cycle charge-discharge profile of a LCO-MCMB full cell tested at 1/20 C. Both electrodes are prepared by the emulsion-based magnetic alignment approach (theoretical areal capacity: LCO cathode 13.7 mAh/cm ² , MCMB anode 14.4 mAh/cm ²).	8
Figure 6. Cycling performance of the control SiO _x /NMC full cell without prelithiation.	10
Figure 7. Cycling performance of the prelithiated SiO _x /NMC full cell.	10
Figure 8. Cycling stability of NMC-porous-Si-graphite full cell.	13
Figure 9. Specific discharge capacity vs. cycle numbers for nc-Si/M1O/CNF tested in lithium ion battery. The current rate for first 3 cycles is 50mA/g, and the remaining cycles are tested at a rate of 500mA/g (~1.4C).	13
Figure 10. (a) Synthesis of Li ₃ N material via nitration of lithium metal in N ₂ atmosphere and annealing processes (200°C, 24 hours). (b) The X-ray diffraction (XRD) result shows that the as-formed Li ₃ N flake is pure alpha-phase Li ₃ N. After grinding, the product contains a small portion of beta-phase Li ₃ N. The XRD peaks at 21° arise from the Kapton tape. (c, d) Transmission electron microscopy (TEM) image (c) taken at the edge area of a Li ₃ N particle, and high-resolution TEM image (d) taken at the area labelled by a rectangle in (c). (e) Charge potential profile a Li ₃ N electrode prepared by a slurry manufacturing process. (f) Initial charge and discharge curves of LCO cathodes with and without the addition of Li ₃ N.	16
Figure 11. Scanning transmission electron microscopy – high angle annular dark field (STEM-HAADF) images showing the cathode particle morphology change even after first cycle.	20
Figure 12. Transmission electron microscopy (TEM) observation of Li ₂ Cu _{0.5} Ni _{0.5} O ₂ sample after one cycle. (a) Low magnification bright field image showing layered morphology. (b) A selected area electron diffraction pattern from the particle showing different lattice spacings. (c) High-resolution TEM image showing embedded LiNiO ₂ nano-domains highlighted by dashed red circles.	20
Figure 13. The capacity vs rate of (left) a Li//CuF ₂ cell and (right) a Li//CuF ₂ -VOPO ₄ cell.	23
Figure 14. Charge and discharge curves for the first 10 cycles of a lithiated Sn-Fe//VOPO ₄ cell.	23
Figure 15. (a) Initial charge/discharge profiles. (b) Cycling performance of different NMC cathodes at C/3 after 3 formation cycles at C/10 in the voltage range of 2.7 ~ 4.5 V. (c, d) Charge/discharge profile evolution of (c) LiNi _{0.68} Mn _{0.22} Co _{0.10} O ₂ and (d) LiNi _{0.76} Mn _{0.14} Co _{0.10} O ₂	26
Figure 16. (a) Charge/discharge profiles of LiNi _{0.76} Mn _{0.14} Co _{0.10} O ₂ with different charge cutoff voltage at C/10, and (b) corresponding cycling performance at C/3 after 3 formation cycles at C/10.	26
Figure 17. Structural evolution of the intermediates during synthesis of LiNi _{0.8} Co _{0.2} O ₂ (LNCO). (a) Thermogravimetry analysis curve of LNCO during heating at 800°C in O ₂ , and corresponding morphological evolution of particles by scanning electron microscopy imaging (inset). (b) Neutron powder diffraction patterns and Rietveld refinements of LNCO samples prepared at 800°C in O ₂ as a function of sintering time. The peaks associated with Li ₂ CO ₃ were indicated by green arrows (bottom panel). (c-i) Transmission electron microscopy images and electron energy loss spectroscopy spectra from a single particle of LNCO synthesized at 800°C in O ₂ for 5 hours, indicating high structural ordering with a thin layer of rock-salt on the surface (< 2 nm).	29

Figure 18. Cycling performance of LNCO and pure LiNiO_2 synthesized certain conditions (shown in the legend) under same cycling conditions (0.1 C; 2.7-4.3 V), along with that of LNCO between 2.7-4.6 V.....	29
Figure 19. (a) Ternary diagram showing NMC compositions investigated. (b) First-cycle efficiency as a function of Li loading compared to the baseline loading (0 on the x axis). (c) First-cycle discharge capacity at varied Li loadings for the NMC materials studied.	32
Figure 20. Ternary contour plot of capacity retention (red=high, blue=low) over the NMC compositions studied. The numbers in the ternary plots denote the reduction of lithium loading from the baseline Li/NMC during synthesis.	32
Figure 21. (Left) Elemental association maps of spray pyrolyzed NMC-622 particles. 3D rendering of the elemental associations viewing the particles at different angles, and 2D slices of the elemental associations. The colors presenting the elemental associations are shown in the middle. (Right) Elemental distribution as a function of the distance from the particle surface (both inner and outer surfaces) calculated using the transmission X-ray microscopy data.	35
Figure 22. (a) Li-plating voltage curves of Li/Au/LLZO/Au/Li symmetric cells at 0.1 and 0.5 mA cm^{-2} . (b) Cross-sectional photograph of LLZO after short-circuit (left) and the corresponding scanning electron microscopy image for the dark part (right).....	38
Figure 23. Reversible charge/discharge voltage curves of Li/Au/LLZO/Au/Li symmetric cell at a current density of 0.1 mA cm^{-2} and 50°C.	38
Figure 24. (a) Normalized discharge profile of $\text{Li}(\text{Co}_{0.9}\text{Ni}_{0.05}\text{Mn}_{0.05})\text{O}_2$, (b-d) dQ/dV plots of $\text{Li}(\text{Co}_{1-2x}\text{Ni}_x\text{Mn}_x)\text{O}_2$ fired at 900°C.	40
Figure 25. Voltage profiles and dQ/dV plots (inset) of $0.025\text{Li}_2\text{MnO}_3 \cdot \text{LiCo}_{1-x}\text{Ni}_x\text{O}_2$ fired at (a) 600°C – 72h and (b) 800°C – 24h.....	40
Figure 26. Selected dQ/dV plots of $x \text{Li}_2\text{NiO}_2 \cdot (1-x) \text{Li}_2\text{CuO}_2$ ($x = 1, 0.8, 0.4$) solid solutions.....	43
Figure 27. <i>Ex situ</i> X-ray diffraction patterns of $\text{Li}_2\text{Ni}_{0.8}\text{Cu}_{0.2}\text{O}_2$ electrodes at selected states-of-charge. Dashed lines represent monoclinic $\text{C2/m Li}_{1+\delta}\text{CuO}_2$ phases ($0 \leq \delta \leq 0.5$). NiO , Li_2O , and Li_2CO_3 are indicated by solid circles, open circles, and open squares, respectively.....	43
Figure 28. (a) Selected area electron diffraction pattern collected on a S-Poly crystal. (b) Contrast image taken with one of the reflections shown in green (a). (c) High-resolution high angle annular dark field (HAADF) scanning transmission electron microscopy image collected on the crystal sample. (d) Electron energy loss spectroscopy data collected from the surface-to-bulk region shown in the HAADF image in (c), with the expanded views shown on the left.	47
Figure 29. (a) Illustration of the SEI chemical composition on Si(111) electrode surface that was swept from open circuit potential to 0.5 V in 1 M $\text{LiPF}_6 + 2\% \text{LiBOB}$, EC:DMC (1:1 wt.). (b) <i>Ex situ</i> attenuated total reflectance – Fourier transform infrared spectrum. (c) Synchrotron infrared near-field spectroscopy (SINS) spectrum of the same electrode. (d) SINS of the electrode swept to 1.5 V with signature absorption bands marked to show correspondence to far- and near-field IR spectra of $\text{Li}_x\text{B}_y\text{C}_n\text{O}_{2n}$	51
Figure 30. <i>In situ</i> quick X-ray absorption spectroscopy of NMC during the first charge. The X-ray absorption near-edge spectroscopy results of NMC at (a) Ni, (b) Co, and (c) Mn K-edges during 30C charge, respectively. (d) The Ni K-edge energy shift as a function of nominal lithium content x in NMC during initial charge process at the current rates of 1C, 10C and 30C.	53
Figure 31. Proposed fluoroethylene carbonate and vinylene carbonate (VC) reduction products and possible structure for crosslinking site of poly(VC).	56
Figure 32. C1s X-ray photoelectron spectroscopy spectra (a, b), ^1H - ^{13}C CP dipolar dephasing ssNMR (c, d, MAS = 10 kHz), and ^7Li single pulse ssNMR (e, f, MAS = 60 kHz) of fluoroethylene carbonate (red) and vinylene carbonate (blue) precipitates obtained after reduction with deuterated naphthalene. In (c) and (d), asterisks indicate spinning sidebands and crosses represent deuterated naphthalene.	56
Figure 33. F1s X-ray photoelectron spectroscopy spectrum (a) and ^{19}F Hahn echo ssNMR (b) of fluoroethylene carbonate precipitates after reduction with deuterated naphthalene.	56

Figure 34. (upper) First cycle voltage profile of Li-rich material, where the voltage range is 2.0 – 4.8V, at C/20 = 12.5 mA g ⁻¹ . (lower) Ni 3p, Mn 3p, and O 1s X-ray photoelectron spectroscopy spectra at various charge/discharge states in the first cycle.	59
Figure 35. Cycling performance of Si coated compared to the bare Si.	59
Figure 36. The sum frequency generation (SFG, ssp) signal at the C=O (carbonyl) stretch at open current potential of 1 M LiClO ₄ in EC, and EC : FEC mixtures of 9:1 and 7:3 (w/w) in contact with a-Si anode at open circuit potential.	62
Figure 37. The evolution of sum frequency generation (SFG, ssp) signal associated with EC:FEC (9:1, w/w) in contact with a-Si (s-CH ₂) vibrations under reaction conditions by dividing the SFG spectra by their former potentials.	62
Figure 38. Schematic drawing to illustrate the effect of the thickness of the silicon oxide layer at silicon nanotube on the lithiation behavior of the tube. A tube with native oxide layer only expands outward when lithiated, while with increasing oxide layer thickness at outside well, it begins to expand inward, indicating the volume change of Si nanotube can be controlled by tailoring the oxide layer thickness on the walls of both inside and outside.	65
Figure 39. Laboratory X-ray diffraction (XRD) of the Li _{2-z} MnO _{3-δ} powder samples (a, b), integrated layered and spinel structures in the Li _{2-z} MnO _{3-δ} (z=1.0) LS composite sample supported by synchrotron high-resolution XRD (c), electron diffraction (d), and high-resolution transmission electron microscopy (e) analyses.	68
Figure 40. (a) Concentration-dependent diffusivity of Li ⁺ from LiTFSI salt dissolved in 1:1 DOL/DME solvent. (b) Concentration-dependent diffusivity of polysulfide anions in two different types of polysulfide salts (Li ₂ S ₆ and Li ₂ S ₈) dissolved in 1:1 DOL/DME solvent. (c) Conductivity of the LiTFSI salt dissolved in 1:1 DOL/DME solvent combined with different amounts of polysulfide solution.	71
Figure 41. (a) Experimentally obtained performance curves for lithium-sulfur cells discharged at different C-rates. (b) Comparison between experimental results and computational predictions at two different C-rates.	71
Figure 42. Surface reconstruction rules of Li ions on the surface (a and b) and Mn coordination (c and d). The Li-ions prefer atop of the underlying Li octahedral sites and under-coordinated surface Mn is readily switched with subsurface Li.	73
Figure 43. The calculated Wulff shape of pristine Li ₂ MnO ₃ (inset) and oxygen release energies for each stable surface. Surface oxygen is spontaneously released from all surfaces for x<1.5.	73
Figure 44. Local atomic coordination around oxygen in Li-excess materials and schematic of the band structure for Li-excess layered Li-M oxides.	76
Figure 45. Atomic configurations and the iso-surface of spin density (yellow) around oxygen (red spheres) in (a) Li _{1.17-x} Ni _{0.25} Mn _{0.58} O ₂ and (b) Li _{1.25-x} Mn _{0.5} Nb _{0.25} O ₂	76
Figure 46. Mean square displacements of Li ⁺ in Li ₂ EDC (left) and EC (right) plotted on a log-log scale. Three distinct regions appear: ballistic diffusion at short times, a flat region that indicates trapping of Li ⁺ , and diffusive region at long times. Notice that time scales for Li ⁺ trapping in the EC solvent (right) is several orders of magnitude smaller compared to the solid electrolyte interphase layer (left).	78
Figure 47. In-plane strain under different states of charge.	81
Figure 48. The energy release rate for channel cracking in a silicon island decreases with island size.	81
Figure 49. Voltage profile within different potential windows.	81
Figure 50. The mechanical stresses within different potential windows.	81
Figure 51. Sequential coarse-graining procedure used to speed up finite-volume conductivity calculation.	84
Figure 52. Li modulus recorded for 30 indents for pristine Li film (left, A) and for a Li film following one deep (3 μm) cycle (right, B).	89
Figure 53. Li grain structure of vapor deposited film.	89

Figure 54. Profile of lithium on a thin film battery after 3150 cycles. The uncycled areas of the Li remained very smooth. The Li is protected with a thin coating of parylene.	89
Figure 55. LLZO grain size versus processing time.	92
Figure 56. Energy dispersive X-ray maps of 20- μm thick composite electrolyte membrane formed by aqueous spray coating.	94
Figure 57. Comparison of the spray coated composites plasticized with TEGDME (left) with the melt-formed composites treated with DMC vapor (right). The polymer electrolytes themselves have about the same conductivity, yet as shown by the arrows, 50 vol% ceramic powder has opposite effects. Photographs and scanning electron microscopy images of both composites are also shown.	94
Figure 58. Impedance of a cathode / garnet / cathode symmetric cell with aqueous interface.	97
Figure 59. Voltage profile of the atomic layer deposition treated garnet symmetric cell at a current density of 0.2 mA/cm ²	97
Figure 60. Comparison of cathode/ electrolyte interfacial impedance on flat and 3D-structured garnet pellets, showing reduction of interfacial resistance with increase in surface area.	97
Figure 61. Schematic illustration of the proposed artificial solid electrolyte interphase structure with Li-ion conducting inorganic nanoparticles and polymeric binder.	100
Figure 62. (a) Scanning electron microscopy (SEM) image of the Cu ₃ N nanoparticles. (b) X-ray diffraction patterns of the as-synthesized Cu ₃ N nanoparticles, and Cu ₃ N nanoparticles dispersed in tetrahydrofuran (THF) overnight. The inset picture demonstrates the good dispersity of the Cu ₃ N nanoparticles in THF. (c) Top-view SEM image of the doctor-bladed Cu ₃ N+SBR coating on Cu foil. (d) Cyclic voltammetry scans.	100
Figure 63. Morphological images of Li metal anodes. (a-c) Cross-section view. (d-f) Top view of Li metal anodes retrieved from Li NMC cells after 100 cycles using (a, d) conventional LiPF ₆ electrolyte, (b, e) dual-salt (LiTFSI-LiBOB) electrolyte, and (c, f) 0.05 M LiPF ₆ -added dual-salt electrolyte.	103
Figure 64. Cycling performance of Li NMC cells with 3.0 mAh cm ⁻² NMC loading and using an additive-containing dual-salt electrolyte at 30°C.	103
Figure 65. Cycling performance of Sulfur-infiltrated framework material.	108
Figure 66. (a) Electrolyte uptake of composite polymer electrolyte (CPE) membranes. (b) Cycling behavior of CPE membranes.	108
Figure 67. Polysulfide dissolution thermodynamics in dimethylformamide (top) and diglyme (bottom) calculated from first principles (kcal/mol).	111
Figure 68. Ratio of total sulfur (on an atomic basis) in the back of the cathode (S _T) to the original amount of sulfur in the back of the cathode (S ₀).	111
Figure 69. <i>In operando</i> ⁷ Li NMR studies on the S ₅ Se ₂ /C cathode in the fluorinated electrolyte: fit curves to the ⁷ Li NMR line shape at (a) open circuit voltage, (b) discharged to 1.0 V, and (c) charged back to 3.0 V. (d) Overlap of the fitting for <i>in operando</i> nuclear magnetic resonance spectra versus scan number. (e) Integrated areas of Li ⁺ species as a function of charge/discharge process.	114
Figure 70. Cycle performance of a S ₅ Se ₂ /C cathode in two different electrolytes. Hollow symbols represent charge; solid symbols mean discharge.	114
Figure 71. Scanning electron microscopy of Ketjen Black and MP97.	116
Figure 72. Sulfur electrode cracks after drying.	116
Figure 73. Carbon types vs. coin cell cycling.	116
Figure 74. Sulfur loading effect on discharge.	116
Figure 75. (a) Image of the prepared sulfur cathode with mass loading 4.5 mg cm ⁻² . (b) Image of Li-S pouch cell. (c) First discharge profiles (black-energy density and blue-specific capacity).	119

Figure 76. (a) Cyclic voltammetry (CV) curves of the S-VS ₂ @G/CNT electrode at various scan rates. Plots of CV peak current for the (b) first cathodic reduction process (I_{c1} : $S_8 \rightarrow Li_2S_x$), (c) second cathodic reduction process ($Li_2S_x \rightarrow Li_2S_2/Li_2S$), and (d) anodic oxidation process ($Li_2S_2/Li_2S \rightarrow S_8$) versus the square root of the scan rates.	122
Figure 77: Solid electrolyte interphase layer formation illustrating fast decomposition of salt at a 4M concentration. Left: LiFSI; Right: LiTFSI.	124
Figure 78. The chromatogram of LiTFSI/DME/DOL electrolyte with Li metal for 8 days then derivatized by methyl triflate. The inset spectra are the corresponding mass spectrometry spectra for $(CH_3)_2S_4$ and $(CH_3)_2S_5$	127
Figure 79. 0.1 M LiTFS/DME electrolytes: original polysulfide mixture (a); mixed with LiTFS (20 mM) (b); mixed with LiBOB (20 mM) (c); and mixed with LiDFOB (20 mM) (d). All samples were first derivatized by methyl triflate before high-performance liquid chromatography analysis.	127
Figure 80. Chromatograms of derivatized polysulfide mixtures: original polysulfide mixture (a), polysulfide mixture with Li metal for 1 hour (b), polysulfide mixture with Li metal for 4 hours (c), polysulfide mixture with Li metal for 24 hours (d), and polysulfide mixture with Li metal for 96 hours (e).	127
Figure 81. Chromatograms of derivatized polysulfide mixtures: original polysulfide and $LiNO_3$ mixture (a), polysulfide and $LiNO_3$ mixture with Li metal for 1 hour (b), polysulfide and $LiNO_3$ mixture with Li metal for 4 hours (c), polysulfide and $LiNO_3$ mixture with Li metal for 24 hours (d), and polysulfide and $LiNO_3$ mixture with Li metal for 96 hours (e).	127
Figure 82. Dynamic cycling performances of the cells fabricated with the (a) spherical-carbon single-wall carbon nanotube (SWCNT)-coated separators, (b) layer by layer carbon nanofiber (LBL CNF)-coated separators, and (c-d) layer by layer carbon nanotube (LBL CNT)-coated separators.	130
Figure 83. Static resting performances of the cells fabricated with the (a) spherical-carbon single-wall carbon nanotube (SWCNT)-coated separators and (b) layer by layer carbon nanofiber (LBL CNT)-coated separators.	130
Figure 84. (a) Cycling performance of Li-O ₂ cells with B ₄ C, TiC and carbon nanotubes (CNT)-based air electrodes under 100 mAh g ⁻¹ at 0.1 mA cm ⁻² within the voltage range of 2.0–4.7 V. (b) X-ray diffraction of B ₄ C electrode before test, after the first discharge, after the first recharge, and after 250 cycles.	134
Figure 85. Discharge/charge voltage profiles (a), capacity versus cycle number (b) and cycle curves (c: B ₄ C cell, d: Ir/B ₄ C cell) of Li-O ₂ cells using B ₄ C and Ir/B ₄ C oxygen electrodes under 200 mAh g ⁻¹ at 10 mA g ⁻¹ within the voltage range of 2.0 ~ 4.4 V.	134
Figure 86. (a) Cell discharge/charge current variation with time (2.72 V constant discharge voltage/2.92 V constant charge voltage), under O ₂ gas, at 150°C. (b). Li/O ₂ cell galvanostatic cycling in $LiNO_3$ -KNO ₃ at 150°C under O ₂ at 2 mA constant current (500 mA/g carbon or 2.5 mA/cm ² current density).	137
Figure 87. X-ray diffraction analysis of a ceramic electrolyte aged in $LiNO_3$ -KNO ₃ eutectic at 150°C.	137
Figure 88. Raman spectra of the Ir-rGO cathode after first and second discharge in the Li-O ₂ cell.	138
Figure 89. Raman spectra of the Ir-rGO cathode after discharge in the Li-O ₂ cell as a function of time to investigate stability.	138
Figure 90. Raman spectra of the Ir-rGO cathode after first and second discharge in the Li-O ₂ cell.	138
Figure 91. (a), (c), (e) and (g) Normalized X-ray absorption near-edge spectroscopy (XANES) of O3-NCFT at various stages during the first charge at Ni, Co, Fe, Ti K-edges, respectively. (b), (d), (f) and (h) Normalized XANES at various stages during the first discharge at Ni, Co, Fe, Ti K-edges, respectively. Qu1-Qu5 refer to the different states of charge process, and Qu5-Qu9 refer to the different state of discharge process.	144

LIST OF TABLES

Table 1. Comparison of two model inversion results.....	84
Table 2. Parameters of the Li-sulfur pouch cell.....	119

A MESSAGE FROM THE ADVANCED BATTERY MATERIALS RESEARCH PROGRAM MANAGER

As the Advanced Battery Materials Research (BMR) Program ends the fiscal year, we note that significant research accomplishments were made to identify, develop, and analyze new materials for high-performance, next generation, rechargeable batteries for use in electric vehicles (EVs). A complete summary of the FY 2016 progress will be available in the Vehicle Technologies Office (VTO) Annual Progress report in upcoming months (<http://energy.gov/eere/vehicles/vehicle-technologies-office-annual-progress-reports>). A few notable achievements for this quarter are summarized below:

- University of Maryland (Wachsman's Team) observed less than 10 ohm-cm² for the combined electrode interfaces comprised of atomic layer deposition (ALD)-treated LLZO against lithium metal plus LLZO with a LiFePO₄ cathode wetted with aqueous catholyte.
- Argonne National Laboratory (ANL, Amine's group) is performing investigations in novel S_xSe_y cathode materials and has identified the difference between carbonate electrolytes and fluorinated electrolytes. They observed that reversible capacities in the carbonate electrolytes are only ~ 300 mAh g⁻¹ for 50 cycles due to the nucleophilic reaction between polysulfides and carbonate electrolytes. However, fluorinated electrolytes not only significantly suppress the formation of soluble polysulfides and polyselenides, but also prevent the nucleophilic reaction, which indicates that they are a promising electrolyte for selenium-sulfur (S₅Se₂/C) cathode systems.
- Texas A&M University (TAMU, Balbuena's Team) is conducting detailed *ab initio* molecular dynamics (AIMD) studies of the reactions at the surface of lithium metal and has shown the buildup of various species due to the long-chain polysulfide migration from cathode to anode. These simulations demonstrated the rapid formation of Li₂S on the lithium metal surface and its dependence on the exposed crystallographic surface. In the presence of an oxidant such as LiNO₃, the most likely products would be sulfates and sulfites. However, the polysulfide species continue forming Li₂S even when a sulfate film starts to cover the anode surface, at least up to a certain thickness that would avoid electron transfer.
- Lawrence Berkeley National Laboratory (LBNL, Kostecki's group) correlated the improved passivating properties of silicon in the presence of LiBOB to the formation and incorporation of Li_xB_yC_nO_{2n} (n>6) in the inner part of the solid electrolyte interphase (SEI) layer.
- Pacific Northwest National Laboratory (PNNL, Wang's Group) used *in situ* transmission electron microscopy (TEM) to investigate the lithiation behavior of individual amorphous silicon nanotubes with different thicknesses of surface oxide layers and revealed that outward expansion of the nanotubes can be effectively confined by increasing the thickness of the outer SiO_x coating.

Sincerely,

Tien Q. Duong

Manager, Advanced Battery Materials Research (BMR) Program

Energy Storage R&D

Vehicle Technologies Office

Energy Efficiency and Renewable Energy

U.S. Department of Energy

TASK 1 – ADVANCED ELECTRODE ARCHITECTURES

Summary and Highlights

Energy density is a critical characterization parameter for batteries for EVs as there is only so much room for the battery and the vehicle needs to travel over 200 miles. The U.S. Department of Energy (DOE) targets are 500 Wh/L on a system basis and 750 Wh/L on a cell basis. Not only do the batteries need to have high energy density, they must also still deliver 1000 Wh/L for 30 seconds at 80% depth of discharge. To meet these requirements not only entails finding new, high energy density electrochemical couples, but also highly efficient electrode structures that minimize inactive material content, allow for expansion and contraction from one to several thousand cycles, and allow full access to the active materials by the electrolyte during pulse discharges. Under that context, the VTO supports four projects in the BMR Program under Advanced Electrode Architectures: (1) Higher Energy Density via Inactive Components and Processing Conditions, LBNL, (2) Assembly of Battery Materials and Electrodes, HydroQuebec (HQ), (3) Design and Scalable Assembly of High-Density, Low-Tortuosity Electrodes, Massachusetts Institute of Technology (MIT), and (4) Hierarchical Assembly of Inorganic/Organic Hybrid Si Negative Electrodes, LBNL.

The four subtasks take two general engineering approaches to improving the energy density. Subtasks 1 and 3 attempt to increase energy density by making thicker electrodes and reducing the overall amount of inactive components per cell. Subtasks 2 and 4 attempt to increase the energy density of Li-ion cells by replacing graphitic anodes with Si-based active materials. All four attempts are based on determining a suitable binder and a proper methodology for assembling the active material.

The problem being addressed with the first approach is that the salt in the electrolyte must travel a further distance to meet the current demand during charge or discharge. If the salt cannot reach the back of the electrode at the discharge rates required of batteries for automobiles, the back of the electrode is not used. If the diffusional path through the electrode is tortuous or the volume for electrolyte is too low, the limiting current is reduced. Another problem with thicker electrodes is that they tend to not cycle as well as thinner electrodes and thus reach the end-of-life condition sooner, delivering fewer cycles.

The problem addressed by the second approach is that silicon suffers from two major issues, both associated with the 300% volume change the material experiences as it goes from a fully delithiated state to a fully lithiated one: (1) the alloying with lithium results in freshly exposed surface area to electrolyte during cycling that reduces the electrolyte and results in a lithium imbalance between the two electrodes, and (2) the volume change causes the particles to become electrically disconnected, which is further enhanced if particle fracturing also occurs, during cycling.

Highlight. This quarter, Battaglia's group at LBNL has demonstrated electrodes at 40% porosity with improved energy density up to 8 mAh/cm².

Task 1.1 – Higher Energy Density via Inactive Components and Processing Conditions (Vincent Battaglia, Lawrence Berkeley National Laboratory)

Project Objective. Thicker electrodes with small levels of inactive components that can still deliver most of their energy at C-rates of C/3 should result in batteries of higher energy density. Higher energy density should translate to more miles per charge or smaller, less expensive batteries. Unfortunately, the limit to making thicker electrodes is not based on power capability but on mechanical capability; for example, thicker electrodes delaminate from the current collector during calendaring and slicing. The objective of this research is to produce a high energy density electrode with typical Li-ion components that does not easily delaminate and still meets the EV power requirements through changes to the polymer binder and concomitant changes to the processing conditions.

Project Impact. Today's batteries cost too much on a per kWh basis and have too low of an energy density to allow cars to be driven over 300 miles on a single charge. This research targets both problems simultaneously. By developing thicker, higher energy density electrodes, the fraction of cost relegated to inactive components is reduced, and the amount of energy that can be introduced to a small volume can be increased. Macroscopic modeling suggests that this could have as much as a 20% impact on both numbers.

Out-Year Goals. In the first year, the project will change its binder supplier to a U.S. supplier willing to provide binders of differing molecular weights. The project will then establish the workability of the new binders, establish a baseline binder and processing conditions, and determine how thick an electrode can be made from the project's standard processes for making moderately thick electrodes.

In the outgoing years, changes will be made to the binder molecular weight and electrode processing conditions to whatever degree is necessary to increase the energy density while maintaining power capability. Changes in the processing conditions can include the time of mixing, rate of casting, temperature of the slurry during casting, drying conditions, and hot calendaring. Chemical modifications may include multiple binder molecular weights and changes in the conductive additive.

Collaborations. This project has collaborations with Zaghbi's group (HQ) for materials and cell testing; Wheeler's group (Brigham Young University, BYU) for modeling analysis; Liu's group (LBNL) on polymer properties; Arkema for binders; and a commercial cathode material supplier.

Milestones

1. Fabricate laminates of NCM cast to different thicknesses using standard materials and various processing conditions to determine how thick one can cast an electrode that does not display cracking or delamination. (Q1 – Complete)
2. Fabricate laminates of NCM cast to different thicknesses using higher molecular weight binders and various processing conditions to determine how thick one can cast an electrode that does not show cracking or delamination. (Q2 – Complete)
3. Fabricate laminates of NCM cast to different thicknesses using standard materials and various processing conditions on current collectors with a thin layer of binder and conductive additive pre-coated on the current collector to determine how thick one can cast an electrode that does not show cracking or delamination. (Q3 – Ongoing)
4. *Go/No-Go.* Determine if a higher molecular weight binder is worth pursuing to achieve thicker electrodes based on ease of processing and level of performance. If no, pursue a path of polymer-coated current collectors. (Q4 – Go)

Progress Report

Milestone 3. Fabricate laminates of NCM cast to different thicknesses using standard materials and various processing conditions on current collectors with a thin layer of binder and conductive additive pre-coated on the current collector to determine how thick one can cast an electrode that does not show cracking or delamination. In process – Electrodes were fabricated this quarter with a thin layer of a mixture of polymer/carbon black. The electrodes were assembled into cells, and the cells are being tested.

Quarter 4 Go/No-go. Determine if a higher molecular weight binder is worth pursuing to achieve thicker electrodes based on ease of processing and level of performance. If no, pursue a path of polymer-coated current collectors. (Go)

Research this year has indicated that electrodes made with higher molecular weight binder are no more difficult to prepare than electrodes with standard binder, and the electrodes perform with higher power if all other conditions are equal. Also, electrodes of high loading are only possible when using the higher molecular weight binder, while keeping all other processing conditions the same as standard operating procedures.

Earlier, it was demonstrated that electrodes as high as 5 mAh/cm² could be produced that still meet the 2:1 power to energy requirement at 80% of discharged energy. It was also shown that energy density continues to improve at porosities as low as 22%. This quarter, those parameters were pushed further to 11 mAh/cm² and to 8% porosity.

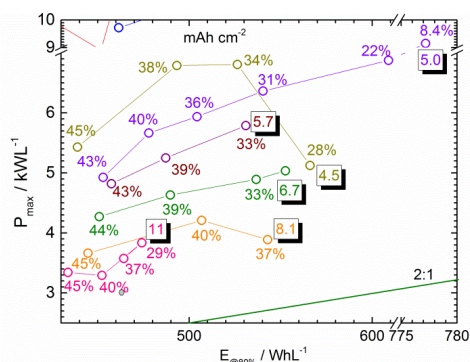


Figure 1. Power v Energy densities x 2 for laminates at different loadings and porosities.

porosities, there is a much greater increase. Also impressive is that energy can still be extracted at 8.4% porosity.

Figure 2 shows the energy density of electrodes at ca. 30% porosity at a C/3 discharge rate for different active material loadings. One sees that the energy density continues to increase up to about 8.1 mAh/cm² and then drops for electrodes at 11 mAh/cm². Questions: Does one see improved performance for even lower porosities? Do these electrodes cycle? Will they easily delaminate?

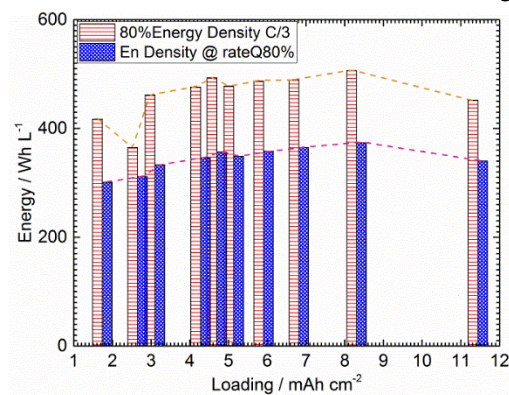


Figure 2. C/3 energy density for different loadings.

Task 1.2 – Electrode Architecture-Assembly of Battery Materials and Electrodes (Karim Zaghib, HydroQuebec)

Project Objective. The project goal is to develop an electrode architecture based on nano-silicon materials and design a full cell having high energy density and long cycle life. To achieve the objective, this project investigates the structure of nano-silicon materials that provide acceptable volume change to achieve long cycle life, while still maintaining the high-capacity performance of Si. The project scope includes the control of the particle size distribution of nano-Si materials, crystallinity, Si composition, and surface chemistry of the nano-Si materials. The focus is to develop electrode formulations and electrode architectures based on nano-Si materials that require optimized nano-Si/C composites and functional binders, as well as a controlled pore distribution in the electrode and the related process conditions to fabricate the electrode.

Project Impact. Silicon is a promising alternative anode material with a capacity of ~4200 mAh/g, which is about an order of magnitude higher than that of graphite. However, many challenges inhibiting the commercialization of Si remain unresolved. The primary culprit is viewed as the large volume variations of Si during charge/discharge cycles that result in pulverization of the particle and poor cycling stability. Success in developing highly reversible Si electrodes with acceptable cost will lead to higher energy density and lower cost batteries that are in high demand, especially for expanding the market penetration for EVs.

Out-Year Goals. This project investigates several steps to prepare an optimized composition and electrode structure of Si-based anode. HQ will use its advanced *in situ* analysis facilities to identify the limitations of the developed Si-based anode materials. *In situ* SEM will be used to monitor crack formations in the particles along with delamination at the binder/particle and current collector/particle interfaces to improve the electrode architecture and cycle life.

Previously, serious gas evolution was observed during the mixing and coating steps of Si-based electrodes. To overcome these technical issues, surface treatment of the nano-Si powder will be considered to utilize the water-based binders. A physical or chemical surface coating to protect the nano-Si powders will be explored. The project will also explore approaches to optimize the particle size distribution (PSD) to achieve better performance.

To achieve high gravimetric energy density (Wh/kg), the electrode loading (mg/cm^2) is a critical parameter in the electrode design. By increasing the anode loading to $2 \text{ mg}/\text{cm}^2$, a higher energy density of more than 300 Wh/kg can be achieved. Higher energy cells will be designed with high loading electrodes of $> 3 \text{ mAh}/\text{cm}^2$ by utilizing an improved electrode architecture. The energy density of these cells will be verified in the format of pouch-type full cells ($< 2 \text{ Ah}$); large format cells ($> 40 \text{ Ah}$) will be evaluated.

Collaborations. This project collaborates with BMR members: V. Battaglia and G. Liu from LBNL, C. Wong and Z. Jiguang from PNNL, and J. Goodenough from the University of Texas (UT).

Milestones

1. Failure mode analysis of large-format cells manufactured in 2015. (December 2015 – Complete)
2. Finalize the structure of nano-Si composite. (March 2016 – Complete)
3. Finalize the architecture of nano-Si composite electrode. *Go/No-Go*: > 300 cycles (80% retention) with loading level of $> 3 \text{ mAh}/\text{cm}^2$. (June 2016 – Complete)
4. Verification of performance in pouch-type full cell ($< 2 \text{ Ah}$). (September 2016 – Complete)

Progress Report

This quarter, Hydro-Quebec extended work on the binder material, which is a key parameter for enabling silicon anodes. To have a coherent comparison with the binders used previously, the same binders were tested with different formulations in the anode. The focus of the previous work was to improve the cycle life by optimization of milling conditions, electrode structures, and electrode formulations. This is especially important in the case of full cells, where the cycle retention was always worse than that of half cells because of the poor discharge/charge efficiency during cycling. The renewal of the unstable SEI as a result of formation and destruction increased Li^+ consumption during cycling. Consequently, the formation of a stable SEI is a critically important factor to improve the cycle life performance.

The voltage profiles during the formation cycle in Figure 3 show the first discharge/charge profiles with different binders in coin half cells. Acrylic resin (Figure 3c) shows the best first efficiency (84.2%) with a reversible capacity of 2973 mAh/g. On the other hand, the lowest efficiency was found with the polyimide at 72.8% first efficiency and with a reversible capacity of 3080 mAh/g.

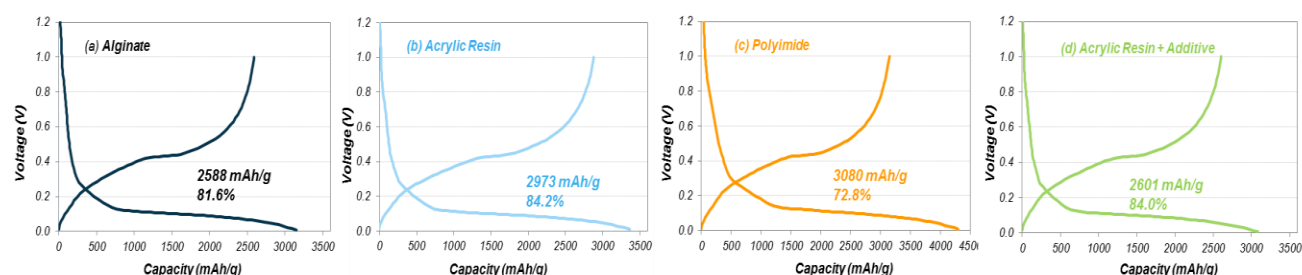


Figure 3. Formation voltage profile of Si/C powder with different binders; (a) Alginate, (b) Acrylic Resins, (c) Polyimide, and (d) Acrylic Resin+Additive.

Figure 4 shows cycle performance with different binders in coin half cells (4a) and with different electrolytes in full cells (based on Si-anode and NMC-cathode, 4b). The cell with acrylic resin shows better cycle retention and was thus adopted for further evaluation in full cells to test the effect of different electrolytes.

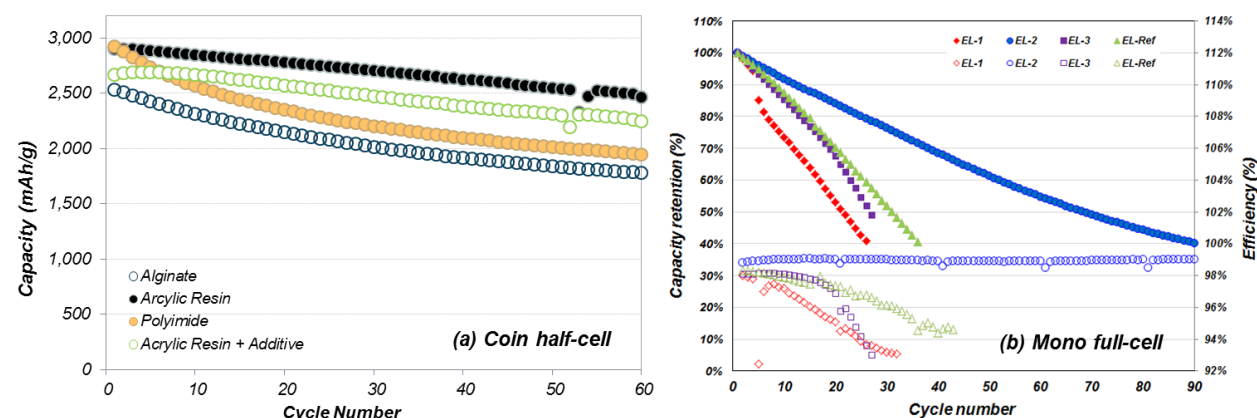


Figure 4. Cycle retention of (a) different binders in coin half-cell level test with low loading level electrode and (b) different electrolytes in full-cell tests.

Figure 4b shows the cycle retention and efficiency during cycle-life testing in full cells; electrolyte no. 2, which is based on a fluorinated component, shows the highest cycle retention and efficiency. However, the cycle life performance is still unacceptable when compared to that of commercialized graphite anodes. Acrylic resin and electrolyte no. 2 were applied for the third deliverable, and are under evaluation.

3rd Deliverable. Supplied 10 laminated-pouch type full cells (~ 35 mAh, 12 cm^2) to LBNL for evaluation.

Task 1.3 – Design and Scalable Assembly of High-Density, Low-Tortuosity Electrodes (Yet-Ming Chiang, Massachusetts Institute of Technology)

Project Objective. The project objective is to develop scalable, high-density, low-tortuosity electrode designs and fabrication processes enabling increased cell-level energy density compared to conventional Li-ion technology, and to characterize and optimize the electronic and ionic transport properties of controlled porosity and tortuosity cathodes as well as densely sintered reference samples. Success is measured by the area capacity (mAh/cm^2) that is realized at defined C-rates or current densities.

Project Impact. The high cost (\$/kWh) and low energy density of current automotive Li-ion technology are in part due to the need for thin electrodes and associated high inactive materials content. If successful, this project will enable use of electrodes based on known families of cathode and anode active compositions, but with at least three times the areal capacity (mAh/cm^2) of current technology while satisfying the duty cycles of vehicle applications. This will be accomplished via new electrode architectures fabricated by scalable methods with higher active materials density and reduced inactive content; this will in turn enable higher energy density and lower cost EV cells and packs.

Approach. Two techniques are used to fabricate thick, high-density electrodes with low tortuosity porosity oriented normal to the electrode plane: (1) directional freezing of aqueous suspensions; and (2) magnetic alignment. Characterization includes measurement of single-phase material electronic and ionic transport using blocking and non-blocking electrodes with ac and dc techniques, electrokinetic measurements, and drive-cycle tests of electrodes using appropriate battery scaling factors for EVs.

Out-Year Goals. The out-year goals are as follows:

- Identify anodes and fabrication approaches that enable full cells in which both electrodes have high area capacity under EV operating conditions. Anode approach will include identifying compounds amenable to the same fabrication approach as cathode, or use of very high-capacity anodes, such as stabilized lithium or Si-alloys that in conventional form can capacity-match the cathodes.
- Use data from best performing electrochemical couple in techno-economic modeling of EV cell and pack performance parameters.

Collaborations. Within BMR, this project collaborates with Antoni P. Tomsia (LBNL) in fabrication of low-tortuosity, high-density electrodes by directional freeze-casting, and with Gao Liu (LBNL) in evaluating Si anodes. Outside of BMR, the project collaborates with Randall Erb (Northeastern University) on magnetic alignment fabrication methods for low-tortuosity electrodes.

Milestones

1. Obtain 2-, 10- and 30- sec pulse discharge data for an electrode of at least $10 \text{ mAh}/\text{cm}^2$ area capacity. (December 2015 – Revised and complete)
2. Test at least one cathode and one anode, each having at least $10 \text{ mAh}/\text{cm}^2$ area capacity under an accepted EV drive cycle. (March 2016 – Complete)
3. *Go/No-Go:* Demonstrate a cathode or anode having at least $10 \text{ mAh}/\text{cm}^2$ area capacity that passes an accepted EV drive cycle. (June 2016 – Complete)
4. Construct and obtain test data for full cell in which area capacity of both electrodes is at least $10 \text{ mAh}/\text{cm}^2$. (September 2016 – Complete)

Progress Report

Milestone. Construct and obtain test data for full cell in which area capacity of both electrodes is at least 10 mAh/cm². (9/30/16).

This quarter, results are reported for mesocarbon microbead (MCMB, 6-28, Osaka Gas) anodes prepared via the emulsion-based magnetic alignment approach, and full cells consisting of a LCO cathode and a MCMB anode, which are both magnetically aligned.

Figure 5a compares the delithiation capacity versus C-rate of an MCMB anode with aligned pores and a reference sample without aligned pores. These two electrodes have similar areal loading of ~39.4 mg/cm² (theoretical areal capacity ~13.8 mAh/cm²). The electrode with aligned pores is thicker and less dense compared to the reference sample without aligned pores (thickness: 485 μ m vs. 425 μ m; porosity: 51% vs. 44%). The MCMB anode with aligned pores clearly outperforms the reference sample, which delivers > 11 mAh/cm² capacity at C/20 C (1C = 350 mA/g) and > 4 mAh/cm² at 1C (red circle in Figure 5a). DC-polarization experiments reveal that the electrode with aligned pores has a low tortuosity of 2.0.

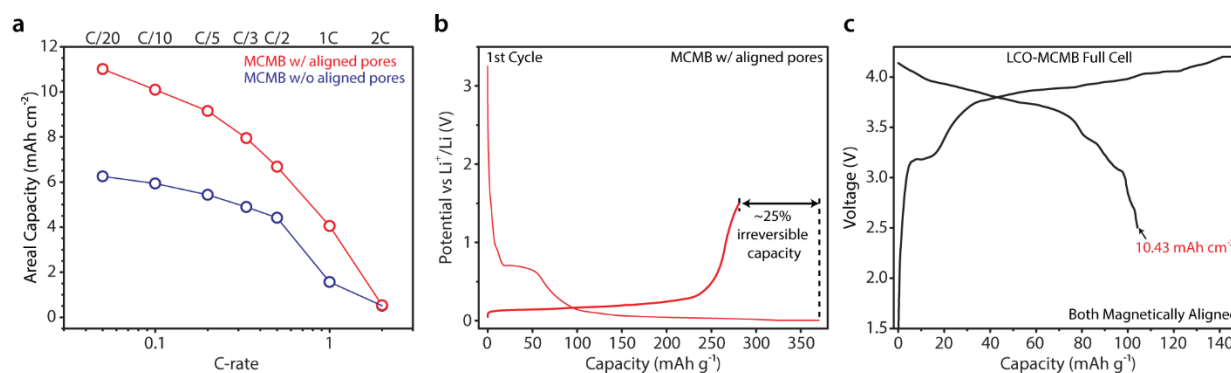


Figure 5. (a) Areal capacity vs. C-rate plot for the low-tortuosity mesocarbon microbead (MCMB) anode in comparison with a high-tortuosity reference sample. (b) First cycle lithiation-delithiation voltage profile of the low-tortuosity MCMB anode tested at 1/20 C. (c) First cycle charge-discharge profile of a LCO-MCMB full cell tested at 1/20 C. Both electrodes are prepared by the emulsion-based magnetic alignment approach (theoretical areal capacity: LCO cathode 13.7 mAh/cm², MCMB anode 14.4 mAh/cm²).

Figure 5b shows the first cycle lithiation-delithiation voltage versus capacity profile of the low-tortuosity MCMB anode. This electrode was lithiated at C/20 to 10 mV and then delithiated to 1.5 V. After the first cycle, approximately 25% of the capacity is lost, possibly due to SEI formation at the MCMB graphite anode. This issue appears in the full-cell tests as well. Figure 5c shows the first charge-discharge voltage profile of a LCO-MCMB full cell tested at C/20. Both electrodes were prepared by the emulsion-based magnetic alignment approach. The LCO cathode is ~440 μ m in thickness and has a theoretical areal capacity of 13.7 mAh/cm². The MCMB anode is ~500 μ m in thickness and has a slightly higher theoretical areal capacity of 14.4 mAh/cm² so that the AC ratio is ca. 1.05:1. Upon charge to 4.2 V (constant current, constant voltage charge), the LCO-MCMB full cell reaches a capacity of 146 mAh/g (calculated based on the weight of the LCO cathode). However, during discharge the full cell only delivers a capacity of 105 mAh/g, ~72% of the charge capacity. Based on the result from the MCMB-Li half-cell test (Figure 5b), the first cycle capacity loss of the full cell should mostly be attributed to the loss at the MCMB anode, which clearly requires further improvement. Nevertheless, the LCO-MCMB full cell delivers an areal capacity of 10.43 mAh/cm². This performance meets the quarterly milestone “Construct and obtain test data for a full cell in which area capacity of both electrodes is at least 10 mAh/cm².”

Task 1.4 – Hierarchical Assembly of Inorganic/Organic Hybrid Silicon Negative Electrodes (Gao Liu, Lawrence Berkeley National Laboratory)

Project Objective. This work aims to enable silicon as a high-capacity and long cycle-life material for negative electrode to address two of the barriers of Li-ion chemistry for EV and plug-in hybrid electric vehicle (PHEV) application: insufficient energy density and poor cycle life performance. The proposed work will combine material synthesis and composite particle formation with electrode design and engineering to develop high-capacity, long-life, and low-cost hierarchical Si-based electrode. State-of-the-art Li-ion negative electrodes employ graphitic active materials with theoretical capacities of 372 mAh/g. Silicon, a naturally abundant material, possesses the highest capacity of all Li-ion anode materials. It has a theoretical capacity of 4200 mAh/g for full lithiation to the $\text{Li}_{12}\text{Si}_5$ phase. However, Si volume change disrupts the integrity of electrode and induces excessive side reactions, leading to fast capacity fade.

Project Impact. This work addresses the adverse effects of Si volume change and minimizes the side reactions to significantly improve capacity and lifetime to develop negative electrode with Li-ion storage capacity over 2000 mAh/g (electrode level capacity) and significantly improve the Coulombic efficiency to over 99.9%. The research and development activity will provide an in-depth understanding of the challenges associated with assembling large volume change materials into electrodes and will develop a practical hierarchical assembly approach to enable Si materials as negative electrodes in Li-ion batteries.

Out-Year Goals. The three main aspects of this proposed work (that is, bulk assembly, surface stabilization, and lithium enrichment) are formulated into 10 tasks in a four-year period.

- Develop hierarchical electrode structure to maintain electrode mechanical stability and electrical conductivity. (bulk assembly)
- Form *in situ* compliant coating on Si and electrode surface to minimize Si surface reaction. (surface stabilization)
- Use prelithiation to compensate first-cycle loss of the Si electrode. (lithium enrichment)

The goal is to achieve a Si-based electrode at higher mass loading of Si that can be extensively cycled with minimum capacity loss at high Coulombic efficiency to qualify for vehicle application.

Collaborations. This project collaborates with the following: Vince Battaglia and Venkat Srinivasan of LBNL; Xingcheng Xiao of GM; Jason Zhang and Chongmin Wang of PNNL; and Phillip B. Messersmith of University of California at Berkeley (UC Berkeley).

Milestones

1. Investigate the impact of different side chain conducting moieties to the electric conductivity of the functional conductive binders. (December 2015 – Complete)
2. Quantify the adhesion group impact to the electrode materials and current collector. (March 2016 – Complete)
3. Fabricate higher loading electrode ($> 3 \text{ mAh/cm}^2$) based on the Si electrode materials and select binder; test cycling stability. (June 2016 – Complete)
4. Fabricate NMC/Si full cell and quantify the performance. (September 2016 – Complete)

Progress Report

Stabilized Lithium Metal Powder (SLMP®) was directly loaded on top of a high loading SiO_x anode (SiO_x , 3 mg/cm²). The SLMP® was activated by subsequent compression calendaring of the electrode. The amount of loaded SLMP® is calculated to be equivalent to the irreversible capacity of the first cycle of the SiO_x electrode. Lithium-ion cells of prelithiated SiO_x anodes and NMC cathodes were fabricated. As a control, a SiO_x /NMC full cell, without prelithiation, was also fabricated and tested similarly. The cycling performance of the full-cell configuration *without* prelithiation is shown in Figure 6. The porosity of the SiO_x electrode was adjusted to 47% to deliver good cycling performance. The first-cycle Coulombic efficiency (CE) is below 50% for the control cell. The low first-cycle CE is due to the high irreversible lithium consumption (~60%) at the SiO_x anode. After the first cycle, the specific capacity is stable around 60 mAh/g of cathode. The poor cycling performance is attributed to the initial consumption of lithium-ions in the SiO_x anode. The cycling performance of the prelithiated SiO_x cell is shown in Figure 7. The first-cycle CE improves to 70%. The following cycling capacity is much higher than that of the controlled cell with a maximum of 122 mAh/g of cathode.

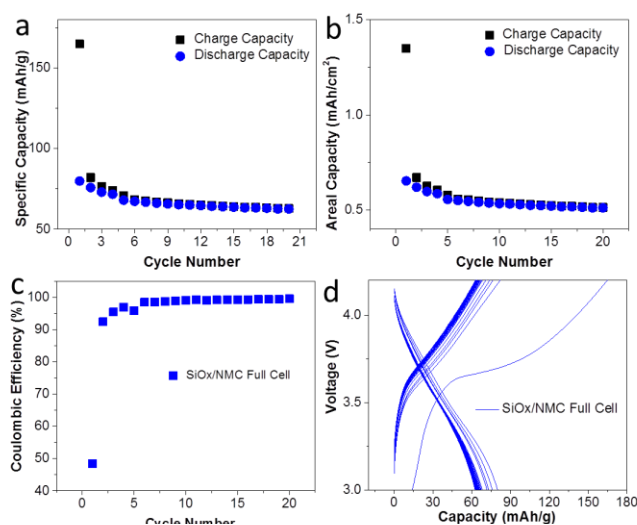


Figure 6. Cycling performance of the control SiO_x /NMC full cell without prelithiation.

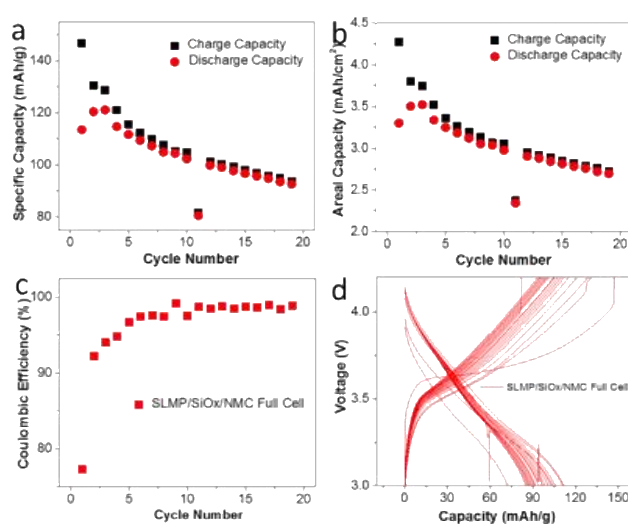


Figure 7. Cycling performance of the prelithiated SiO_x /NMC full cell.

Patents/Publications/Presentations

Publications

- Ai, Guo, and Yiling Dai, Wenfeng Mao, Hui Zhao, Yanbao Fu, Xiangyun Song, Yunfei En, Vincent S. Battaglia, Venkat Srinivasan, and Gao Liu. "Biomimetic Ant-Nest Electrode Structures for High Sulfur Ratio Lithium–Sulfur Batteries." *Nano Letters* 16 (2016): 5365-5372.
- Ai, Guo, and Zhihui Wang, Yiling Dai, Wenfeng Mao, Hui Zhao, Yanbao Fu, Yunfei En, Vincent Battaglia, and Gao Liu. "Conductive Polymer Binder for Nano-silicon/Graphite Composite Electrode in Lithium-ion Batteries towards a Practical Application." *Electrochimica Acta* 209 (2016): 159-162.

Task 2 – Silicon Anode Research

Summary and Highlights

Most Li-ion batteries used in state-of-the-art EVs contain graphite as their anode material. Limited capacity of graphite (LiC_6 , 372 mAh/g) is one barrier that prevents the long-range operation of EVs required by the EV Everywhere Grand Challenge proposed by the DOE Office of Energy Efficiency and Renewable Energy (EERE). In this regard, silicon is one of the most promising candidates as an alternative anode for Li-ion battery applications. Silicon is environmentally benign and ubiquitous. The theoretical specific capacity of silicon is 4212 mAh/g ($\text{Li}_{21}\text{Si}_5$), which is 10 times greater than the specific capacity of graphite. However, the high specific capacity of silicon is associated with large volume changes (more than 300 percent) when alloyed with lithium. These extreme volume changes can cause severe cracking and disintegration of the electrode and can lead to significant capacity loss.

Significant scientific research has been conducted to circumvent the deterioration of Si-based anode materials during cycling. Various strategies, such as reduction of particle size, generation of active/inactive composites, fabrication of Si-based thin films, use of alternative binders, and the synthesis of one-dimensional silicon nanostructures have been implemented by several research groups. Fundamental mechanistic research also has been performed to better understand the electrochemical lithiation and delithiation processes during cycling in terms of crystal structure, phase transitions, morphological changes, and reaction kinetics. Although significant progress has been made on developing Si-based anodes, many obstacles still prevent their practical application. Long-term cycling stability remains the foremost challenge for Si-based anode, especially for the high loading electrode ($> 3\text{mAh/cm}^2$) required for many practical applications. The cyclability of full cells using Si-based anodes is also complicated by multiple factors, such as diffusion-induced stress and fracture, loss of electrical contact among silicon particles and between silicon and current collector, and the breakdown of SEI layers during volume expansion/contraction processes. The design and engineering of a full cell with a Si-based anode still needs to be optimized. Critical research remaining in this area includes, but is not limited to, the following:

- Low-cost manufacturing processes must be found to produce nano-structured silicon with the desired properties.
- The effects of SEI formation and stability on the cyclability of Si-based anodes need to be further investigated. Electrolytes and additives that can produce a stable SEI layer need to be developed.
- A better binder and a conductive matrix need to be developed. They should provide flexible but stable electrical contacts among silicon particles and between particles and the current collector under repeated volume changes during charge/discharge processes.
- The performances of full cells using silicon-based anode need to be investigated and optimized.

The main goal of this project is to have a fundamental understanding on the failure mechanism on Si-based anode and improve its long-term stability, especially for thick electrode operated at full-cell conditions. Success of this project will enable Li-ion batteries with a specific energy of $>350\text{ Wh/kg}$ (in cell level), 1000 deep-discharge cycles, 15-year calendar life, and less than 20% capacity fade over a 10-year period to meet the goal of the EV Everywhere Grand Challenge.

Highlight. The Stanford group developed a facile route to prepare a surface-passivated Li_3N material used for cathode prelithiation.

Task 2.1 – Development of Silicon-Based High-Capacity Anodes (Ji-Guang Zhang/Jun Liu, PNNL; Prashant Kumta, U Pittsburgh)

Project Objective. The project objective is to develop high-capacity and low-cost silicon-based anodes with good cycle stability and rate capability to replace graphite in Li-ion batteries. In one approach, the low-cost Si-graphite-carbon (SGC) composite will be developed to improve the long-term cycling performance while maintaining a reasonably high capacity. Si-based secondary particles with a nano-Si content of ~10 to 15 wt% will be embedded in the matrix of active graphite and inactive conductive carbon materials. Controlled void space will be pre-created to accommodate the volume change of silicon. A layer of highly graphitized carbon coating at the outside will be developed to minimize the contact between silicon and electrolyte, and hence minimize the electrolyte decomposition. New electrolyte additives will be investigated to improve the stability of the SEI layer. In another approach, nanoscale silicon and Li-ion conducting lithium oxide composites will be prepared by *in situ* chemical reduction methods. The stability of Si-based anode will be improved by generating the desired nanocomposites containing nanostructured amorphous or nanocrystalline Si as well as amorphous or crystalline lithium oxide (Si+Li₂O) by the direct chemical reduction of a mixture and variety of silicon sub oxides (SiO and SiO_x) and/or dioxides. Different synthesis approaches comprising direct chemical reduction using solution, solid-state, and liquid-vapor phase methods will be utilized to generate the Si+Li₂O nanocomposites. The electrode structures will be modified to enable high utilization of thick electrode.

Project Impact. Si-based anodes have much larger specific capacities compared with conventional graphite anodes. However, the cyclability of Si-based anodes is limited because of the large volume expansion characteristic of these anodes. This work will develop a low-cost approach to extend the cycle life of high-capacity, Si-based anodes. The success of this work will further increase the energy density of Li-ion batteries and accelerate market acceptance of EVs, especially for the PHEVs required by the EV Everywhere Grand Challenge proposed by the DOE/EERE.

Out-Year Goals. The main goal of the proposed work is to enable Li-ion batteries with a specific energy of > 200 Wh/kg (in cell level for PHEVs), 5000 deep-discharge cycles, 15-year calendar life, improved abuse tolerance, and less than 20% capacity fade over a 10-year period.

Milestones

1. Identify and synthesize the active-inactive Si-based nanocomposite with low-cost approach and a specific capacity ~800 mAh/g. (December 2015 – Complete)
2. Achieve 80% capacity retention over 200 cycles for graphite supported nano Si-carbon shell composite. (March 2016 – Complete)
3. Develop interface control agents and surface electron conducting additives to reduce the first-cycle irreversible loss and improve the Coulombic efficiency of Si-based anode. (June 2016 – Complete)
4. Optimize the cost-effective, scalable high-energy mechanical milling (HEMM) and solid state synthesis techniques for generation of active-inactive composite with capacities ~1000-1200 mAh/g. (December 2016 – Ongoing)
5. Achieve > 80% capacity retention over 300 cycles for thick electrodes (> 2 mAh cm⁻²) through optimization of the silicon electrode structure and binder. (September 2016 – Complete)
6. Synthesize the suitable active-inactive nanocomposite with Li₂O as matrix (Si+Li₂O) or intermetallic matrix (Si+ MnBm) of specific capacity ~1000-1200mAh/g. (December 2016 – Ongoing)

Progress Report

This quarter, the electrochemical performance of porous-Si-graphite composite with higher Si/graphite ratio (1:2 instead of 1:3 used in the last quarter) was evaluated. The electrode loading was $\sim 3 \text{ mAh cm}^{-2}$ at a low current density of $\sim 0.06 \text{ mA cm}^{-2}$. The areal capacity is $\sim 2.5 \text{ mAh cm}^{-2}$ at a charge-discharge current density of $\sim 0.4 \text{ mA cm}^{-2}$. The specific capacity calculated based on the active material (porous Si and graphite) is $\sim 640 \text{ mAh g}^{-1}$. The capacity retention is $\sim 80\%$ in 450 cycles. The porous Si-graphite electrodes after prelithiation were assembled into full cells with NMC electrodes. The full cell was cycled at 0.08 mA cm^{-2} for two formation cycles and then charged at 0.5 mA cm^{-2} and discharged at 0.75 mA cm^{-2} . Good cycling stability was obtained. Figure 8 shows the typical cycling performance of a NMC/porous Si-graphite full cell with $\sim 83\%$ capacity retention over 300 cycles. In another effort, a low temperature thermite approach was developed to synthesize porous Si from porous SiO_2 . A category of metal salts was developed as molten media for the thermite reaction. Preliminary results show that the porous structure of the silica precursor could be largely maintained and hence the porous Si can deliver good cycling stability. Further investigation is under way.

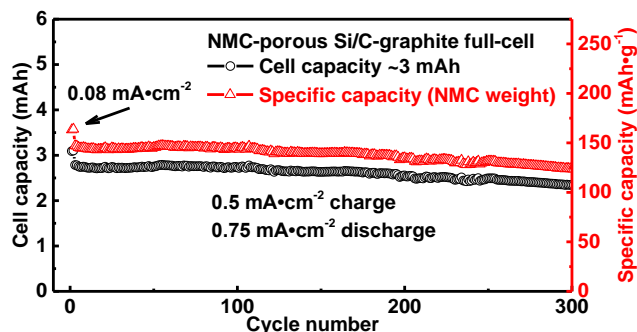


Figure 8. Cycling stability of NMC-porous-Si-graphite full cell.

In addition to development of Si anode based on porous Si, a nanocrystalline-Si/metal oxide/carbon nanofiber composite (nc-Si/ M_1O /CNF) has been synthesized and studied as a promising anode material for Li-ion batteries. Initially, nc-Si/ M_1O composite was prepared using high energy mechano chemical reduction (HEMR) of SiO_x using metal-based reductant (M_1X) as a reducing agent for 40h in argon atmosphere. The ball milled powder was heat treated at 500°C for 4h to enable completion of the reduction reaction to form the nc-Si/ M_1O composite. The X-ray diffraction (XRD) pattern shows the evolution of nc-Si during the high energy mechanical reduction of SiO with M_1X followed by heat treatment of the milled material at 500°C for 4h to form nc-Si/ M_1O composite. The obtained nc-Si/ M_1O composites were then embedded in carbon nanofiber (CNF) using a solution coating technique followed by thermally induced carbonization. Figure 9 shows the cycling performance of the nc-Si/ M_1O /CNF, tested in lithium-ion battery, with an active material loading density of $\sim 3\text{-}5 \text{ mg cm}^{-2}$. The nc-Si/ M_1O /CNF system shows a first- and second-cycle discharge capacity $\sim 1500 \text{ mAh g}^{-1}$ and $\sim 1340 \text{ mAh g}^{-1}$ at a current rate of $\sim 50 \text{ mA/g}$ with a first-cycle irreversible (FIR) loss of ~ 25 to 35% . The obtained capacities were in accordance with the theoretical calculated specific capacity of Si/ M_1O /CNF composite. Following long-term cycling, the system shows a stable specific capacity of $\sim 730 \text{ mAh/g}$ at the end of 120 cycles at a charge/discharge rate of $\sim 500 \text{ mA/g}$ with a Coulombic efficiency of $\sim 99.65\text{-}99.82\%$ and a fade rate of $\sim 0.15\%$ capacity loss per cycle. Retention of the metal oxide matrix in the HEMR-generated composite coupled with the interconnected CNF acts as an efficient buffer to relieve the stresses generated during alloying/dealloying and also maintain the electrical continuity during expansion of the nc-Si. This results in improved electrochemical performance and cycling stability of the Si composite electrode when tested in lithium-ion batteries. Extensive electrochemical characterization including electrochemical impedance, rate capability, degradation mechanism, etc. will be reported soon.

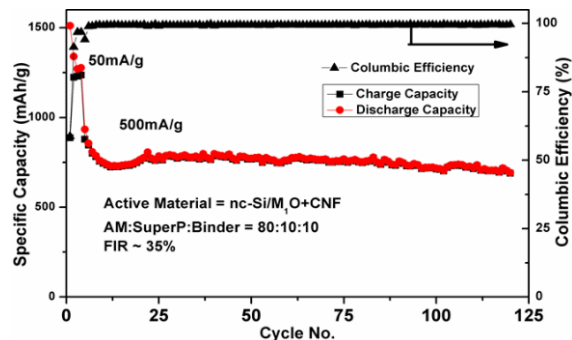


Figure 9. Specific discharge capacity vs. cycle numbers for nc-Si/ M_1O /CNF tested in lithium ion battery. The current rate for first 3 cycles is 50 mA/g , and the remaining cycles are tested at a rate of 500 mA/g ($\sim 1.4\text{C}$).

Patents/Publications/Presentations

Publications

- Jeong, Sookyung, and Xiaolin Li, Jianming Zheng, Pengfei Yan, Ruiguo Cao, Hee Joon Jung, Chongmin Wang, Jun Liu, and Ji-Guang Zhang. “Hard Carbon Coated Nano-Si/Graphite Composite as a High Performance Anode for Li-ion Batteries.” *Journal of Power Sources* 329 (2016): 323-329.
- Gattu, Bharat, and Rigved Epur, Prashanth H. Jampani, Ramalinga Kuruba, Moni K. Datta, and Prashant N. Kumta. “Carbon Coated Hollow Silicon Nanostructures: High Performance Anode for Lithium Ion Batteries.” Submitted to *Journal of Power Sources*, 2016.

Presentation

- 229th Electrochemical Society (ECS) Meeting, San Diego, California (May 2016): “Synthesis of High Performance Si Nanoflakes and Nanorod Anode Morphologies Using Water Soluble Recyclable Templates for Lithium Ion Batteries”; B. Gattu, P. M. Shanthi, P. Jampani, M. K. Datta, and P. N. Kumta.

Task 2.2 – Pre-Lithiation of Silicon Anode for High-Energy Lithium-Ion Batteries (Yi Cui, Stanford University)

Project Objective. Prelithiation of high-capacity electrode materials such as silicon is an important means to enable those materials in high-energy batteries. This study pursues two main directions: (1) developing facile and practical methods to increase first-cycle Coulombic efficiency of silicon anodes, and (2) synthesizing fully lithiated silicon and other lithium compounds for pre-storing lithium.

Project Impact. The lithium loss for first cycle in existing Li-ion batteries will be compensated by using these cathode prelithiation materials. The cathode prelithiation materials have good compatibility with ambient air, regular solvent, binder, and the thermal processes used in current Li-ion battery manufacturing. This project's success will improve the energy density of existing Li-ion batteries and help to achieve high-energy-density Li-ion batteries for electric vehicles.

Out-Year Goals. Compounds containing a large quantity of lithium will be synthesized for pre-storing lithium ions inside batteries. First-cycle lithium loss will be compensated (for example, ~10%) by prelithiation with the synthesized conversion materials.

Collaborations. The project works with the following collaborators: (1) BMR principal investigators, (2) Stanford Linear Accelerator Center (SLAC): *in situ* X-ray, Dr. Michael Toney, and (3) Stanford: mechanics, Professor Nix.

Milestones

1. Synthesize LiF/metal nanocomposite for cathode prelithiation with high capacity and good air stability (> 500 mAh/g) (March 2016 – Complete)
2. Synthesize $\text{Li}_x\text{Si}/\text{Li}_2\text{O}$ composites for anode prelithiation with improved stability in ambient air with 40% relative humidity (June 2016 – Complete)
3. Synthesize stabilized Li_3N for cathode prelithiation with high capacity of > 1700 mAh/g (September 2016 – Complete)

Progress Report

Li_3N can deliver more than 10 times the theoretical capacity of existing cathode materials and can serve as an excellent cathode prelithiation additive to offset the initial lithium loss in lithium-ion batteries. However, Li_3N has intrinsic problems of poor environmental and chemical stability in battery electrode processing environments due to its reactivity with moisture in ambient conditions and incompatibility with solvents used for battery slurry mixing. Therefore, a facile route to prepare a surface-passivated Li_3N material was developed through a spontaneous chemical reaction between lithium metal and nitrogen, followed by an annealing process in a nitrogen-filled glovebox with trace oxygen species (Figure 10a). The XRD result shows that the as-formed Li_3N flake is pure *alpha*-phase Li_3N . After grinding, the product contains a small portion of *beta*-phase Li_3N (Figure 10b). Transmission electron microscopy (TEM) was performed at the edge area of a Li_3N particle to investigate the structure and composition of the passivation layer of Li_3N particles at a low temperature of ~ 100 K (Figure 10c). The high-resolution TEM (HRTEM) image taken at the area labelled by a rectangle confirmed that there exists a dense layer of highly crystalline Li_2O and Li_2CO_3 on the surface of Li_3N particles (Figure 10d). Similar to previous work, the dense and highly crystalline Li_2O and Li_2CO_3 isolate the active composition of materials from air and thus enable active prelithiation materials to have enhanced stability in ambient conditions.

Electrochemical investigations were carried out on Li_3N electrodes to test the performance of the as-fabricated Li_3N powder. A slurry casting process was employed to fabricate the Li_3N electrodes using the surface-passivated Li_3N powder and a low-polarity tetrahydrofuran (THF) solvent. The as-prepared Li_3N electrodes exhibit a relatively high open circuit voltage of 1.16 V and a high decomposition potential above 4 V. Impressively, a high specific capacity of 1761 mAh/g is achieved with a charge cut-off potential of 4.8 V, which is ~ 10 times that of current cathode materials (Figure 10e). After confirming the high capacity of the as-synthesized Li_3N material, the project investigated the electrochemical performance of LiCoO_2 (LCO) cathodes with the addition of various amounts of Li_3N powder. Compared with the pristine LCO electrode, the potential profile of the LCO cathode with Li_3N additive extends above 3.8 V in the charge process, arising from the decomposition of Li_3N during charging (Figure 10f). With the addition of 2.5% Li_3N , the initial charge capacity of the LCO cathode reaches 246 mAh/g, which is 51 mAh/g higher than the pristine LCO electrode. This increased capacity corresponds to 1782 mAh/g from Li_3N , indicating that high utilization of Li_3N is achieved in LCO cathodes. When 5% Li_3N is included into a LCO electrode, the cathode delivers an even higher initial charge capacity of 291 mAh/g with an extra capacity supply of 96 mAh/g from Li_3N . Therefore, the as-prepared Li_3N particles are suitable for potential application in lithium-ion batteries to offset the first-cycle lithium loss and thus improve the overall battery energy density.

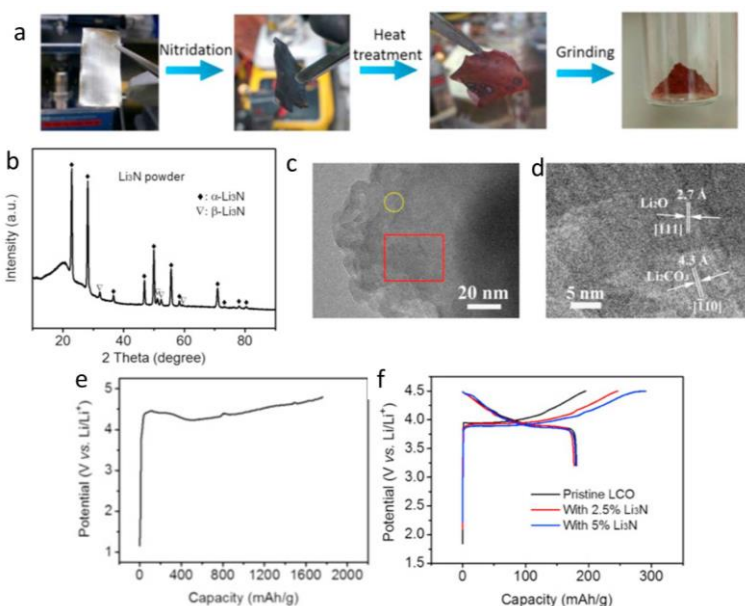


Figure 10. (a) Synthesis of Li_3N material via nitridation of lithium metal in N_2 atmosphere and annealing processes (200°C , 24 hours). (b) The X-ray diffraction (XRD) result shows that the as-formed Li_3N flake is pure *alpha*-phase Li_3N . After grinding, the product contains a small portion of *beta*-phase Li_3N . The XRD peaks at 21° arise from the Kapton tape. (c, d) Transmission electron microscopy (TEM) image (c) taken at the edge area of a Li_3N particle, and high-resolution TEM image (d) taken at the area labelled by a rectangle in (c). (e) Charge potential profile a Li_3N electrode prepared by a slurry manufacturing process. (f) Initial charge and discharge curves of LCO cathodes with and without the addition of Li_3N .

Patents/Publications/Presentations

Publication

- Sun, Y., and Y. Li, J. Sun, Y. Li, A. Pei, and Y. Cui.* “Stabilized Li_3N for Efficient Battery Cathode Prelithiation.” *Energy Storage Materials*, accepted.

TASK 3 – HIGH ENERGY DENSITY CATHODES FOR ADVANCED LITHIUM-ION BATTERIES

Summary and Highlights

Developing high energy density, low-cost, thermally stable, and environmentally safe electrode materials is a key enabler for advanced batteries for transportation. High energy density is synonymous with reducing cost per unit weight or volume. Currently, one major technical barrier toward developing high energy density Li-ion batteries is the lack of robust, high-capacity cathodes. As an example, the most commonly used anode material for Li-ion batteries is graphitic carbon, which has a specific capacity of 372 mAh/g, while even the most advanced cathodes like lithium nickel manganese cobalt oxide (NMC) have a maximum capacity of ~180 mAh/g. This indicates an immediate need to develop high-capacity (and voltage) intercalation type cathodes that have stable reversible capacities of 250 mAh/g and beyond. High volumetric density is also critical for transportation applications. Alternative high-capacity cathode chemistries such as those based on conversion mechanisms, Li-S, or metal air chemistries still have fundamental issues that must be addressed before integration into cells for automotive use. Successful demonstration of practical high energy cathodes will enable high energy cells that meet or exceed the DOE cell level targets of 400 Wh/kg and 600 Wh/L with a system-level cost target of \$125/kWh.

During the last decade, many high-voltage cathode chemistries were developed under the BATT (now BMR) program, including Li-rich NMC and Ni-Mn spinels. Current efforts are directed toward new syntheses and modifications to improve their stability under high-voltage cycling condition (> 4.4 V) for Ni-rich NMC and Li-Mn-rich NMC (LMR-NMC) [Zhang/Jie, PNNL; Thackeray/Croy, ANL; Doeff and Tong, LBNL]. Three other subtasks are directed toward synthesis and structural stabilization of high-capacity polyanionic cathodes that can have > 1 lithium per transition metal (TM) and can be in crystalline or amorphous phases [Nanda, Oak Ridge National Laboratory (ORNL); Wei Tong, LBNL; Looney/Wang, BNL; and Whittingham, State University of New York (SUNY) at Binghamton. Approaches also include aliovalent or isovalent doping to stabilize cathode structures during delithiation as well as stabilizing oxygen. John Goodenough's group at UT Austin is developing membranes to stabilize lithium metal anodes and eventually enable high-capacity cathodes in full-cell configuration.

Highlights. The highlights for this quarter are as follows:

- **Task 3.1.** High-resolution electron microscopy confirms formation of LiNiO_2 phase during charging of $\text{Li}_2\text{-Cu-NiO}_2$ high capacity cathodes.
- **Task 3.2.** Demonstrated cycling of lithiated $\text{CuF}_2/\text{VOPO}_4$ and Sn-Fe/VOPO_4 full cells.
- **Task 3.3.** Achieved more than 200 mAh g^{-1} and capacity retention higher than 90% in 100 cycles by optimizing various Ni-rich NMC compositions.
- **Task 3.4.** Demonstrated high capacity and good cycling stability (> 200 mAh/g) in stoichiometric NMC cathodes via kinetic control of the cationic ordering during synthesis.
- **Task 3.5.** Carried out a systematic phase study of a portion of the NMC ternary space showing electrochemical improvements when a 'layered-layered-spinel' synthesis methodology is applied.
- **Task 3.6.** TXM analyses of spray pyrolyzed NMC-622 and NMC-422 compositions shows Mn-rich composition on the surface with hollow interiors.
- **Task 3.7.** Tested Li/Au/LLZO/Au/Li symmetric cells at 0.1 and 0.5 mA/cm² at 50°C for Li-transport.
- **Task 3.8.** Reported synthesis and electrochemical testing of $\text{Li}(\text{Co}_{1-2x}\text{Ni}_x\text{Mn}_x)\text{O}_2$ ($x = 0.025, 0.05, \text{ and } 0.1$) at various temperatures between 500 and 900°C.
- **Task 3.9.** Reported detailed structural investigation to understand the role of Cu substitution on the phase transformation for high capacity $\text{Li}_2\text{Ni}(\text{Cu})\text{O}_2$ cathode system.

Task 3.1 – Studies of High-Capacity Cathodes for Advanced Lithium-Ion Systems (Jagjit Nanda, Oak Ridge National Laboratory)

Project Objective. The overall project goal is to develop high energy density Li-ion electrodes for EV and PHEV applications that meet and/or exceed the DOE energy density and life-cycle targets from the USDRIVE/USABC roadmap. Specifically, this project aims to mitigate the technical barriers associated with high-voltage cathode compositions such as LMR-NMC, and $\text{Li}_2\text{M}_x^{\text{I}}\text{M}_{1-x}^{\text{II}}\text{O}_2$, where M^{I} and M^{II} are transition metals that do not include Mn or Co. Major emphasis is placed on developing new materials modifications (including synthetic approaches) for high-voltage cathodes that will address issues such as: (i) voltage fade associated with LMR-NMC composition that leads to loss of energy over the cycle life; (ii) transition metal dissolution that leads to capacity and power fade; (iii) thermal and structural stability under the operating state-of-charge (SOC) range; and (iv) voltage hysteresis associated with multivalent transition metal compositions. Another enabling feature of the project is utilizing (and developing) various advanced characterization and diagnostic methods at the electrode and/or cell level for studying cell and/or electrode degradation under abuse conditions. The techniques include electrochemical impedance spectroscopy (EIS), micro-Raman spectroscopy; aberration corrected electron microscopy combined with electron energy loss spectroscopy (EELS), X-ray photoelectron spectroscopy (XPS), inductively coupled plasma – atomic emission spectroscopy (ICP-AES), fluorescence, and X-ray and neutron diffraction.

Project Impact. The project has short- and long- term deliverables directed toward VTO Energy Storage 2015 and 2022 goals. Specifically, work focuses on advanced electrode couples that have cell level energy density targets of 400 Wh/kg and 600 Wh/l for 5000 cycles. Increasing energy density per unit mass or volume reduces the cost of battery packs consistent with the DOE 2022 EV Everywhere goal of \$125/kWh.

Out-Year Goals. The project is directed toward developing high-capacity cathodes for advanced Li-ion batteries. The goal is to develop new cathode materials that have high capacity, use low cost materials, and meet the DOE road map in terms of safety and cycle life. Under this project two kinds of high energy cathode materials are studied. Over the last few years, the principal investigator has worked on improving cycle life and mitigating energy losses of high-voltage Li-rich composite cathodes (referred to as LMR-NMC) in collaboration with the voltage fade team at ANL. Efforts also include surface modification of LMR-NMC cathode materials to improve their electrochemical performance under high-voltage cycling ($> 4.5\text{V}$). The tasks also include working in collaboration with researchers at Stanford Synchrotron Research Laboratory (SSRL) and Advanced Light Source (ALS, LBNL) to understand local changes in morphology, microstructure, and chemical composition under *in situ* and *ex situ* conditions.

Collaborations. This project collaborates with Johanna Nelson, SSRL, SLAC: X-ray imaging XANES; Guoying Chen, LBNL: *in situ* XAS and XRD; Feng Wang, BNL: X-ray synchrotron spectroscopy and microscopy; and Bryant Polzin, Argonne Research Laboratory: CAMP Facility for electrode fabrication.

Milestones

1. Synthesize three compositions of $\text{Li}_2\text{Cu}_x\text{Ni}_{1-x}\text{O}_2$ cathodes with x between 0.4-0.6 and improve their anionic stability by fluorination. *Subtask 1.1:* Fluorination of Li_2CuO_2 (Q1 – Complete). *Subtask 1.2:* Fluorination of $\text{Li}_2\text{Cu}_x\text{Ni}_{1-x}\text{O}_2$ with $x \sim 0.4-0.6$ (Q2 – Complete).
2. Identify roles of Ni and F in obtaining reversible redox capacity at higher voltage, and stabilize Ni-rich compositions. *Subtask 2.1:* XANES, microscopy, and XPS studies (Q3 – Complete). *Subtask 2.2:* Gas evolution and electrochemistry (Q4 – Smart Milestone).

Progress Report

This quarter, the project carried out HRTEM microscopy to monitor the changes in particle morphology and evolution of intermediate phases as it cycles, and monitored the gas evolution in $\text{Li}_2\text{Cu}_{0.5}\text{Ni}_{0.5}\text{O}_2$. This provides insights for plausible reasons behind the capacity loss and addresses structural and electrochemical irreversibility. The microscopy work is done as a part of collaboration with Drs. Chongmin Wang and Pengfei Yang at PNNL. As reported previously, $\text{Li}_2\text{Cu}_{0.5}\text{Ni}_{0.5}\text{O}_2$ undergoes significant changes in electrochemical signature after the first charge-discharge cycle. The scanning transmission electron microscopy – high angle annular dark field (STEM-HAADF) images show that even after one charge-discharge cycle the particle morphology has converted to form exfoliated layers, and the morphology does not change significantly even after 100 cycles (Figure 11c). Additional images collected (not shown here) show evidence of breakdown into smaller particles with cycling. Transmission X-ray microscopy (TXM)-XANES studies reported earlier indicate formation of amorphous phases that are clearly not captured either from XRD or HRTEM. XRD data

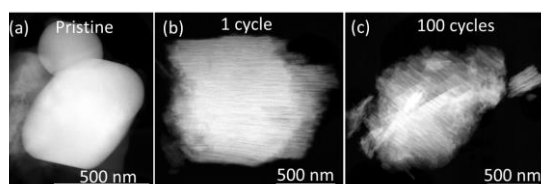


Figure 11. Scanning transmission electron microscopy – high angle annular dark field (STEM-HAADF) images showing the cathode particle morphology change even after first cycle.

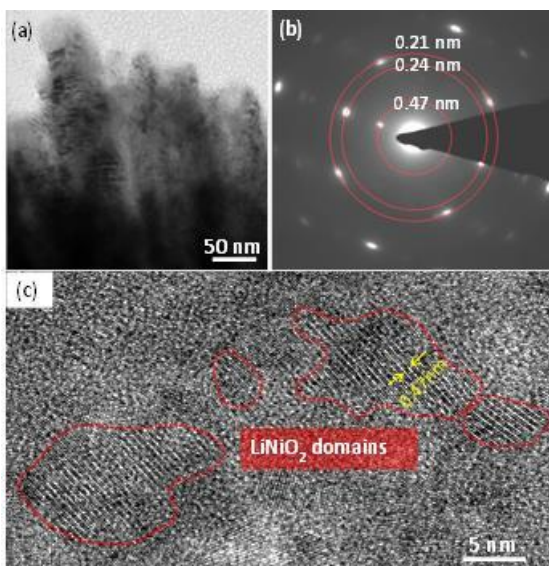


Figure 12. Transmission electron microscopy (TEM) observation of $\text{Li}_2\text{Cu}_{0.5}\text{Ni}_{0.5}\text{O}_2$ sample after one cycle. (a) Low magnification bright field image showing layered morphology. (b) A selected area electron diffraction pattern from the particle showing different lattice spacings. (c) High-resolution TEM image showing embedded LiNiO_2 nano-domains highlighted by dashed red circles.

reported earlier (not shown here) show formation of LiNiO_2 phase after one charge-discharge cycle. From TEM investigation, the project further confirmed this process. As shown in Figure 12, from the layered region (12a) a selected area electron diffraction (SAED) pattern was obtained (12b). The 0.47 nm spacing corresponds to the (003) plane of LiNiO_2 . HRTEM images also confirmed LiNiO_2 phase featured by the 0.47 nm lattice spacing. Figure 12c shows the LiNiO_2 type nano-domains embedded by rock-salt type nano-crystals. The formation of a layered morphology supports the formation of phases with short-range order similar to the layered 1T- Li_2NiO_2 or LiNiO_2 . Exfoliation of the layers accommodates the significant change in density that occurs when the particles transform from orthorhombic (3.7 g/cm^3) to trigonal (4.8 g/cm^3 for LiNiO_2 and 4.1 g/cm^3 for 1T- Li_2NiO_2). No further evolution in particle morphology or structure was observed compared to the cathode particles cycled only once. This is consistent with the electrochemical data reported earlier showing that the voltage profiles also stabilize after the initial cycle.

In conjunction with microscopy and spectroscopy studies, the project also measured the gas evolution from $\text{Li}_2\text{Cu}_{0.5}\text{Ni}_{0.5}\text{O}_2$ electrodes as a function of SOC. Results showed that after 3.9V charge, all capacity originates from oxygen loss from the cathode surface. This clearly is not from the electrolyte decomposition, since it is much below the 4.2V threshold beyond which instability begins.

Patents/Publications/Presentations

Presentations

- International Materials Research Congress (IMRC), Cancun, Mexico (August 2016): “Meso and Microscale Chemical and Morphological Heterogeneities in High Capacity Battery Materials”; invited.
- Telluride Science Workshop, Telluride, Colorado (July 2016): “Charge Transfer across Lithium-Garnet Solid Electrolyte Interface”; invited.

Task 3.2 – High Energy Density Lithium Battery (Stanley Whittingham, SUNY Binghamton)

Project Objective. The project objective is to develop the anode and cathode materials for high energy density cells for use in PHEVs and EVs that offer substantially enhanced performance over current batteries used in PHEVs and with reduced cost. Specifically, the primary objectives are to:

- Increase the volumetric capacity of the anode by a factor of 1.5 over today's carbons
 - Using a SnFeC composite conversion reaction anode
- Increase the capacity of the cathode
 - Using a high-capacity conversion reaction cathode, CuF_2 , and/or
 - Using a high-capacity 2 Li intercalation reaction cathode, VOPO_4
- Enable cells with an energy density exceeding 1 kWh/liter

Project Impact. The volumetric energy density of today's Li-ion batteries is limited primarily by the low volumetric capacity of the carbon anode. If the volume of the anode could be cut in half, and the capacity of the cathode to over 200 Ah/kg, then the cell energy density can be increased by over 50% to approach 1 kWh/liter (actual cell). This will increase the driving range of vehicles.

Moreover, smaller cells using lower cost manufacturing will lower the cost of tomorrow's batteries.

Out-Year Goals. The long-term goal is to enable cells with an energy density of 1 kWh/liter. This will be accomplished by replacing both the present carbon used in Li-ion batteries with anodes that approach double the volumetric capacity of carbon, and the present intercalation cathodes with materials that significantly exceed 200 Ah/kg. By the end of this project, it is anticipated that cells will be available that can exceed the volumetric energy density of today's Li-ion batteries by 50%.

Collaborations. The Advanced Photon Source (APS) at ANL and, when available, the National Synchrotron Light Source II at Brookhaven National Laboratory (BNL) will be used to determine the phases formed in both *ex situ* and *operando* electrochemical cells. University of Colorado, Boulder, will provide some of the electrolytes to be used.

Milestones

1. Determine the optimum composition Li_xVOPO_4 . (December 2015 – Complete)
2. Demonstrate VOPO_4 rate capability. (March 2016 – Complete)
3. Demonstrate Sn_2Fe rate capability. (June 2016 – Complete)
4. Demonstrate CuF_2 rate capability. (September 2016 – Complete)
5. *Go/No-Go*: Demonstrate lithiation method. *Criteria*: A cycling cell containing lithium in one of the intercalation or conversion electrodes must be achieved. (September 2016 – Complete)

Progress Report

The goal of this project is to synthesize tin-based anodes that have 1.5 times the volumetric capacity of the present carbons, and conversion and intercalation cathodes with capacities over 200 Ah/kg. The major efforts in this fourth quarter of year two were to demonstrate the rate capability of the conversion cathode material, CuF_2 , and demonstrate a lithiation method for a full cell containing the Sn/Fe/C conversion anode and either a Li_xVOPO_4 or a CuF_2 cathode.

Milestone 4. The goal of this milestone is to demonstrate the rate capability of the CuF_2 cathode. The discharge capacity over a range of rates is shown in Figure 13 for a CuF_2/C composite and a $\text{CuF}_2/\text{VOPO}_4/\text{C}$ composite. Although the latter shows a higher capacity, the former shows a higher energy density. Also, the project identified conclusively that Cu^+ ions diffuse readily in the common battery liquid electrolytes and in some solid electrolytes. This results in some copper metal being plated on the anode during charge, rather than the active CuF_2 compound being reformed. Thus, extended high capacity cycling of the CuF_2 cathode has not been accomplished. The search for electrolytes that do not transport Cu species continues.

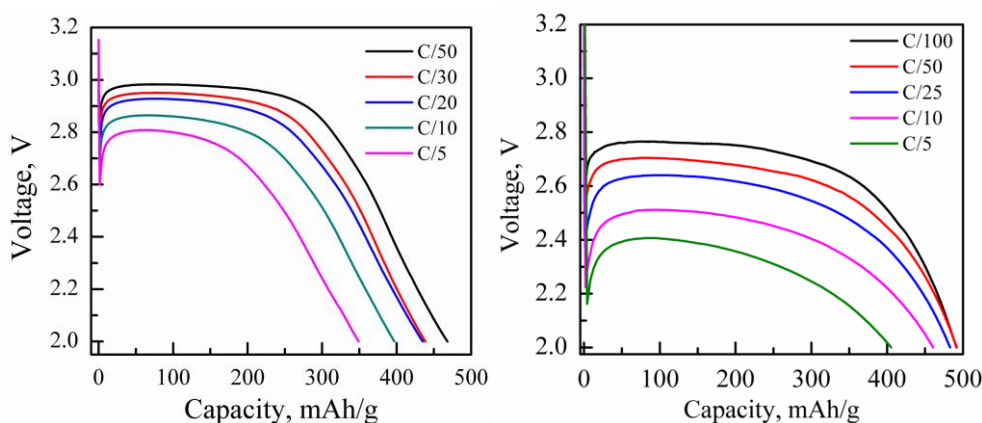


Figure 13. The capacity vs rate of (left) a Li//CuF_2 cell and (right) a $\text{Li//CuF}_2\text{-VOPO}_4$ cell.

Go-No Go. Demonstrate lithiation method. Several methods are under study to lithiate either or both of the Sn/Fe/C composite anode and the VOPO_4 cathode. These include pre-lithiation of the electrodes, addition of lithium or lithiating agents to the anode, and addition of compounds, like Li_2O , to the cathode that will provide lithium on the first charge. Figure 14 demonstrates that constructing a cell of electrochemically lithiated Sn/Fe/C and VOPO_4 allows a functional cell.

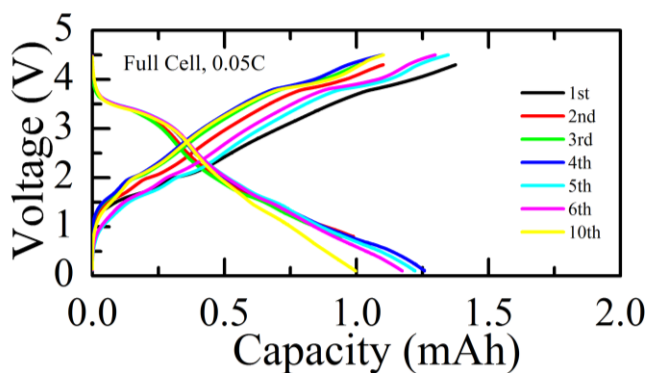


Figure 14. Charge and discharge curves for the first 10 cycles of a lithiated Sn-Fe/VOPO_4 cell.

Patents/Publications/Presentations

Presentations

- National Renewable Energy Laboratory (NREL), Golden, Colorado (September 22, 2016): “What are the Ultimate Limits of Intercalation Reactions for Li-Batteries, and Some Approaches to Get There?”; M. S. Whittingham.
- American Chemical Society (ACS) Northeast Regional Meeting (NERM), Binghamton, New York (October 7, 2016): “FeSn₂ and FeSn₅ Alloy with High and Stable Capacity as Anodes in Lithium-Ion Batteries”; Fengxia Xin.
- ACS NERM, Binghamton, New York (October 6, 2016): “Intrinsic Challenges in Creating a Reversible Copper(II) Fluoride Cathode for Lithium-Ion Batteries”; Nik Zagarella.
- ACS NERM, Binghamton, New York (October 6, 2016): “Synthesis, Characterization, and Optimization of Vanadium Phosphates as Cathode Material for Lithium-Ion Batteries”; Yong Shi.

Task 3.3 – Development of High-Energy Cathode Materials (Ji-Guang Zhang and Jianming Zheng, Pacific Northwest National Laboratory)

Project Objective. The project objective is to develop high-energy-density, low-cost, cathode materials with long cycle life. The previous investigation demonstrates that synthesis condition, synthesis approach, and surface modification have significant effects on the performances of high-voltage spinel and LMR-NCM cathodes. These valuable understandings will be used to guide the development of high-energy-density, enhanced long-term cycling stability of Ni-rich $\text{LiNi}_x\text{Mn}_y\text{Co}_z\text{O}_2$ (NMC) cathode materials that can deliver a high discharge capacity with long-term cycling stability.

Project Impact. Although state-of-the-art layered structure cathode materials such as $\text{LiNi}_{1/3}\text{Mn}_{1/3}\text{Co}_{1/3}\text{O}_2$ and $\text{LiNi}_{0.4}\text{Mn}_{0.4}\text{Co}_{0.2}\text{O}_2$, have relatively good cycling stability at charge to 4.3 V, their energy densities need to be further improved to meet the requirements of EVs. This work focuses on the two closely integrated parts: (1) Develop the high-energy-density NMC layered cathode materials for Li-ion batteries; and (2) characterize the structural properties of the NMC materials by various diagnostic techniques including STEM/EELS, energy dispersive X-ray (EDX) mapping and secondary ion mass spectrometry (SIMS), and correlate with part (1). The success of this work will increase the energy density of Li-ion batteries and accelerate market acceptance of EVs, especially for PHEVs required by the EV Everywhere Grand Challenge proposed by the DOE/EERE.

Out-Year Goals. The long-term goal of the proposed work is to enable Li-ion batteries with a specific energy of $> 96 \text{ Wh kg}^{-1}$ (for PHEVs), 5000 deep-discharge cycles, 15-year calendar life, improved abuse tolerance, and less than 20% capacity fade over a 10-year period.

Collaborations. This project engages with the following collaborators:

- Dr. Bryant Polzin (ANL) – NMC electrode supply
- Dr. X.Q. Yang (BNL) – *in situ* XRD characterization during cycling
- Dr. Kang Xu (U.S. Army Research Laboratory) – new electrolyte

Milestones

1. Identify NMC candidates that can deliver 190 mAh g^{-1} at high voltages. (December 2015 – Complete)
2. Complete multi-scale quantitative atomic level mapping to identify the behavior of Co, Ni, and Mn in NMC during battery charge/discharge, correlation with battery fading characteristics. (March 2016 – Complete)
3. Identify structural/chemical evolution of modified-composition NMC cathode during cycling. (June 2016 – Complete)
4. Optimize compositions of NMC materials to achieve improved electrochemical performance (90% capacity retention in 100 cycles). (September 2016 – Complete)

Progress Report

This quarter's milestone was completed. The compositions of NMC materials with respect to their Ni, Co, Mn contents and the effect of charge cutoff voltage have been systematically optimized to achieve improved electrochemical performances. An initial discharge capacity of more than 200 mAh g⁻¹ and capacity retention higher than 90% in 100 cycles were obtained.

The initial charge/discharge voltage curves demonstrated that discharge capacities of 200 mAh g⁻¹ or higher could be achieved at a Ni content ≥ 0.5 with charge cutoff of 4.5 V (Figure 15a). The long-term cycle life of these NMC cathodes, as presented in Figure 15b, has been found to be very sensitive to the Ni content in the prepared materials. The capacity retention in 100 cycles of the NMCs follows the trend of Ni_{0.33} (97.7%) > Ni_{0.50} (97.6%) > Ni_{0.62} (97.2%) > Ni_{0.68} (93.8%) > Ni_{0.76} (88.5%) during cycling at C/3. The comparison of voltage profiles of LiNi_{0.68}Mn_{0.22}Co_{0.10}O₂ (Figure 15c) and LiNi_{0.76}Mn_{0.14}Co_{0.10}O₂ (Figure 15d) illustrated that the material with higher Ni content showed faster capacity decay, as labeled by the red arrows in Figure 15c-d. This could be attributed to the poor interfacial stability of high-Ni NMC materials due to the parasitic reactions between Ni⁴⁺ and the electrolyte as well as the structural instability owing to large volume variation upon deep delithiation process.

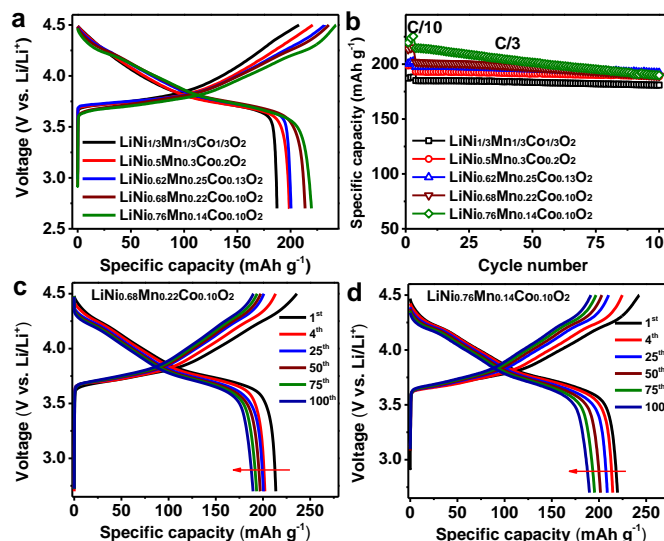


Figure 15. (a) Initial charge/discharge profiles. (b) Cycling performance of different NMC cathodes at C/3 after 3 formation cycles at C/10 in the voltage range of 2.7 ~ 4.5 V. (c, d) Charge/discharge profile evolution of (c) LiNi_{0.68}Mn_{0.22}Co_{0.10}O₂ and (d) LiNi_{0.76}Mn_{0.14}Co_{0.10}O₂.

The effect of charge cutoff voltage on the cycling stability of the Ni-rich cathode material LiNi_{0.76}Mn_{0.14}Co_{0.10}O₂ was also investigated in detail (Figure 16). It is found that lowering the charge cutoff voltage significantly improved the cycling stability (Figure 16a). The capacity retention in 100 cycles was improved from 88.5% to 97.6% when the charged cutoff was reduced from 4.5 V to 4.4 V. There was no capacity fade observed at cutoff 4.3 V and 4.2 V. This could be ascribed to the side reactions that occurred at electrode surface at lower charge voltage along with the decreased extraction of lithium ion at each charge that mitigated the structural degradation. However, considerably decreased accessible discharge capacity was obtained at lower cutoff voltages, especially when 4.2 V was used as a cutoff. The initial discharge capacities at cutoff 4.5 V, 4.4 V, 4.3 V, and 4.2 V are 219, 207, 200 and 176 mAh g⁻¹ (Figure 16b), respectively. In this regard, a good trade-off between discharge capacity and cycling stability was achieved at charge cut-off ~4.4 V. In the future study, additional lattice doping, surface modification, and electrolyte additives will be adopted for high-Ni NMC cathodes to achieve both high discharge capacity and improved long-term cycling stability.

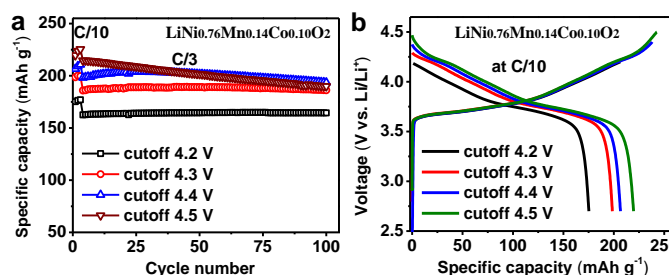


Figure 16. (a) Charge/discharge profiles of LiNi_{0.76}Mn_{0.14}Co_{0.10}O₂ with different charge cutoff voltage at C/10, and (b) corresponding cycling performance at C/3 after 3 formation cycles at C/10.

Patents/Publications/Presentations

Publication

- Zheng, Jianming, and Jie Xiao and Ji-Guang Zhang. “The Roles of Oxygen Non-Stoichiometry on the Electrochemical Properties of Oxide-based Cathode Materials.” *Nano Today*, 2016, in press (<http://dx.doi.org/10.1016/j.nantod.2016.08.011>).

Task 3.4 – *In Situ* Solvothermal Synthesis of Novel High-Capacity Cathodes (Feng Wang and Jianming Bai, Brookhaven National Laboratory)

Project Objective. The goal is to develop novel high-capacity cathodes with precise control of the phase, stoichiometry, and morphology. Despite considerable interest in developing low-cost, high-energy cathodes for Li-ion batteries, designing and synthesizing new cathode materials with the desired phases and properties has proven difficult, due to complexity of the reactions involved in chemical synthesis. Building on established *in situ* capabilities/techniques for synthesizing and characterizing electrode materials, this project will undertake *in situ* studies of synthesis reactions under real conditions to identify the intermediates and to quantify the thermodynamic and kinetic parameters governing the reaction pathways. The results of such studies will enable strategies to “dial in” desired phases and properties, opening a new avenue for synthetic control of the phase, stoichiometry, and morphology during preparation of novel high-capacity cathodes.

Project Impact. Present-day Li-ion batteries are incapable of meeting the targeted miles of all-electric-range within the weight and volume constraints, as defined by the DOE in the EV Everywhere Grand Challenge. New cathodes with higher energy density are needed for Li-ion batteries so that they can be widely commercialized for plug-in electric vehicle (PEV) applications. The effort will focus on increasing energy density (while maintaining the other performance characteristics of current cathodes) using synthesis methods that have the potential to lower cost.

Out-Year Goals. This project is directed toward developing novel high-capacity cathodes, with a focus on Ni-rich layered oxides. Specifically, synthesis procedures will be developed for making LiNiO_2 and a series of Co/Mn substituted solid solutions, $\text{LiNi}_{1-x}\text{M}_x\text{O}_2$ ($\text{M}=\text{Co}, \text{Mn}$); through *in situ* studies, this project undertakes systematic investigations of the impact of synthesis conditions on the reaction pathways and cationic ordering processes toward the final layered phases. The structural and electrochemical properties of the synthesized materials will be characterized using s-XRD, neutron scattering, transmission electron microscopy (TEM), EELS, and various electrochemical techniques. The primary goal is to develop a reversible cathode with an energy density of 660 Wh/kg or higher.

Collaborations. This project engages with the following collaborators: Lijun Wu and Yimei Zhu at BNL; Khalil Amine, Zonghai Chen, and Yang Ren at ANL; Jagjit Nanda and Ashfia Huq at ORNL; Nitash Balsara, Wei Tong, and Gerbrand Ceder at LBNL; Arumugam Manthiram at UT Austin; Scott Misture at Alfred University; Peter Khalifha at SUNY; Kirsuk Kang at Seoul National University; Brett Lucht at University of Rhode Island; and Jason Graetz at HRL Laboratories.

Milestones

1. Develop synthesis procedures for preparing Ni-Mn-Co layered oxides. (December 2015 – Complete)
2. Identify the impact of synthesis conditions on the reaction kinetics and pathways toward forming layered Ni-Mn-Co oxides via *in situ* studies. (March 2016 – Complete)
3. Develop new capabilities for monitoring synthesis parameters (pressure, temperature, and *PH* values) in real time during solvothermal synthesis of cathode materials. (June 2016 – Complete)
4. Identify synthetic approaches for stabilizing the layered structure of Ni-Mn-Co cathodes. (September 2016 – Complete)

Progress Report

Synthesis of stoichiometric Ni-rich layered oxides, $\text{LiNi}_{1-x}\text{M}_x\text{O}_2$ ($\text{M}=\text{Co}, \text{Mn}; x < 0.5$), has proven difficult due to cation mixing in octahedral sites. Temperature-resolved *in situ* XRD studies of synthesis reactions in preparing $\text{LiNi}_{0.8}\text{Co}_{0.2}\text{O}_2$ (LNCO) were carried out in previous quarters, indicating the importance of

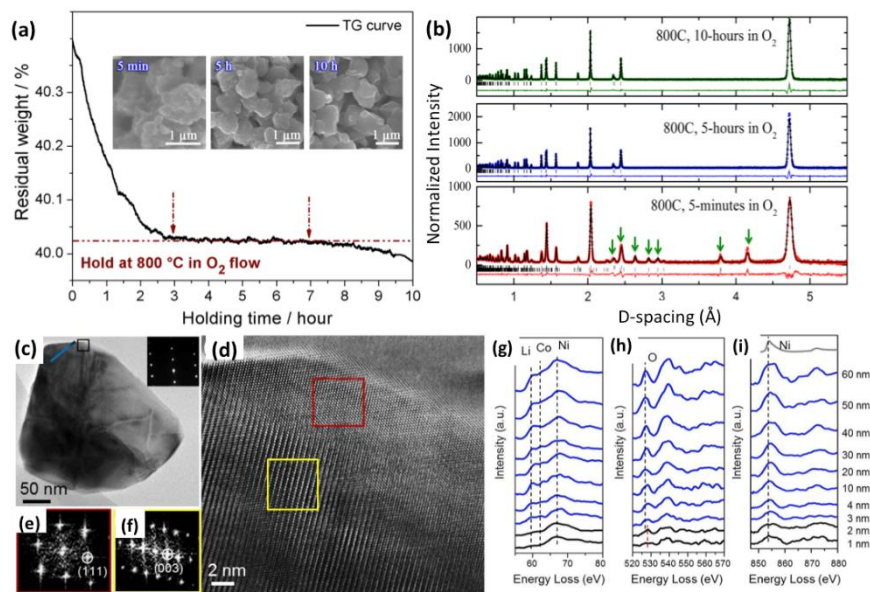


Figure 17. Structural evolution of the intermediates during synthesis of $\text{LiNi}_{0.8}\text{Co}_{0.2}\text{O}_2$ (LNCO). (a) Thermogravimetry analysis curve of LNCO during heating at 800°C in O_2 , and corresponding morphological evolution of particles by scanning electron microscopy imaging (inset). (b) Neutron powder diffraction patterns and Rietveld refinements of LNCO samples prepared at 800°C in O_2 as a function of sintering time. The peaks associated with Li_2CO_3 were indicated by green arrows (bottom panel). (c-i) Transmission electron microscopy images and electron energy loss spectroscopy spectra from a single particle of LNCO synthesized at 800°C in O_2 for 5 hours, indicating high structural ordering with a thin layer of rock-salt on the surface (< 2 nm).

is evident, kinetic control of the cationic ordering is important to achieving high stoichiometry in LNCO. Figure 18 shows the electrochemical performance of electrodes made from the LNCO samples synthesized under different conditions ($\text{LiNi}_{0.8}\text{Co}_{0.2}\text{O}_2$ -800- O_2 -5h), compared with pure LiNiO_2 (LiNiO_2 -750- O_2 -5h), and with LNCO synthesized in air at 900°C for 20 hours ($\text{LiNi}_{0.8}\text{Co}_{0.2}\text{O}_2$ -900-A-20h). Through optimization of the synthesis process, stoichiometric LNCO with high capacity (up to ~ 200 mAh/g) and good cycling stability was obtained. Results from this study provide insights into designing high performance Ni-rich layered oxide cathodes through synthetic control of the structural ordering in the materials.

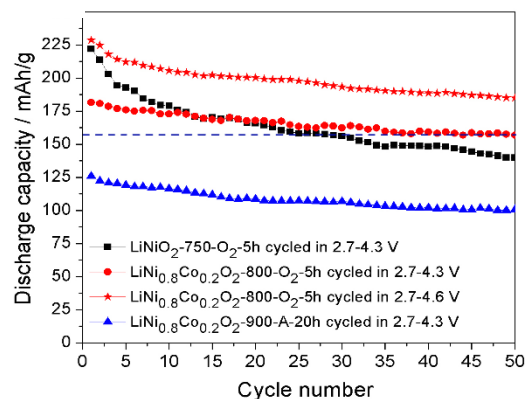


Figure 18. Cycling performance of LNCO and pure LiNiO_2 synthesized certain conditions (shown in the legend) under same cycling conditions (0.1 C; 2.7 - 4.3 V), along with that of LNCO between 2.7 - 4.6 V.

Patents/Publications/Presentations

Publications

- Zhao, J., and W. Zhang, A. Huq, S. T. Misture, B. Zhang, S. Guo, L. Wu, Y. Zhu, Z. Chen, K. Amine, F. Pan, J. Bai, and F. Wang. “*In Situ* Probing and Synthetic Control of Cationic Ordering in Ni-Rich Layered Oxide Cathodes.” *Adv. Energy Mater.* 1601266, 2016 (*in press*).
- Bai, J., and J. Zhao, D. Wang, J. P. Ko, A. Huq, and F. Wang. “*In Situ* Tracking of the Structural Chemistry during Synthesis of Ni-Rich Layered Oxides as High-Energy Cathodes for Li-Ion Batteries.” Submitted.

Presentations

- International Materials Research Congress (IMRC), Cancun, Mexico (August 2016): “Insights into Designing Electrodes and Interfaces for Li-Ion Batteries from *In Situ* Studies”; F. Wang.
- International Meeting on Lithium Batteries (IMLB) 2016, Chicago, Illinois (June 19-24, 2016): “Cu-Based Ternary Fluorides as High-Energy Cathodes for Rechargeable Lithium Batteries”; F. Wang, S-W. Kim, D-H. Seo, K. Kang, L. Wang, D. Su, J. Vajo, J. Wang, and J. Graetz.

Task 3.5 – Novel Cathode Materials and Processing Methods (Michael M. Thackeray and Jason R. Croy, Argonne National Laboratory)

Project Objective. The project goal is to develop low-cost, high-energy, and high-power Mn-oxide-based cathodes for Li-ion batteries that will meet the performance requirements of PHEVs and EVs. Improving the design, composition, and performance of advanced electrodes with stable architectures and surfaces, facilitated by an atomic-scale understanding of electrochemical and degradation processes, is a key objective.

Project Impact. Standard Li-ion battery technologies are unable to meet the demands of the next-generation EVs and PHEVs. Battery developers and scientists will take advantage of both the applied and fundamental knowledge generated from this project to advance the field. In particular, this knowledge should enable progress toward meeting DOE goals for 40-mile, all-electric range PHEVs.

Approach. This project will exploit the concept and optimize the electrochemical properties of structurally integrated “composite” electrode structures with a prime focus on layered-layered-spinel (LLS) materials. Alternative processing routes will be investigated. The comprehensive characterization facilities at ANL will be used to explore novel surface and bulk structures by both *in situ* and *ex situ* techniques in pursuit of advancing the electrochemical performance of state-of-the-art cathode materials. A theoretical component will complement the experimental work of this project.

Out-Year Goals. The out-year goals are as follows:

- Identify high-capacity (‘layered-layered’ and ‘layered-spinel’) composite electrode structures and compositions that are stable to electrochemical cycling at high potentials (~4.5 V).
- Identify and characterize surface chemistries and architectures that allow fast Li-ion transport and mitigate or eliminate transition-metal dissolution.
- Use complementary theoretical approaches to further the understanding of electrode structures and electrochemical processes to accelerate the progress of materials development.
- Scale-up, evaluate, and verify promising cathode materials in conjunction with scale-up and cell fabrication facilities at ANL.

Collaborators. This project engages with the following collaborators: Joong Sun Park, Bryan Yonemoto, Eunje Lee, and Roy Benedek (Chemical Sciences and Engineering, ANL).

Milestones

1. Optimize the composition, capacity, and cycling stability of structurally integrated cathode materials with a low (~10 – 20%) Li_2MnO_3 content. Target capacity = 200 mAh/g or higher (baseline electrode). (September 2016 – In progress)
2. Scale up the most promising materials to batch sizes required for evaluation by industry (10g-100g-1kg). (September 2016 – In progress)
3. Synthesize and determine the electrochemical properties of unique surface architectures that enable > 200 mAh/g at a > 1C rate. (September 2016 – In progress)

Progress Report

‘Layered-layered-spinel’ materials are promising as next-generation, Mn-rich cathodes wherein a ‘layered-layered’ (LL) $x\text{Li}_2\text{MnO}_3 \cdot (1-x)\text{LiMO}_2$ ($M=\text{Ni}, \text{Mn}, \text{Co}$, ‘NMC’) material is stabilized via the intentional integration of spinel-type nanodomains. The integrated domains can be induced by under lithiation (with respect to the nominal LL composition) of the LL precursor material during synthesis. This strategy has consistently

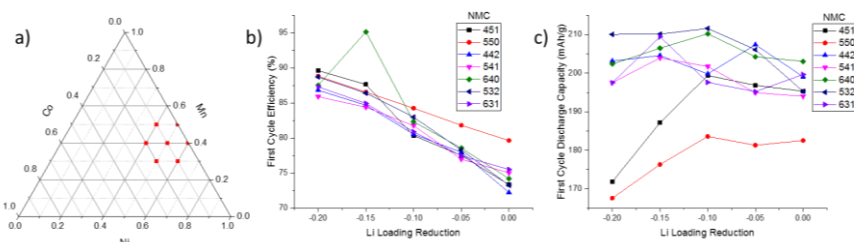


Figure 19. (a) Ternary diagram showing NMC compositions investigated. (b) First-cycle efficiency as a function of Li loading reduction compared to the baseline loading (0 on the x axis). (c) First-cycle discharge capacity at varied Li loadings for the NMC materials studied.

shown improvements in first-cycle efficiency and rate capability in comparison to LL counterpart materials. To better understand the role of composition on the formation and structure property-electrochemical-relationships of NMC-based LLS materials, and search for improved LLS compositions, a compositional study was performed over the region shown (red dots) in the ternary diagram of Figure 19a. Data points are labeled by their intended Li:Ni:Mn:Co molar ratios (with $\text{Ni}+\text{Mn}+\text{Co} = 1$). To ensure reliable and consistent comparisons between the materials, all $[\text{NiMnCo}](\text{OH})_2$ precursors were prepared in a 4L stirred-tank reactor with automated pH control.

After synthesis of the NMC precursors, the materials were divided and fired with targeted lithium amounts to give the different, nominal Li:NMC ratios. Figure 19b shows the first-cycle efficiency of all materials. A clear trend appears where decreasing the lithium loading resulted in increasing the Coulombic efficiency, consistent with prior observations of various other LLS materials synthesized using this method. The improved efficiencies result in better utilization of available capacity at lower lithium loadings.

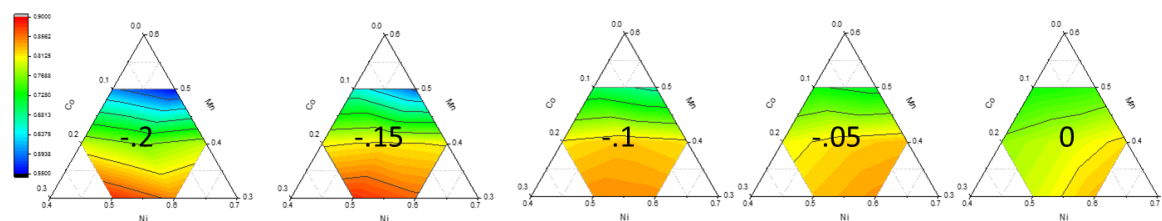


Figure 20. Ternary contour plot of capacity retention (red=high, blue=low) over the NMC compositions studied. The numbers in the ternary plots denote the reduction of lithium loading from the baseline Li/NMC during synthesis.

In Figure 20, the rate retention of a 300 mA/g discharge cycle, compared to a 15mA/g cycle, is presented for the ternary phase space investigated. Capacity retention during higher rate testing increased at higher Ni loadings in the NMC-based cathodes. As the lithium loading decreases to -0.15 or -0.2 from the baseline loading (0), capacity retention becomes very poor for materials with 50% Mn. These same materials also showed the lowest first-cycle capacities, Figure 19c; this was likely the result of rock-salt-type impurities impeding Li diffusion, as was evidenced in XRD data (not shown).

In summary, a systematic phase study of a portion of the NMC ternary space shows electrochemical improvements when a LLS synthesis methodology (targeted lithium loadings) is applied. The large data set (35 samples) is being used to identify compositions of interest, and general electrochemical trends of NMC-based, LLS cathodes.

Patents/Publications/Presentations

Publication

- Croy, Jason R., and Joong Sun Park, Youngho Shin, Bryan T. Yonemoto, Mahalingam Balasubramanian, Brandon R. Long, Yang Ren, and Michael M. Thackeray. “Prospects for Spinel-Stabilized, High-Capacity Lithium-Ion Battery Cathodes.” *J. Power Sources*, accepted (2016).

Task 3.6 – Advanced Cathode Materials for High-Energy Lithium-Ion Batteries (Marca Doeff, Lawrence Berkeley National Laboratory)

Project Objective. Microscopy and synchrotron X-ray absorption and photoemission techniques will be used to study the phenomenon of surface reconstruction to rock salt on NMC particle surfaces as a function of composition, synthesis method, surface chemistry, and electrochemical history. Because the surface reconstruction is implicated in capacity fading and impedance rise during high-voltage cycling, a thorough understanding of this phenomenon is expected to lead to principles that can be used to design robust, high-capacity NMC materials for Li-ion cells. The emphasis will be on stoichiometric NMCs with high Ni contents such as 622 and 523 compositions.

Project Impact. To increase the energy density of Li-ion batteries, cathode materials with higher voltages and/or higher capacities are required, but safety and cycle life cannot be compromised. Nickel-rich NMCs can provide higher capacities and lower cost in comparison with low nickel content NMCs, but surface reactivity is an issue. A systematic evaluation of the effects of synthesis method, composition, and cell history on the surface reconstruction phenomenon will lead to higher capacity, robust, and structurally stable positive electrode materials that result in higher energy density Li-ion cells than are currently available.

Out-Year Goals. The information generated by the in-depth characterization will be used to design robust NMC materials that can withstand cycling to high potentials and deliver >200 mAh/g.

Collaborations. TXM was used this quarter to characterize NMC materials, with work done in collaboration with Yijin Liu (SSRL). Synchrotron and computational efforts continued in collaboration with Professor M. Asta (UC Berkeley); and Dr. Dennis Nordlund, Dr. Yijin Liu, and Dr. Dimosthenis Sokaras (SSRL). The TEM effort is in collaboration with Dr. Huolin Xin (BNL).

Milestones

1. Synthesize baseline NMC-523 and NMC-622 and Ti-substituted variants by spray pyrolysis and co-precipitation. (December 2015 – Completed)
2. Complete surface characterization of pristine materials by XAS and XPS. (March 2016 – Complete)
3. Complete soft XAS experiments on electrodes cycled to high potentials. (June 2016 – Complete)
4. *Go/No-Go*: Core-shell composites made by infiltration and re-firing of spray-pyrolyzed hollow spherical particles. (September 2016 – Decision is postponed until March 2017)

Progress Report

Co-precipitation and spray pyrolysis have been both employed in research to prepare nickel-rich NMC materials. The project has reported the structural stability of these materials, both the crystalline structure and electronic structure, in our previous reports.

Spray pyrolysis has also been used to prepare NMC-442, and results were reported in previous publications. The pristine NMC-442 shows inhomogeneous elemental distribution when analyzed by full-field TXM. In particular, the material has a Mn-rich surface, which results in reduced surface reconstruction and improved cycling.¹

Similar characterization was applied to NMC-622 materials. As shown in Figure 21 (left), the elemental information is color mapped and an inhomogeneous transition metal distribution is observed in the particles. A more quantitative analysis was achieved by performing a correlation analysis of the absorption coefficient as a function of the transition metal K-edges. Only 70.54% of the voxels (32.5 x 32.5 x 32.5 nm) contain all three transition metals (Ni, Mn and Co). According to the cross-section images, the inhomogeneity is mainly found on the surface of the particles. The Mn-rich surface behavior for both NMC-442 and NMC-622 demonstrates the uniqueness of spray pyrolysis in preparing NMC materials. However, with the current synthesis condition, the particles generated with spray pyrolysis are mostly hollow structures. The large surface area of these hollow particles may promote side reactions of NMCs with electrolyte. A future research goal is to make solid spherical particles by this method, by changing the reaction parameters. Specifically, the project will use drying agents and control the solution viscosity.

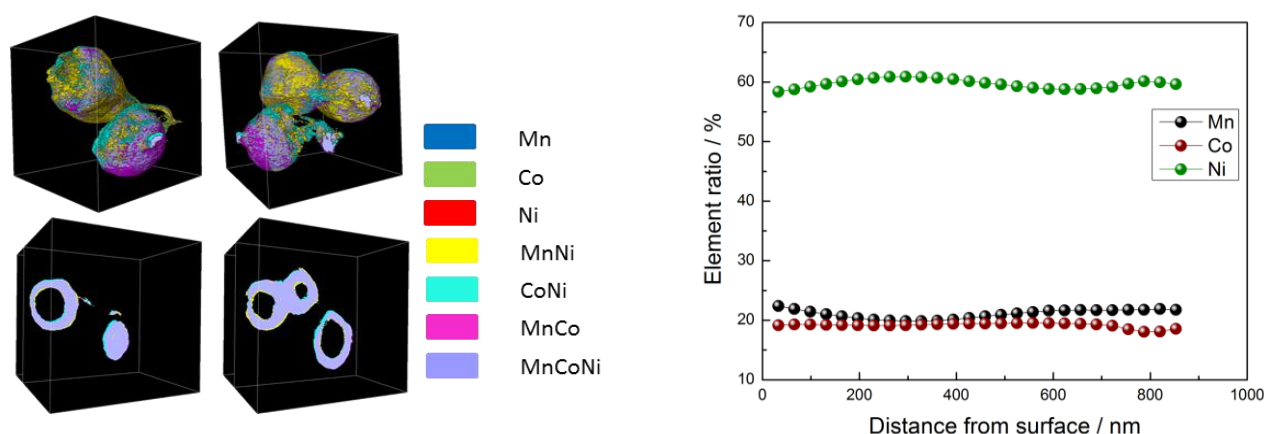


Figure 21. (Left) Elemental association maps of spray pyrolyzed NMC-622 particles. 3D rendering of the elemental associations viewing the particles at different angles, and 2D slices of the elemental associations. The colors presenting the elemental associations are shown in the middle. (Right) Elemental distribution as a function of the distance from the particle surface (both inner and outer surfaces) calculated using the transmission X-ray microscopy data.

- (1) Lin, F., and D. Nordlund, Y. Li, M. K. Quan, L. Cheng, T.-C. Weng, Y. Liu, H. L. Xin, M. M. Doeff, M. S. Whittingham, et al. "Metal Segregation in Hierarchically Structured Cathode Materials for High-Energy Lithium Batteries." *Nat. Energy* 1, no. 1 (2016): 15004.

Patents/Publications/Presentations

Publication

- Ludwig, Jennifer, and Cyril Marino, Dominik Haering, Christoph Stinner, Dennis Nordlund, Marca Doeff, Hubert Gasteiger, and Tom Nilges. “Facile Ethylene Glycol-Promoted Microwave-Assisted Solvothermal Synthesis of High-Performance LiCoPO_4 as a High-Voltage Cathode Material for Lithium-Ion Batteries.” *RSC Advances* 6 (2016): 82984–82994. doi: 10.1039/C6RA19767A (2016).

Presentations

- 2016 University of California Industry Battery Workshop, LBNL, Berkeley, California (September 29, 2016): “Structural Stability of Nickel-Rich Layered Cathode Materials”; Chixia Tian and Marca Doeff. Poster presentation.
- Molecular Foundry 2016 User Meeting, LBNL, Berkeley, California (August 7-8, 2016): “NMC Cathode and LLZO Electrolyte Studies”; Marca M. Doeff, Feng Lin, Lei Cheng, Chixia Tian, Dennis Nordlund, and Huolin Xin.
- 67th Annual Meeting of the International Society of Electrochemistry, The Hague, Netherlands (August 21-26, 2016): “The Promise of Sodium Ion Batteries”; Marca M. Doeff. Invited.

Task 3.7 – Lithium Batteries with Higher Capacity and Voltage (John B. Goodenough, UT Austin)

Project Objective. The project objective is to develop an electrochemically stable alkali-metal anode that can avoid the SEI layer formation and the alkali-metal dendrites during charge/discharge. To achieve the goal, a thin and elastic solid electrolyte membrane with a Fermi energy above that of metallic lithium and an ionic conductivity $\sigma > 10^{-4} \text{ S cm}^{-1}$ will be tested in contact with alkali-metal surface. The interface between the alkali-metal and the electrolyte membrane should be free from liquid electrolyte, have a low impedance for alkali-metal transport and plating, and keep good mechanical contact during electrochemical reactions.

Project Impact. An alkali-metal anode (lithium or sodium) would increase the energy density for a given cathode by providing a higher cell voltage. However, lithium is not used as the anode in today's commercial Li-ion batteries because electrochemical dendrite formation can induce a cell short-circuit and critical safety hazards. This project aims to find a way to avoid the formation of alkali-metal dendrites and to develop an electrochemical cell with dendrite-free alkali-metal anode. Therefore, once realized, the project will have a significant impact by an energy-density increase and battery safety; it will enable a commercial Li-metal rechargeable battery of increased cycle life.

The key approach is to introduce a solid-solid contact between an alkali metal and a solid electrolyte membrane. Where SEI formation occurs, the creation of new anode surface at dendrites with each cycle causes capacity fade and a shortened cycle life. To avoid the SEI formation, a thin and elastic solid electrolyte membrane will be introduced, and liquid electrolyte will be eliminated from the anode surface.

Out-Year Goals. The out-year goals are to increase cell energy density for a given cathode and to allow low-cost, high-capacity rechargeable batteries with cathodes other than insertion compounds.

Collaborations. This project collaborates with A. Manthiram at UT Austin and with Karim Zaghib at HQ.

Milestones

1. Fabricate and test glass-fiber and cross-linked polymer membranes impregnated with Li^+ glass electrolytes. (December 2015 – Complete)
2. Test cycle life of plating/stripping lithium across Li^+ glass electrolyte. (March 2016 – Complete)
3. Optimize the heat treatment of the Li^+ and Na^+ glass electrolytes for achieving rapidly a $\sigma_i > 10^{-2} \text{ S cm}^{-1}$ at room temperature (June 2016 – Complete)
4. Test the cyclability of plating of metallic lithium and sodium anodes through the glass electrolyte. (September 2016 – Complete)

Progress Report

High-density LLZO ($\text{Li}_7\text{La}_3\text{Zr}_2\text{O}_{12}$) pellets were prepared by sintering at 1150°C . Typical pellet density was $\sim 93\%$ in our experiment. Li-ion conductivity was measured to be $1.0 \times 10^{-4} \text{ S cm}^{-1}$ at room temperature. First, the project checked the Li transport properties with Li/Au/LLZO/Au/Li symmetric cells. To lower interfacial impedance, gold layers on both sides of the LLZO pellet were deposited before testing. Figure 22a clearly demonstrates short circuits in 591 and 28 seconds at 0.1 and 0.5 mA cm^{-2} , respectively. Lithium dendrites can penetrate through open pores and grain boundaries at room temperature, as is shown in Figure 22b. Cross-sectional area of the short-circuited LLZO turned black, and the SEM image for the corresponding area showed deposit of a secondary material that should be lithium metal. Since it is essential to get stable and reversible Li^+ transport properties across the LLZO electrolyte, the project increased the cell temperature to 50°C . Figure 23 shows charge/discharge voltage curves of a Li/Au/LLZO/Au/Li symmetric cell. It shows a reversible cycling at a current density of 0.1 mA cm^{-2} , unlike the room-temperature test results. It is suggested that a higher atomic mobility of Li atoms at a higher temperature can help reduce the surface area of the metastable dendrites and promote isotropic lithium growth.

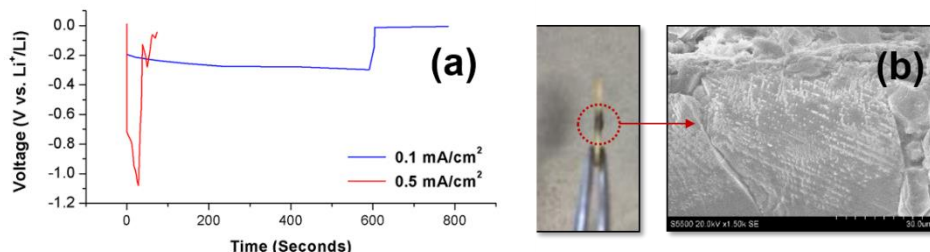


Figure 22. (a) Li-plating voltage curves of Li/Au/LLZO/Au/Li symmetric cells at 0.1 and 0.5 mA cm^{-2} . (b) Cross-sectional photograph of LLZO after short-circuit (left) and the corresponding scanning electron microscopy image for the dark part (right).

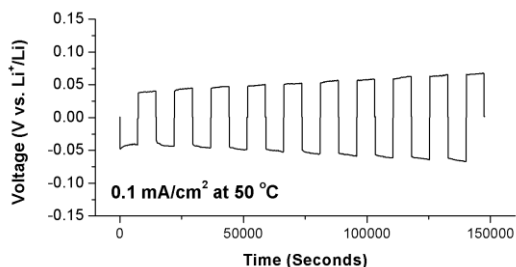


Figure 23. Reversible charge/discharge voltage curves of Li/Au/LLZO/Au/Li symmetric cell at a current density of 0.1 mA cm^{-2} and 50°C .

Patents/Publications/Presentations

Publication

- Park, K., and B. C. Yu, J. W. Jung, Y. Li, W. Zhou, H. Gao, S. Son, and J. B. Goodenough. "Electrochemical Nature of the Cathode Interface for a Solid-State Lithium-Ion Battery: Interface between LiCoO_2 and Garnet- $\text{Li}_7\text{La}_3\text{Zr}_2\text{O}_{12}$." *Chem. Mater.* 28, no. 21 (2016): 8051–8059. doi: 10.1021/acs.chemmater.6b03870.

Task 3.8 – Exploiting Cobalt and Nickel Spinel in Structurally Integrated Composite Electrodes (Michael M. Thackeray and Jason R. Croy, Argonne National Laboratory)

Project Objective. The project goal is to stabilize high-capacity, composite ‘layered-layered’ electrode structures with lithium-cobalt-oxide and lithium-nickel-oxide spinel components (referred to as LCO-S and LNO-S, respectively), or solid solutions thereof (LCNO-S), which can accommodate lithium at approximately 3.5 V versus metallic lithium. This approach and the motivation to use LCO-S and LNO-S spinel components, about which relatively little is known, is novel.

Project Impact. State-of-the-art Li-ion batteries are unable to satisfy the performance goals for PHEVs and all-electric EVs. If successful, this project will impact the advance of energy storage for electrified transportation as well as other applications, such as portable electronic devices and the electrical grid.

Approach. This work will focus on the design and synthesis of new spinel compositions and structures that operate above 3 V and below 4 V and to determine their structural and electrochemical properties through advanced characterization. This information will subsequently be used to select the most promising spinel materials for integration as stabilizers into high-capacity composite electrode structures.

Out-Year Goals. The electrochemical capacity of most high-potential Li-metal oxide insertion electrodes is generally severely compromised by their structural instability and surface reactivity with the electrolyte at low lithium loadings (that is, at highly charged states). Although some progress has been made by cation substitution and structural modification, the practical capacity of these electrodes is still restricted to approximately 160-170 mAh/g. This project proposes a new structural and compositional approach with the goal of producing electrode materials that can provide 200-220 mAh/g without significant structural or voltage decay for 500 cycles. If successful, the materials processing technology will be transferred to the ANL Materials Engineering and Research Facility (MERF) for scale up and further evaluation.

Collaborations. This project collaborates with Eungje Lee, Joong Sun Park, and Roy Benedek (Chemical Sciences and Engineering, ANL), Mali Balasubramanian (Advanced Photon Source, ANL), and V. Dravid and C. Wolverton (Northwestern University).

Milestones

1. Synthesize and optimize spinel compositions and structures with a focus on Co-based systems for use in structurally integrated layered-spinel electrodes. (Q4 – In progress; see text)
2. Determine electrochemical properties of Co-based spinel materials, and when structurally integrated in composite layered-spinel electrodes. (Q4 – In progress)
3. Evaluate the electrochemical migration of TM ions in Co-based layered-spinel electrodes. (Q4 – In progress)

Progress Report

Previous synthesis efforts to explore lithiated spinel compositions that may be used as structural stabilizers for high-capacity, ‘layered-layered’ (LL), $x\text{Li}_2\text{MnO}_3 \cdot (1-x)\text{LiMO}_2$ ($M=\text{Mn, Ni, Co}$) electrode materials have shown interesting results. Reports on $\text{LiCo}_{1-x}\text{Ni}_x\text{O}_2$ ($0 \leq x \leq 0.2$) materials show that the structurally integrated, local spinel configurations, which are characterized by the presence of cobalt (and nickel) in the lithium-rich layers, are formed via solid-state synthesis at intermediate temperatures of $\sim 700^\circ\text{C}$. Data also suggests that such spinel-like structures could be stabilized at higher temperatures when Co is partially substituted with other metals such as Ni. Encouraged by these findings, this study further expands synthesis efforts to explore Co-based, spinel-type materials containing Ni, Mn, and excess Li that may be stabilized at higher temperatures within LL composite electrodes. The amount of the integrated spinel-type configurations is sensitive to both chemical composition and synthesis temperatures. However, the content of Ni, Mn, and excess Li in target materials should be kept low to avoid formation of impurity phases such as NiO rock salt or Co_3O_4 spinel.

A series of $\text{Li}(\text{Co}_{1-2x}\text{Ni}_x\text{Mn}_x)\text{O}_2$ ($x = 0.025, 0.05$, and 0.1) was prepared at various synthesis temperatures between 500 and 900°C . Figure 24a shows normalized discharge curves of $\text{Li}(\text{Co}_{0.9}\text{Ni}_{0.05}\text{Mn}_{0.05})\text{O}_2$. The 3.5 V plateau, attributable to the lithiated spinel structure, is clearly seen in the sample fired at 500°C . Although the length of the 3.5 V plateau decreases significantly after the synthesis temperature is increased above 600°C , it is still noticeable in samples annealed up to 800°C . The differential capacity (dQ/dV) plots in Figure 24b-d reveal a weak but clear oxidation peak at ~ 3.7 V for the $x = 0.05$ and 0.1 samples prepared at 900°C . It is noteworthy that the dQ/dV curve is noticeably more stable with cycling as the degree of Ni and Mn substitution, x , increases.

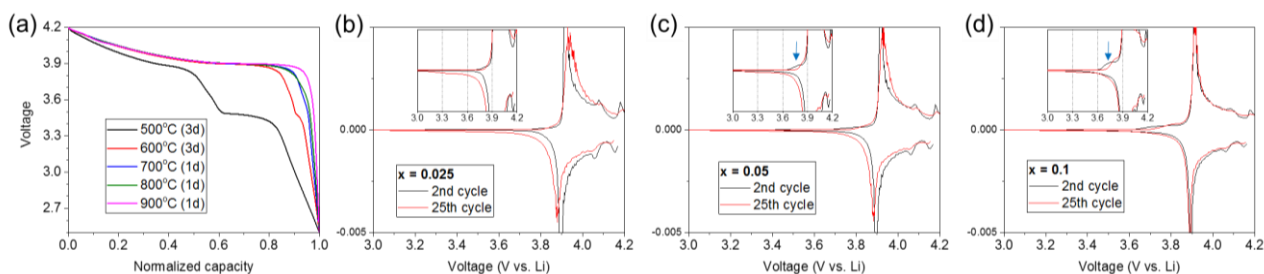


Figure 24. (a) Normalized discharge profile of $\text{Li}(\text{Co}_{0.9}\text{Ni}_{0.05}\text{Mn}_{0.05})\text{O}_2$, (b-d) dQ/dV plots of $\text{Li}(\text{Co}_{1-2x}\text{Ni}_x\text{Mn}_x)\text{O}_2$ fired at 900°C .

In addition, $0.025\text{Li}_2\text{MnO}_3 \cdot \text{LiCo}_{1-x}\text{Ni}_x\text{O}_2$ ($x = 0$ and 0.025) materials have been synthesized at $500 - 900^\circ\text{C}$. Power XRD data (not shown) confirmed the quality of the Co, Ni, and Mn oxide structures and the absence of significant impurities. In Figure 25a, the voltage profiles of the 600°C fired samples show the presence of the 3.6 V plateau of the lithiated spinel phase (arrows). Although the structural development toward a perfectly layered structure progresses with increasing synthesis temperature, the voltage profiles of the 800°C fired samples suggest that a remnant of the low-voltage electrochemical process may yet remain (Figure 25b).

These data corroborate that the local spinel-like atomic configurations can be stabilized at higher synthesis temperatures when composition and synthesis conditions are controlled.

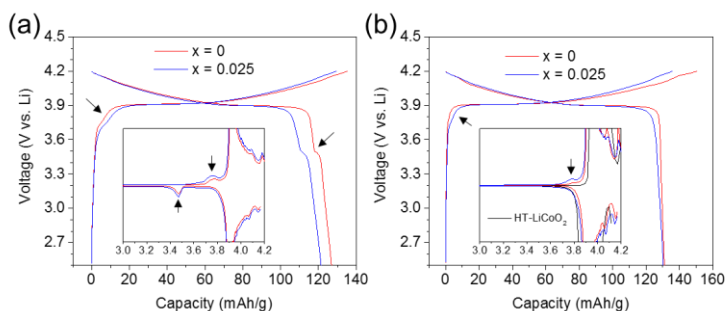


Figure 25. Voltage profiles and dQ/dV plots (inset) of $0.025\text{Li}_2\text{MnO}_3 \cdot \text{LiCo}_{1-x}\text{Ni}_x\text{O}_2$ fired at (a) $600^\circ\text{C} - 72\text{h}$ and (b) $800^\circ\text{C} - 24\text{h}$.

Patents/Publications/Presentations

Publication

- Lee, E., and J. Blauwkamp, F. C. Castro, J. Wu, V. P. Dravid, P. Yan, C. Wang, S. Kim, C. Wolverton, R. Benedek, F. Dogan, J. S. Park, J. R. Croy, and M. M. Thackeray. “Exploring Lithium-Cobalt-Nickel-Oxide Spinel Electrodes for ≥ 3.5 V Li-Ion Cells.” *ACS Applied Materials & Interfaces* (2016). doi: 10.1021/acsami.6b09073 (2016).

Task 3.9 – Discovery of High-Energy Lithium-Ion Battery Materials (Wei Tong, Lawrence Berkeley National Laboratory)

Project Objective. This project aims to develop a cathode that can cycle > 200 mAh/g while exhibiting minimal capacity and voltage fade. The emphasis will be on oxides with high nickel contents. This task focuses on the compositions in the Li-Ni-O phase space, which will be explored using a combinatorial materials approach to search for new high-capacity cathodes. The specific objectives of this project are to: (1) investigate and understand the correlation between the synthesis and electrochemical performance of Ni-based compounds, and (2) design, synthesize, and evaluate the potential new high-capacity cathodes within Li-Ni-O composition space using the percolation theory as a guideline.

Project Impact. In commercial Li-ion batteries, the well-ordered, close-packed oxides, particularly, layered lithium transition metal oxides (LiTmO_2 , Tm is transition metal) are widely used. However, the energy density needs to be at least doubled to meet the performance requirements of EVs (300 to 400 miles). Although capacities approaching 300 mAh/g have been reported in Li-, Mn-rich layered oxide compounds, capacity decay and voltage fading in the long-term cycling are always observed. Therefore, new materials are urgently needed to make the breakthrough in Li-ion battery technology.

Approach. The recent discovery of high-capacity materials with lithium excess provides new insights into design principles for potential high-capacity cathode materials. According to the percolation theory, lithium excess is required to access 1 lithium exchange capacity in LiTmO_2 compounds. This seems to be independent of TM species; therefore, it could open a composition space for the search of new materials with high capacity. The interesting $\text{Ni}^{2+}/\text{Ni}^{4+}$ redox is selected as the electrochemically active component, and combinatorial materials design concept will be used to discover the potential cathode material candidates in the Li-Ni-O phase space.

Out-Year Goals. The long-term goal is to search new high-energy cathodes that can potentially meet the performance requirements of EVs with a 300- to 400-mile range in terms of cost, energy density, and performance.

Collaborations. The PI closely collaborates with M. Doeff (LBNL) on soft XAS, C. Ban (NREL) on ALD coating, B. McCloskey (LBNL) for differential electrochemical mass spectrometry (DEMS), and R. Kostecki (LBNL) for Raman spectroscopy. Collaboration is also in progress with other BMR PIs (X.-Q. Yang and F. Wang, BNL; and K. Persson, LBNL) for crystal structure evolution on cycling and material computation.

Milestones

1. Determine synthetic approach and identify the key synthetic parameters for Ni^{3+} -containing compounds, for example, LiNiO_2 . (Q1 – Complete)
2. Complete the structural and electrochemical characterization of LiNiO_2 . (Q2 – Complete)
3. Determine synthetic approach and identify the key synthetic parameters for Ni^{2+} -containing compounds, for example, Li_2NiO_2 . (Q3 – Complete)
4. Complete the structural and electrochemical characterization of Li_2NiO_2 , and down select the synthetic approach for the phase screening within Li-Ni-O chemical space. (Q4 – Ongoing)

Progress Report

Preliminary electrochemical studies on $x \text{Li}_2\text{NiO}_2 \cdot (1-x) \text{Li}_2\text{CuO}_2$ solid solutions indicated Cu substitution improved the discharge capacity in the initial cycle; however, the capacity retention was not effectively enhanced within the tested voltage window (4.6 - 1.5 V). This quarter, the project aimed to understand the role of Cu substitution on the structural transformation during the electrochemical reaction because it presents a critical challenge for this family of materials.

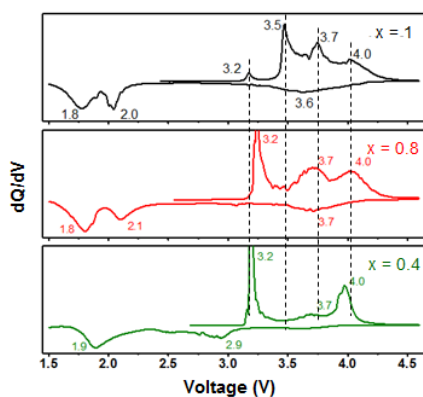


Figure 26. Selected dQ/dV plots of $x \text{Li}_2\text{NiO}_2 \cdot (1-x) \text{Li}_2\text{CuO}_2$ ($x = 1, 0.8, 0.4$) solid solutions.

Phase transformation is typically reflected by several oxidation/reduction peaks on the differential capacity curves (Figure 26). The dQ/dV plot of Li_2NiO_2 during the charge was featured by several small oxidation peaks around 3.2, 3.5, 3.7, and 4.0 V. With 0.2 Cu substitution, oxidation peaks around 3.7, and 4.0 V remained as the main features, but the oxidation peak around 3.2 V appeared to grow at the expense of the peak at 3.5 V. When further increasing Cu content to 0.6, only sharp oxidation peaks at 3.2 and 4.0 V were observed. The discharge profiles of Li_2NiO_2 and $\text{Li}_2\text{Ni}_{0.8}\text{Cu}_{0.2}\text{O}_2$ were featured by three reduction peaks around 3.6, 2.0, and 1.8 V. When increasing Cu content to 0.6, the 3.6 and 2.0 V plateaus gradually diminished and a new plateau around 2.9 V was observed, which was a direct indication of Cu-related phase transformation. Of the four materials, $\text{Li}_2\text{Ni}_{0.8}\text{Cu}_{0.2}\text{O}_2$ was chosen for the electrochemical mechanism study considering a substantial change in the first charge profile and preserved features during the first discharge.

To elucidate the structural evolution, *ex situ* XRD patterns were collected at various states of charge. As shown in Figure 27a-b, a new set of diffraction peaks represented by the dashed lines developed after charging the electrode to 3.8 V, which could be indexed as monoclinic $\text{Li}_{1+\delta}\text{CuO}_2$ ($0 \leq \delta \leq 0.5$) with $C2/m$ space group. Meanwhile, another set of broad diffraction peaks (solid circles) showed a match with phases belonging to $Fm\bar{3}m$ space group (for example, NiO and $\text{Li}_{1-x}\text{Ni}_x\text{O}$). This observation confirmed the different phase transformation routes during the delithiation process for $Immm$ -type Li_2NiO_2 and Li_2CuO_2 . In other words, Ni and Cu followed its delithiation mechanism and did not form a solid solution any more.

When further charging the electrode to 4.6 V (Figure 27c), changes in the XRD peaks of $Fm\bar{3}m$ NiO were almost negligible, and an increase in the amount of Li_2CO_3 was revealed. The main features of $\text{Li}_{1+\delta}\text{CuO}_2$ (peaks marked by dashed lines) were mostly preserved through the rest of the first cycle. Interestingly, this structural variation associated with lithium copper oxides when charging the electrode from 3.8 to 4.6 V was reversible once the electrode was discharged to 2.6 V (Figure 27d). On the other hand, the original $Immm$ structure was not recovered after discharged to 1.5 V (Figure 27e), indicating the irreversible structural change during the first charge for $\text{Li}_2\text{NiO}_2 - \text{Li}_2\text{CuO}_2$ solid solution. Instead, the monoclinic $C2/m$ phase dismissed after further discharging $\text{Li}_2\text{Ni}_{0.8}\text{Cu}_{0.2}\text{O}_2$ electrode to 1.5 V, and the formation of Li_2O crystalline phase ($R\bar{3}m$) was revealed. The underlying reaction that leads to the formation of Li_2O remains unclear here, partially due to the loss in crystallinity when discharging electrode to 1.5 V.

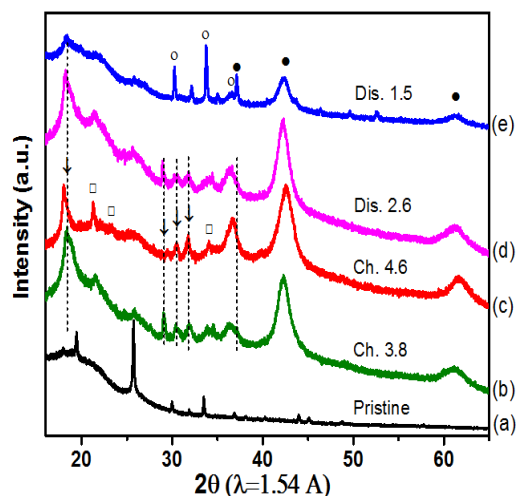


Figure 27. *Ex situ* X-ray diffraction patterns of $\text{Li}_2\text{Ni}_{0.8}\text{Cu}_{0.2}\text{O}_2$ electrodes at selected states-of-charge. Dashed lines represent monoclinic $C2/m$ $\text{Li}_{1+\delta}\text{CuO}_2$ phases ($0 \leq \delta \leq 0.5$). NiO , Li_2O , and Li_2CO_3 are indicated by solid circles, open circles, and open squares, respectively.

TASK 4 – ELECTROLYTES FOR HIGH-VOLTAGE, HIGH-ENERGY, LITHIUM-ION BATTERIES

NOTE: This task is now closed, with limited extension work being completed this fiscal year. The BMR has awarded new tasks in this area, which will begin next fiscal year.

Summary

The current Li-ion electrolyte technology is based on LiPF_6 solutions in organic carbonate mixtures with one or more functional additives. Li-ion battery chemistries with energy density of 175~250 Wh/Kg are the most promising choice. To further increase the energy density, the most efficient way is to raise either the voltage and/or the capacity of the positive materials. Several high-energy materials including high-capacity composite cathode $x\text{Li}_2\text{MnO}_3 \cdot (1-x)\text{LiMO}_2$ and high-voltage cathode materials such as $\text{LiNi}_{0.5}\text{Mn}_{1.5}\text{O}_4$ (4.8 V) and LiCoPO_4 (5.1 V) have been developed. However, their increased operating voltage during activation and charging poses great challenges to the conventional electrolytes, whose organic carbonate-based components tend to oxidatively decompose at the threshold beyond 4.5 V vs Li^+/Li .

Other candidate positive materials for PHEV application that have potential of providing high capacity are the layered Ni-rich NCM materials. When charged to a voltage higher than 4.5 V, they can deliver a much higher capacity. For example, $\text{LiNi}_{0.8}\text{Co}_{0.1}\text{Mn}_{0.1}\text{O}_2$ (NCM 811) only utilizes 50% of its theoretical capacity of 275 mAh/g when operating in a voltage window of 4.2 V – 3.0 V. Operating voltage higher than 4.4 V would significantly increase the capacity to 220 mAh/g; however, the cell cycle life becomes significantly shortened mainly due to the interfacial reactivity of the charged cathode with the conventional electrolyte. The oxidative voltage instability of the conventional electrolyte essentially prevents the practicality to access the extra capacities of these materials.

To address the above challenges, new electrolytes that have substantial high-voltage tolerance at high temperature with improved safety are needed urgently. Organic compounds with low HOMO (highest occupied molecular orbital) energy level are suitable candidates for high-voltage application. An alternative approach to address the electrolyte challenges is to mitigate the surface reactivity of high-voltage cathodes by developing cathode passivating additives. Like the indispensable role of SEI on the carbonaceous anodes, cathode electrolyte interphase (CEI) formation additives could kinetically suppress the thermodynamic reaction of the delithiated cathode and electrolyte, thus significantly improving the cycle life and calendar life of the high energy density Li-ion battery.

An ideal electrolyte for high-voltage, high-energy cathodes also requires high compatibility with anode materials (graphite or silicon). New anode SEI formation additives tailored for the new high-voltage electrolyte are equally critical for the high-energy Li-ion battery system. Such an electrolyte should have the following properties: high stability against 4.5 – 5.0 V charging state, particularly with cathodes exhibiting high surface oxygen activity; high compatibility with a strongly reducing anode under high-voltage charging; high lithium salt solubility ($> 1.0 \text{ M}$) and ionic conductivity ($> 6 \times 10^{-3} \text{ S/cm}$ @ room temperature); and non-flammability (no flash point) for improved safety and excellent low-temperature performance (-30°C).

TASK 5 – DIAGNOSTICS

Summary and Highlights

To meet the goals of VTO-Multi Year Program Plan and develop lower-cost, abuse-tolerant batteries with higher energy density, higher power, better low-temperature operation and longer lifetimes suitable for the next-generation of HEVs, PHEVs and EVs, there is a strong need to identify and understand structure-property-electrochemical performance relationships in materials, life-limiting and performance-limiting processes, and various failure modes to guide battery development activities and scale-up efforts. In the pursuit of batteries with high energy density, high cell operating voltages and demanding cycling requirements lead to unprecedented chemical and mechanical instabilities in cell components. Successful implementation of newer materials such as Si anode and high-voltage cathodes also requires better understanding of fundamental processes, especially those at the solid/electrolyte interface of both anode and cathode.

The BMR Task 5 takes on these challenges by combining model system, *ex situ*, *in situ*, and *operando* approaches with an array of the start-of-the-art analytical and computational tools. Four subtasks are tackling the chemical processes and reactions at the electrode/electrolyte interface. Researchers at LBNL use *in situ* and *ex situ* vibrational spectroscopy, far- and near-field scanning probe spectroscopy and laser-induced breakdown spectroscopy (LIBS) to understand the composition, structure, and formation/degradation mechanisms of the SEI at silicon anode and high-voltage cathodes. The University of California at San Diego (UCSD) subtask combines STEM/EELS, XPS, and *ab initio* computation for surface and interface characterization and identification of instability causes at both electrodes. At Cambridge University, nuclear magnetic resonance (NMR) is being used to identify major SEI components, their spatial proximity, and how they change with cycling. Subtasks at BNL and PNNL focus on the understanding of fading mechanisms in electrode materials, with the help of synchrotron based X-ray techniques (diffraction and hard/soft X-ray absorption) at BNL and HRTEM and spectroscopy techniques at PNNL. At LBNL, model systems of electrode materials with well-defined physical attributes are being developed and used for advanced diagnostic and mechanistic studies at both bulk and single-crystal levels. These controlled studies remove the ambiguity in correlating material physical properties and reaction mechanisms to performance and stability, which is critical for further optimization. The final subtask takes advantage of the user facilities at ANL that bring together X-ray and neutron diffraction, X-ray absorption, emission and scattering, HRTEM, Raman spectroscopy, and theory to look into the structural, electrochemical, and chemical mechanisms in the complex electrode/electrolyte systems. The diagnostics team not only produces a wealth of knowledge that is key to developing next-generation batteries, it also advances analytical techniques and instrumentation that have a far-reaching effect on material and device development in a range of fields.

Highlights. The highlights this quarter are as follows:

- LBNL (Kostecki's group) correlated the improved passivating properties of silicon in the presence of LiBOB to the formation and incorporation of $\text{Li}_x\text{B}_y\text{C}_n\text{O}_{2n}$ ($n>6$) in the inner part of the SEI layer.
- PNNL (Wang's Group) used *in situ* TEM to investigate the lithiation behavior of individual amorphous silicon (a-Si) nanotubes with different thicknesses of surface oxide layers and revealed that outward expansion of the nanotubes can be effectively confined by increasing the thickness of the outer SiO_x coating.

Task 5.1 – Design and Synthesis of Advanced High-Energy Cathode Materials (Guoying Chen, Lawrence Berkeley National Laboratory)

Project Objective. The successful development of next-generation electrode materials requires particle-level knowledge of the relationships between materials' specific physical properties and reaction mechanisms to their performance and stability. This single-crystal-based project was developed specifically for this purpose, and it has the following objectives: (1) obtain new insights into electrode materials by utilizing state-of-the-art analytical techniques that are mostly inapplicable on conventional, aggregated secondary particles, (2) gain fundamental understanding on structural, chemical, and morphological instabilities during lithium extraction/insertion and prolonged cycling, (3) establish and control the interfacial chemistry between the cathode and electrolyte at high operating voltages, (4) determine transport limitations at both particle and electrode levels, and (5) develop next-generation electrode materials based on rational design as opposed to more conventional empirical approaches.

Project Impact. The project will reveal performance-limiting physical properties, phase-transition mechanisms, parasitic reactions, and transport processes based on the advanced diagnostic studies on well-formed single crystals. The findings will establish rational, non-empirical design methods that will improve the commercial viability of next-generation $\text{Li}_{1+x}\text{M}_{1-x}\text{O}_2$ ($\text{M}=\text{Mn}, \text{Ni}, \text{and Co}$) and spinel $\text{LiNi}_x\text{Mn}_{2-x}\text{O}_4$ cathode materials.

Approach. This project scope will encompass the following: (1) Prepare crystal samples of Li-rich layered oxides and high-voltage Ni/Mn spinels with well-defined physical attributes, (2) Perform advanced diagnostic and mechanistic studies at both bulk and single-crystal levels, and (3) Establish global properties and performance of the samples from the bulk analyses, while, for the single-crystal based studies, utilizing time- and spatial-resolved analytical techniques to probe material redox transformation and failure mechanisms.

Out-Year Goals. This project aims to determine performance and stability limiting fundamental properties and processes in high-energy cathode materials and to outline mitigating approaches. Improved electrode materials will be designed and synthesized.

Collaborations. This project collaborates with Drs. Y. Liu (SSRL), M. Doeff and P. Ross (LBNL), Simon Mun (GIST), J. Guo (ALS), C. Wang (PNNL), C. Grey (Cambridge), and A. Huq and J. Nanda (ORNL).

Milestones

1. Establish synthesis-structure-electrochemical property relationship in high-voltage Li-TM-oxides. (December 2015 – Complete)
2. *Go/No-Go*: Downselect alternative high-energy cathode materials for further investigation, if the material delivers > 200 mAh/g capacity in the voltage window of 2 – 4.5 V. (March 2016 – Complete, with a No-Go decision)
3. Determine lithium concentration and cycling dependent TM movement in and out of oxide particles. Examine the mechanism. (June 2016 – Complete)
4. Identify key surface properties and features hindering stable high-voltage cycling of Li-TM-oxides. (September 2016 – Complete)

Progress Report

This quarter, facet-dependent surface properties of pristine Li- and Mn-rich (LMR) layered oxide were directly visualized on crystal samples, and their impact on cycling stability was further elucidated. Figure 28a shows an SAED pattern collected on a polyhedron-shaped $\text{Li}_{1.2}\text{Mn}_{0.13}\text{Mn}_{0.54}\text{Co}_{0.13}\text{O}_2$ crystal (~ 200 nm in size), recorded by using an aperture covering the entire particle in TEM. In addition to the reflections from the three variants of monoclinic C2/m structure, a second set of reflections (highlighted in green circles) was also observed. Comparison with the simulated SAED pattern reveals that the secondary phase belongs to a spinel structure. The dark-field image collected by using the spinel reflections only allowed location of the spinel's exclusive presence on particle surface, as shown by the bright contrast in Figure 28b. The extent of spinel formation is non-uniform throughout the surface, which reveals the facet-dependent nature. When the spinel slab was parallel to the electron beam, Co and Ni enrichment was also observed on the surface, suggesting facet-dependent elemental composition. Structural transformation on pristine surface was further confirmed by STEM/EELS studies. Figure 28c shows the HAADF STEM image where a thin surface layer (about 2 nm) with a different atomic arrangement from that of the bulk is clearly shown. Atomic simulation of the surface layer shows that some lithium sites are occupied by the transition metals to form a spinel phase with antisite defects. EEL spectra including O K-edge, Mn, Ni and Co L-edges were collected from the bulk to the surface, and the results are shown in Figure 28d (with the expanded regions of Ni, Co, Mn and O also shown on the left). Ni was found to remain at 2+, while the spectra of both Mn and Co show a gradual increase in the L3/L2 ratio when going from the bulk toward the surface, corresponding to a decrease in oxidation state of both transition metals. The reduction in the TM oxidation state is also supported by the lower O pre-peak intensity observed on the surface, where the O profile resembles that of a spinel. EELS Li K-edge imaging in the low-loss region confirms the presence of Li in the surface region where Mn and Co are reduced. These results are consistent with the previously reported soft XAS data, providing further evidence that instead of the layered structure, the reduced transition metals reside in a defective spinel on the pristine surface, similar to what was reported on the cycled conventional secondary particles in the literature. All three transition metals as well as Li are present in the surface layer.

These pristine surface properties and their changes were further correlated to cycling stability by using an intricate electrochemical protocol, high-resolution microscopy/ spectroscopy and high throughput ensemble-averaged spectroscopy on crystal samples with various morphologies. It was found that particle morphology determines the extent of TM reduction, both during synthesis and cycling, which directly correlates to cathode rate performance and stability. Oxide structure and cycling stabilities, therefore, improve with maximum expression of surface facets stable against TM reduction. These results provide important material optimization strategies in addressing critical issues facing this family of cathode materials.

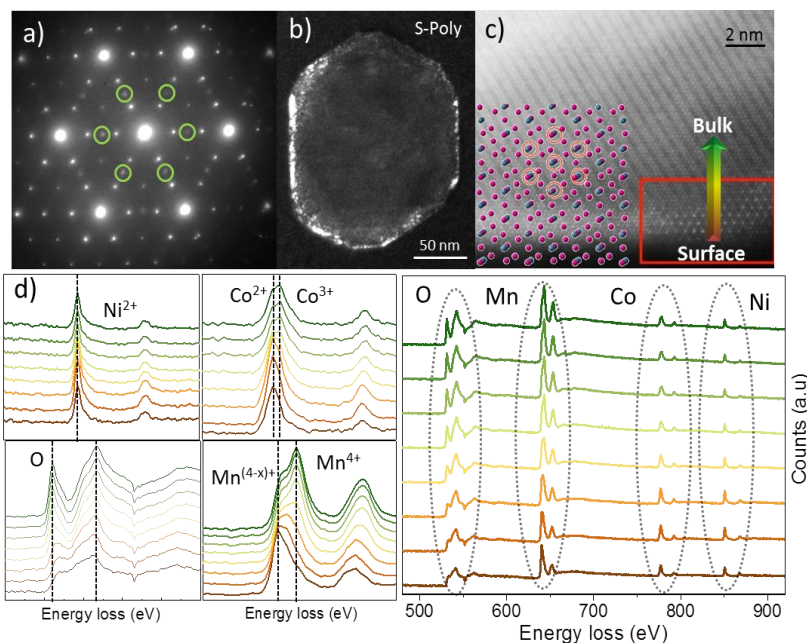


Figure 28. (a) Selected area electron diffraction pattern collected on a S-Poly crystal. (b) Contrast image taken with one of the reflections shown in green (a). (c) High-resolution high angle annular dark field (HAADF) scanning transmission electron microscopy image collected on the crystal sample. (d) Electron energy loss spectroscopy data collected from the surface-to-bulk region shown in the HAADF image in (c), with the expanded views shown on the left.

Patents/Publications/Presentations

Presentations

- 2016 Molecular Foundry Users Meeting, Berkeley, California (August 2016): “Crystal-Based Microscopy and Spectroscopy Diagnostics for Lithium-ion Battery Cathode Development,”; S. Kuppan, A. K. Shukla, and G. Chen. Invited.
- 2016 University of California (UC) Industry Battery Workshop, LBNL, Berkeley, California (September 29, 2016): “Advanced High-Energy Cathode Materials for Lithium-Ion Batteries”; W.-H. Kan, S. Kuppan, and G. Chen.

Task 5.2 – Interfacial Processes – Diagnostics (Robert Kostecki, Lawrence Berkeley National Laboratory)

Project Objective. The main task objective is to obtain detailed insight into the dynamic behavior of molecules, atoms, and electrons at electrode/electrolyte interfaces of high-voltage $\text{Li}[\text{Ni}_x\text{Mn}_y\text{Co}_z]\text{O}_2$ materials at a spatial resolution that corresponds to the size of basic chemical or structural and chemical building blocks. This project focuses on high Ni content NMC compositions such as 523 and 622, which are expected to achieve high discharge capacities even within conservative electrode potential limits. The aim of these studies is to unveil the structure and reactivity at hidden or buried interfaces and interphases that determine material, composite electrode and battery cell performance and failure modes. To accomplish these goals, novel far- and near-field optical multifunctional probes must be developed and deployed *in situ*. This work constitutes an integral part of the concerted effort within the BMR Program, and it attempts to establish clear connections between diagnostics, theory/modeling, materials synthesis, and cell development efforts.

Project Impact. This project provides better understanding of the underlying principles that govern the function and operation of battery materials, interfaces, and interphases, which is inextricably linked with successful implementation of high-energy density materials such as $\text{Li}[\text{Ni}_x\text{Mn}_y\text{Co}_z]\text{O}_2$ compounds (NMCs) that can cycle stably to high potentials and deliver $> 200 \text{ mAh/g}$ at Coulombic efficiency close to 100%. This task also involves development and application of novel innovative experimental methodologies to study and understand the basic function and mechanism of operation of materials, composite electrodes, and high-energy Li-ion battery systems for PHEV and EV applications.

Approach. The *in situ/ex situ* investigations of surface reconstruction into rock salt on NMC samples of different morphology and composition will be linked with investigations of interfacial reactivity toward organic electrolytes. Pristine and cycled NMC powders and electrodes will be probed using surface- and bulk-sensitive techniques, including Fourier transform infrared (FTIR), attenuated total reflectance (ATR)-FTIR, near-field IR, and Raman spectroscopy and microscopy and scanning probe microscopy to identify and characterize changes in structure and composition. The effect of electrolyte composition, additives, and protective coatings will be explored to determine the mechanism and kinetics of surface phenomena and implications for long-term electrochemical performance of NMC cathodes in high-energy Li-ion systems.

Out-Year Goals. The requirements for long-term stability of Li-ion batteries are extremely stringent and necessitate control of the chemistry at a wide variety of temporal and structural length scales. Progress toward identifying the most efficient mechanisms for electrical energy storage and the ideal material depends on a fundamental understanding of how battery materials function and what structural/electronic properties limit their performance. This project provides better understanding of the underlying principles that govern the function and operation of battery materials, interfaces, and interphases, which is inextricably linked with successful implementation of high energy density materials in Li-ion cells for PHEVs and EVs.

Collaborations. This project collaborates with Marca Doeff, Vincent Battaglia, Chunmei Ban, Vassilia Zorba, and Bryan D. McCloskey.

Milestones

1. Build and test binder- and carbon-free model NMC electrodes. (December 2015 – Complete)
2. Complete preliminary characterization of interfacial activity of the baseline NMC material in organic carbonate electrolytes. (Q3 – Complete)
3. Determine relationship between surface reconstruction and surface layer formation during cycling in NMC electrodes. (Q4 – Complete)
4. *Go/No-Go*: Demonstrate feasibility of *in situ* near-field FTIR microscopy and spectroscopy to study interfacial phenomena at Li-battery electrodes. *Criteria*: Stop development of near-field and LIBS techniques, if the experiments fail to deliver adequate sensitivity. (Q4 – Complete)

Progress Report

This quarter, the project exploited the exceptional spatial resolution (ca. 20 nm), surface sensitivity, and chemical selectivity of near-field FTIR microscopy and spectroscopy to identify individual chemical building blocks of the SEI film on a silicon model electrode. The project looked at the influence of LiBOB as an additive in the standard electrolyte on the SEI film chemical composition, morphology, and individual component distribution. LiBOB is an effective electrolyte additive known for its positive effect on interfacial properties of the anode in Li-ion batteries via formation of $\text{Li}_x\text{B}_y\text{C}_n\text{O}_{2n}$ ($n>3$) oligomers. $\text{Li}_2\text{C}_2\text{O}_4$ and $\text{Li}_x\text{B}_y\text{C}_n\text{O}_{2n}$ form and get incorporated in the SEI layer upon LiBOB electroreduction during initial cycles. These compounds can be used as spectroscopic markers to map SEI layer chemical composition because of their very distinguishable spectroscopic signature in IR that is easily identifiable by synchrotron infrared near-field spectroscopy (SINS). Varying LiBOB content in the electrolyte and probing the corresponding SEI films formed on Si with SINS in combination with other techniques can help to unravel the correlation between the function and chemical composition of an effective SEI layer. The samples were characterized by near-field IR spectroscopy using the Advanced Light Source Synchrotron (ALSS) beamline 5.4.1. Figure 29 shows conclusive SINS identification of $\text{Li}_2\text{C}_2\text{O}_4$ and $\text{Li}_x\text{B}_y\text{C}_n\text{O}_{2n}$ in the surface film on Si (111) wafer electrode swept to 1.5 and 0.5 V in 1 M LiPF_6 + 2% LiBOB in EC:DMC 1:2, by comparison to a standard average ATR-FTIR spectrum.

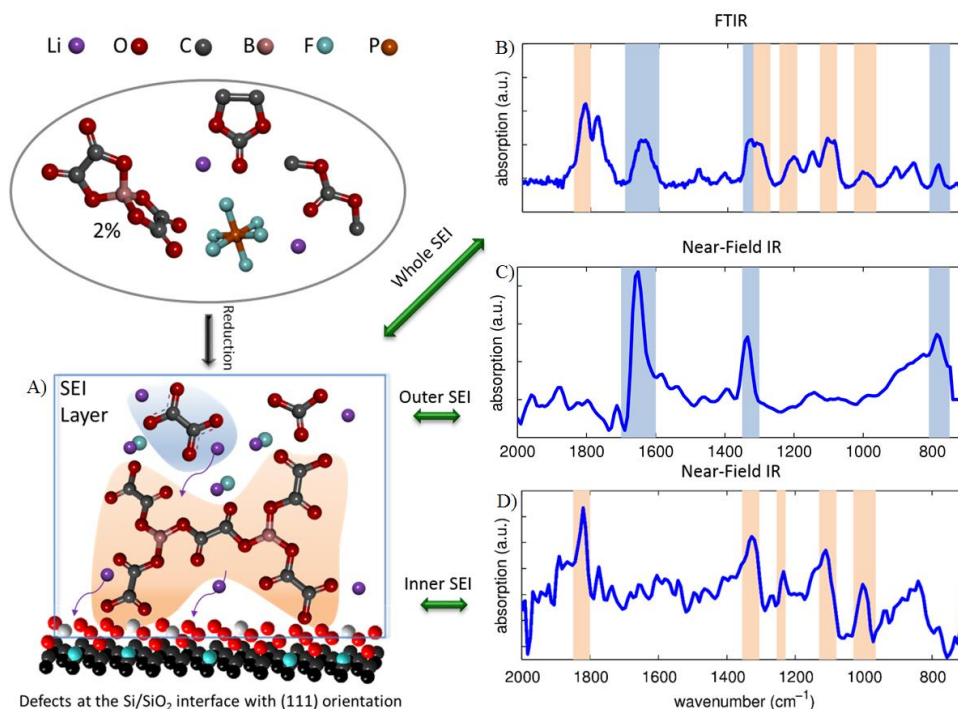


Figure 29. (a) Illustration of the SEI chemical composition on Si(111) electrode surface that was swept from open circuit potential to 0.5 V in 1 M LiPF_6 + 2% LiBOB, EC:DMC (1:1 wt.). (b) *Ex situ* attenuated total reflectance – Fourier transform infrared spectrum. (c) Synchrotron infrared near-field spectroscopy (SINS) spectrum of the same electrode. (d) SINS of the electrode swept to 1.5 V with signature absorption bands marked to show correspondence to far- and near-field IR spectra of $\text{Li}_x\text{B}_y\text{C}_n\text{O}_{2n}$.

The project was able to correlate for the first time the improved passivating properties of silicon in the presence of LiBOB to the formation and incorporation of $\text{Li}_x\text{B}_y\text{C}_n\text{O}_{2n}$ ($n>6$) in the inner part of the SEI layer. This completes efforts toward milestone 4. Further investigations are under way to evaluate the influence of rock salt surface layer formation on the battery performance in high Ni content NMC based battery systems.

Task 5.3 – Advanced *In Situ* Diagnostic Techniques for Battery Materials (Xiao-Qing Yang and Xiqian Yu, Brookhaven National Laboratory)

Project Objective. The primary project objective is to develop new advanced *in situ* material characterization techniques and to apply these techniques to support development of new cathode and anode materials for the next generation of Li-ion batteries for PHEVs. To meet the challenges of powering the PHEV, Li-ion batteries with high energy and power density, low cost, good abuse tolerance, and long calendar and cycle life must be developed.

Project Impact. The VTO Multi Year Program Plan describes the goals for battery: “Specifically, lower-cost, abuse-tolerant batteries with higher energy density, higher power, better low-temperature operation, and longer lifetimes are needed for the development of the next-generation of HEVs, PHEVs, and EVs.” The knowledge gained from diagnostic studies through this project will help U.S. industries develop new materials and processes for new generation Li-ion batteries in the effort to reach these VTO goals.

Approach. This project will use the combined synchrotron based *in situ* X-ray techniques (XRD, and hard and soft XAS) with other imaging and spectroscopic tools such as HRTEM and MS to study the mechanisms governing the performance of electrode materials and provide guidance for new material and new technology development regarding Li-ion battery systems.

Out-Year Goals. Complete the first-stage development of diagnostic technique to study kinetic property of advanced Li-ion electrode materials using time-resolved XRD and XAS (TR-XRD, TR-XAS) combined with STEM imaging and TXM. Apply this technique to study the structural changes of new cathode materials including various NCM and high-voltage spinel materials during high-rate cycling.

Collaborations. The BNL team will work closely with material synthesis groups at ANL (Drs. Thackeray and Amine) for the high-energy composite; and at PNNL for the Si-based anode materials. Such interaction between the diagnostic team at BNL and synthesis groups of these other BMR members will catalyze innovative design and synthesis of advanced cathode and anode materials. The project will also collaborate with industrial partners at General Motors and Johnson Controls, as well as with international collaborators.

Milestones

1. Complete the thermal stability studies of Fe substituted high-voltage spinel cathode materials $\text{LiNi}_{1/3}\text{Mn}_{4/3}\text{Fe}_{1/3}\text{O}_4$ in comparison with unsubstituted $\text{LiNi}_{0.5}\text{Mn}_{1.5}\text{O}_4$ using *in situ* TR-XRD and MS techniques. (December 2015 – Complete)
2. Complete the energy resolved TXM investigation on new concentration gradient NCM cathode sample particles in a noninvasive manner with 3D reconstructed by images through tomography scans to study the 3D Ni, Co, and Mn elemental distribution from surface to the bulk. (March 2016 – Complete)
3. Complete the *in situ* TR-XRD studies of the structural changes of $\text{Li}_{1-x}\text{Ni}_{1/3}\text{Co}_{1/3}\text{Mn}_{1/3}\text{O}_2$ from $x=0$ to $x=0.7$ during high-rate charge process at different C rates at 10C, 30C, and 60C. (June 2016 – Complete)
4. Complete the *in situ* TR-XAS of $\text{Li}_{1-x}\text{Ni}_{1/3}\text{Co}_{1/3}\text{Mn}_{1/3}\text{O}_2$ cathode material at Ni, Co, and Mn K-edge during 30C high-rate charge. (September 2016 – Complete)

Progress Report

This quarter, milestone 4 was completed. BNL has been focused on the studies of *in situ* TR-XAS on a widely used $\text{LiNi}_{1/3}\text{Mn}_{1/3}\text{Co}_{1/3}\text{O}_2$ (NMC) cathode material during high-rate cycling at 30C.

The valence state and local environment of each transition metal element in NMC are monitored by *in situ* quick X-ray absorption technique. Figure 30a-c shows the changes of the XANES at the Ni, Co and Mn K-edges during 30C charge, respectively. The K-edge of Ni shifts continuously to higher energy, indicating the oxidation of Ni ions from Ni^{2+} to Ni^{4+} during the charging process. In contrast, the K-edges of Co and Mn exhibit almost no energy shift. The Co and Mn K-edge features change shape, indicating that the local environment changes around Co and Mn ions, but Co and Mn do not contribute much to the charge compensation. The same results are obtained at 1C and 10C rates. These results suggest that charge compensation during charging mainly arises from Ni. The results of these studies were presented in a paper published in *Advanced Energy Materials*.

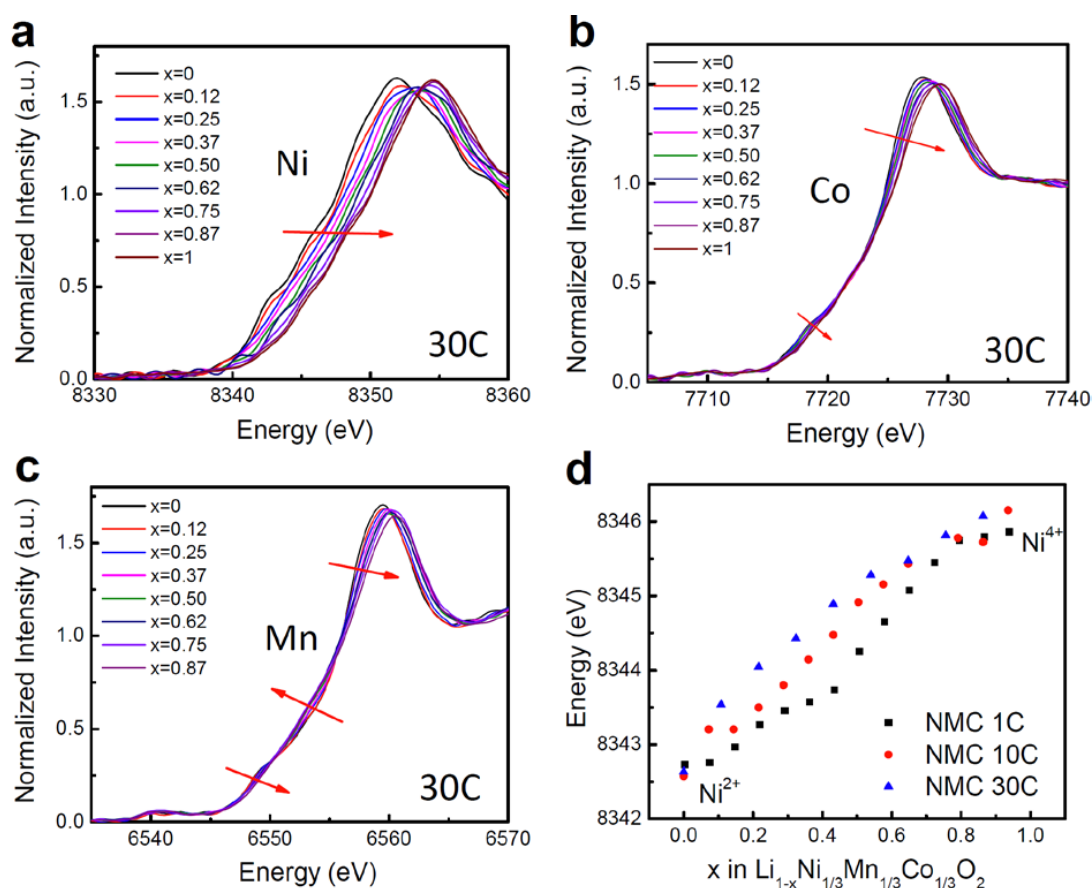


Figure 30. *In situ* quick X-ray absorption spectroscopy of NMC during the first charge. The X-ray absorption near-edge spectroscopy results of NMC at (a) Ni, (b) Co, and (c) Mn K-edges during 30C charge, respectively. (d) The Ni K-edge energy shift as a function of nominal lithium content x in NMC during initial charge process at the current rates of 1C, 10C and 30C.

Patents/Publications/Presentations

Publications

- Zhou, Jigang, and Jian Wang, Jeffrey Cutler, Enyuan Hu, and Xiao-Qing Yang. “Imaging the Surface Morphology, Chemistry and Conductivity of $\text{LiNi}_{1/3}\text{Fe}_{1/3}\text{Mn}_{4/3}\text{O}_4$ Crystalline Facets using Scanning Transmission X-ray Microscopy.” *Phys. Chem. Chem. Phys.* 18 (2016): 22789-22793. doi: 10.1039/C6CP03511F (web publication date, July 2016).
- Zhou, Yong-Ning, and Ji-Li Yue, Enyuan Hu, Hong Li, Lin Gu, Kyung-Wan Nam, Seong-Min Bak, Xiqian Yu, Jue Liu, Jianming Bai, Eric Dooryhee, Zheng-Wen Fu, and Xiao-Qing Yang. “High-Rate Charging Induced Intermediate Phases and Structural Changes of Layer-Structured Cathode for Lithium-Ion Batteries.” *Adv. Energy Mater.* (August 2016). doi: 10.1002/aenm.201600597.

Presentation

- Seminar at Energy Sciences Institute, Yale University – New Haven, New Haven, Connecticut (September 14, 2016): “Using Synchrotron Based *In Situ* X-ray Diffraction and Absorption and TXM Techniques to Study the New Electrode Materials for Next Generation of Batteries”; Enyuan Hu, Xiao-Qing Yang*, Xiqian Yu, Yongning Zhou, Seong-Min Bak, Hung-sui Lee, Zhaoxiang Wang, and Yijin Liu. Invited.

Task 5.4 – NMR and Pulse Field Gradient Studies of SEI and Electrode Structure (Clare Grey, Cambridge University)

Project Objective. The formation of a stable SEI is critical to the long-term performance of a battery, since the continued growth of the SEI on cycling/aging results in capacity fade (due to lithium consumption) and reduced rate performance due to increased interfacial resistance. Although arguably a (largely) solved problem with graphitic anodes/lower voltage cathodes, this is not the case for newer, much higher capacity anodes such as silicon, which suffer from large volume expansions on lithiation, and for cathodes operating above 4.3 V. Thus, it is essential to identify how to design a stable SEI. The objectives are to identify major SEI components, and their spatial proximity, and how they change with cycling. SEI formation on silicon versus graphite and high-voltage cathodes will be contrasted. Li⁺ diffusivity in particles and composite electrodes will be correlated with rate. The SEI study will be complemented by investigations of local structural changes of high-voltage/high-capacity electrodes on cycling.

Project Impact. The first impact of this project will be an improved, molecular based understanding of the surface passivation (SEI) layers that form on electrode materials, which are critical to the operation of the battery. Second, the project will provide direct evidence for how additives to the electrolyte modify the SEI. Third, it will provide insight to guide and optimize the design of more stable SEIs on electrodes beyond LiCoO₂/graphite.

Out-Year Goals. The project goals are to identify the major components of the SEI as a function of state of charge and cycle number on different forms of silicon. The project will determine how the surface oxide coating affects the SEI structure and will establish how the SEI on silicon differs from that on graphite and high-voltage cathodes. The project will determine how the additives that have been shown to improve SEI stability affect the SEI structure and will explore the effect of different additives that react directly with exposed fresh silicon surfaces on SEI structure. Via this program, the project will develop new NMR-based methods for identifying different components in the SEI and their spatial proximities within the SEI, which will be broadly applicable to the study of SEI formation on a much wider range of electrodes. These studies will be complemented by studies of electrode bulk and surface structure to develop a fuller model with which to describe how these electrodes function.

Collaborations. This project collaborates with B. Lucht (Rhode Island); J. Cabana, (University of Illinois at Chicago); G. Chen and K. Persson (LBNL); S. Whittingham (Binghamton); P. Bruce (St. Andrews); S. Hoffman and A. Morris (Cambridge); and P. Shearing (University College London).

Milestones

1. Identify the major carbon-containing break-down products that form on graphene platelets. (December 2015 – Complete; paper being written.)
2. *Go/No-Go:* Establish the difference between extrinsic and P-doped silicon nanowires. *Criteria:* If no difference in performance of P-doped wires established after the first cycle, terminate project. (March 2016 – Complete. No clear differences under conditions used to date. In process of terminating project and writing results.)
3. Complete SEI study of silicon nanoparticles by NMR spectroscopy. (June 2016 – Complete) Develop NMR methodology to examine cathode SEI. (Ongoing)
4. Produce first optimized coating for Si electrode. (September 2016 – Ongoing; initial coatings produced)

Progress Report

In collaboration with Prof. B. Lucht (U. Rhode Island), the project directly synthesized the reduction products of fluoroethylene carbonate (FEC) and vinylene carbonate (VC) via lithium naphthalene reduction to (a) identify which products are formed and (b) provide spectral fingerprints of these species, which can then be used to search for/identify similar products in the SEI formed in the presence of these additives. (Deuterated lithium naphthalene was used to separate decomposition products from the reductant in the ^1H - ^{13}C cross-polarization (CP) solid-state nuclear magnetic resonance (ssNMR) experiments).

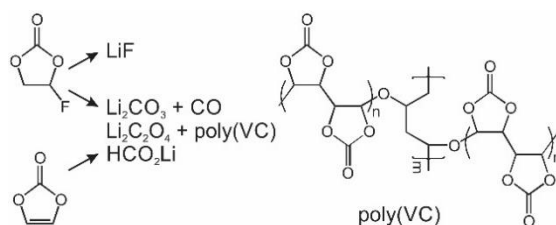


Figure 31. Proposed fluoroethylene carbonate and vinylene carbonate (VC) reduction products and possible structure for crosslinking site of poly(VC).

Analysis of the resulting solid precipitates formed from both VC and FEC and gas evolution with multinuclear ssNMR, XPS, FTIR, and gas chromatography mass spectrometry (GC-MS) reveals that both FEC and VC decomposition products include HCO_2Li , $\text{Li}_2\text{C}_2\text{O}_4$, Li_2CO_3 , and polymerized VC (Figure 31), albeit in different relative quantities. For example, in the case of VC reduction (Figure 32b/d/f), greater quantities of

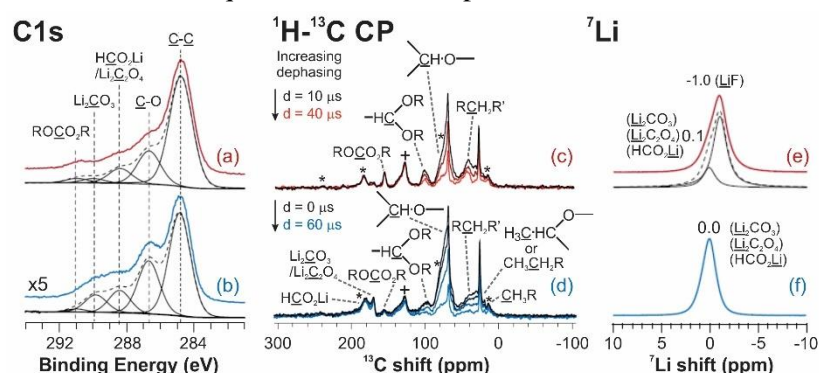


Figure 32. C1s X-ray photoelectron spectroscopy spectra (a, b), ^1H - ^{13}C CP dipolar dephasing ssNMR (c, d, MAS = 10 kHz), and ^7Li single pulse ssNMR (e, f, MAS = 60 kHz) of fluoroethylene carbonate (red) and vinylene carbonate (blue) precipitates obtained after reduction with deuterated naphthalene. In (c) and (d), asterisks indicate spinning sidebands and crosses represent deuterated naphthalene.

additional fluorine environments, other than LiF , detected by ^{19}F ssNMR or F1s XPS (Figure 33). This is contrary to previous reports where fluorinated organic products are proposed.

FEC and VC are used in higher (FEC) and lower (VC) concentrations in the base electrolytes of lithium-ion batteries. The findings suggest that the different relative ratios of the inorganic and organic reduction products formed by their decomposition are relevant to the chemical composition and morphology of the SEI formed in their presence and likely impact Li^+ transport in systems containing FEC and VC additives. Experiments are now in progress to compare these reduction products with those found in the SEIs formed in Si anodes with FEC additives.

- (1) Zhang, B.; and M. Metzger, S. Solchenbach, M. Payne, S. Meini, H. A. Gasteiger, A. Garsuch, B. L. Lucht. *J. Phys. Chem. C* 119 (2015): 11337.

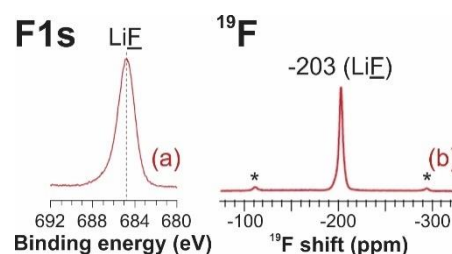


Figure 33. F1s X-ray photoelectron spectroscopy spectrum (a) and ^{19}F Hahn echo ssNMR (b) of fluoroethylene carbonate precipitates after reduction with deuterated naphthalene.

Patents/Publications/Presentations

Publications

- R. J. Clément, J. Billaud, A. R. Armstrong, G. Singh, T. Rojo, P. G. Bruce, and C. P. Grey. “Structurally Stable Mg-Doped $P2\text{-Na}_{2/3}\text{Mn}_{1-y}\text{Mg}_y\text{O}_2$ Sodium-Ion Battery Cathodes with High Rate Performance: Insights from Electrochemical, NMR, and Diffraction Studies.” *Energy Environ. Sci.* 9 (2016): 3240-3251.
- A. L. Michan, B. S. Parimalam, M. Leskes, R. N. Kerber, T. Yoon, C. P. Grey, B. L. Lucht. “Fluoroethylene Carbonate and Vinylene Carbonate Reduction: Understanding Lithium-Ion Battery Electrolyte Additives and Solid Electrolyte Interphase Formation.” *Chem. Mater.* Accepted. doi: 10.1021/acs.chemmater.6b02282 (2016).

Presentations

- Euromar, Aarhus, Denmark (July 2016)
- Smarter Conference, Bayreuth, Germany (September 2016)
- Challenges and Prospects for Solid State Chemistry, Seville, Spain (September 2016)
- PNMR ITN meeting, Venice, Italy (September 2016)

Task 5.5 – Optimization of Ion Transport in High-Energy Composite Cathodes (Shirley Meng, UC San Diego)

Project Objective. This project aims to probe and control the atomic-level kinetic processes that govern the performance limitations (rate capability and voltage stability) in a class of high-energy composite electrodes. A systematic study with a powerful suite of analytical tools [including atomic resolution STEM (a-STEM) and EELS, neutron, XPS and first principles (FP) computation] will elucidate approaches to optimize ion transport. Ultimately, this will hone in on the optimum bulk compositions and surface characteristics to improve the mechanistic rate and cycling performance of high-energy composite electrodes. Moreover, it aims to develop the large-scale synthesis efforts to produce materials with consistent performance. The surface-sensitive characterization tools will be extended to diagnose various silicon anode types.

Project Impact. If successful, this research will provide a major breakthrough in commercial applications of the class of high energy density cathode material for Li-ion batteries. Additionally, it will provide in-depth understanding of the role of surface modifications and bulk substitution in the high-voltage composite materials. The diagnostic tools developed here can also be leveraged to study a wide variety of cathode and anode materials for rechargeable batteries.

Approach. This unique approach combines STEM/EELS, XPS, and *ab initio* computation as diagnostic tools for surface and interface characterization. This allows for rapid identification of surface interphases that provide surface instability or stability in various types of electrode materials including both high-voltage cathodes and low-voltage anodes. Neutron enables the characterization of bulk material properties to enhance and further optimize high-energy electrode materials.

Out-Year Goals. The goal is to control and optimize Li-ion transport, TM migration, and oxygen activity in the high-energy composite cathodes and to optimize electrode/electrolyte interface in silicon anodes so that their power performance and cycle life can be significantly improved.

Collaborations. This work funds collaborations on EELS (Miaofang Chi, ORNL); molecular layer deposition (MLD, Chunmei Ban, NREL); neutron diffraction (Ken An, ORNL); soft XAS (Marca Doeff, LBNL); and XPS, time-of-flight SIMS (TOF-SIMS) characterization (Keith Stevenson, UT Austin). It supports collaborative work with Zhaoping Liu and Yonggao Xia at Ningbo Institute of Materials Technology and Engineering China.

Milestones

1. Quantify the SEI characteristics of MLD coated silicon anode on long cycling with a combination of STEM/EELS and XPS. (March 2016 – Complete)
2. Complete investigation of coating and morphology control for Li-rich, Mn-rich, layered oxides. (June 2016 – Complete)
3. Obtain the optimum nanoscale uniform surface oxygen vacancy amount in Li-rich layered oxides when charged up to 4.8 V (or 5.0 V). (September 2016 – Complete)
4. Apply the optimum surface modification and electrolyte additives for silicon/carbon anode with more than 87% first-cycle capacity retention and greater than 99.9% Coulombic efficiency. (On schedule)

Progress Report

Probing the surface transition metal oxidation state and oxygen activities of Li-rich layered oxides

X-ray photoelectron spectroscopy is a powerful surface sensitive characterization tool that can determine chemical species and oxidation state of the transition metals. To study the surface chemistry including redox process of transition metal and oxygen activities of Li-rich oxides, XPS data were collected from electrodes at different charge/discharge states. Figure 34 shows the resulting XPS spectra for the Ni 3p, Mn 3p, and O 1s region. The pristine Ni 3p shows a binding energy of ~67.6 eV. After charged to 4.4 V, where the $\text{Ni}^{2+}/\text{Ni}^{4+}$ redox occurs, the peak shifts to a higher binding energy of ~68.6 eV. When further charged to 4.8V, the peak slightly shifts back to a lower binding energy, which is caused by the oxygen oxidation at high voltage. The peak shifts back to 67.6 eV when discharged to 3.3 V and remains unchanged upon full discharge. The Mn 3p region shows a major peak at 49.8 eV corresponding to Mn^{4+} , a minor peak at 48.6 eV ascribed to Mn^{3+} . At pristine state, not all the Mn ions are in Mn^{4+} , indicating that Mn on the surface is reduced to some extent after contact with electrolyte. During the charging/discharging process, Mn ions experience $\text{Mn}^{3+}/\text{Mn}^{4+}$ redox reaction, contributing certain amount of capacity. For the O 1s spectra, at pristine state, the two main peaks at ~529.1 and ~531.5 eV are assigned to O^{2-} anions in the crystal lattice and carbonate species on the surface, respectively. The minor component at ~533.0 eV is ascribed to adsorbed species from the electrolyte. Another peak component at ~530.5 eV, which is associated with peroxo-like species (O_2)ⁿ⁻ or undercoordinated oxygen atoms, is dramatically increased after charge to high voltage (larger than 4.4 V). More interestingly, this component corresponding to peroxo-like species gradually reduced back to the pristine state after one cycle. This oxygen activity observed by XPS clearly indicates that oxygen anion redox reversibly contributes to the overall capacity of Li-rich layered oxides.

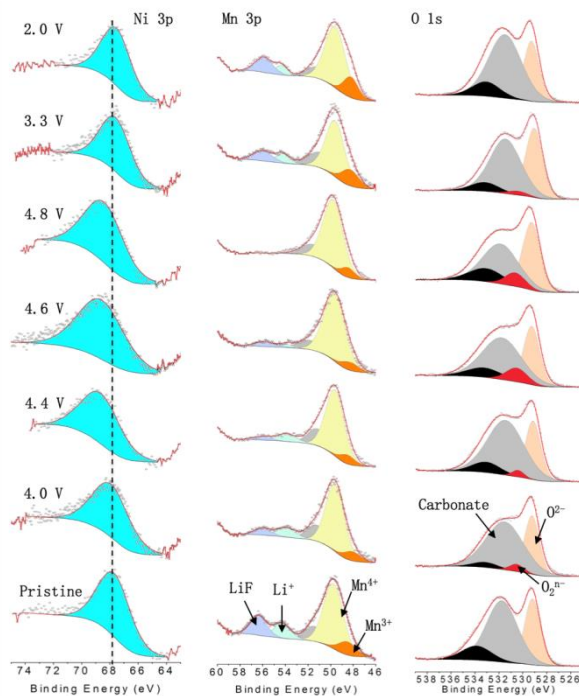


Figure 34. (upper) First cycle voltage profile of Li-rich material, where the voltage range is 2.0 – 4.8V, at C/20 = 12.5 mA g⁻¹. (lower) Ni 3p, Mn 3p, and O 1s X-ray photoelectron spectroscopy spectra at various charge/discharge states in the first cycle.

Aluminum hydroquinone coated Si nanoparticles using MLD

One of the successful strategies for stabilizing the Si surface chemistry has been surface modification. Herein, Si surface modification has been applied via MLD of alucone to improve the interfacial chemistry of Si anode upon cycling. The electrochemical performance of the coated Si is shown in Figure 35, which does not demonstrate significant changes in comparison with the bare Si anode. The coated and the bare Si electrodes cycled in $\text{LiPF}_6/\text{EC}/\text{DEC}$ at C/10 within the potential window of 0.05-1V. The major difference of this work from the literature is that it uses CMC-based binder. The alucone coating may have more significant effect on the electrode made from the PVDF type of binder than the electrode made from CMC binder. This indicates the importance of understanding the effect of surface coating on binder chemistry.

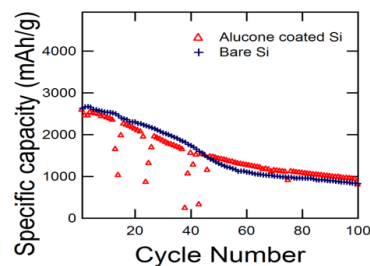


Figure 35. Cycling performance of Si coated compared to the bare Si.

Patents/Publications/Presentations

Patent

- Meng, Y. S., and M. Zhang, H. D. Liu, C. Fang, D. Qian. “Lithium Excess Cathode Material and Co-Precipitation Formation Method.” Patent Provisional, 2016.

Publication

- Sina, M., and J. Alvarado, H. Shobukawa, K. W. Schroder, K. Stevenson, and Y.S. Meng. “Direct Visualization of the Solid Electrolyte Interphase and Its Effects on Silicon Electrochemical Performance.” *Advanced Materials Interfaces* (2016). doi: 10.1002/admi.201600438.

Presentation

- Microscopy and Microanalysis Meeting, Columbus, Ohio (2016): “Morphological and Chemical Evolution of Silicon Nanocomposite during Cycling”; M. Sina, J. Alvarado, H. Shobukawa, and Y.S. Meng. Invited.

Task 5.6 – Analysis of Film Formation Chemistry on Silicon Anodes by Advanced *In Situ* and *Operando* Vibrational Spectroscopy

(Gabor Somorjai, UC Berkeley; Phil Ross, Lawrence Berkeley National Laboratory)

Project Objective. Understand the composition, structure, and formation/degradation mechanisms of the SEI on the surfaces of silicon anodes during charge/discharge cycles by applying advanced *in situ* vibrational spectroscopies. Determine how the properties of the SEI contribute to failure of silicon anodes in Li-ion batteries in vehicular applications. Use this understanding to develop electrolyte additives and/or surface modification methods to improve Si anode capacity loss and cycling behavior.

Project Impact. A high-capacity alternative to graphitic carbon anodes is silicon, which stores 3.75 lithium per silicon versus 1 lithium per 6 carbon, yielding a theoretical capacity of 4008 mAh/g versus 372 mAh/g for carbon. But silicon anodes suffer from large first-cycle irreversible capacity loss and continued parasitic capacity loss on cycling, leading to battery failure. Electrolyte additives and/or surface modification developed from new understanding of failure modes will be applied to reduce irreversible capacity loss, and to improve long-term stability and cyclability of silicon anodes for vehicular applications.

Approach. Model silicon anode materials including single crystals, e-beam deposited polycrystalline films, and nanostructures are studied using baseline electrolyte and promising electrolyte variations. A combination of *in situ* and *operando* FTIR, Sum Frequency Generation (SFG), and ultraviolet Raman vibrational spectroscopies are used to directly monitor the composition and structure of electrolyte reduction compounds formed on the silicon anodes. Pre-natal and post-mortem chemical composition is identified using XPS. The silicon films and nanostructures are imaged using SEM.

Out-Year Goals. Extend study of interfacial processes with advanced vibrational spectroscopies to high-voltage oxide cathode materials. The particular oxide to study will be chosen based on materials of interest and availability of the material in a form suitable for these studies (for example, sufficiently large crystals or sufficiently smooth/reflective thin films). The effect of electrolyte composition, electrolyte additives, and surface coatings will be determined, and new strategies for improving cycle life developed.

Milestones

1. Modifying the SFG apparatus to obtain high-resolution SFG spectra further allowing particles, thin film, and microstructures of silicon and the electrolyte interface research. (October 2015 – Complete)
2. Performing phase-specific SFG measurement under constant and dynamic potentials (-0.01 V, 0.5 V, and 1.0 V vs. Li/Li⁺) of 1 M LiPF₆ in EC without DEC to probe the SEI formed on amorphous silicon anodes. (January 2016 – Complete)
3. *Go/No-Go*: Can this task distinguish between the various SEI products in the C-H stretch mode (2800 – 3200 cm⁻¹)? If not, proceed to conventional C-O region (1700 – 1800 cm⁻¹). (June 2016 – Complete)
4. Performing fs-SFG measurement in tandem with cyclic voltammetry (CV, potential sweep) to find the ring opening kinetics of EC. (September 2016 – Ongoing)

Progress Report

The project has synthesized the following electrolyte solutions: 1.0 M LiClO₄ in EC, 1.0 M LiClO₄ : in FEC and their mixtures EC:FEC in a 9:1 and 7:3 w/w ratio to investigate the effect of fluorinated additives (FEC) on chemical composition of the SEI and surface ordering of electrolytes at electrolyte/a-Si interface. The main conclusion this quarter is that FEC induces ordering of the adsorbed EC on a-Si anode. The results suggest that FEC induces a tighter packing of EC at the anode surface, consequently yielding a better SEI in Li-ion batteries. By tuning the SFG polarization configuration to *ssp* the project has enhanced the SF signal sensitivity to adsorbates with a perpendicular dipole orientation in respect to the electrode surface. Figure 36 presents the a-Si / EC and EC:FEC based electrolyte interphase at open circuit potential (OCP) at the C=O stretch range. No prominent SFG features corresponding to FEC were detected from the interface. The main broad peak of EC (black curve) is ~ 1820 cm⁻¹ (fundamental stretching, yellow bar) with a shoulder around 1780 cm⁻¹ (Fermi resonance, green bar). Noticeably, upon adding FEC, for example, EC:FEC 9:1 (red curve), the Fermi resonance at 1780 cm⁻¹ intensifies. This trend continues with the addition of more FEC to form EC:FEC 7:3 (blue curve). This trend suggests a solid-like EC packing at the anode surface presumably due to better dipole-dipole stacking. Figure 37 shows the trend of EC ring opening frequencies (s-CH₂, ~ 2880 cm⁻¹) arising from EC:FEC 9:1 (w/w) mixture in contact with a-Si anode after the first lithiation / delithiation (Figure 37a) and the second cycle (Figure 37b) at the C-H stretch region. By dividing the SFG spectra (SFG_{GA}/SFG_{OCP}), the project emphasizes the appearance (or trend) of vibrational peaks that are less clear in a regular SFG scan since in most cases the SFG from the a-Si/SEI interferes with the SFG generated from the Si substrate. In Figure 37a, the shoulder around 2880 cm⁻¹ (s-CH₂) suggests that EC undergoes a ring opening, but still its products are tightly packed upon (black dots). On discharge (open red squares), most of the EC molecules are converted to linear moieties such as -OCH₂CH₂O- expressed by the major peak at 2950 cm⁻¹. In Figure 37b, no major trend features are detectable and so it is presumed that the SEI first layer consists of mainly R-OCH₂-CH₂O-R'. In conclusion, the project observes that FEC on a-Si induces better ordering of the adsorbed EC on the silicon anode. The C-H stretch range suggests that the SEI does not change in chemistry after the first delithiation, but maintains a tightly packed layer of linear products.

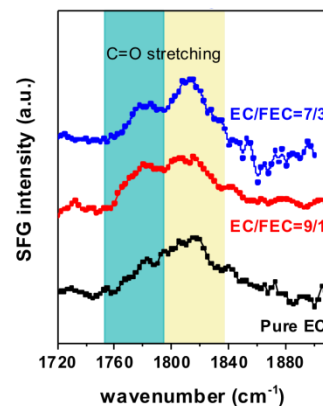


Figure 36. The sum frequency generation (SFG, *ssp*) signal at the C=O (carbonyl) stretch at open circuit potential of 1 M LiClO₄ in EC, and EC : FEC mixtures of 9:1 and 7:3 (w/w) in contact with a-Si anode at open circuit potential.

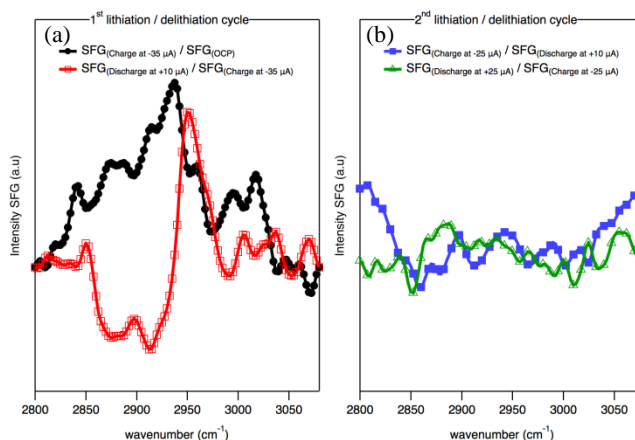


Figure 37. The evolution of sum frequency generation (SFG, *ssp*) signal associated with EC:FEC (9:1, w/w) in contact with a-Si (s-CH₂) vibrations under reaction conditions by dividing the SFG spectra by their former potentials.

Patents/Publications/Presentations

Publication

- “Fluoroethylene Carbonate Aligns Ethylene Carbonate on Amorphous Silicon Anodes to Produce Better Solid Electrolyte Interphase as Probed by Sum Frequency Generation Vibrational Spectroscopy under Reaction Conditions”; in preparation.

Task 5.7 – Microscopy Investigation on the Fading Mechanism of Electrode Materials (Chongmin Wang, Pacific Northwest National Laboratory)

Project Objective. The overall objective is to develop low-cost, high-energy cathode materials with long cycle life. This part is focused on microscopy investigation on the fading mechanism of the electrode materials. The focus will be on using *ex situ*, *in situ*, and *operando* HR-TEM and spectroscopy to probe the structural evolution of electrodes and interfaces between the electrode and electrolyte and correlate this structural and chemical evolution with battery performance.

Project Impact. Both *ex situ* and *in situ* TEM have been demonstrated to be critical for probing the structure and chemistry of electrode and SEI layer. Recently, this task developed new *operando* characterization tools to characterize SEI formation and electrode/electrolyte interaction using a practical electrolyte, which is critical for making new breakthroughs in the battery field. The success of this work will increase the energy density of Li-ion batteries and accelerate market acceptance of EV, especially for PHEV required by the EV Everywhere Grand Challenge proposed by the DOE/EERE.

Approach. Extend and enhance the unique *ex situ* and *in situ* TEM methods for probing the structure of Li-ion batteries, especially for developing a biasing liquid electrochemical cell that uses a real electrolyte in a nano-battery configuration. Use various microscopic techniques, including *ex situ*, *in situ*, and especially the *operando* TEM system, to study the fading mechanism of electrode materials in batteries. This project will be closely integrated with other research and development efforts on high-capacity cathode and anode projects in the BMR Program to (1) discover the origins of voltage and capacity fading in high-capacity layered cathodes and (2) provide guidance for overcoming barriers to long cycle stability of electrode materials.

Out-Year Goals. The out-year goals are as follows:

- Multi-scale (ranging from atomic scale to meso-scale) *ex situ/in situ* and *operando* TEM investigation of failure mechanisms for energy-storage materials and devices. Atomic-level *in situ* TEM and STEM imaging to help develop a fundamental understanding of electrochemical energy storage processes and kinetics of electrodes.
- Extension of the *in situ* TEM capability for energy storage technology beyond lithium ions, such as Li-S, Li-air, Li-metal, sodium ions, and multi-valence ions.

Collaborations. The project is collaborating with the following PIs: Michael M. Thackeray and Khalil Amine (ANL); Chunmei Ban (NREL); Donghai Wang (Pennsylvania State University); Arumugam Manthiram (UT Austin); Guoying Chen, Wei Tong, and Gao Liu (LBNL); Yi Cui (Stanford University); Jason Zhang and Jun Liu (PNNL); and Xingcheng Xiao (GM).

Milestones

1. Complete multi-scale quantitative atomic level mapping to identify the behavior of Co, Ni, and Mn in NCM during battery charge/discharge. (March 2016 – Complete)
2. Complete quantitative measurement of structural/chemical evolution of modified-composition NCM cathode during cycling of battery. (June 2016 – Complete)
3. Complete the correlation between structure stability and charge voltage of NCM for optimized charge voltage. (September 2016 – Complete)

Progress Report

This work combines *in situ* TEM experiment and chemomechanical modeling to study the electrochemically induced swelling of a-Si nanotubes with different thicknesses of surface SiO_x layers. No inward expansion occurs at the inner surface during lithiation of a-Si nanotubes with native oxides. In contrast, inward expansion can be induced by increasing the thickness of SiO_x on the outer surface, thus reducing the overall outward swelling of the lithiated nanotube. The chemomechanical modeling reveals the mechanical confinement effects in lithiated a-Si nanotubes with and without SiO_x coatings. This work not only provides insights into the degradation of nanotube anodes with surface coatings but also sheds light onto the optimal design of anode materials based on hollow structure for high-performance lithium-ion batteries.

During the past few years, considerable efforts have been made to mitigate the mechanical degradation of Si anodes by using nanostructures, nanocomposites, and surface coatings. In these engineered Si anodes, open space or flexible matrix (for example, carbon nanofiber) was introduced to accommodate the lithiation-induced large volume changes. Surface coatings (for example, SiO_2 , Al_2O_3 , TiO_2 , and carbon) were also often applied to alleviate the mechanical degradation and/or improve the conductivity and surface stability of Si anodes. Recently, Si-based anodes with hollow structures, including nanotubes, porous nanowires, and nanoparticles, have attracted great interest in development of high-performance lithium-ion batteries. The free space inside these hollow structures is expected to accommodate the volume change and thus reduce the outward expansion, thereby mitigating the degradation of both Si nanostructures and SEI. However, the actual morphological changes and degradation of these hollow Si nanostructures during electrochemical cycling remain largely unexplored. On the other hand, surface coatings have been widely applied to hollow Si nanostructures for constraining the volume expansion and/or serving as artificial SEIs. Among the various coatings, silicon oxide (SiO_x) has gained considerable attention for Si-based anodes due to easy processing via thermal treatment. In principle, the SiO_x coating can mechanically confine the outward expansion of Si-based hollow structures and reduce the fracture of SEIs, leading to improved battery performance. However, it is still unclear to what degree the swelling of Si-based hollow nanostructures can be confined by the surface SiO_x layers and whether the lithiation mechanism of Si nanostructures remains unchanged with the application of surface coatings. To address these questions, the a-Si nanotubes with surface SiO_x layers represent a clean system to study the effect of SiO_x coatings.

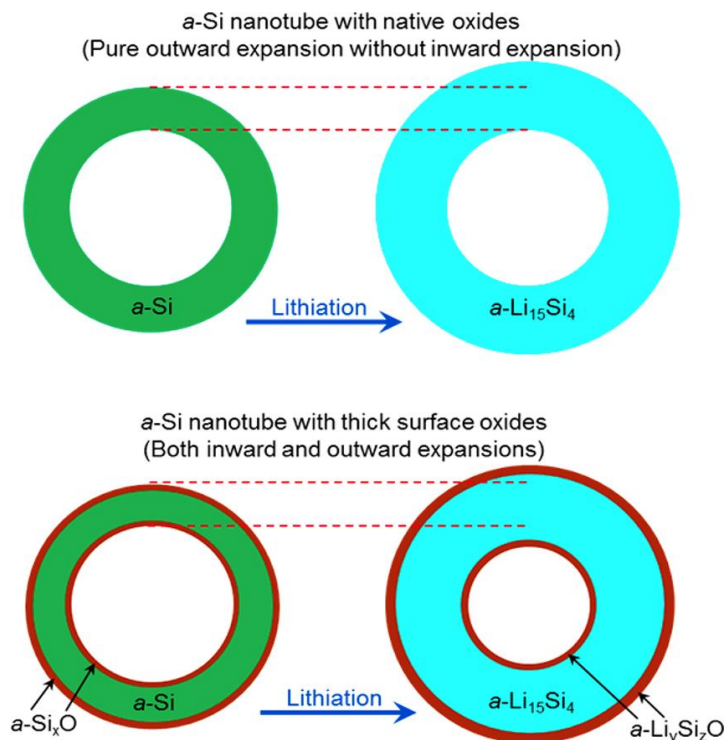


Figure 38. Schematic drawing to illustrate the effect of the thickness of the silicon oxide layer at silicon nanotube on the lithiation behavior of the tube. A tube with native oxide layer only expands outward when lithiated, while with increasing oxide layer thickness at outside well, it begins to expand inward, indicating the volume change of Si nanotube can be controlled by tailoring the oxide layer thickness on the walls of both inside and outside.

The *in situ* TEM experiments have revealed the detailed lithiation behavior of individual a-Si nanotubes with different thicknesses of surface oxide layers. The real-time, high-resolution imaging enables a precise measurement of the geometrical changes (with the nanometer resolution) during lithiation of a-Si nanotubes. Our results unambiguously show that outward expansion at the outer surface of lithiated a-Si nanotubes can be effectively confined by increasing the thickness of the outer SiO_x coating, while minimizing the thickness of the inner SiO_x coating can facilitate a more effective confinement by the outer SiO_x coating. Moreover, a high mechanical stability of lithiated SiO_x (that is, no cracking after full lithiation) could avoid the repeated growth of SEI layers, thereby enhancing the cycle performance of Si nanotube electrodes.

Patents/Publications/Presentations

Publications

- Wang, Jiangwei, and Hao Luo, Yang Liu, Yang He, Feifei Fan, Ze Zhang, Scott X. Mao, Chongmin Wang, and Ting Zhu. “Tuning the Outward to Inward Swelling in Lithiated Silicon Nanotubes via Surface Oxide Coating.” *Nano Lett.* 16 (2016): 5815–5822.
- He, Yang, and Meng Gu, Haiyan Xiao, Langli Luo, Yuyan Shao, Fei Gao, Yingge Du, Scott X. Mao, and Chongmin Wang. “Atomistic Conversion Reaction Mechanism of WO₃ in Secondary Ion Batteries of Li, Na, and Ca.” *Angew. Chem. Int. Ed.* 55 (2016): 6244–6247.

Presentations

- 2016 Microscopy and Microanalysis, Columbus, Ohio (July 24-29, 2016): “*In Situ* TEM Study of Coating Layer Function on Silicon Anode Particle for Lithium Ion Battery”; Chongmin Wang and Langli Luo.
- 2016 Microscopy and Microanalysis, Columbus, Ohio (July 24-29, 2016): “Investigating Side Reactions and Coating Effects on High Voltage Layered Cathodes for Lithium Ion Batteries”; Pengfei Yan and Jianming Zheng, Saravanan Kuppan, Xiaofeng Zhang, Khalil Amine, Jie Xiao, Guoying Chen, Ji-Guang Zhang, and Chong-Min Wang.

Task 5.8 – Characterization and Computational Modeling of Structurally Integrated Electrode (Michael M. Thackeray and Jason R. Croy, Argonne National Laboratory)

Project Objective. The primary project objective is to explore the fundamental, atomic-scale processes that are most relevant to the challenges of next-generation, energy-storage technologies, in particular, high-capacity, structurally integrated electrode materials. A deeper understanding of these materials relies on novel and challenging experiments that are only possible through unique facilities and resources. The goal is to capitalize on a broad range of facilities to advance the field through cutting-edge science, collaborations, and multi-disciplinary efforts to characterize and model structurally integrated electrode systems, notably those with both layered and spinel character.

Project Impact. This project capitalizes on and exploits DOE user facilities and other accessible national and international facilities (including skilled and trained personnel) to produce knowledge to advance Li-ion battery materials. Specifically, furthering the understanding of structure-electrochemical property relationships and degradation mechanisms will contribute significantly to meeting the near- to long-term goals of PHEV and EV battery technologies.

Approach. A wide array of characterization techniques including X-ray and neutron diffraction, X-ray absorption, emission and scattering, HR-TEM, Raman spectroscopy, and theory will be brought together to focus on challenging experimental problems. Combined, these resources promise an unparalleled look into the structural, electrochemical, and chemical mechanisms at play in novel, complex electrode/electrolyte systems being explored at ANL.

Out-Year Goals. The out-year goals are as follows:

- Gain new, fundamental insights into complex structures and degradation mechanisms of high-capacity composite cathode materials from novel, probing experiments carried out at user facilities and beyond.
- Investigate structure-property relationships that will provide insight into the design of improved cathode materials.
- Use knowledge and understanding gained from this project to develop and scale up advanced cathode materials in practical Li-ion prototype cells.

Collaborators. This project engages in collaboration with Eungje Lee, Joong Sun Park, Joel Blauwkamp, and Roy Benedek (Chemical Sciences and Engineering, ANL).

Milestones

1. Characterize bulk and surface properties of structurally integrated electrode materials using DOE user facilities at Argonne (APS, Electron Microscopy Center, and Argonne Leadership Computing Facility) and facilities elsewhere, for example, Spallation Neutron Source (ORNL) and the Northwestern University Atomic and Nanoscale Characterization Experimental Center (NUANCE). (September 2016 – In progress)
2. Use complementary theoretical approaches to further the understanding of the structural and electrochemical properties of layered-spinel electrodes and protective surface layers. (September 2016 – In progress)
3. Analyze, interpret, and disseminate collected data for publication and presentation. (September 2016 – In progress)

Progress Report

Embedding local spinel (S) or spinel-type configurations within a composite matrix of layered (L) and layered-layered (LL) structures provides a unique opportunity to address the limitations of high-capacity, lithium- and manganese-rich cathode materials including voltage fade, initial irreversible capacity loss, low rate performance, and surface instabilities. Optimization of the synergistic effects of structurally integrated components requires an understanding of the structures that are formed under various conditions (for example, synthesis procedures and composition). Obtaining a systematic understanding of the interplay between targeted composition, the resulting structures, and electrochemical performance is also a non-trivial task. To gain insight into these complex relationships, a series of lithium-manganese-oxide materials within the system $\text{Li}_{2-z}\text{MnO}_{3-\delta}$ ($0 \leq z \leq 1.5$) with layered (Li_2MnO_3 , $z=0$) and spinel (LiMn_2O_4 , $z=1.5$) end-members was selected for detailed structure analysis.

Laboratory XRD data (Figure 39a) and electrochemical charge-discharge voltage profiles (data not shown) confirmed that $\text{Li}_{2-z}\text{MnO}_{3-\delta}$ electrode samples with $z=0.5$, 0.75 , and 1.0 had composite structures containing a layered component and a spinel component. Although the electrochemical signature of a spinel phase could not be unequivocally detected for $z=0.25$, the XRD data of this sample provided evidence of a trace amount of spinel (Figure 39b). The results therefore highlight the complex relationship that exists between the integrated structures and their electrochemical response. Largely coherent crystallographic relationships between the layered and spinel components were observed. For $z=1.0$, high-resolution (synchrotron) XRD data showed distinct L and S peaks as well as single, overlapping $(111)_\text{S} // (001)_\text{L}$ and $(222)_\text{S} // (002)_\text{L}$ peaks (Figure 39c), the former set corresponding to diffraction from the close-packed oxygen planes in the layered and spinel structures. The overlap of the two main peaks therefore indicates almost identical interplanar distances of the corresponding planes. The crystallographic coherency of the layered and spinel structures in the direction of the closed-packed oxygen planes was also observed by high-resolution electron microscopy (HREM). As shown in Figure 39d-e, both lattice structures are coherently arranged in the direction of the oxygen close packed planes, that is, $(001)_\text{L}$ and $(111)_\text{S}$. A coherent interface region that connects the layered and spinel components was also observed. The findings provide an importance basis for the on-going development of LLS composite cathode structures. Furthermore, the results support and validate the strategy that is being followed to induce the formation of a spinel component in LL $x\text{Li}_2\text{MnO}_3 \bullet (1-x)\text{LiMO}_2$ ($\text{M}=\text{Mn}, \text{Ni}, \text{Co}$) composite electrode structures by slightly reducing amount of lithium in the Li_2MnO_3 component prior to firing and annealing the reagents at elevated temperatures ($\sim 850^\circ\text{C}$).

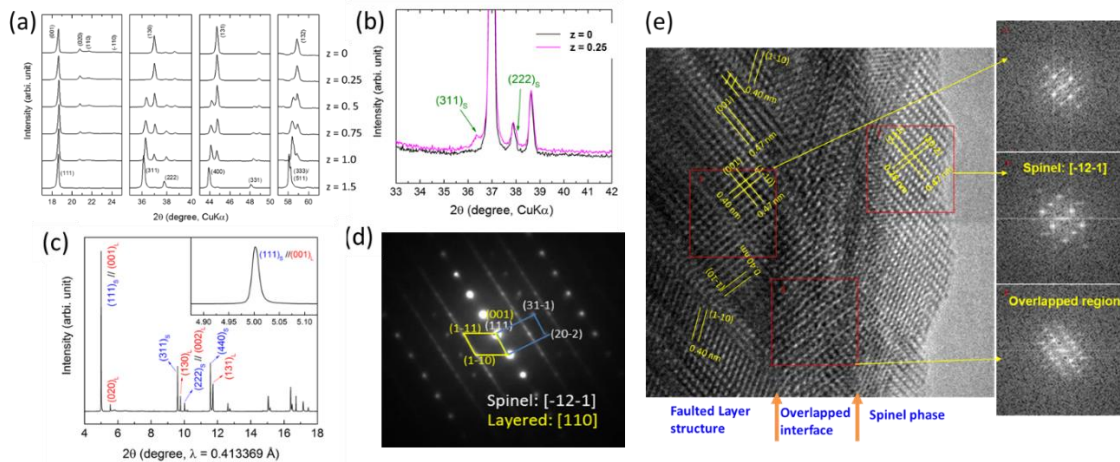


Figure 39. Laboratory X-ray diffraction (XRD) of the $\text{Li}_{2-z}\text{MnO}_{3-\delta}$ powder samples (a, b), integrated layered and spinel structures in the $\text{Li}_{2-z}\text{MnO}_{3-\delta}$ ($z=1.0$) LS composite sample supported by synchrotron high-resolution XRD (c), electron diffraction (d), and high-resolution transmission electron microscopy (e) analyses.

TASK 6 – MODELING ADVANCED ELECTRODE MATERIALS

Summary and Highlights

Achieving the performance, life, and cost targets outlined in the EV Everywhere Grand Challenge will require moving to next generation chemistries, such as higher capacity Li-ion intercalation cathodes, silicon and other alloy-based anodes, Li-metal anode, and sulfur cathodes. However, numerous problems plague the development of these systems, from material-level challenges in ensuring reversibility to electrode-level issues in accommodating volume changes, to cell-level challenges in preventing cross talk between the electrodes. In this task, a mathematical perspective is applied to these challenges to provide an understanding of the underlying phenomenon and to suggest solutions that can be implemented by the material synthesis and electrode architecture groups.

The effort spans multiple length scales from *ab initio* methods to continuum-scale techniques. Models are combined with experiments and extensive collaborations are established with experimental groups to ensure that the predictions match reality. Efforts are also focused on obtaining the parameters needed for the models, either from lower-length scale methods or from experiments. Projects also emphasize pushing the boundaries of the modeling techniques used to ensure that the task stays at the cutting edge.

In the area of intercalation cathodes, the effort is focused on understanding the working principles of the high Ni layered materials with an aim of understanding structural changes and the associated changes in transport properties. In addition, focus is paid to the assembling of porous electrodes with particles to predict the conduction behavior and developing tools to measure electronic conduction. This quarter, using calculations of oxygen stability, the project found that the surface of the excess Li materials will spontaneously release oxygen at $x < 1.75$, consistent with experimental evidence. In addition, results of calculations on the excess lithium materials reveal the origin of oxygen oxidation and the excess capacity. Finally, the conductivity probe method was improved this quarter to show a factor of two difference between in-plane and out of plane conductivity of cathode laminates.

In the area of silicon anodes, the effort is in trying to understand the interfacial instability and suggest ways to improve the cyclability of the system. In addition, effort is focused on designing artificial SEI layers that can accommodate the volume change, and in understanding the ideal properties for a binder to accommodate the volume change without delamination. Work on the Li-ion transport through the SEI was conducted, and three regions were identified: ballistic, trapping, and diffusive regions. Simulations of the silicon islands were conducted to identify the design space where it is possible to prevent cracking while allowing partial delamination.

In the area of sulfur cathodes, the focus is on developing better models for the chemistry with the aim of describing the precipitation reactions accurately. Efforts are focused on performing the necessary experiments to obtain a physical picture of the phase transformations in the system and in measuring the relevant thermodynamic, transport, and kinetic properties. In addition, changes in the morphology of the electrode are described and tested experimentally. This quarter, the diffusion coefficient of lithium and the polysulfide were measured as a function of concentration. These parameters were incorporated into a porous electrode model and compared to experimental rate data.

Finally, microstructure models are an area of focus to ensure that the predictions move away from average techniques to more sophisticated descriptions of processes inside electrodes. Efforts are focused on understanding conduction within the electrode and on simulating the full electrode that describes the intricate physics inside the battery electrode. These efforts are combined with tomography information as input into the models.

Task 6.1 – Electrode Materials Design and Failure Prediction (Venkat Srinivasan, Lawrence Berkeley National Laboratory)

Project Objective. The project goal is to use continuum-level mathematical models along with controlled experiments on model cells to (i) understand the performance and failure models associated with next-generation battery materials, and (ii) design battery materials and electrodes to alleviate these challenges. The research will focus on the Li-S battery chemistry and on microscale modeling of electrodes. Initial work on the Li-S system will develop a mathematical model for the chemistry along with obtaining the necessary experimental data, using a single ion conductor (SIC) as a protective layer to prevent polysulfide migration to the lithium anode. The initial work on microscale modeling will use the well understood $\text{Li}(\text{NiMnCo})_{1/3}\text{O}_2$ (NMC) electrode to establish a baseline for modeling next-generation electrodes.

Project Impact. Li-S cells promise to increase the energy density and decrease the cost of batteries compared to the state of the art. If the performance and cycling challenges can be alleviated, these systems hold the promise for meeting the EV Everywhere targets.

Out-Year Goals. At the end of this project, a mathematical model will be developed that can address the power and cycling performance of next-generation battery systems. The present focus is on microscale modeling of electrodes and Li-S cells, although the project will adapt to newer systems, if appropriate. The models will serve as a guide for better design of materials, such as in the kinetics and solubility needed to decrease the morphological changes in sulfur cells and increase the power performance.

Milestones

1. Replace parameters (porosity gradient and tortuosity) in macroscale NMC model with corresponding values or functions obtained from tomography data. (December 2015 – Complete)
2. Measure the relationship of film growth to electrochemical response and develop a model to interpret the relationship. (March 2016 – Complete)
3. Measure transport properties of polysulfide solutions using electrochemical methods. If unsuccessful at obtaining concentration-dependent diffusion coefficient, use fixed diffusion coefficient value in upcoming simulations. (June 2016 – No-Go)
4. Incorporate measured properties into porous-electrode model of Li-S cell and compare to data. (September 2016 – Complete)

Progress Report

Incorporate measured properties into porous-electrode model of a Li-S cell and compare to data

Experiments this quarter were conducted to extend the transport property measurements previously reported. A methodology based on the restricted diffusion technique has been developed to measure concentration-dependent diffusion coefficients of Li^+ and polysulfide species (S_8^{2-} and S_6^{2-}), as reported in Figure 40a-b. This analysis uses the slope of the log(potential) vs. time curve obtained during relaxation of a cell constructed with lithium metal and glassy carbon electrodes. The magnitude of diffusivity is seen to decrease with species concentration. Additional experiments were performed this quarter to explore the dependence of LiTFSI salt solution conductivity with polysulfide (Li_2S_6 and Li_2S_8) concentration. It was observed that the conductivity variation is very similar for both of these polysulfide species. As shown in Figure 40c, the presence of polysulfides does not impact the conductivity significantly at low concentration of LiTFSI salt. However, the maximum conductivity and conductivity at high concentration both experience rapid decay with increasing polysulfide concentration.

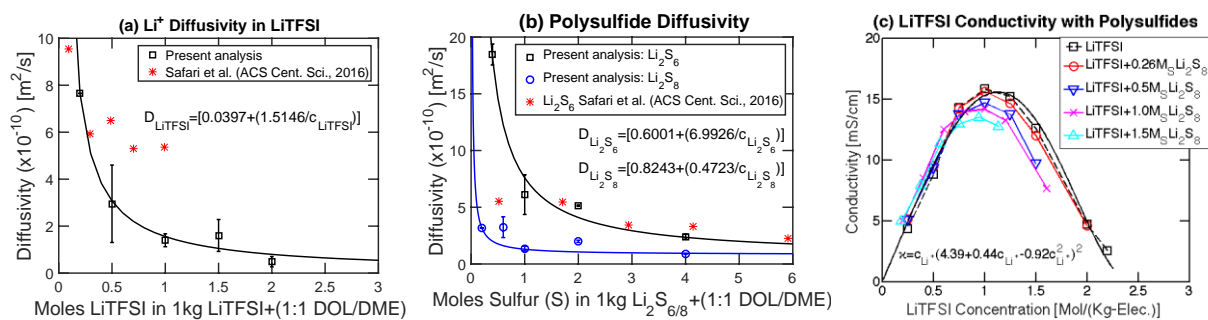


Figure 40. (a) Concentration-dependent diffusivity of Li^+ from LiTFSI salt dissolved in 1:1 DOL/DME solvent. (b) Concentration-dependent diffusivity of polysulfide anions in two different types of polysulfide salts (Li_2S_6 and Li_2S_8) dissolved in 1:1 DOL/DME solvent. (c) Conductivity of the LiTFSI salt dissolved in 1:1 DOL/DME solvent combined with different amounts of polysulfide solution.

Sulfur cathode laminates were prepared from slurries of conductive carbon, sulfur, and PVDF binder, with a dried coating thickness of 75 μm . These were incorporated into coin cells with lithium metal anodes and 1M LiTFSI salt dissolved in 1:1 (by vol) DOL/DME solvent as electrolyte solution. The cells were cycled at different C-rates at room temperature. The discharge curves shown in Figure 41a show significant capacity losses with increasing rate of operation.

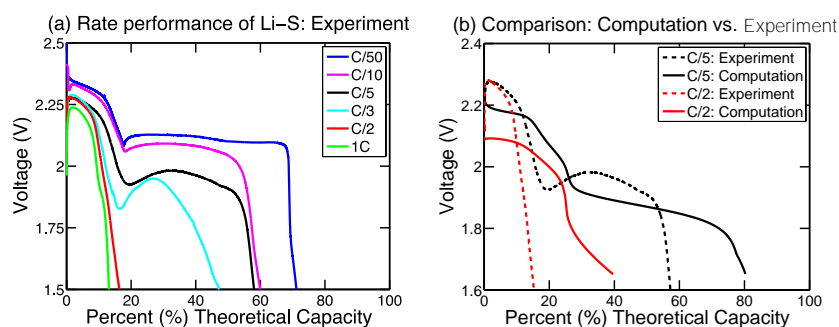


Figure 41. (a) Experimentally obtained performance curves for lithium-sulfur cells discharged at different C-rates. (b) Comparison between experimental results and computational predictions at two different C-rates.

Finally, a computational methodology has been developed, combining porous electrode theory and concentrated solution theory, and incorporating the concentration-dependent transport properties. Model predictions are plotted in Figure 41b, along with corresponding experimental results. The discrepancies might be attributed to several causes, such as unknown electrochemically active surface area, unknown porosity and tortuosity, isolation of sulfur, limited information about side reactions, and polysulfide shuttling. This new model will be refined as additional experimental results become available. Its development fulfills this quarter's milestone.

Task 6.2 – Predicting and Understanding Novel Electrode Materials from First Principles (Kristin Persson, Lawrence Berkeley National Laboratory)

Project Objective. The project aim is to model and predict novel electrode materials from first-principles focusing on (1) understanding the atomistic interactions behind the behavior and performance of the high-capacity lithium excess and related composite cathode materials, and (2) predicting new materials using the recently developed Materials Project high throughput computational capabilities at LBNL. More materials and new capabilities will be added to the Materials Project Lithium Battery Explorer App (www.materialsproject.org/apps/battery_explorer/).

Project Impact. The project will result in a profound understanding of the atomistic mechanisms underlying the behavior and performance of the lithium excess as well as related composite cathode materials. The models of the composite materials will result in prediction of voltage profiles and structural stability—the ultimate goal being to suggest improvements based on the fundamental understanding that will increase the life and safety of these materials. The Materials Project aspect of the work will result in improved data and electrode properties being calculated to aid predictions of new materials for target chemistries relevant for ongoing BMR experimental research.

Out-Year Goals. During years one and two, the bulk phase diagram will be established, including bulk defect phases in layered Li_2MnO_3 , layered LiMO_2 ($M = \text{Co}, \text{Ni}, \text{and Mn}$), and LiMn_2O_4 spinel to map out the stable defect intermediate phases as a function of possible TM rearrangements. Modeling of defect materials (mainly Li_2MnO_3) under stress/strain will be undertaken to simulate effect of composite nano-domains. The composite voltage profiles as function of structural change and lithium content will be obtained. In years two to four, the project will focus on obtaining lithium activation barriers for the most favorable TM migration paths as a function of lithium content, as well as electronic density of states (DOS) as a function of lithium content for the most stable defect structures identified in years one to two. Furthermore, stable crystal facets of the layered and spinel phases will be explored, as a function of O_2 release from surface and oxygen chemical potential. Within the project, hundreds of novel lithium intercalation materials will be calculated and made available.

Collaborations. This project engages in collaboration with Gerbrand Ceder (LBNL), Clare Grey (Cambridge), Mike Thackeray (ANL), and Guoying Chen (LBNL).

Milestones

1. Mn mobilities as a function of lithium content in layered Li_xMnO_3 and related defect spinel and layered phases. (March 2015 – Complete)
2. Surface facets calculated and validated for Li_2MnO_3 . (March 2016 – Complete)
3. Calculate stable crystal facets. Determine whether facet stabilization is possible through morphology tuning. (March 2016 – Complete)
4. *Go/No-Go*: Stop this approach if facet stabilization cannot be achieved. (May 2016 – Complete)
5. Lithium mobilities as a function of lithium content in layered Li_xMnO_3 and related defect spinel and layered phases. (September 2015 – Complete)

Progress Report

The final effort of this study is focused on the surface stability of the Li-excess layered materials using first-principles calculations. By applying reconstruction rules and dipole corrections, Li_xMnO_3 is found to exhibit five reconstructed stable surfaces. It is known that the surface stability depends strongly on the surface cation arrangement. This project systematically investigated the surface environments with respect to the Li and Mn ions locations. Through probing the Li-ion arrangement on the surface (Figure 42a-b), it was found that the Li-ions prefer the atop site of the underlying Li octahedral site. Furthermore, the surface under-coordinated Mn are swapped with subsurface Li-ions (Figure 42c). Calculations show that only the first subsurface Li-sites are energetically favorable for Mn swapping, (Figure 42d).

The Wulff structure (Figure 43-inset) of Li_2MnO_3 is calculated according to the obtained stable, reconstructed surfaces. The Wulff shape exhibits two majority surfaces ((001) and (010)) and three minority surfaces ((100), (110), and (111)). By averaging the oxygen defect energies over all surface sites, the project calculated the oxygen release energies for each surface. The surface oxygen release energies start out positive (stable) at discharge ($x=2$), but rapidly turn negative at $x=1.5$ and $x=1.0$. It is worth noting that there is very little kinetic hindrance to removing the surface oxygen ions. In comparison, previous research indicated that the oxygen defect energies in bulk Li_xMnO_3 are 2.6 eV ($x=2.0$) and 0.4 eV ($x=1.0$) (star marks in Figure 43). Barriers for oxygen migration remain high throughout the composition range.

Therefore, the combined investigation demonstrates that the oxygen—even when oxidized to O^{-1} —prefers to stay in the bulk of the Li excess material, while surface oxygen is spontaneously released for $x < 1.7$. This is consistent with experimental observations of oxygen evolution initiated at 19% of Li extraction ($x=1.63$). However, while all stable facets exhibit spontaneous oxygen evolution for $x < 1.5$, the (110) surface is consistently more stable as compared to the other surfaces. Conversely, the (010) surface presents less stability against oxygen release than the other surfaces. Hence, to optimize the morphology of Li excess particles, the project would expect Li_2MnO_3 particles with minimized (010) surfaces and enhanced (110) facets to exhibit improved oxygen retention.

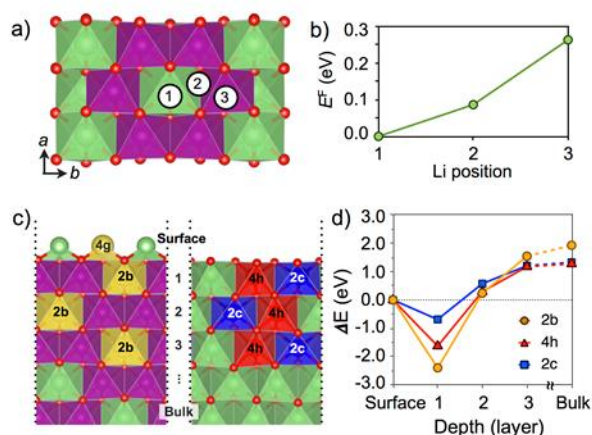


Figure 42. Surface reconstruction rules of Li ions on the surface (a and b) and Mn coordination (c and d). The Li-ions prefer atop of the underlying Li octahedral sites and under-coordinated surface Mn is readily switched with subsurface Li.

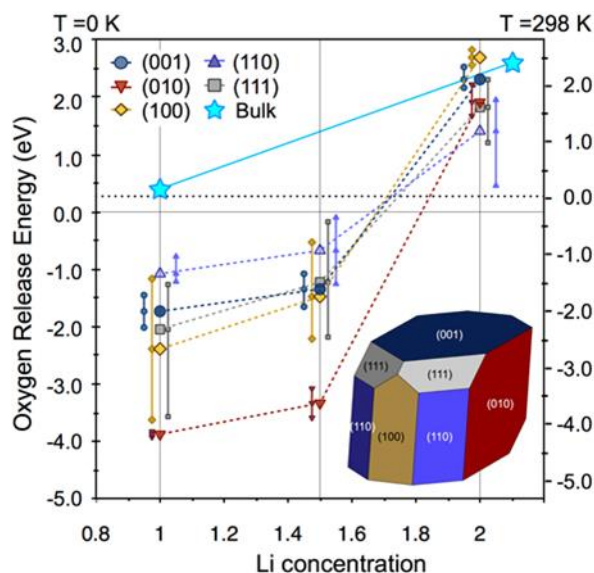


Figure 43. The calculated Wulff shape of pristine Li_2MnO_3 (inset) and oxygen release energies for each stable surface. Surface oxygen is spontaneously released from all surfaces for $x < 1.5$.

Patents/Publications/Presentations

Publication

- Shin, Yongwoo, and Kristin A. Persson. “Surface Morphology and Surface Stability against Oxygen Loss of the Li-excess Li_2MnO_3 Cathode Material as a Function of Li Concentration.” *ACS Appl. Mater. Interfaces* 8 (2016): 25595–25602.

Task 6.3 – First Principles Calculations of Existing and Novel Electrode Materials (Gerbrand Ceder, LBNL)

Project Objective. Identify the structure of layered cathodes that leads to high capacity. Clarify the role of the initial structure as well as structural changes upon first charge and discharge. Give insight into the role of lithium excess, and develop methods to predict ion migration in layered cathodes upon cycling and during overcharge. Develop predictive modeling of oxygen charge transfer and oxygen loss. Give insight into the factors that control the capacity and rate of Na-intercalation electrodes, as well as Na-vacancy ordering. Develop very high-capacity layered cathodes with high structural stability (> 250 mAh/g).

Project Impact. The project will lead to insight in how lithium excess materials work and ultimately to higher capacity cathode materials for Li-ion batteries. The project will help in the design of high-capacity cathode materials that are tolerant to TM migration.

Out-Year Goals. The out-year goals are as follows:

- Higher capacity Li-ion cathode materials
- Novel chemistries for higher energy density storage devices
- Guidance for the field in search for higher energy density Li-ion materials

Collaborations. This project collaborates with Kristin Persson (LBNL) and Clare Grey (Cambridge).

Milestones

1. Model to predict compositions that will disorder as synthesized. (December 2015 – Complete)
2. At least one Ti-based compound with high capacity. (March 2016 – Complete)
3. Predictive model for the voltage curve (slope) of cation-disordered materials. (June 2016 – Complete)
4. Modeling capability for materials with substantial oxygen redox capability. (September 2016 – Complete)

Progress Report

As part of the objective to develop predictive modeling of oxygen charge transfer and materials with substantial oxygen redox capability, the project has investigated the chemical and structural origin of oxygen redox activities in Li-excess cathode materials using first-principles calculations. The reversible oxygen redox in Li-excess materials can substantially enlarge the composition space of potential high-capacity and high-energy-density cathodes because it can deliver excess capacity beyond the theoretical TM redox capacity, eliminating the need for heavy and expensive TM ions. Nevertheless, the origin of the oxygen redox process is not understood, preventing the rational design of better Li-excess cathodes with oxygen redox. Using first-principles calculations, the project demonstrated that specific chemical and structural features in layered and cation-disordered Li-excess cathode materials lead to labile oxygen electrons that can be easily extracted and participate in the practical capacity of these materials.

The first-principles calculations on the cation-mixed layered LiNiO_2 and Li_2MnO_3 showed that some electronic states of oxygen ions that are linearly coordinated by two Li ions (Li–O–Li configuration) are less stable than those of other oxygen ions. O 2p orbitals along the Li–O–Li configurations do not have an M (metal ion) d orbital with which to hybridize and do not hybridize with the Li 2s orbital either because of the large energy difference between the O 2p and Li 2s orbitals. Consequently, their energy levels are close to that of the unhybridized O 2p orbital, which has higher energy than the hybridized O bonding states (t_{1u}^b , a_{1g}^b , and e_g^b states), as shown in Figure 44. The project applied this understanding to practical Li-excess materials to reveal the origin of oxygen oxidation and the excess capacity. The first-principles calculations showed that the hole is localized around oxygen ions along the Li–O–Li configuration, as illustrated in Figure 45, indicating that these states are oxidized and the extraction of electrons from such unstable oxygen states is the origin of the oxygen redox activity and the extra capacity beyond theoretical TM redox capacity in Li-excess TM oxides.

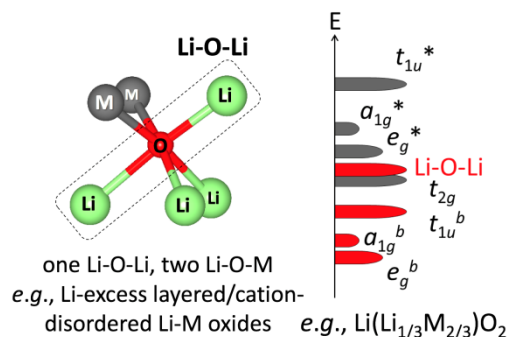


Figure 44. Local atomic coordination around oxygen in Li-excess materials and schematic of the band structure for Li-excess layered Li-M oxides.

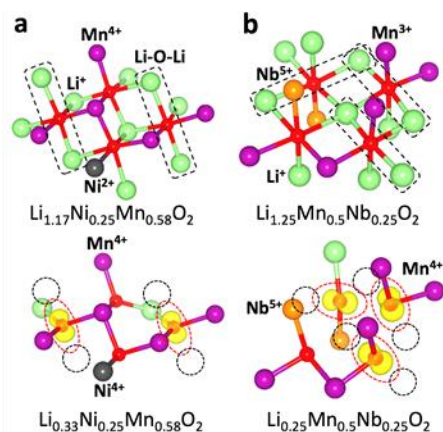


Figure 45. Atomic configurations and the iso-surface of spin density (yellow) around oxygen (red spheres) in (a) $\text{Li}_{1.17-x}\text{Ni}_{0.25}\text{Mn}_{0.58}\text{O}_2$ and (b) $\text{Li}_{1.25-x}\text{Mn}_{0.5}\text{Nb}_{0.25}\text{O}_2$.

The project finding is distinct from the prevailing argument that the covalency of TM–O bonding leads to excess capacity beyond TM redox capacity. In stark contrast with this current belief, the project demonstrated that only oxygen oxidation by extracting labile electrons from unhybridized O 2p states sitting in Li–O–Li configurations can create the excess capacity. This distinction is important because the number of electrons, and thus the capacity, from the hybridized TM d states (for example, e_g^* states) remains the same regardless of covalency, which is already counted as TM redox capacity. This work has been published in *Nature Chemistry*.¹

[1] Seo, D.-H., and J. Lee, A. Urban, R. Malik, S. Kang, and G. Ceder. “The Structural and Chemical Origin of the Oxygen Redox Activity in Layered and Cation-Disordered Li-Excess Cathode Materials.” *Nature Chem.* 8 (2016): 692.

Task 6.4 – First Principles Modeling of SEI Formation on Bare and Surface/Additive Modified Silicon Anode (Perla Balbuena, Texas A&M University)

Project Objective. This project aims to develop fundamental understanding of the molecular processes that lead to the formation of a SEI layer due to electrolyte decomposition on Si anodes, and to use such new knowledge in a rational selection of additives and/or coatings. The focus is on SEI layer formation and evolution during cycling and subsequent effects on capacity fade through two concatenated problems: (1) SEI layers formed on lithiated silicon surfaces, and (2) SEI layers formed on coated surfaces. Key issues being addressed include the dynamic evolution of the system and electron transfer through solid-liquid interfaces.

Project Impact. Finding the correspondence between electrolyte molecular properties and SEI formation mechanism, structure, and properties will allow the identification of new/improved additives. Studies of SEI layer formation on modified surfaces will allow the identification of effective coatings able to overcome the intrinsic deficiencies of SEI layers on bare surfaces.

Approach. Investigating the SEI layer formed on modified silicon surfaces involves analysis of the interfacial structure and properties of specific coating(s) deposited over the silicon anode surface, characterization of the corresponding surface properties before and after lithiation, especially how such modified surfaces may interact with electrolyte systems (solvent/salt/additive), and what SEI layer structure, composition, and properties may result from such interaction. This study will allow identification of effective additives and coatings able to overcome the intrinsic deficiencies of SEI layers on bare surfaces. Once the SEI layer is formed on bare or modified surfaces, it is exposed to cycling effects that influence its overall structure (including the anode), chemical, and mechanical stability.

Out-Year Goals. Elucidating SEI nucleation and electron transfer mechanisms leading to growth processes using a molecular level approach will help establish their relationship with capacity fading, which will lead to revisiting additive and/or coating design.

Collaborations. Work with Chunmei Ban (NREL) consists in modeling the deposition-reaction of alucone coating on silicon surfaces and their reactivity. Reduction of solvents and additives on silicon surfaces were studied in collaboration with K. Leung and S. Rempe, from SNL. Collaborations with Professor Jorge Seminario (TAMU) on electron and ion transfer reactions, and Dr. Partha Mukherjee (TAMU) focusing on the development of a multi-scale model to describe the SEI growth on silicon anodes.

Milestones

1. Identify SEI nucleation and growth on silicon surfaces modified by deposition of alucone coatings as a function of degree of lithiation of the film. (December 2015 – Complete)
2. Quantify chemical and electrochemical stability of various SEI components: competition among polymerization, aggregation, and dissolution reactions. Evaluate voltage effects on SEI products stability. (March 2016 – Complete)
3. Identify alternative candidate electrolyte and coating formulations. (June 2016 – In progress)
4. *Go/No-Go*: Test potential candidate electrolyte and coating formulations using coarse-grained model and experimentally via collaborations. (September 2016 – In progress)

Progress Report

Alternative electrolytes and coatings. The effect of fluorinated additives resulting from modifications of FEC, such as trifluoropropylene carbonate (TFPC) and trifluoroethyl ethyl carbonate (TFEEC) reported last quarter were further examined with AIMD simulations. A partially lithiated model Si nanoparticle was further lithiated in contact with an electrolyte phase containing the tested additive (solvent) + salt (LiPF_6). Initial results indicated the formation of a very thick layer upon volume expansion of the Si nanoparticle. However irreversible trapping of the lithium ions inside the SEI layer could not be proved yet. Further analyses are being carried out to identify whether particle size is a limiting constraint for obtaining reversible lithiation. In addition, together with collaborator Chunmei Ban from NREL, the project is modeling coating effects on Si particles. In particular, the NREL group is depositing a thin Al_2O_3 layer over a silicon anode using MLD methods, and the TAMU team has carried out density functional theory (DFT) and AIMD simulations to elucidate the effects of such a layer on the reactivity of a lithiated Si anode. In summary, it was found that the Al_xO_y groups in the film may play a significant role in the formation of an SEI layer with a larger inorganic component. New experiments are being conducted to investigate the effect of the layer thickness on the reactivity, and capacity fade of the electrochemical cell. Consequently, this team is modeling the thickness effect in the models studied previously.

Li-ion transport through SEI layer. Rempe's group (Sandia National Laboratories, SNL) thoroughly investigated the transport properties of Li^+ in Li_2EDC and ethylene carbonate (precursor to EDC) using mean squared displacements (MSD). The diffusion process involves three distinct regions: a ballistic, trapping, and diffusive region. High-resolution simulation data is required to observe these behaviors.

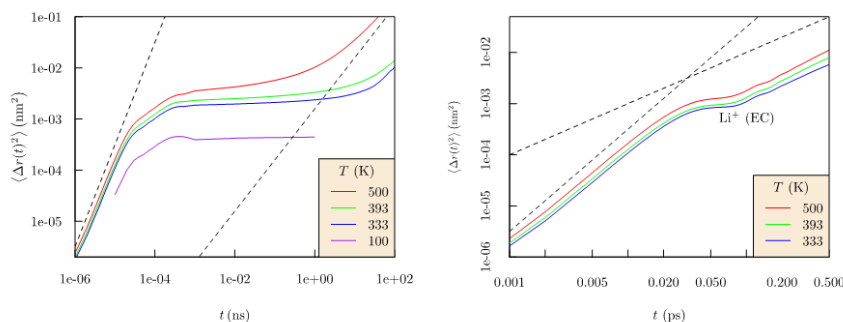


Figure 46. Mean square displacements of Li^+ in Li_2EDC (left) and EC (right) plotted on a log-log scale. Three distinct regions appear: ballistic diffusion at short times, a flat region that indicates trapping of Li^+ , and diffusive region at long times. Notice that time scales for Li^+ trapping in the EC solvent (right) is several orders of magnitude smaller compared to the solid electrolyte interphase layer (left).

In Figure 46, Li^+ MSD plots show that all three regions were observed in Li_2EDC and EC. In the case of Li_2EDC , Li^+ can get trapped into a relatively viscous Li_2EDC layer, as shown by the flat region on the MSD plot. EC, being relatively fluid in comparison, does not trap Li^+ ions. Hence, the flat region is significantly smaller. These subtle differences are important for understanding the Li^+ ion transport mechanism in the SEI layer. The team has also identified vibrational modes important for Li^+ transport in Li_2EDC and EC, and are investigating these modes using electronic structure calculations to understand their influence on Li^+ transport mechanisms in Li_2EDC and EC.

Effects of the SEI structural heterogeneity at the atomic scale. Previous findings of this team suggest that LiF and Li_2O are key SEI inorganic components on the immediate surfaces of reactive anode materials. The $\text{LiF}/\text{Li}_2\text{O}$ “grain boundary” model described last quarter exhibits substantial spatial variation in its effective “local potential” $V(x)$. Therefore, Leung's group at SNL has focused on the reactivity of FEC molecules at Li_2O surfaces and grain boundaries. It was found that an FEC molecule initially placed on a $V(x) \sim -0.3$ V region, is rapidly electrochemically decomposed. This qualitatively illustrates that the spatial heterogeneities (“hot spots”) can accelerate electrolyte decomposition. Here $V(x)$ represents local voltage variation due to the effects of the local electrostatics added to the constant voltage.

Patents/Publications/Presentations

Publications

- Perez-Beltrán, S., and G. E. Ramirez-Caballero, and P. B. Balbuena. “First Principles Calculations of Lithiation of a Hydroxylated Surface of Amorphous Silicon Dioxide.” *J. Phys. Chem. C* 119 (2015): 16424-16431.
- Ma, Y., and J. M. Martinez de la Hoz, I. Angarita, J. M. Berrio-Sanchez, L. Benitez, J. M. Seminario, S.-B. Son, S.-H. Lee, S. M. George, C. M. Ban, and P. B. Balbuena. “Structure and Reactivity of Alucone-Coated Films on Si and Li_xSi_y Surfaces.” *ACS Appl. Mater. Inter.* 7 (2015): 11948-11955.
- Martinez de la Hoz, J. M., and F. A. Soto, and P. B. Balbuena. “Effect of the Electrolyte Composition on SEI Reactions at Si Anodes of Li-Ion Batteries.” *J. Phys. Chem. C* 119 (2015): 7060-7068. doi: 10.1021/acs.jpcc.5b01228.
- Soto, F. A., and Y. Ma, J. M. Martinez de la Hoz, J. M. Seminario, and P. B. Balbuena. “Formation and Growth Mechanisms of Solid-Electrolyte Interphase Layers in Rechargeable Batteries.” *Chem. Mater.* 27, no. 23 (2015): 7990-8000.
- You, X., and M. I. Chaudhari, S. B. Rempe, and L. R. Pratt. “Dielectric Relaxation of Ethylene Carbonate and Propylene Carbonate from Molecular Dynamics Simulations.” *J. Phys. Chem. B.* doi: 10.1021/acs.jpcc.5b09561.
- Leung, K., and F. A. Soto, K. Hankins, P. B. Balbuena, and K. L. Harrison. “Stability of Solid Electrolyte Interphase Components on Reactive Anode Surfaces.” *J. Phys. Chem. C* 120 (2016): 6302-6313.
- Kumar, N., and J. M. Seminario. “Lithium-Ion Model Behavior in an Ethylene Carbonate Electrolyte Using Molecular Dynamics.” *J. Phys. Chem. C* 120 (2016): 16322-16332.
- Chaudhari, M., and J. Nair, L. Pratt, F. A. Soto, P. B. Balbuena, and S. Rempe. “Scaling Atomic Partial Charges of Carbonate Solvents for Lithium Ion (Li^+) Solvation and Diffusion.” *J. Chem. Theory and Comp.*, under review.
- Galvez-Aranda, D. E., and V. Ponce-Valderrama, and J. M. Seminario. “Molecular Dynamics Simulations of the First Charge of a Li-Ion-Si-Anode Nanobattery.” *J. Phys. Chem. C*, submitted.

Task 6.5 – A Combined Experimental and Modeling Approach for the Design of High Current Efficiency Silicon Electrodes (Xingcheng Xiao, General Motors; Yue Qi, Michigan State University)

Project Objective. The use of high-capacity, Si-based electrode has been hampered by its mechanical degradation due to large volume expansion/contraction during cycling. Nanostructured silicon can effectively avoid silicon cracking/fracture. Unfortunately, the high surface to volume ratio in nanostructures leads to an unacceptable amount of SEI formation and growth, and thereby low current/Coulombic efficiency and short life. Based on mechanics models, the project demonstrates that the artificial SEI coating can be mechanically stable despite the volume change in silicon, if the material properties, thickness of SEI, and the size/shape of silicon are optimized. Therefore, the project objective is to develop an integrated modeling and experimental approach to understand, design, and make coated silicon anode structures with high current efficiency and stability.

Project Impact. The validated model will ultimately be used to guide the synthesis of surface coatings and the optimization of silicon size/geometry that can mitigate SEI breakdown. The optimized structures will eventually enable a negative electrode with a 10x improvement in capacity (compared to graphite), while providing > 99.99% Coulombic efficiency; this could significantly improve the energy/power density of current Li-ion batteries.

Out-Year Goals. The out-year goal is to develop a well validated mechanics model that directly imports material properties either measured from experiments or computed from atomic simulations. The predicted SEI induced stress evolution and other critical phenomena will be validated against *in situ* experiments in a simplified thin film system. This comparison will also allow fundamental understanding of the mechanical and chemical stability of artificial SEI in electrochemical environments and the correlation between the Coulombic efficiency and the dynamic process of SEI evolution. Thus, the size and geometry of coated silicon nanostructures can be optimized to mitigate SEI breakdown, providing high current efficiency.

Collaborations. This project engages in collaboration with LBNL, PNNL, and NREL.

Milestones

1. Identify critical mechanical and electrochemical properties of the SEI coating that can enable high current efficiency. (December 2015 – Complete)
2. Design a practically useful silicon electrode where degradation of the SEI layer is minimized during lithiation and delithiation. (March 2016 – Complete)
3. Construct an artificial SEI design map for silicon electrodes, based on critical mechanical and transport properties of desirable SEI for a given silicon architecture. (June 2016 – Complete)
4. Validated design guidance on how to combine the SEI coating with a variety of silicon nano/microstructures. *Go/No-Go*: Decision based on whether the modeling guided electrode design can lead to high Coulombic efficiency > 99.9%. (September 2016 – Complete; Go)

Progress Report

Modeling SEI failure on Si. This project has demonstrated that properly designed Si islands could provide a feasible platform to decouple SEI failure from electrode fracture. In this platform, Si islands of selected dimension (lateral width and thickness) were designed to adhere stably to the current collector, while the SEI layer underwent accumulative mechanical degradation due to the in-plane strain of a Si island upon lithiation (Figure 47). The full design space for such a system was explored. It was indicated that the energy release rate for channel cracking in a silicon island decreases with the island size (Figure 48) and that there exists an interesting design window in which channel cracking can be fully suppressed, but stable partial delamination of the islands is allowed; this results in nearly free-expanding particles on a substrate.

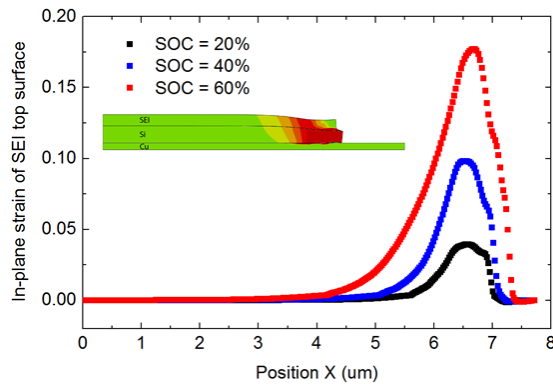


Figure 47. In-plane strain under different states of charge.

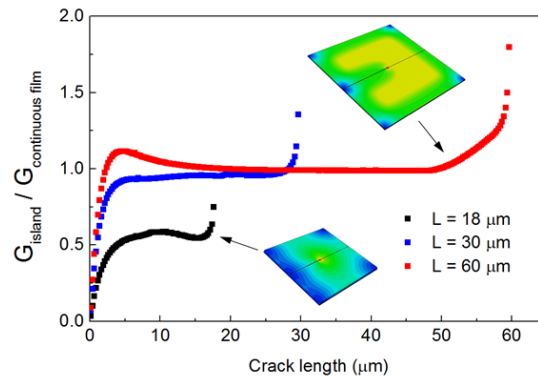


Figure 48. The energy release rate for channel cracking in a silicon island decreases with island size.

Binder free thick Si film electrode. The project further elucidated the effects of voltage limits on the operational performance of cells employing a Li-Si thick-film negative electrode, and a lithium or a $\text{Li-Ni}_{0.6}\text{Mn}_{0.2}\text{Co}_{0.2}\text{O}_2$ counter electrode (Figure 49). When the Li-Si electrode is operated between 0.13 and 0.55 V versus a lithium reference, promising cycling operation is achieved (that is, greater than 500 cycles with retention of 75% of initial cell capacity). It was also demonstrated that mechanical stress in film can retain compressive by controlling the potential window, leading to significantly improved cycle life (Figure 50).

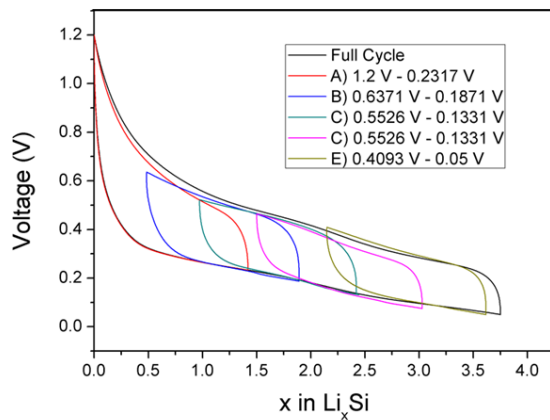


Figure 49. Voltage profile within different potential windows.

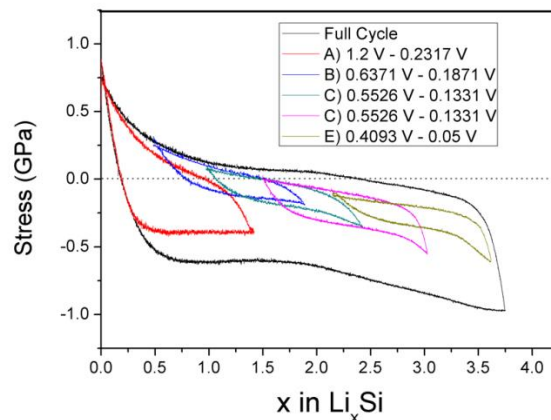


Figure 50. The mechanical stresses within different potential windows.

Patents/Publications/Presentations

Publication

- Kumar, Ravi, and Anton Tokranov, Brian W. Sheldon, Xingcheng Xiao, Zhuangqun Huang, Chunzeng Li, and Thomas Mueller. “Direct Observations of Cracking in the Solid Electrolyte Interphase on Silicon Electrodes for Li-Ion Batteries.” *ACS Energy Lett.* 1 (2016): 689–697. (Research Highlights: “Silicon Islands under Strain,” *Nature Reviews Materials*. doi:10.1038/natrevmats.2016.77.)

Presentation

- Mechanics and Electrochemistry of Energy Materials, 2016 Society of Engineering Science, University of Maryland, College Park, Maryland (October 2-5, 2016): Symposium E-1, “Understanding the Mechanical Behavior of Materials for Electrochemical Energy Storage”; Yang-Tse Cheng.

Task 6.6 – Predicting Microstructure and Performance for Optimal Cell Fabrication (Dean Wheeler and Brian Mazzeo, Brigham Young University)

Project Objective. This work uses microstructural modeling coupled with extensive experimental validation and diagnostics to understand and optimize fabrication processes for composite particle-based electrodes. The first main outcome will be revolutionary methods to assess electronic and ionic conductivities of porous electrodes attached to current collectors, including heterogeneities and anisotropic effects. The second main outcome is a particle-dynamics model parameterized with fundamental physical properties that can predict electrode morphology and transport pathways resulting from particular fabrication steps. These two outcomes will enable the third, which is an understanding of the effects of processing conditions on microscopic and macroscopic properties of electrodes.

Project Impact. This work will result in new diagnostic tools for rapidly and conveniently interrogating electronic and ionic pathways in porous electrodes. A new mesoscale 3D microstructure prediction model, validated by experimental structures and electrode-performance metrics, will be developed. The model will enable virtual exploration of process improvements that currently can only be explored empirically.

Out-Year Goals. This project was initiated April 2013 and concludes December 2016. Goals by fiscal year are as follows.

- 2013: Fabricate first-generation micro-four-line probe, and complete associated computer model.
- 2014: Assess conductivity variability in electrodes; characterize microstructures of multiple electrodes.
- 2015: Fabricate first-gen ionic conductivity probe, N-line probe, and dynamic particle packing (DPP) model.
- 2016: Improve robustness of N-line probe and DPP model; assess structure correlation to conductivity.

Collaborations. Bryant Polzin (ANL) and Karim Zaghib (HQ) provided battery materials. Transfer of technology to A123 to improve their electrode production process took place in FY 2015. There are ongoing collaborations with Simon Thiele (IMTEK, University of Freiburg) and Mårten Behm (KTH, Sweden).

Milestones

1. Demonstrate that the DPP model can accurately imitate the mechanical calendaring process for a representative electrode film. (December 2015 – Complete)
2. Develop a robust numerical routine for interpreting N-line conductivity measurements. (March 2016 – Complete)
3. *Go/No-Go*: Continue work on N-line probe and inversion routine if they can accurately determine anisotropic conductivity for test materials. (June 2016 – Complete)
4. *Go/No-Go*: Demonstrate correlations between DPP modeled conductivities and those determined by focused ion beam (FIB)/SEM and N-line probe. (September 2016 – Partially Complete)

Progress Report

Milestone 3 Go/No-Go (Complete). One of the final goals of this work was to determine by means of the N-line probe the degree of anisotropy, meaning the difference in electronic conductivity in the in-plane and through-plane directions. This was measured for a baseline Toda 523 cathode (provided by ANL) to show less through-plane conductivity than the in-plane conductivity by a factor of around 2. This anisotropy represents inefficiency in the structure of typical electrodes, because higher through-plane conductivity is more desirable for battery performance. The major development that allowed this measurement was an improvement in the N-line probe inversion routine. Nevertheless, it was found that results are sensitive to experimental noise. It is believed that improvements in the probe design (FY 2017) coupled with the improved model will enable this measurement to be improved in accuracy. Table 1 contrasts the results on the same electrode film using the old (isotropic) and new (anisotropic) inversion routines.

Table 1. Comparison of two model inversion results.

	Isotropic Model	Anisotropic Model
Conductivity – out of plane (mS/cm)	474±32	230±31
Conductivity – in plane (mS/cm)	474±32	542±46
Current collector contact resistance ($\Omega\text{-cm}^2$)	0.165±0.013	0.179±0.022

Milestone 4 (Partially Complete). Substantial progress was made toward the final milestone of FY 2016, though it was not fully completed; a related milestone will be completed in FY 2017 under a new contract. The essence of the milestone is to demonstrate substantial agreement between experiment and the predicted conductivity of the DPP model for realistic battery electrode microstructures. It was determined that while the predicted conductivities were qualitatively correct, this was only for uncalendered electrodes. The model needs additional improvements in order to predict the anisotropic structures of realistically coated and calendered electrodes. Such improvements were begun and will be at a stage in FY 2017 that the accuracy of the model can again be assessed. The ultimate goal is to have a quantitatively accurate structure prediction model that will allow process changes to be assessed.

Figure 51 shows a finite-volume method used to assess the conductivity of an uncalendered electrode. Three phases are shown: active (red), carbon/binder domain (black), and pore (white). The method has novel features, namely a multigrid/coarse-graining technique, to speed up computation, causing it to take only a few minutes for a typical set of results.

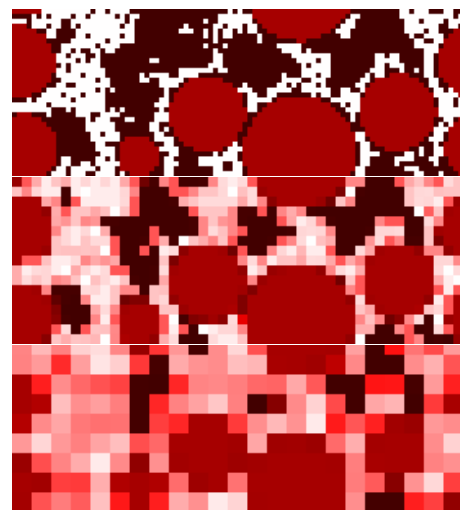


Figure 51. Sequential coarse-graining procedure used to speed up finite-volume conductivity calculation.

Patents/Publications/Presentations

Publications

- Two publications are being prepared.

Presentations

- Electrochemical Society (ECS) Pacific Rim Meeting on Electrochemical and Solid-State Science (PRiME), Honolulu, Hawaii, (October 2016): “A Predictive Model of Lithium-Ion Electrode Fabrication, including Mixing, Coating, Drying, and Calendering”; M. Mehdi Forouzan, Anthony Gillespie, Nicholas Lewis, Brian A. Mazzeo, and Dean R. Wheeler.
- Electrochemical Society (ECS) Pacific Rim Meeting on Electrochemical and Solid-State Science (PRiME), Honolulu, Hawaii, (October 2016): “Correlation of Local Conductivity to Microstructure for Li-Ion Battery Electrodes by Use of a Contact Probe and SEM/FIB”; John E. Vogel, William Lange, Derek Clement, Brian A. Mazzeo, and Dean R. Wheeler.

TASK 7 – METALLIC LITHIUM AND SOLID ELECTROLYTES

Summary and Highlights

The use of a metallic lithium anode is required for advanced battery chemistries like Li-air and Li-S to realize dramatic improvements in energy density, vehicle range, cost economy, and safety. However, the use of metallic lithium with liquid and polymer electrolytes has so far been limited due to parasitic SEI reactions and dendrite formation. Adding excess lithium to compensate for such losses effectively negates the high energy density for lithium in the first place. For a long lifetime and safe anode, it is essential that no lithium capacity is lost to physical isolation from roughening, to dendrites or delamination processes, or to chemical isolation from side reactions. The key risk and current limitation for this technology is the gradual loss of lithium over the cycle life of the battery.

To date there are no examples of battery materials and architectures that realize such highly efficient cycling of metallic lithium anodes for a lifetime of 1000 cycles due to degradation of the Li-electrolyte interface. A much deeper analysis of the degradation processes is needed, so that materials can be engineered to fulfill the target level of performance for EV, namely 1000 cycles and a 15-year lifetime, with adequate pulse power. Projecting the performance required in terms of just the lithium anode, this requires a high rate of lithium deposition and stripping reactions, specifically about 40 μm Li per cycle, with pulse rates up to 10 and 20 nm/s (15 mA/cm²) charge and discharge, respectively. This is a conservative estimate, yet daunting in the total mass and rate of material transport. While such cycling has been achieved for state-of-the-art batteries using *molten* sodium in Na-S and zebra cells, solid sodium and lithium anodes are proving more difficult.

The efficient and safe use of metallic lithium for rechargeable batteries is then a great challenge, and one that has eluded research and development efforts for years. BMR Task 7 takes a broad look at this challenge for both solid-state batteries and batteries continuing to use liquid electrolytes. For the liquid electrolyte batteries, PNNL researchers are examining the use of dual Li salts and organic additives to the typical organic carbonate electrolytes to impede Li corrosion and dendrite formation at both the lithium and graphite anodes. If successful, this is the simplest approach to implement. At Stanford, novel coatings and 3D structures are applied to the lithium surface and appear to suppress roughening and lengthen cycle life. A relatively new family of solid electrolytes with a garnet crystal structure shows superionic conductivity and good electrochemical stability. Four programs chose this family of solid electrolytes for investigation. Aspects of the processing of this ceramic garnet electrolyte are addressed at the University of Maryland and at the University of Michigan (UM), with attention to effect of flaws and the critical current density. Computational models will complement their experiments to better understand interfaces and guide reduction of the lithium and cathode area specific resistance (ASR). At ORNL, composite electrolytes composed of ceramic and polymer phases are being investigated, anticipating that the mixed phase structures may provide additional means to adjust the mechanical and transport properties. The last project takes on the challenge to use nano-indentation methods to measure the mechanical properties of the solid electrolyte, the Li-metal anode, and the interface of an active electrode. Each of these projects involves a collaborative team of experts with the skills needed to address the challenging materials studies of this dynamic electrochemical system.

Highlights. The highlights for this quarter are as follows:

- Less than 10 ohm-cm² was found for the combined electrode interfaces comprised of ALD-treated LLZO against Li metal plus LLZO with a LiFePO₄ cathode wetted with aqueous catholyte. (Task 7.4)
- A candidate Li SEI protection composed of Cu₃N nanoparticles in styrene-butadiene rubber was cast and cycled on copper foil. (Task 7.5)

- Using a dual LiTFSI+LiBOB liquid electrolyte with a special additive provided stable cycling of a 4V Li||NMC half cells for more than 500 1C cycles at 0.6 mA cm⁻². Higher currents shortened the cycle life. (Task 7.6)
- Thin films of lithium ~3μm thick, as demonstrated for prolonged cycling of thin film batteries, are metastable and gradually form pits or disconnected islands. (Task 7.1)
- The effect of grain boundaries on Li dendrites growth across LLZO electrolytes was evaluated by promoting grain growth. (Task 7.2)
- For polymer-ceramic composite electrolytes plasticized with TEGDME, the electrolyte is stable with Li anodes, but the ceramic component does not contribute to the conduction. (Task 7.3)

Task 7.1 – Mechanical Properties at the Protected Lithium Interface (Nancy Dudney, ORNL; Erik Herbert, Michigan Technological U; Jeff Sakamoto, UM)

Project Objective. This project will develop understanding of the Li-metal SEI through state-of-the-art mechanical nano-indentation methods coupled with solid electrolyte fabrication and electrochemical cycling. The goal is to provide the critical information that will enable transformative insights into the complex coupling between the microstructure, its defects, and the mechanical behavior of Li-metal anodes.

Project Impact. Instability and/or high resistance at the interface of lithium metal with various solid electrolytes limit the use of the metallic anode for batteries with high-energy density batteries, such as Li-air and Li-S. The critical impact of this endeavor will be a much deeper analysis of the degradation, so that materials can be engineered to fulfill the target level of performance for EV batteries, namely 1000 cycles and a 15-year lifetime, with adequate pulse power.

Approach. Mechanical properties studies through state-of-the-art nano-indentation techniques will be used to probe the surface properties of the solid electrolyte and the changes to the lithium that result from prolonged electrodeposition and dissolution at the interface. An understanding of the degradation processes will guide future electrolyte and anode designs for robust performance. In the first year, the team will address the two critical and poorly understood aspects of the protected Li-metal anode assembly: (1) the mechanical properties of the solid electrolyte and (2) the morphology of the cycled lithium metal.

Out-Year Goals. Work will progress toward study of the electrode assembly during electrochemical cycling of the anode. This project hopes to capture the formation and annealing of vacancies and other defects in the lithium and correlate this with the properties of the solid electrolyte and the interface.

Collaborations. This project funds work at ORNL, Michigan Technological University (MTU), and UM. Asma Sharafi (UM, Ph. D. student) and Dr. Robert Schmidt (UM) also contribute to the project. Steve Visco (PolyPlus) will serve as a technical advisor.

Milestones

1. Determine elastic properties of battery grade lithium from different sources and preparation, comparing to values from the reference literature. (September 2015 – Complete)
2. Compare lithium properties, uncycled versus cycled, using thin film battery architecture. (June 2016 – Complete)
3. View annealing of defects following a single stripping and plating half cycle, using thin film battery architecture. (September 2016 – Delayed)

Progress Report

For milestones 2 and 3, the project has opted to look at much higher areal capacity than can be achieved with a thin film battery. Using a symmetric Li//Li device, and LLZO electrolyte, the project is looking at deposition and removal of 2-5 μm of Li in a cycle that is $> 10\text{X}$ more than possible with thin film cathode.

Preparing and shipping high quality Li to MTU for nano-indentation continues to be a problem, particularly for the cycled samples where the Li invariably roughens and reacts at the unprotected surface. Consequently, the project is jumping ahead to planned work for Year 3, where equipment is being assembled at MTU to cycle the Li as mounted on the nano-indentation. In this way, the change in Li defect structures with plating or adsorption at the electrolyte can be probed from initiation, as current is applied and as the structure equilibrates. (Milestone 3)

Figure 52 illustrates the problem. With uncycled Li, determination of the elastic modulus and other properties is well behaved. At small depth, the variation is due to the thin reaction

layer at the surface; at large depth, correction must be made for the influence of the rigid LLZO pellet. After transport of Li, however, the shiny silver Li becomes discolored and dull and the results of indent mapping are erratic. This is true for both the source and sink Li electrodes. The problem may be due to inadequate protection of the Li or lack of any stack pressure on the Li. Coordinating the Li transport with the nanoindentation measurements should allow the project to distinguish changes to the bulk Li from the surface.

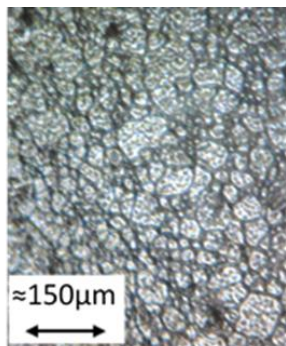


Figure 53. Li grain structure of vapor deposited film.

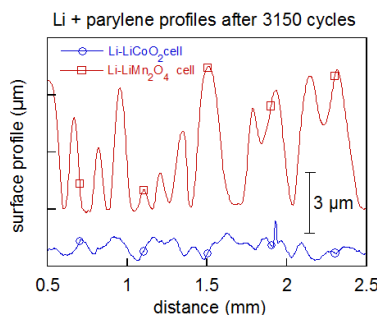


Figure 54. Profile of lithium on a thin film battery after 3150 cycles. The uncycled areas of the Li remained very smooth. The Li is protected with a thin coating of parylene.

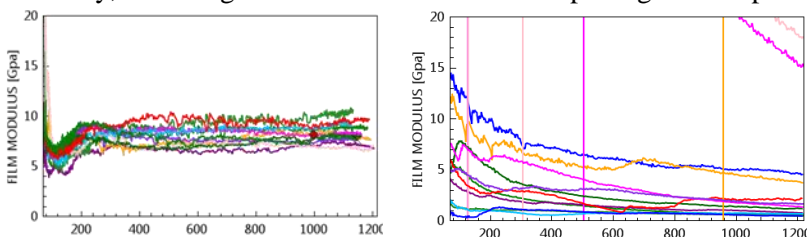


Figure 52. Li modulus recorded for 30 indents for pristine Li film (left, A) and for a Li film following one deep (3 μm) cycle (right, B).

Note that in addition to indentation studies, vapor deposited lithium electrodes from ORNL are also being used in coordination with Task 7.2. Here the thin film Li electrodes are compared side-by-side with Li applied as bulk foils and conditioned with pressure and heating. This is helping to address the source of the high ASR of the interface. As part of both studies, efforts are directed toward learning to control the microstructure of the Li films. Figure 53 shows the larger Li grains achieved this quarter, about 100 μm in size for a $\sim 20\text{-}\mu\text{m}$ thick films.

A final activity this quarter focused on analysis, addressing the causes for the Li redistribution in thin film batteries. This was followed by stylus profilometry. An example of the Li waviness that develops over 3000 cycles is shown in Figure 54. This instability is attributed to the fact that thin films are metastable and tend to form islands. The surprising outcome of the study is that the structure evolution depends on the cathode material and on the duty cycle.

Patents/Publications/Presentations

Publication

- Dudney, Nancy J. “Evolution of the Lithium Morphology from Cycling of Thin Film Solid-State Batteries.” Submitted to *Journal of Electroceramics*. Invited for issue dedicated to Solid State Batteries.

Presentation

- Gordon Research Conference on Thin Film and Small Scale Mechanical Behavior, Lewiston, ME (July 24, 2016): “Dynamic Nanoindentation: State of the Art Experimental Methods”; Erik G. Herbert, Nancy J Dudney, Owen Mills, and Violet Thole. Invited presentation.

Task 7.2 – Solid Electrolytes for Solid-State and Lithium–Sulfur Batteries (Jeff Sakamoto, University of Michigan)

Project Objectives. *Enable advanced Li-ion solid-state and lithium-sulfur EV batteries using LLZO solid-electrolyte membrane technology.* Owing to its combination of fast ion conductivity, stability, and high elastic modulus, LLZO exhibits promise as an advanced solid-state electrolyte. To demonstrate relevance in EV battery technology, several objectives must be met. First, LLZO membranes must withstand current densities approaching $\sim 1 \text{ mA/cm}^2$ (commensurate with EV battery charging and discharging rates). Second, low ASR between lithium and LLZO must be achieved to achieve cell impedance comparable to conventional Li-ion technology ($\sim 10 \text{ Ohms/cm}^2$). Third, low ASR and stability between LLZO and sulfur cathodes must be demonstrated.

Project Impact. The expected outcomes will: (i) enable Li-metal protection, (ii) augment DOE access to fast ion conductors and/or hybrid electrolytes, (iii) mitigate Li-polysulfide dissolution and deleterious passivation of Li-metal anodes, and (iv) prevent dendrite formation. Demonstrating these aspects could enable Li-S batteries with unprecedented end-of-life, cell-level performance: $> 500 \text{ Wh/kg}$, $> 1080 \text{ Wh/l}$, > 1000 cycles, and lasting > 15 years.

Approach. This effort will focus on the promising new electrolyte known as LLZO ($\text{Li}_7\text{La}_3\text{Zr}_2\text{O}_{12}$). LLZO is the first bulk-scale ceramic electrolyte to simultaneously exhibit the favorable combination of high conductivity ($\sim 1 \text{ mS/cm}$ at 298K), high shear modulus (61 GPa) to suppress Li-dendrite penetration, and apparent electrochemical stability ($0\text{--}6 \text{ V}$ vs Li/Li^+). While these attributes are encouraging, additional research and development is needed to demonstrate that LLZO can tolerate current densities in excess of 1 mA/cm^2 , thereby establishing its relevance for PHEV/EV applications. This project hypothesizes that defects and the polycrystalline nature of realistic LLZO membranes can limit the critical current density. However, the relative importance of the many possible defect types (porosity, grain boundaries, interfaces, surface and bulk impurities), and the mechanisms by which they impact current density, have not been identified. Using experience with the synthesis and processing of LLZO (Sakamoto and Wolfenstine), combined with sophisticated materials characterization (Nanda), this project will precisely control atomic and microstructural defects and correlate their concentration with the critical current density. These data will inform multi-scale computation models (Siegel and Monroe), which will isolate and quantify the role(s) that each defect plays in controlling the current density. By bridging the knowledge gap between composition, structure, and performance, this project will determine if LLZO can achieve the current densities required for vehicle applications.

Collaborations. This project collaborates with Don Siegel (UM atomistic modeling), Chuck Monroe (UM, continuum scale modeling), Jagjit Nanda (ORNL, sulfur chemical and electrochemical spectroscopy), and Jeff Wolfenstine (ARL, atomic force microscopy of Li-LLZO interfaces).

Milestones

1. Establish a process to control the microstructural defect that governs the critical current density (CCD) to achieve a $\text{CCD} \geq 1 \text{ mA/cm}^2$. (December 2016 – On schedule)
2. Establish a process to control the atomic-scale defect that governs the CCD to achieve a $\text{CCD} \geq 1 \text{ mA/cm}^2$. (December 2016 – On schedule)
 - 2.1. Design, fabricate, and test beginning of life performance of hybrid Li-LLZO-liquid-S+carbon cells (UM, ORNL). (March 2016 – On schedule)

Progress Report

Milestone 1.6 – Establish a process to control the microstructural defect that governs the CCD to achieve a CCD of ≥ 1 mA/cm². (UM, ORNL, ARL, Oxford).

Several approaches for controlling the microstructural feature that controls the CCD were pursued. One approach was identified and successfully demonstrated control of the grain size, which affects the ratio of grain/grain boundary volume in a polycrystalline material (Figure 55). No other variables such as phase purity or chemical contamination are expected. Next quarter, materials characterization and statistical analysis will be conducted to better understand how the new materials process affects the microstructure and eventually the CCD.

Theory was used to complement the experimental materials development. Atomistic simulation is an integral part of this task and is used to determine how ions flow through and/or around the key microstructural defect.

Milestone 1.7 – Establish a process to control the atomic-scale defect that governs the CCD to achieve a CCD of ≥ 1 mA/cm². (UM, ORNL, ARL, Oxford).

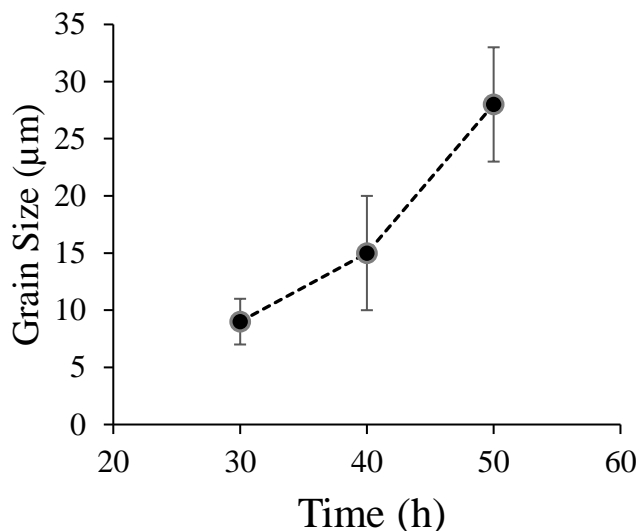


Figure 55. LLZO grain size versus processing time.

Last quarter, atomistic simulations indicated certain atomistic defects, incorporated through adventitious reactions, affect Li-ion transport. Based on the concentration of the defect, the Li-ion transport and the activation was predicted. To validate the simulations, LLZO membranes were fabricated. Next quarter, the atomic defect will be incorporated into the LLZO membranes followed by salient property measurements.

Milestone 2.1. – Design, fabricate, and test beginning of life performance of hybrid Li-LLZO-liquid-S+carbon or SOA cathode cells (UM, ORNL).

Because the counter electrode is Li in Li-LLZO-Li cells, interpretation of cycling data can be difficult. Hybrid Li-LLZO-liquid electrolyte+cathode cells were designed and are being implemented.

Patents/Publications/Presentations

Publication

- Cheng, M., and Y. Cheng, K. Yin, J. Luo, A. Sharafi, J. Sakamoto, K. L. More, N. J. Dudney, and M. Chi. “Interfacial Stability of the Li Metal-Solid Electrolyte Elucidated via *In Situ* Electron Microscopy.” *NanoLetters*, accepted October 2016.

Presentation

- The American Chemical Society Meeting, Philadelphia, Pennsylvania (August 2016): “J. Sakamoto, Solid-State Electrolytes Enabling Beyond Li-Ion Cell Chemistries”; invited speaker.

Task 7.3 – Composite Electrolytes to Stabilize Metallic Lithium Anodes (Nancy Dudney and Frank Delnick, Oak Ridge National Laboratory)

Project Objective. Prepare composites of representative polymer and ceramic electrolyte materials to achieve thin membranes that have the unique combination of electrochemical and mechanical properties required to stabilize the metallic lithium anode while providing for good power performance and long cycle life. Understand the Li-ion transport at the interface between polymer and ceramic solid electrolytes, which is critical to the effective conductivity of the composite membrane. Identify key features of the composite composition, architecture, and fabrication that optimize the performance. Fabricate thin electrolyte membranes to use with a thin metallic lithium anode to provide good power performance and long cycle life.

Project Impact. A stable lithium anode is critical to achieve high energy density with excellent safety, lifetime, and cycling efficiency. This study will identify the key design strategies that should be used to prepare composite electrolytes to meet the challenging combination of physical, chemical, and manufacturing requirements to protect and stabilize the Li-metal anode for advanced batteries. By utilizing well characterized and controlled component phases, the design rules developed for the composite structures will be generally applicable toward the substitution of alternative and improved solid electrolyte component phases as they become available. Success in this program will enable these specific DOE technical targets: 500-700 Wh/kg, 3000-5000 deep discharge cycles, and robust operation.

Approach. This project seeks to develop practical solid electrolytes that will provide stable and long-lived protection for the Li-metal anode. Current electrolytes all have serious challenges when used alone: oxide ceramics are brittle, sulfide ceramics are air sensitive, polymers are too resistive and soft, and many electrolytes react with lithium. Composites provide a clear route to address these issues. This project does not seek discovery of new electrolytes; rather, the goal is to study combinations of current well known electrolytes. The project emphasizes the investigation of polymer-ceramic interfaces formed as bilayers and as simple composite mixtures where the effects of the interface properties can be readily isolated. In general, the ceramic phase is several orders of magnitude more conductive than the polymer electrolyte, and interfaces can contribute an additional source of resistance. Using finite element simulations as a guide, composites with promising compositions and architectures are fabricated and evaluated for Li-transport properties using ac impedance and dc cycling with lithium in symmetric or half cells. General design rules will be determined that can be widely applied to other combinations of solid electrolytes.

Out-Year Goal. Use advanced manufacturing processes where the architecture of the composite membrane can be developed and tailored to maximize performance and cost-effective manufacturing.

Collaborations. Electrolytes under investigation include a garnet electrolyte from Jeff Sakamoto (UM) and ceramic powder from Ohara. Staff at Corning Corporation will serve as the industrial consultant. The student intern from Virginia Technological University (Cara Herwig) assisted this quarter.

Milestones

1. Measure the removal of solvent molecules introduced via solution synthesis or gas absorption from ceramic-polymer composite sheets under vacuum and heating conditions. (March 2016 – Complete)
2. Prepare ceramic-polymer electrolyte sheets with a coating, and map the uniformity with nano-indentation and by profiling the lithium plating. (September 2016 – Completed; Phases are uniformly distributed, but lithium transport is not. See text.)

Progress Report

Additional composite electrolyte membranes were spray coated from aqueous slurry. All membranes were 50 volume % of the ceramic Ohara powders. The uniformity and density of the membranes were investigated by EDX maps in SEM and TEM. For TEM, the slurry was sprayed directly onto holey carbon membranes. The ceramic particles are coated with the polymer and salt, identified by C and F associated with the PEO and the Li Triflate salt. For cross sections of a membrane sprayed on copper foil, see Figure 56, the structure is uniform with even distribution of all the expected elements, including C, O, Ti, P, and F. Figure 56 is a small view of the total area mapped. As will be shown below, the Li ion motion through this composite is still not accessing the ceramic powders, and the conductivity restricted to the polymer phase is inadequate for the EV application. The milestone for this quarter called for mapping the uniformity of the Li plating; obviously, this will not prove uniform because the ceramic effectively blocks the Li^+ ion transport.

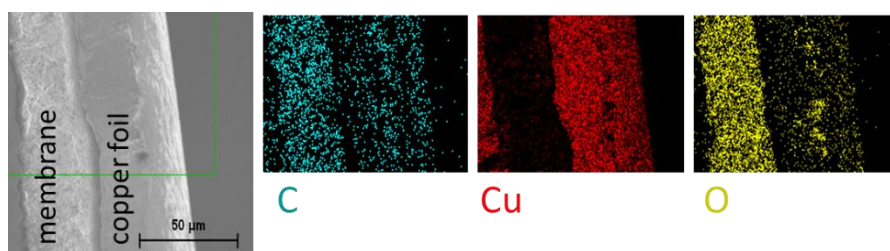


Figure 56. Energy dispersive X-ray maps of 20- μm thick composite electrolyte membrane formed by aqueous spray coating.

Thus, there is a dilemma. The project's most conductive composite is not stable with lithium, and so far, the lithium-stable composite has a higher resistivity. This is summarized as collected plots and images of Figure 57.

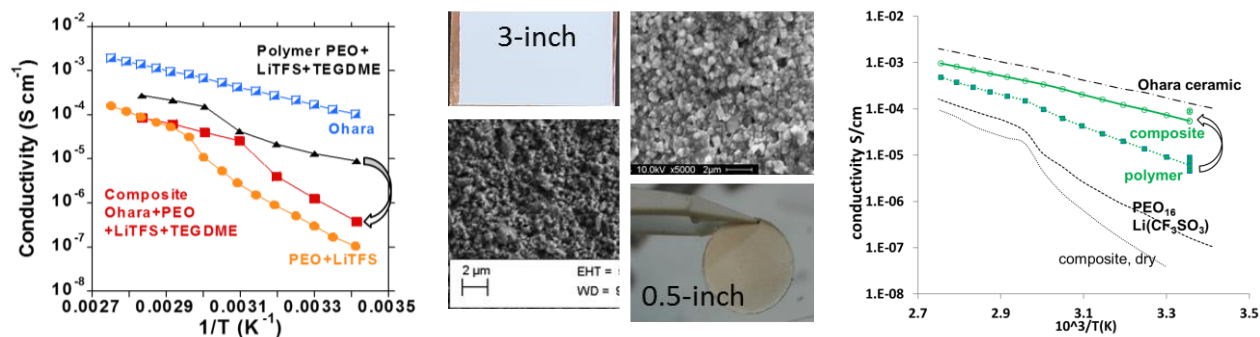


Figure 57. Comparison of the spray coated composites plasticized with TEGDME (left) with the melt-formed composites treated with DMC vapor (right). The polymer electrolytes themselves have about the same conductivity, yet as shown by the arrows, 50 vol% ceramic powder has opposite effects. Photographs and scanning electron microscopy images of both composites are also shown.

Clearly the effects of TEGDME plasticizer differs from that of DMC and other small molecules. While the small molecules may promote Li^+ ion transport across the polymer/ceramic interface, TEGDME likely encapsulates the Li^+ ion, like the PEO matrix. The solvation impedes the transfer to/from the ceramic. Interestingly, the spray-coated composites will not adsorb DMC vapor. Surface modifications of the ceramic powder and adjustments of the polymer composition are being pursued for the spray processed material, as this spray processing is more practical for forming large area and very thin sheets.

Patents/Publications/Presentations/Presentations

Presentation

- Electrochemical Society (ECS) Pacific Rim Meeting on Electrochemical and Solid-State Science (PRiME), Honolulu, Hawaii, (October 2016): “Composite Polymer-Ceramic Electrolyte for High Energy Lithium Secondary Batteries”; Amaresh Samuthira Pandian, Frank Delnick, and Nancy Dudney.

Task 7.4 – Overcoming Interfacial Impedance in Solid-State Batteries (Eric Wachsman, Liangbing Hu, and Yifei Mo, University of Maryland College Park)

Project Objective. Develop a multifaceted and integrated (experimental and computational) approach to solve the key issue in solid-state, Li-ion batteries (SSLIBs), interfacial impedance, with a focus on garnet-based solid-state electrolytes (SSEs), the knowledge of which can be applied to other SSE chemistries. The focus is to develop methods to decrease the impedance across interfaces with the solid electrolyte, and ultimately demonstrate a high power/energy density battery employing the best of these methods.

Project Impact. Garnet electrolytes have shown great promise for safer and high-energy density batteries. The success of the proposed research can lead to dramatic progress on development of SSLIBs based on garnet electrolytes. Regarding fundamental science, the project methodology by combining computations and experiments can lead to an understanding of the thermodynamics, kinetics and structural stability, and evolution of SSLIBs with the garnet electrolytes. Due to the ceramic nature of garnet electrolyte, being brittle and hard, garnet electrolyte particles intrinsically lead to poor contacts among themselves or with electrode materials. A fundamental understanding at the nanoscale and through computations, especially with interface layers, can guide design improvements and eventually lead to commercial use of such technologies.

Approach. SSLIB interfaces are typically planar, resulting in high impedance due to low specific surface area, and attempts to make 3D high surface area interfaces can also result in high impedance due to poor contact (for example, pores) at the electrode-electrolyte interface that hinders ion transport or degrades due to expansion/contraction with voltage cycling. This project will experimentally and computationally determine the interfacial structure-impedance relationship in SSLIBs to obtain fundamental insight into design parameters to overcome this issue. Furthermore, it will investigate interfacial modification (layers between SSE and electrode) to see if it can extend these structure-property relationships to higher performance.

Collaborations. This project is in collaboration with Dr. Venkataraman Thangadurai on garnet synthesis. It will collaborate with Dr. Leonid A. Bendersky (Leader, Materials for Energy Storage Program at NIST) and use neutron scattering to investigate the lithium profile across the bilayer interface with different charge-discharge rates. The project is in collaboration with Dr. Kang Xu in U.S. Army Research Laboratory (ARL) with preparation of perfluoropolyether (PFPE) electrolyte.

Milestones

1. Identify compositions of gel electrolyte to achieve $100 \Omega \cdot \text{cm}^2$. (Milestone 1 – Complete)
2. Determination of interfacial impedance in layered and 3D controlled solid state structures. (Milestone 2 – Complete)
3. Develop computation models to investigate interfacial ion transport with interlayers. (Milestone 3 – Complete)
4. Identify compositions out of 4 types of interlayers and processing with electrolyte/electrode interfacial impedance of $\sim 10 \Omega \cdot \text{cm}^2$. (Milestone 4 – complete)
5. *Go/No Go:* Achieve low impedance resistance ($\sim 10 \Omega \cdot \text{cm}^2$) between electrolyte and anode or between electrolyte and cathode. (Complete)

Progress Report

Reducing the Interfacial Impedance to $10 \Omega \text{ cm}^2$ between Garnet Electrolyte and Electrodes

This project employed a Li-salt aqueous electrolyte as a new interface to reduce the cathode/garnet interfacial resistance. Different from the conventional cathode preparation method using aluminum foil as current collect, the project used carbon cloth to support cathode material (LiFePO_4 , Carbon black and PVDF), because carbon cloth shows much higher resistance to aqueous solution corrosion. Two identical electrodes were pressed on both sides of garnet pellet by titanium foil for electrochemical test.

As shown in Figure 58, the EIS plot of symmetrical cell shows a total resistance of $253 \Omega \text{ cm}^2$. After subtracting the resistance of $238 \Omega \text{ cm}^2$ from garnet (based on conductivity and thickness calculation) and dividing by 2, the interfacial resistance from single cathode/garnet interface is only $7.5 \Omega \text{ cm}^2$, which achieved this quarter's Go/No-Go milestones.

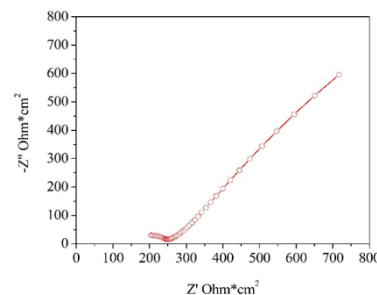


Figure 58. Impedance of a cathode / garnet / cathode symmetric cell with aqueous interface.

For garnet/Li metal anode interface, the project optimized the ALD interface-treating technique. A $\sim 5\text{-}6 \text{ nm}$ thick layer was coated onto the garnet surface by ALD. Then two pieces of Li metal foil were pressed on both sides of the garnet pellet and

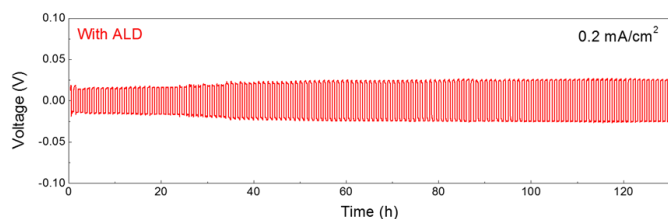


Figure 59. Voltage profile of the atomic layer deposition treated garnet symmetric cell at a current density of 0.2 mA/cm^2 .

heated at 250°C for 1 hour under a small pressure. Figure 59 shows that the cell maintains a stable voltage around 20 mV. Thus, the DC ASR of Li/garnet/Li symmetric cell with ALD interface is $100 \Omega \text{ cm}^2$. The resistance of garnet is $90 \Omega \text{ cm}^2$. The DC ASR of interface is $(\text{Total ASR} - \text{Bulk ASR})/2 = (100 - 90)/2 = 5 \Omega \text{ cm}^2$, which has achieved this quarter's Go/No-Go milestones.

Effect of Structure on Interface

A 3D garnet surface structure can dramatically increase the effective surface area compared with the planar surface. 3D structured garnet line patterns were printed on surface polished garnet pellets and sintered to form structured ionic conductive paths with varying line spacing (Figure 60). Cathode slurries (LiFePO_4 , CNT, and gel) were coated on both flat and 3D structured garnet surfaces. EIS of the symmetrical cells were obtained at room temperature.

The 3D printed lines ($40 \mu\text{m}$ height and $70 \mu\text{m}$ width) increased the effective sample surface areas from 36 mm^2 for polished pellet to 39.9 , 42.3 and 48 mm^2 with increasing line density, resulting in 22%, 35% and 52% reduction of interfacial resistance proportional to the increase in effective surface area (Figure 60). Therefore, as expected the 3D-printed structures reduced the cathode-electrolyte interfacial resistance linearly by increasing effective surface area. Further impedance reduction is anticipated by increasing line density (using smaller printing tips and reduced particle sizes).

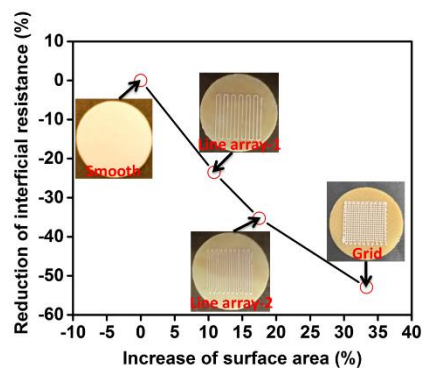


Figure 60. Comparison of cathode/ electrolyte interfacial impedance on flat and 3D-structured garnet pellets, showing reduction of interfacial resistance with increase in surface area.

Patents/Publications/Presentations

Patent

- Liangbing Hu. “Engineered Interface of Solid State Electrolyte and Li Metal Anode with Li-Metal Alloys toward All Solid State Batteries.” PS-2016-053.

Publication

- Luo, W., and Y. Gong, Y. Zhu, K. Fu, J. Dai, S. D. Lacey, C. Wang, B. Liu, X. Han, Y. Mo, E. D. Wachsman, and L. Hu. “Transition from Super-Lithiophobicity to Super-Lithiophilicity of Garnet Solid-State Electrolyte.” *J Am Chem Soc* (2016). doi. 10.1021/jacs.6b06777.

Presentation

- Future Strategies in Electrochemical Technologies for Efficient Energy Utilization, Tours, France (September 7-9, 2016): “Ion Conducting Oxides for Electrochemical Energy Conversion and Storage”; Eric Wachsman.

Task 7.5 – Nanoscale Interfacial Engineering for Stable Lithium-Metal Anodes (Yi Cui, Stanford University)

Project Objective. This study aims to render Li-metal anode with high capacity and reliability by developing chemically and mechanically stable interfacial layers between lithium metal and electrolytes, which is essential to couple with sulfur cathode for high-energy, Li-S batteries. With the nanoscale interfacial engineering approach, various kinds of advanced thin films will be introduced to overcome issues related to dendritic growth, reactive surface, and virtually “infinite” volume expansion of Li-metal anode.

Project Impact. Cycling life and stability of Li-metal anode will be dramatically increased. The success of this project, together with breakthroughs of sulfur cathode, will significantly increase the specific capacity of lithium batteries and decrease cost as well, therefore stimulating the popularity of EVs.

Out-Year Goals. Along with suppressing dendrite growth, the cycle life, Coulombic efficiency, and current density of Li-metal anode will be greatly improved (that is, no dendrite growth for current density up to 3.0 mA/cm², with Coulombic efficiency greater than 99.5%) by choosing the appropriate interfacial nanomaterial along with rational electrode material design.

Milestones

1. Demonstrate the improved cycling performance and effective dendrite suppression using nanoporous Li metal electrode with largely increased electrode active surface area. (December 2015 – Completed)
2. Achieve minimum relative volume change during electrochemical cycling via host-Li composite electrode design. (December – Completed)
3. Study the relative affinity of lithium for different materials. (March 2016 – Completed)
4. Demonstrate facile, low-cost, scalable fabrication of porous host-lithium composite electrodes. (March 2016 – Completed)
5. Detailed study on the Li-rGO composite anode. (June 2016 – Completed)
6. Propose promising material design strategies for the surface protection of three-dimensional nanoporous Li metal anode. (September 2016 – Completed)

Progress Report

In recognition of the problems associated with the “hostless” nature of Li metal, the project successfully introduced stable hosts for metallic Li such as layered reduced graphene oxide and nanofibers with ‘lithiophilic’ coatings. The approach minimized the volumetric change at the whole electrode level, and resulted in 3D, porous Li, which reduced the effective current density and the degree of interface fluctuation during cycling; this led to more uniform Li deposition with greatly improved cycling stability. Engineering the SEI layer on porous Li electrodes is the next step needed to further improve cycling efficiency. Several requirements need to be satisfied for an ideal SEI layer. First, it must be homogeneous in all aspects (composition and morphology, etc.) to ensure uniform Li metal nucleation and growth. Second, it must possess high elastic modulus and compact structure to mechanically suppress Li dendrite. Third, the SEI layer must be flexible enough to accommodate the inevitable interface fluctuation during battery cycling without repeated breakdown/repair. Importantly, high ionic conductivity of the SEI layer is essential to facilitate the uniform transport of Li ions throughout the whole electrode surface.

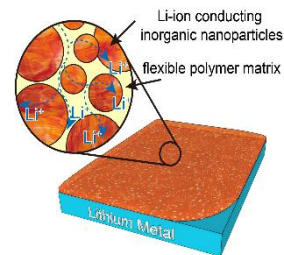


Figure 61. Schematic illustration of the proposed artificial solid electrolyte interphase structure with Li-ion conducting inorganic nanoparticles and polymeric binder.

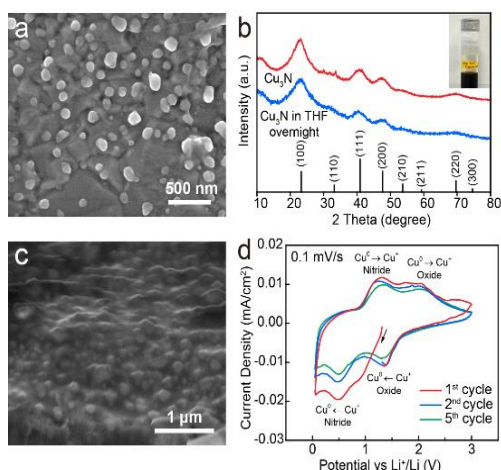


Figure 62. (a) Scanning electron microscopy (SEM) image of the Cu_3N nanoparticles. (b) X-ray diffraction patterns of the as-synthesized Cu_3N nanoparticles, and Cu_3N nanoparticles dispersed in tetrahydrofuran (THF) overnight. The inset picture demonstrates the good dispersity of the Cu_3N nanoparticles in THF. (c) Top-view SEM image of the doctor-bladed Cu_3N +SBR coating on Cu foil. (d) Cyclic voltammetry scans.

During the first delithiation, the anodic peak centered at ~ 1.3 V corresponds well with the oxidation of Cu^0 to Cu^+ in Cu_3N , while the anodic peak at ~ 2.1 V is associated with the oxidation of Cu^0 to Cu^+ in Cu_2O . Fortunately, the electrochemical potential of Li metal anode will usually not exceed the decomposition voltage (~ 0.5 V theoretically) of Li_3N under normal operation conditions, guaranteeing validity of the proposed coating as a Li-ion conducting artificial SEI on Li metal electrode.

This project would like to propose a composite artificial SEI layer design for the stabilization of Li metal anode, which will be composed of a mechanically robust and Li-ion conducting inorganic phase connected by a flexible organic binder to maintain structural integrity during cycling, as illustrated in Figure 61. For the proof-of-concept, the project has chosen Cu_3N nanoparticles as the inorganic phase, and a common binder material, styrene-butadiene rubber (SBR), as the polymeric phase. Sub 100-nm Cu_3N nanoparticles can be easily obtained by a one-step solution reaction, and they afford a stable dispersion with SBR in solvents such as tetrahydrofuran (Figure 62a-b). Notably, the Cu_3N nanoparticles will be passivated spontaneously when in contact with metallic Li to form Li_3N , which is among one of the fastest Li-ion conductors, with ionic conductivity on the order of $\sim 10^{-3}$ – 10^{-4} S cm^{-1} at room temperature. To evaluate the electrochemical properties of the Cu_3N +SBR artificial SEI layer, it was first applied on Cu foil current collector via doctor blading (Figure 62c). CV was carried out to confirm the conversion of Cu_3N to Li_3N in the presence of Li (Figure 62d). During the first CV cycle, a main cathodic peak at ~ 0.48 V was observed, confirming the lithiation of Cu_3N . It is noted that the conversion reaction is only partially reversible.

Patents/Publications/Presentations

Publications

- Liu, Y., and D. Lin, Z. Liang, J. Zhao, K. Yan, and Y. Cui. “Lithium-Coated Polymeric Matrix as a Minimum Volume-Change and Dendrite-Free Lithium Metal Anode.” *Nat. Commun.* 7 (2016): 10992.
- Liang, Z., and D. Lin, J. Zhao, Z. Lu, Y. Liu, C. Liu, Y. Lu, H. Wang, K. Yan, X. Tao, and Y. Cui. “Composite Lithium Metal Anode by Melt Infusion of Lithium into a 3D Conducting Scaffold with Lithiophilic Coating.” *Proc. Natl. Acad. Sci. U.S.A.* 113 (2016): 2862.

Task 7.6 – Lithium Dendrite Suppression for Lithium-Ion Batteries (Wu Xu and Ji-Guang Zhang, Pacific Northwest National Laboratory)

Project Objective. The project objective is to enable lithium metal to be used as an effective anode in rechargeable Li-metal batteries for long cycle life at a reasonably high current density. The investigation will focus on the effects of various lithium salts, additives, and carbonate-based electrolyte formulations on Li-anode morphology, lithium Coulombic efficiency, and battery performances in terms of long-term cycling stability at room temperature and elevated temperatures and at various current density conditions, rate capability, and low-temperature discharge behavior. The surface layers on lithium anode and cathode will be systematically analyzed. The properties of solvates of cation-solvent molecules will also be calculated to help explain the obtained battery performances.

Project Impact. Lithium metal is an ideal anode material for rechargeable batteries. Unfortunately, uncontrollable dendritic lithium growth and limited Coulombic efficiency during lithium deposition/stripping inherent in these batteries have prevented their practical applications. This work will explore the new electrolyte additives that can lead to dendrite-free lithium deposition with high Coulombic efficiency. The success of this work will increase energy density of lithium and Li-ion batteries and accelerate market acceptance of EVs, especially for PHEVs required by the EV Everywhere Grand Challenge proposed by the DOE/EERE.

Out-Year Goals. The long-term goal of the work is to enable lithium and Li-ion batteries with >120 Wh/kg (for PHEVs), 1000 deep-discharge cycles, a 10-year calendar life, improved abuse tolerance, and less than 20% capacity fade over a 10-year period.

Collaborations. This project engages in collaboration with the following:

- Bryant Polzin (ANL) – NCA, NMC, and graphite electrodes
- Vincent Battaglia (LBNL) – LFP electrode
- Chongmin Wang (PNNL) – Characterization by TEM/SEM

Milestones

1. Develop mixed salts electrolytes to protect aluminum substrate and Li-metal anode, and to maintain lithium Coulombic efficiency over 98%. (December 2015 – Complete)
2. Demonstrate over 500 cycles for Li|LFP cells with high LFP loading and at high current density cycling. (March 2016 – Complete)
3. Demonstrate over 200 cycles for 4-V Li-metal batteries with high cathode loading and at high current density cycling. (June 2016 – Complete)
4. Achieve over 500 cycles for 4-V Li-metal batteries with high cathode loading and at high current density cycling. (September 2016 – Complete)

Progress Report

This quarter, the effects of the additive X in the LiTFSI-LiBOB dual-salt electrolyte on the performances of Li||NMC coin cells were further investigated and compared with the dual-salt electrolyte without additive and the conventional LiPF₆ electrolyte. The NMC cathode had a moderately high areal capacity of $\sim 1.75 \text{ mAh cm}^{-2}$ ($\sim 10.8 \text{ mg active material cm}^{-2}$). The amount of the additive in the dual-salt electrolytes was optimized to be 0.05 M. With the electrolyte containing optimized amount of additive, the Li||NMC cells can be stably cycled for at least 400 cycles at a charging/discharging current density of 1.75 mA cm^{-2} at 60°C and at least 800 cycles when the cells were cycled at room temperature at the charging current density of 0.58 mA cm^{-2} and the discharging current density of 1.75 mA cm^{-2} . Detailed analyses were conducted to identify the fundamental mechanism for the significantly improved long-term cycling stability and fast charging capability of Li||NMC cells with the additive X containing LiTFSI-LiBOB dual-salt electrolyte. The SEM images of Li metal anodes after 100 cycles are shown in Figure 63. The LiPF₆-electrolyte caused significant cracking and severe corrosion of bulk Li anode (Figure 63a) and sporadic needle-like dendritic Li (Figure 63d) and led to high resistance of the cell. In contrast, when dual-salt electrolytes were used, the bulk Li metal was well reserved with a corrosion depth of about only 30–50 μm (Figure 63b-c) and the Li surface had a fibrous morphology (Figure 63e-f). Furthermore, the Li metal cycled in the additive X containing dual-salt electrolyte had more compact and well adhesive surface layer and uniform fibrous Li morphology with a diameter of $\sim 1 \mu\text{m}$ and a length ranging from $\sim 10 \mu\text{m}$ to several tens microns. This electrolyte also gave very small cell impedance. The XPS results show that the SEI layers formed in the dual-salt electrolytes were dominated by polycarbonate species, especially when additive X was used.

The Li||NMC cells with high NMC loading (3.0 mAh cm^{-2}) were also tested with an additive-containing dual-salt electrolyte. After formation cycles at 0.3 mA cm^{-2} (that is, C/10 rate), the cells can be stably cycled for about 100 cycles at 3.0 mA cm^{-2} (that is, 1C), 300 cycles at 1.0 mA cm^{-2} (that is, C/3) charging and at least 500 cycles at 0.6 mA cm^{-2} (that is, 1C) charging (Figure 64). These results indicated that increased charging current density led to a shorter cycle life of Li||NMC cells.

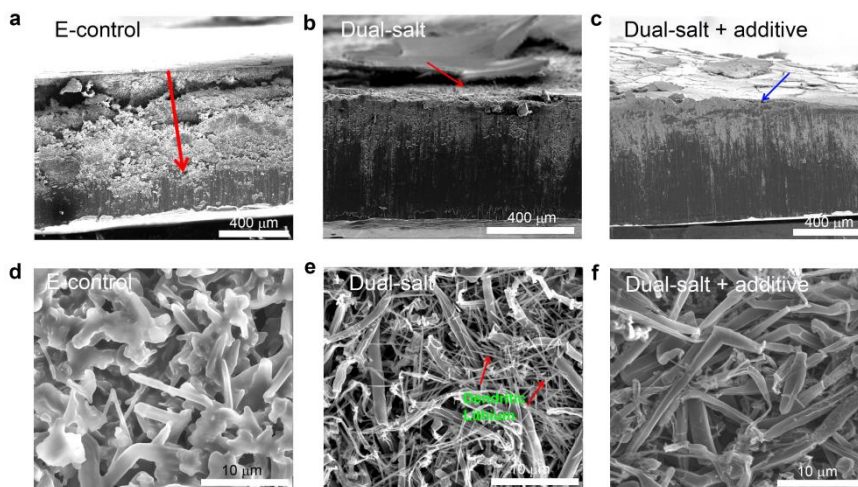


Figure 63. Morphological images of Li metal anodes. (a-c) Cross-section view. (d-f) Top view of Li metal anodes retrieved from Li||NMC cells after 100 cycles using (a, d) conventional LiPF₆ electrolyte, (b, e) dual-salt (LiTFSI-LiBOB) electrolyte, and (c, f) 0.05 M LiPF₆-added dual-salt electrolyte.

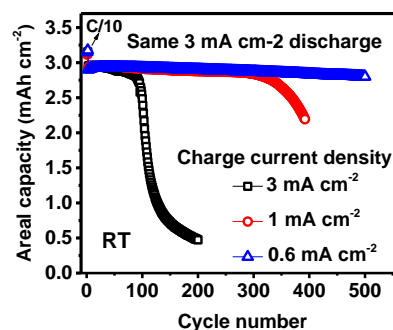


Figure 64. Cycling performance of Li||NMC cells with 3.0 mAh cm^{-2} NMC loading and using an additive-containing dual-salt electrolyte at 30°C .

Patents/Publications/Presentations

Publication

- Zheng, J., and M. H. Engelhard, D. Mei, S. Jiao, B. J. Polzin, J.-G. Zhang,* and W. Xu.* “Fast Charging and Stable Cycling Lithium Metal Batteries.” Submitted for publication.

TASK 8 – LITHIUM–SULFUR BATTERIES

Summary and Highlights

Advances in Li-ion technology have been stymied by challenges involved in developing high reversible capacity cathodes and stable anodes. Hence, there is a critical need for development of alternate battery technologies with superior energy densities and cycling capabilities. In this regard, Li-S batteries have been identified as the next flagship technology, holding much promise due to the attractive theoretical specific energy densities of 2,567 Wh/kg. In addition, realization of the high theoretical specific capacity of 1,675 mAh/g corresponding to formation of Li_2S using earth-abundant sulfur renders the system highly promising compared to other available cathode systems. Thus, the research focus has shifted to developing Li–S batteries. This system, however, suffers from major drawbacks, as elucidated below.

- Limited inherent electronic conductivity of sulfur and sulfur compound based cathodes.
- Volumetric expansion and contraction of both the sulfur cathode and lithium anode.
- Soluble polysulfide formation/dissolution and sluggish kinetics of subsequent conversion of polysulfides to Li_2S resulting in poor cycling life.
- Particle fracture and delamination as a result of the repeated volumetric expansion and contraction.
- Irreversible loss of lithium at the sulfur cathode, resulting in poor Coulombic efficiency.
- High diffusivity of polysulfides in the electrolyte, resulting in plating at the anode and consequent loss of driving force (that is, drop in cell voltage).

These major issues cause sulfur loss from the cathode, leading to mechanical disintegration. Additionally, surface passivation of anode and cathode systems results in a decrease in the overall specific capacity and Coulombic efficiency upon cycling. As a result, the battery becomes inactive within the first few charge-discharge cycles. Achievement of stable high capacity in Li-S batteries requires execution of fundamental studies to understand the degradation mechanisms in conjunction with engineered solutions. BMR Task 8 addresses both aspects with execution of esoteric, fundamental *in situ* XAS and *in situ* electron paramagnetic resonance (EPR) studies juxtaposed with applied research comprising use of suitable additives, coatings, and exploration of composite morphologies. Both ANL and LBNL use X-ray based techniques to study phase evolution and loss of Coulombic efficiency in Se_8 during lithiation/delithiation, while understanding polysulfide formation in sulfur and polysulfides (PSL) in oligomeric PEO solvent, respectively. Work from PNNL, University of Pittsburgh (U Pitts), and Stanford University demonstrates high areal capacity electrodes in excess of 2 mAh/cm². Following loading studies reported in the first quarter, PNNL has performed *in situ* EPR to study reaction pathways mediated by sulfur radical formation. Coating/encapsulation approaches adopted by U Pitts and Stanford comprise flexible sulfur wire (FSW) electrodes coated with Li-ion conductors, and TiS_2 encapsulation of Li_2S in the latter, both ensuring polysulfide retention at sulfur cathodes. BNL work has focused on benchmarking of pouch cell testing by optimization of the voltage window and study of additives such as LiI and LiNO_3 . *Ab initio* studies at Stanford and U Pitts involving calculation of binding energies and reaction pathways, respectively, augment the experimental results. AIMD simulations performed at TAMU reveal multiple details regarding electrolyte decomposition reactions and the role of soluble polysulfides (PS) on such reactions. Using kinetic Monte Carlo (KMC) simulations, electrode morphology evolution and mesostructured transport interaction studies were also executed. Each of these projects has a collaborative team of experts with the required skill set needed to address the EV Everywhere Grand Challenge of 350 Wh/kg and 750 Wh/l, and cycle life of at least 1000 cycles.

Highlights. Studies at ANL (Khalil Amine-ANL) have identified the difference between carbonate electrolytes and fluorinated electrolytes. They observed that reversible capacities in the carbonate electrolytes are only around 300 mAh g⁻¹ for 50 cycles due to the nucleophilic reaction between polysulfides and carbonate electrolytes. However, fluorinated electrolytes not only significantly suppress the formation of soluble polysulfides and polyselenides, but also prevent the nucleophilic reaction, which indicates that they are a very promising electrolyte for selenium-sulfur (S₅Se₂/C) cathode systems.

A detailed AIMD study (Balbuena-TAMU) of the reactions at the surface of Li metal has shown the buildup of the various species due to the long-chain polysulfide migration from cathode to anode. These simulations demonstrated the rapid formation of Li₂S on the Li metal surface and its dependence on the exposed crystallographic surface. In the presence of an oxidant such as LiNO₃, the most likely products would be sulfates and sulfites. However, the polysulfide species continue forming Li₂S even when a sulfate film starts to cover the anode surface, at least up to a certain thickness that would avoid electron transfer.

Task 8.1 – New Lamination and Doping Concepts for Enhanced Lithium–Sulfur Battery Performance (Prashant N. Kumta, University of Pittsburgh)

Project Objective. The project objective is to successfully demonstrate generation of novel sulfur cathodes for Li-S batteries meeting targeted gravimetric energy densities ≥ 350 Wh/kg and ≥ 750 Wh/l with a cost target \$125/kWh and cycle life of at least 1000 cycles for meeting the EV Everywhere blueprint. The proposed approach will yield sulfur cathodes with specific capacity ≥ 1400 mAh/g, at ≥ 2.2 V, generating ~ 460 Wh/kg energy density higher than the target. Full cells meeting the required deliverables will also be made.

Project Impact. Identifying new laminated S-cathode-based systems displaying higher gravimetric and volumetric energy densities than conventional Li-ion batteries will likely result in new commercial battery systems that are more robust, capable of delivering better energy and power densities, and more lightweight than current Li-ion battery packs. Strategies and configurations based on new Li-ion conductor (LIC)-coated sulfur cathodes will also lead to more compact battery designs for the same energy and power density specifications as current Li-ion systems. Commercialization of these new S-cathode-based Li-ion battery packs will represent, fundamentally, a major hallmark contribution of the DOE VTO and battery community.

Out-Year Goals. This is a multi-year project comprising of three major phases to be successfully completed in three years. Phase 1 (Year 1): Synthesis, Characterization, and Scale up of suitable LIC matrix materials and multilayer composite sulfur cathodes. This phase is completed. Phase 2 (Year 2): Development of LIC-coated sulfur nanoparticles, scale up of high-capacity engineered LIC-coated multilayer composite electrodes and doping strategies for improving electronic conductivity of sulfur. Phase 3 (Year 3): Advanced high energy density, high rate, extremely cyclable cell development.

Collaborations. The project collaborates with the following members with the corresponding expertise:

- Dr. Spandan Maiti (U Pitts): for mechanical stability and multi-scale modeling
- Dr. A. Manivannan (NETL): for XPS for surface characterization
- Dr. D. Krishnan Achary (U Pitts): for solid-state MAS-NMR characterization

Milestones

1. Develop novel LIC membrane systems using *ab initio* methods displaying impermeability to sulfur diffusion and demonstrate generation of novel sulfur 1D, 2D and 3D morphologies exhibiting superior stability and capacity. (June 2015 – Complete)
2. Identification of suitable dopants and dopant compositions to improve electronic conductivity of sulfur. (October 2015 – Complete)
3. Preparing doped LIC with improved ionic conductivity. (January 2016 – Complete)
4. Doping Sulfur with like-sized dopants with enhanced electronic properties. (April 2016 – Complete)
5. Developing organic and inorganic Complex Framework Networks (CFN) as effective polysulfide traps. (July 2016 – Complete)
6. Application of inorganic framework material to improve the specific capacity of commercial sulfur to ~ 712 mAh/g for over 100 cycling and developed ceramic filler incorporated composite polymer electrolytes (CPE) with improved lithium ionic conductivity. (October 2016 – Complete)
7. Synthesis of vertically aligned carbon nanotube and LIC coated nanosulfur based composite materials. (Ongoing)
8. Design and engineering of high-capacity, LIC-coated sulfur nanoparticles. (Ongoing)

Progress Report

Phase 1 concluded with replacement of the commercial separator with a LIC with and successful demonstration of prevention of polysulfide dissolution. Development of LIC-coated sulfur nanoparticles, improvement in the conductivity of LIC by coating, and development of engineered coating strategies are the primary aims of Phase 2. The first three quarters focused on improving the ionic conductivity of LIC by doping, altering the electronic structure of sulfur with size-matched dopants, and designing effective methods for coating LIC onto sulfur cathodes. Accordingly, sulfur infiltrated framework materials (SFM) with higher ionic conductivities

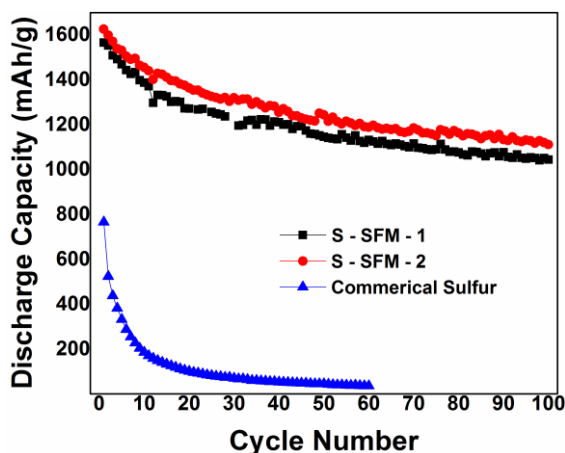


Figure 65. Cycling performance of Sulfur-infiltrated framework material.

were developed and upon testing showed an initial capacity of 1626 mAh/g with stable performance of 1044 mAh/g for over 100 cycles (Figure 65). This quarter involved the development of CPE with solid-state fillers using simple wet-chemical techniques that demonstrated high capacity and prevention of polysulfide dissolution. The CPE demonstrated an electrolyte uptake of ~200 wt% (Figure 66a) with room-temperature ionic conductivities similar to organic liquid electrolytes. Testing of these CPEs with commercial sulfur cathodes showed an initial capacity of 894 mAh/g, which remained very stable demonstrating capacity of ~809 mAh/g after 50 cycles (Figure 66b). Commercial sulfur electrodes normally undergo capacity loss to < 100 mAh/g after 10 cycles. Thus, the CPE material demonstrates significant advancement in sulfur electrolytes. The cycling

stability of the cathodes tested with CPE is likely due to the physical properties and optimized electrolyte content of these separator-electrolytes.

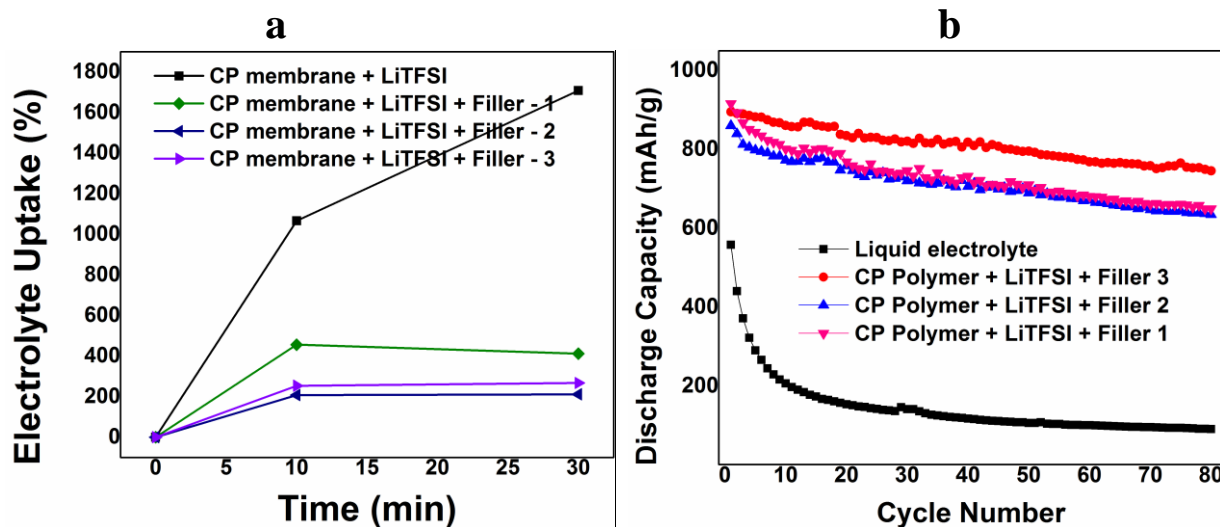


Figure 66. (a) Electrolyte uptake of composite polymer electrolyte (CPE) membranes. (b) Cycling behavior of CPE membranes.

Patents/Publications/Presentations

Patent

- Jampani, P. H., and B. Gattu, P. M. Shanthi, and P. N. Kumta. Novel Electro-Spun Sulfur Wires for Fabricating Mattes of Lithium-Sulfur Batteries. International Patent Number: WO 2016/145429 A1. Awarded: September 15, 2016.

Publication

- Shanthi, P. M, and P. H. Jampani, B. Gattu, M. Sweeney, M. K. Datta, and P. N. Kumta. “Nanoporous Non-Carbonized Metal Organic Frameworks (MOFs): Effective Sulfur Hosts for High Performance Li-S Batteries.” Manuscript submitted, 2016.

Presentation

- The Electrochemical Society, Honolulu, Hawaii (Fall 2016): “Doped Lithium Orthosilicates – Promising High Rate Lithium-Ion Conductors for Li-S Batteries”; P. M. Shanthi, and P. H. Jampani, B. Gattu, O. I. Velikokhatnyi, and P. N. Kumta.

Task 8.2 – Simulations and X-Ray Spectroscopy of Lithium–Sulfur Chemistry (Nitash Balsara, Lawrence Berkeley National Laboratory)

Project Objective. Li-S cells are attractive targets for energy storage applications as their theoretical specific energy of 2600 Wh/kg is much greater than the theoretical specific energy of current Li-ion batteries. Unfortunately, the cycle-life of Li-S cells is limited due to migration of species generated at the sulfur cathode. These species, collectively known as polysulfides, can transform spontaneously, depending on the environment, and it has thus proven difficult to determine the nature of redox reactions that occur at the sulfur electrode. The project objective is to use XAS to track species formation and consumption during charge-discharge reactions in a Li-S cell. Molecular simulations will be used to obtain X-ray spectroscopy signatures of different polysulfide species, and to determine reaction pathways and diffusion in the sulfur cathode. The long-term objective is to use mechanistic information to build high specific energy lithium-sulfur cells.

Project Impact. Enabling rechargeable Li-S cells has potential to change the landscape of rechargeable batteries for large-scale applications beyond personal electronics due to: (1) high specific energy, (2) simplicity and low cost of cathode (the most expensive component of Li-ion batteries), and (3) earth abundance of sulfur. The proposed diagnostic approach also has significant potential impact, as it represents a new path for determining the species that form during charge-discharge reactions in a battery electrode.

Approach. Experimental XAS of charging/discharging lithium sulfur batteries will be used to examine battery reaction mechanisms *in situ*. Theoretical XAS calculations and molecular dynamics simulations will be used to provide a molecular-level understanding and conclusive interpretation of experimental observations.

Out-Year Goals. The out-year goals are as follows:

- Year 1: Simulations of sulfur and PSL in oligomeric PEO solvent. Prediction of X-ray spectroscopy signatures of PSL/PEO mixtures. Measurement of X-ray spectroscopy signatures of PSL/PEO mixtures.
- Year 2: Use comparisons between theory and experiment to refine simulation parameters. Determine speciation in PSL/PEO mixtures without resorting to ad hoc assumptions.
- Year 3: Build an all-solid lithium-sulfur cell that enables measurement of X-ray spectra *in situ*. Conduct simulations of reduction of sulfur cathode.
- Year 4: Use comparisons between theory and experiment to determine the mechanism of sulfur reduction and Li₂S oxidation in all-solid Li-S cell. Use this information to build Li-S cells with improved life-time.

Collaborations. This project collaborates with Tsu-Chien Weng, Dimosthenis Sokaras, and Dennis Nordlund at SSRL, SLAC National Accelerator Laboratory in Stanford, California.

Milestones

1. Establish disproportionation thermodynamics in solvents with high and low electron pair donor (EPD) numbers using theoretical calculations. (December 2015 – Complete)
2. Extend theoretical calculations of XAS to dimethylformamide, a model solvent for high EPD number solvents that stabilize radical polysulfide anions. (February 2016 – Complete)
3. Perform *in situ* XAS tests of Li-S charge/discharge. (May 2016 – Complete)
4. Vary charge/discharge rate for *in situ* XAS testing; compare reaction pathways. (August 2016 – Ongoing)

Progress Report

While dissolution of lithium polysulfides is a well-known problem in Li-S batteries, there is a lack of fundamental understanding of how the polysulfides are dissolved and solvated in battery electrolytes. The recent work herein has focused on elucidating the thermodynamic origins of the solubility of polysulfides. The solubility of isolated lithium polysulfides is calculated from first-principles molecular dynamics simulations. The project explored the associated changes in the dissolution free energy, enthalpy, and entropy in two solvents: dimethylformamide (DMF) and 2-methoxyethyl ether (diglyme). The calculated results show that while the dissolution free energy and solubility of neutral S_8 in diglyme is similar to DMF, lithium polysulfides are significantly less soluble in diglyme than in DMF (Figure 67). A decrease in solvent entropy is associated with the dissolution because solvent molecules need to reorient to screen the electrostatic environment presented by the polysulfides. The losses in the dissolution entropy are far more pronounced in diglyme than in DMF, owing to the rigid solvate structures with highly chelated lithium ions, which greatly restricts the mobility of the associated solvent molecules and the solvate self-diffusion. The entropic losses in the radicals are even larger than in the dianions, due to the more rigid and polar solvate structure of LiS_x motif; this results in a net unfavorable free energy of dissolution.

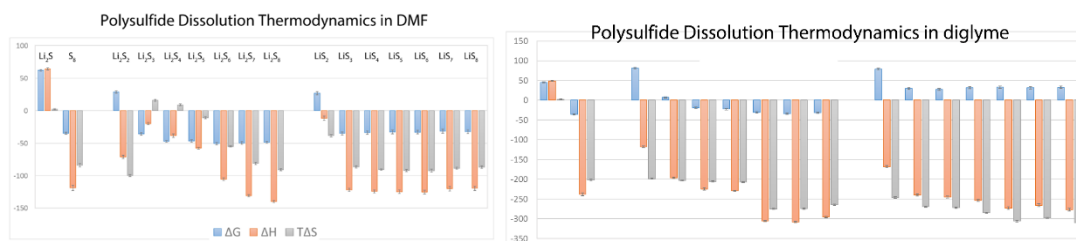


Figure 67. Polysulfide dissolution thermodynamics in dimethylformamide (top) and diglyme (bottom) calculated from first principles (kcal/mol).

In situ X-ray absorption spectroscopy at the sulfur K-edge was used to probe the back of a thick Li-S cathode during discharge. The experimentally obtained spectra were interpreted using theoretical spectral standards previously generated by this group. Analysis of spectra and fluorescence intensity measured during each scan showed that polysulfide dianion species produced by electrochemical reactions diffused to the back of the cathode during discharge. To the best of the group's knowledge, this is the first

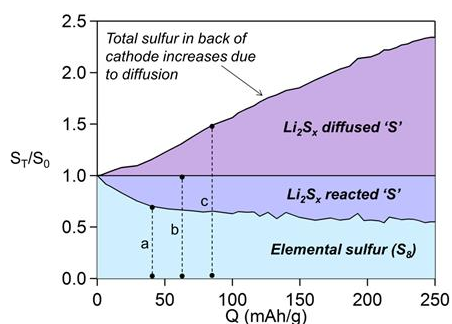


Figure 68. Ratio of total sulfur (on an atomic basis) in the back of the cathode (S_T) to the original amount of sulfur in the back of the cathode (S_0).

time this phenomenon has been quantified. This finding is explained as follows: the limited diffusion of lithium ions to the back of a thick Li-S cathode will lead to higher reaction rates in the front of the cathode relative to the back of the cathode. This difference in reaction rate leads to a higher concentration of polysulfide dianions in the front of the cathode, which creates a concentration gradient that leads to diffusion of polysulfide dianions to the back of the cathode (Figure 68).

The conversion of sulfur in the back of the cathode occurs in two distinct steps. In the first step, elemental sulfur is consumed by a combination of electrochemical reduction and chemical reactions. In the second step, elemental sulfur is consumed by chemical reactions alone. Going further, the group's results suggest that intermediate chain polysulfide dianions (Li_2S_x , $4 \leq x \leq 6$) are the

dominant species at the back of the cathode. Since elemental sulfur is a crystalline insulating solid, it is likely that reactions between elemental sulfur and these intermediate chain length polysulfide dianions are essential for complete utilization of a sulfur cathode.

Patents/Publications/Presentations

Publications

- Wujcik, K. H., and D. R. Wang, A. Raghunathan, M. Drake, T. A. Pascal, D. Prendergast, N. P. Balsara. “Lithium Polysulfide Radical Anions in Ether-Based Solvents.” *Journal of Physical Chemistry C* 120, no. 33 (2016): 18403-18410. doi: 10.1021/acs.jpcc.6b04264.
- Pascal, T., and K. Wujcik, D. Wang, N. Balsara, and D. Prendergast. “Thermodynamic Origins of the Solvent-Dependent Solubility of Lithium Polysulfides from First Principles.” *Journal of the American Chemical Society*, under review.
- Wujcik, K., and D. Wang, T. Pascal, D. Prendergast, and N. Balsara. “*In Situ* X-ray Absorption Spectroscopy Studies of Discharge Reactions in a Thick Cathode of a Lithium Sulfur Battery.” *Journal of the Electrochemical Society*, under review.

Task 8.3 – Novel Chemistry: Lithium Selenium and Selenium Sulfur Couple (Khalil Amine, Argonne National Laboratory)

Project Objective. The project objective is to develop a novel S_xSe_y cathode material for rechargeable lithium batteries with high energy density and long life, as well as low cost and high safety.

Project Impact. Development of a new battery chemistry is promising to support the goal of PHEV and EV applications.

Approach. The dissolution of lithium polysulfides in nonaqueous electrolytes has been the major contribution to the low energy efficiency and short life of Li/S batteries. In addition, the insulating characteristics of both end members during charge/discharge (S and Li_2S) limit their rate capacity. To overcome this problem, sulfur or Li_2S are generally impregnated in a carbon conducting matrix for better electronic conductivity. However, this makes it difficult to increase the loading density of practical electrodes. It is proposed here to solve the above barriers using the following approaches: (1) partially replace S with Se and (2) nano-confine the S_xSe_y in a nanoporous conductive matrix.

Out-Year Goals. When this new cathode is optimized, the following result can be achieved:

- A cell with nominal voltage of 2 V and energy density of 600 Wh/kg.
- A battery capable of operating for 500 cycles with low capacity fade.

Collaborations. This project engages in collaboration with the following:

- Professor Chunsheng Wang of University of Maryland
- Dr. Yang Ren and Dr. Chengjun Sun of APS at ANL

Milestones

1. Investigate the phase diagram of S_xSe_y system. (Q1 – Complete)
2. Encapsulating Se_2S_5 in nanoporous carbon. (Q1 – Complete)
3. Investigating the impact of fluorinated solvents. (Ongoing)
4. Stabilizing materials with a higher sulfur content for a higher energy density. (Ongoing)
5. Investigating the impact of the pore structure of carbon matrix. (Ongoing)

Progress Report

In previous studies, it was found that a fluorinated electrolyte could significantly improve the cycle life and suppress the shuttle effect of selenium-sulfur cathodes. *In operando* ^7Li NMR studies were used to unravel the reaction mechanism.

To quantify changes in the dissolved and solid Li^+ -species during cycling, the *in operando* NMR data set was fitted by fixing the widths of the sharp resonances, but allowing the line width of the broad resonance to float (Figure 69a-c). This resulted in good fits being obtained throughout (Figure 69d). The integrated areas of high frequency, low frequency, and broad resonance along with the charge/discharge process are compared in Figure 69e. As shown, the integrated areas of the dissolved Li^+ -species at both high and low frequency have a slight increase at the very beginning of the discharge process and then keep relatively stable at the end of the charge/discharge process, which means that there are very few soluble polysulfides and polyselenides in the fluorinated electrolyte. Meanwhile, it is obvious to see that the integrated area of the Li^+ -containing solid changes little at the very beginning of the discharge. However, its intensity significantly increased after the consumption of the trace polysulfides and polyselenides and reached the maximum at the end of the discharge process. *In operando* ^7Li NMR studies have confirmed that there are very few dissolved polysulfides and polyselenides in the fluorinated electrolyte during the whole charge/discharge process; most of the S_5Se_2 converts directly to Li_2S and Li_2Se , indicating a solid state lithiation-delithiation process.

The group has previously reported that lithium-selenium batteries also undergo solid-state lithiation-delithiation process in carbonate electrolytes. Therefore, the group further compared the cycle performance of $\text{S}_5\text{Se}_2/\text{C}$ cathode in the fluorinated and carbonate electrolytes. Although the $\text{S}_5\text{Se}_2/\text{C}$ cathode did not show any shuttle effect, the reversible capacities in the carbonate electrolytes are only around 300 mAh g^{-1} for 50 cycles. This should be due to the nucleophilic reaction between polysulfides and carbonate electrolytes. Therefore, the fluorinated electrolytes not only significantly suppress the formation of soluble polysulfides and polyselenides, but also prevent the nucleophilic reaction; this indicates that they are very promising electrolytes for selenium-sulfur systems.

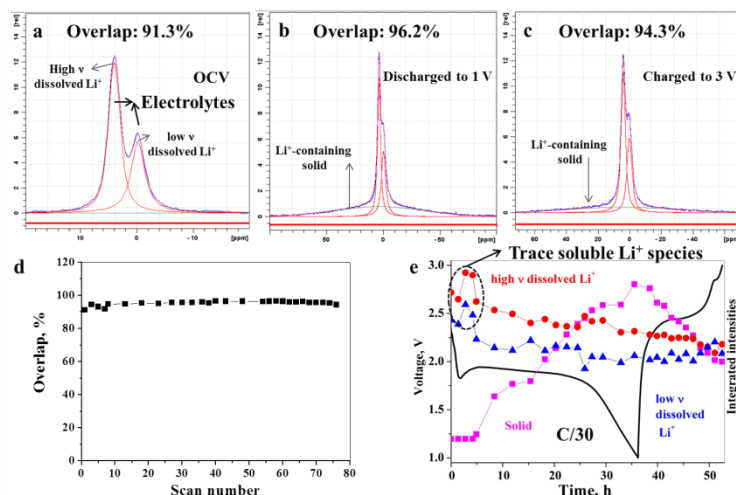


Figure 69. *In operando* ^7Li NMR studies on the $\text{S}_5\text{Se}_2/\text{C}$ cathode in the fluorinated electrolyte: fit curves to the ^7Li NMR line shape at (a) open circuit voltage, (b) discharged to 1.0 V, and (c) charged back to 3.0 V. (d) Overlap of the fitting for *in operando* nuclear magnetic resonance spectra versus scan number. (e) Integrated areas of Li^+ species as a function of charge/discharge process.

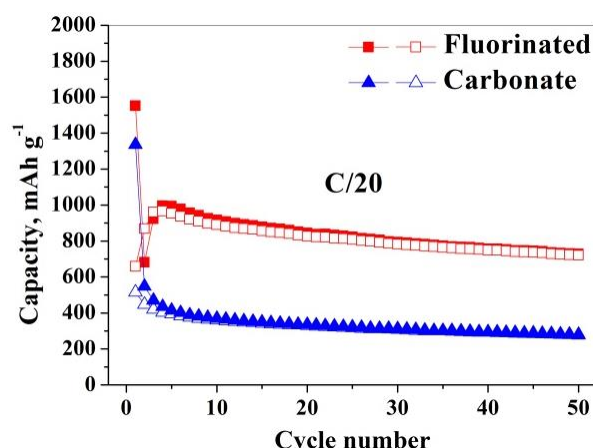


Figure 70. Cycle performance of a $\text{S}_5\text{Se}_2/\text{C}$ cathode in two different electrolytes. Hollow symbols represent charge; solid symbols mean discharge.

Task 8.4 – Multi-Functional Cathode Additives (MFCA) for Lithium–Sulfur Battery Technology (Hong Gan, Brookhaven National Laboratory; and Co-PI Esther Takeuchi, Brookhaven National Laboratory and Stony Brook University)

Project Objective. Develop a low-cost battery technology for PEV application utilizing Li-S electrochemical system by incorporating multifunctional cathode additives (MFCA), consistent with the long-term goals of the DOE EV Everywhere Grand Challenge.

Project Impact. The Li-S battery system has gained significant interest due to its low material cost potential (35% cathode cost reduction over Li-ion) and its attractive 2.8x (volumetric) to 6.4x (gravimetric) higher theoretical energy density compared to conventional Li-ion benchmark systems. Commercialization of this technology requires overcoming several technical challenges. This effort will focus on improving the cathode energy density, power capability, and cycling stability by introducing MFCA. The primary deliverable is to identify and characterize the best MFCA for Li-S cell technology development.

Approach. Transition metal sulfides are evaluated as cathode additives in sulfur cathode due to their high electronic conductivity and chemical compatibility to the sulfur cell system. Electrochemically active additives are also selected for this investigation to further improve energy density of the sulfur cell system. In the first year, the team has established the individual baseline sulfur and TM sulfide coin cell performances, and demonstrated the strong interactions between sulfur and various MFCA within the hybrid electrode. TiS_2 and FeS_2 were selected as the leading candidates for additional optimization studies with synthetic method developed. During the second year, leading candidates for the cathode optimization studies will be further narrowed down. More attention will be directed into electrode optimization and cell system optimization for improved electrode integrity, energy density, and electrochemical charge/discharge cycling performance. Examples for these efforts include electrode components (binder, carbon), electrode formulation optimization, and electrolyte optimization.

Out-Year Goals. This is a multi-year project comprised of two major phases to be successfully completed in three years. Phase 1 includes cathode and MFCA proof-of-concept investigations to be mostly completed during year-1 investigations. Phase 2 will include cell component interaction studies and full cell optimization. The work scope for year 2 will focus on the leading MFCA candidate selection, followed by hybrid electrode processing, material and formulation studies for optimized energy density, and cell electrochemical performance testing. The mechanistic studies of MFCA and sulfur interaction will continue throughout the year to advance fundamental understanding of the system.

Collaborations. This project collaborates with Dong Su, Xiao Tong, and Yu-chen Karen Chen-Wiegar at BNL and with Amy Marschilok and Kenneth Takeuchi at SBU.

Milestones

1. Synthesized MFCA evaluation and selection. (Q1 – Complete)
2. MFCA particle size effect study and best candidate selection. (Q2 – Complete)
3. Cathode process and material optimization. (Q3 – Complete)
4. Cathode formulation optimization. (Q4 – In progress – Completed carbon selection)

Progress Report

Last quarter, the group selected the Cellulose Polymer (CP) as the leading binder for improved sulfur cathode adhesion/cohesion based on the cathodes with sulfur loading of $< 1.5 \text{ mg/cm}^2$, using Super C65 as the conductive carbon additive. However, severe electrode cracks and delamination were observed when the group attempted to increase sulfur loading to $> 4 \text{ mg/cm}^2$. To achieve $> 350 \text{ kW/kg}$ energy density at the cell level, targeted by VTO, sulfur loading of $> 6 \text{ mg/cm}^2$ is desirable at the practical level. The focus this quarter is to achieve cathode of sulfur loading $> 6 \text{ mg/cm}^2$ with good mechanical integrity and handle-ability by optimizing the carbon additives, along with additional binder adjustment.

Carbon selection to achieve $> 6 \text{ mg/cm}^2$ sulfur loading. To maintain low cost, the group evaluated seven commercially available carbons, including Super C65 (control), Ketjen Black, three micro-porous carbons (MP62, MP83, and MP97) and two fibrous carbons (Fiber 150 and Fiber 200). These carbons have wide variety of physical properties, such as particle size (30 nm – 40 μm) (Figure 71), BET surface area (3 – 1200 m^2/g), pore size (0 - 20A) and pore volume (0 - 1.1 cc/g), etc. Sulfur cathode slurries using formulation of S:C:CP = 62:30:8 were tape casted on aluminum foil, with targeted sulfur loading ranging from 1.1 to 10.0 mg/cm^2 . Electrodes with sulfur loading of $> 3.5 \text{ mg/cm}^2$ using carbons of small particle sizes (Super C65 and Ketjen Black) exhibited severe cracks and delamination after drying with exposed aluminum foil, while electrodes using micro-porous carbons with large particle sizes

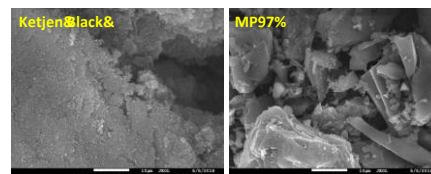


Figure 71. Scanning electron microscopy of Ketjen Black and MP97.



Figure 72. Sulfur electrode cracks after drying.

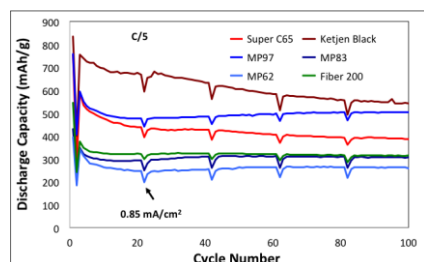


Figure 73. Carbon types vs. coin cell cycling.

exhibited no visible cracks and delamination after drying, as shown in Figure 72. Using MP97, sulfur loading up to 9 mg/cm^2 without electrode cracks was achieved. Electrochemical performance of coin cells using six carbon additives with low sulfur loading ($\sim 1.3 \text{ mg/cm}^2$) were examined (Figure 73). Among them only Ketjen Black and MP97 exhibited equal or better coin cell cycling performance relative to the control cell with Super C65. Since both Super C65 and Ketjen Black did not achieve $> 3.5 \text{ mg/cm}^2$ sulfur loading without mechanical defects, MP97 was selected for additional sulfur electrode development.

High sulfur loading electrode optimization. With MP97 as carbon additive, it was observed that the coated electrode has very rough surface and is also brittle for handling and pouching. The group further improved the electrode by using composite carbon additives (MP97/Super C65 for electrode surface smoothness) and composite binders (CP/PVDF for reduced electrode brittleness). Electrodes with sulfur loading up to 10 mg/cm^2 were obtained with good mechanical integrity. Under low current density, linear relationship between sulfur loading and the delivered areal capacity is observed in coin cell test, with up to 12 mAh/cm^2 delivered for the 10 mg/cm^2 sulfur loading sample (Figure 74). Higher sulfur loading cells exhibited the decreased rate capability at higher current density discharge.

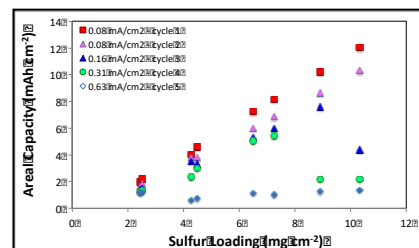


Figure 74. Sulfur loading effect on discharge.

As part of the cathode formulation optimization, the group has completed carbon additive selection for high sulfur loading during this quarter. The work on cathode formulation optimization for high energy density with TiS_2 additive is initiated.

Patents/Publications/Presentations

Publication

- Sun, Ke, and Christina A. Cama, Rachel A. DeMayo, David C. Bock, Xiao Tong, Dong Su, Amy C. Marschilok, Kenneth J. Takeuchi, Esther S. Takeuchi, and Hong Gan. “Interaction of FeS₂ and Sulfur in Li-S Battery System.” *J. Electrochem. Soc.* 164, no. 1 (2017): A6039-A6046.

Presentation

- 2016 BMR Li-S Meeting, LBNL, Berkeley, California (August 9, 2016): “Multi-Functional Cathode Additives (MFCA) for Li-S Battery Technology”; Hong Gan and Esther Takeuchi.

Task 8.5 – Development of High-Energy Lithium–Sulfur Batteries (Jun Liu and Dongping Lu, Pacific Northwest National Laboratory)

Project Objective. The project objective is to develop high-energy, low-cost Li-S batteries with long lifespan. All proposed work will employ thick sulfur cathode (≥ 2 mAh/cm² of sulfur) at a relevant scale for practical applications. The diffusion process of soluble polysulfide out of thick cathode will be revisited to investigate cell failure mechanism at different cycling. Alternative anode will be explored to address the lithium anode issue. The fundamental reaction mechanism of polysulfide under the electrical field will be explored by applying advanced characterization techniques to accelerate development of Li-S battery technology.

Project Impact. The theoretical specific energy of Li-S batteries is ~2300 Wh/kg, which is almost three times higher than that of state-of-the-art Li-ion batteries. The major challenge for Li-S batteries is polysulfide shuttle reactions, which initiate a series of chain reactions that significantly shorten battery life. The proposed work will design novel approaches to enable Li-S battery technology and accelerate market acceptance of long-range EVs required by the EV Everywhere Grand Challenge.

Out-Year Goals. This project has the following out-year goals:

- Fabricate Li-S pouch cells with thick electrodes to understand sulfur chemistry/electrochemistry in the environments similar to the real application.
- Leverage the Li-metal protection project funded by the DOE and PNNL advanced characterization facilities to accelerate development of Li-S battery technology.
- Develop Li-S batteries with a specific energy of 400 Wh/kg at cell level, 1000 deep-discharge cycles, improved abuse tolerance, and less than 20% capacity fade over a 10-year period to accelerate commercialization of electrical vehicles.

Collaborations. This project engages in collaboration with the following:

- Dr. Xiao-Qing Yang (LBNL) – *In situ* characterization
- Dr. Bryant Polzin (ANL) – Electrode fabrication
- Dr. Xingcheng Xiao (GM) – Materials testing
- Dr. Jim De Yoreo (PNNL) – *In situ* characterization

Milestones

1. SEI study on graphite surface in the new EC-free electrolyte. (December 2015 – Complete)
2. Demonstrate prototype Li-ion sulfur cells with > 95% Coulombic efficiency (no additive) and > 80% capacity retention for 100 cycles. (March 2016 – Complete)
3. Identify effective approaches to facilitate electrolyte penetration within thick sulfur cathode (≥ 4 mg/cm²). (June 2016 – Complete)
4. Complete pouch cell assembly and testing by using optimized electrode and electrolyte. (September 2016 – complete)

Progress Report

The PNNL study in previous quarters indicates that improving sulfur utilization rate in high loading sulfur electrode is quite challenging due to the electrode wetting problems. To address these problems, the group has proposed and demonstrated that using electrode additives during electrode preparation process or employing functionalized carbon/sulfur composite as cathode are effective approaches to improve electrode wetting and sulfur utilization rate. With coin cells, high capacities over 1100 mAh g⁻¹ can be achieved for sulfur electrode, with mass loading up to 8 mg cm⁻². To verify the feasibility of the proposed approaches for practical applications, pouch cells were prepared using thick sulfur electrode for electrochemical evaluation. Using sulfur electrode with mass loading around 4.5 mg cm⁻², Li-S pouch cells prepared in this work exhibit energy densities of 250 Wh kg⁻¹ with a cell capacity of 1.6 Ah. More work will be done to improve the energy density of these cells.

In addition to using the electrode additive approach to enhance the sulfur utilization rate in thick electrode (reported last quarter), the group also modified the synthesis of integrated Ketjen Black (IKB) by introducing functional groups into material. Significant improvement in electrode wetting for thick electrode was demonstrated, and related mechanism understanding is in progress. One of the foci in this quarter is to use this modified material to prepare thick sulfur electrodes and do electrochemical evaluation in large-scale pouch cells. Table 2 shows detailed parameter information of the Li-S pouch cell. The sulfur electrode with mass loadings around 4.5 mg cm⁻² (Figure 75a) was coated and processed at the Advanced Battery Facility at PNNL. The pouch cell has a dimension of 72 mm×41mm×4mm and a total mass of 14 g including 1.72 g sulfur active material and 5 g electrolyte, with an electrolyte/sulfur ratio of 2.9. The capacity achieved from the cell is 1.68 Ah at a current of 100 mA and room temperature. Figure 75c shows the first discharge curves of the cell plotted in forms of both specific capacity and energy density. The actual specific capacity of sulfur is near 1000 mAh g⁻¹ (blue curve), indicating a comparable sulfur utilization rate with those obtained in coin cells. Based on the output energy and total mass of the cell, the measured energy density of the system is 247 Wh kg⁻¹ (black curve in Figure 75c), which can be further improved to 300 Wh kg⁻¹ by optimizing the inactive components of the pouch cell (for example, electrode current collector and separator). To obtain Li-S cells with elevated energy density for practical applications, continued efforts of the PNNL group will be focused on the following: (1) optimization of sulfur electrode with higher mass loading, (2) introduction of electrode additives into electrode to improve sulfur utilization rate, and (3) optimization of electrolyte for long-term cycling stability.

Table 2. Parameters of the Li-sulfur pouch cell.

Parameters	Values
Cell dimension (mm)	72(length)×41(width) ×4 (thickness)
Total capacity (Ah)	1.68
Total mass of cell (g)	14
Mass of sulfur (g)	1.72
Mass of electrolyte	5
Energy density	247 Wh kg ⁻¹

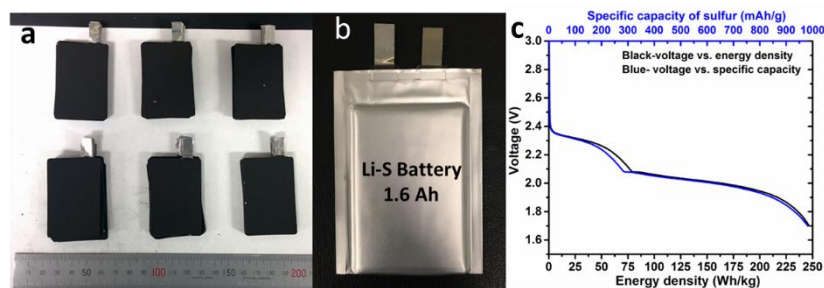


Figure 75. (a) Image of the prepared sulfur cathode with mass loading 4.5 mg cm⁻². (b) Image of Li-S pouch cell. (c) First discharge profiles (black-energy density and blue-specific capacity).

Patents/Publications/Presentations

Publication

- Lu, D., and J. Tao, P. Yan, W. A. Henderson, Q. Li, Y. Shao, G. L. Graff, B. Polzin, C. Wang, J. Zhang, J.D. Yoreo, J. Liu, and J. Xiao. “Reversible Shielding of Electrodes.” Submitted for publication.

Presentation

- 2016 BMR Li-S Meeting, LBNL, Berkeley, California (August 9, 2016): “Development of High Energy Lithium Sulfur Battery”; J. Liu, et al.

Task 8.6 – Nanostructured Design of Sulfur Cathodes for High-Energy Lithium–Sulfur Batteries (Yi Cui, Stanford University)

Project Objective. The charge capacity limitations of conventional TM oxide cathodes are overcome by designing optimized nano-architected sulfur cathodes.

This study aims to enable sulfur cathodes with high capacity and long cycle life by developing sulfur cathodes from the perspective of nanostructured materials design, which will be used to combine with Li-metal anodes to generate high-energy Li-S batteries. Novel sulfur nanostructures as well as multifunctional coatings will be designed and fabricated to overcome issues related to volume expansion, polysulfide dissolution, and the insulating nature of sulfur.

Project Impact. The capacity and the cycling stability of sulfur cathode will be dramatically increased. This project's success will make Li-S batteries to power electric vehicles and decrease the high cost of batteries.

Out-Year Goals. The cycle life, capacity retention, and capacity loading of sulfur cathodes will be greatly improved (200 cycles with 80% capacity retention, $> 0.3 \text{ mAh/cm}^2$ capacity loading) by optimizing material design, synthesis, and electrode assembly.

Collaborations. This project engages in collaboration with the following:

- BMR PIs
- SLAC: *In situ* X-ray, Dr. Michael Toney
- Stanford: Professor Nix, mechanics; Professor Bao, materials

Milestones

1. Demonstrate synthesis to generate monodisperse sulfur nanoparticles with/without hollow space. (October 2013 – Complete)
2. Develop surface coating with one type of polymers and one type of inorganic materials. (January 2014 – Complete)
3. Develop surface coating with several types of polymers; Understand amphiphilic interaction of sulfur and sulfide species. (April 2014 – Complete)
4. Demonstrate sulfur cathodes with 200 cycles with 80% capacity retention and 0.3 mAh/cm^2 capacity loading. (July 2014 – Complete)
5. Demonstrate Li_2S cathodes capped by layered metal disulfides. (December 2014 – Complete)
6. Identify the interaction mechanism between sulfur species and different types of sulfides/oxides/metals, and find the optimal material to improve the capacity and cycling of sulfur cathode. (July 2015 – Complete)
7. Demonstrate the balance of surface adsorption and diffusion of Li_2S_x species on nonconductive metal oxides. (December 15 – Complete)
8. The selection criterion of metal oxide is proposed to guide the rational design of cathode materials for advanced Li-S batteries. (April 2016 – Complete)
9. Demonstrate lithium polysulfides adsorption and diffusion on the metal sulfides surface. (July 2016 – Complete)
10. Investigate the lithium-ion diffusion mechanism in different types of metal sulfides. (October 2016 – On track)

Progress Report

Last quarter, the interaction mechanism between sulfur species and different types of metal sulfides was explored. The results indicate that all the sulfide materials in the study can induce larger binding strength than that by graphene, which exhibits very weak chemical binding to Li_2S_6 with adsorption dominated by physical van der Waals interaction. This is why these sulfides can mitigate polysulfide dissolution and suppress shuttle effect, leading to better performance in Li-S battery than that of commonly adopted sp^2 carbon materials. This quarter, the group further explored the lithium-ion diffusion mechanism in different types of metal sulfides.

The lithium-ion diffusion coefficient can serve as a good descriptor to verify whether metal sulfides (M_xS_y) can propel the polysulfide redox reaction process as fast lithium-ion diffusion facilitates the sulfur transformation chemistry at the M_xS_y interface. CV was used to investigate electrode kinetics with respect to the lithium-ion diffusion coefficient. Taking the $\text{S-VS}_2@\text{G/CNT}$ electrode as a representative example, Figure 76a shows the CV curves of the electrode measured under different scanning rates ranging from 0.2 to 0.5 mV s^{-1} between 1.5 and 2.8 V (versus Li/Li^+). At all scan rates, there are two cathodic peaks at around 2.30 V (I_{C1}) and 1.95 V (I_{C2}), corresponding to the reduction of elemental sulfur (S_8) to long-chain lithium polysulfides and subsequent formation of short-chain $\text{Li}_2\text{S}_2/\text{Li}_2\text{S}$. The anodic peak at around 2.50 V in the anodic sweep results from transition of $\text{Li}_2\text{S}_2/\text{Li}_2\text{S}$ to polysulfides and elemental sulfur (I_{A}). The cathodic and anodic current peaks (I_{C1} , I_{C2} , I_{A}) of the M_xS_y containing electrodes have a linear relationship with the square root of scanning rates (Figure 76b-d), indicative of the diffusion-limited process. Therefore, the classical Randles Sevcik equation can be applied to describe the lithium diffusion process: $\text{I}_p = (2.69 \times 10^5) n^{1.5} S D_{\text{Li}^+}^{0.5} C_{\text{Li}} v^{0.5}$, where I_p is the peak current, n is the charge-transfer number, S is the geometric area of the active electrode, D_{Li^+} is the lithium-ion diffusion coefficient, C_{Li} is the concentration of lithium ions in the cathode, and v is the potential scan rate. The slope of the curve ($\text{I}_p/v^{0.5}$) represents the lithium-ion diffusion rate as n , S , and C_{Li} are unchanged. It can be seen that the $\text{S}@G/\text{CNT}$ electrode exhibits the lowest lithium-ion diffusivity, which mainly arises from the weak lithium polysulfides adsorption and Li_2S conversion capability, induced high polysulfides viscosity in the electrolyte or deposition of a thick insulating layer on the electrode. In contrast, the $\text{S-VS}_2@\text{G/CNT}$, $\text{S-CoS}_2@\text{G/CNT}$, and $\text{S-TiS}_2@\text{G/CNT}$ electrodes demonstrate much faster diffusion compared to the $\text{S}@G/\text{CNT}$ electrode and better reaction kinetics than the $\text{S-Ni}_3\text{S}_2@\text{G/CNT}$, $\text{S-SnS}_2@\text{G/CNT}$, and $\text{S-FeS}@G/\text{CNT}$ electrodes, indicating that the introduction of M_xS_y hosts enables highly efficient conversion of sulfur redox.

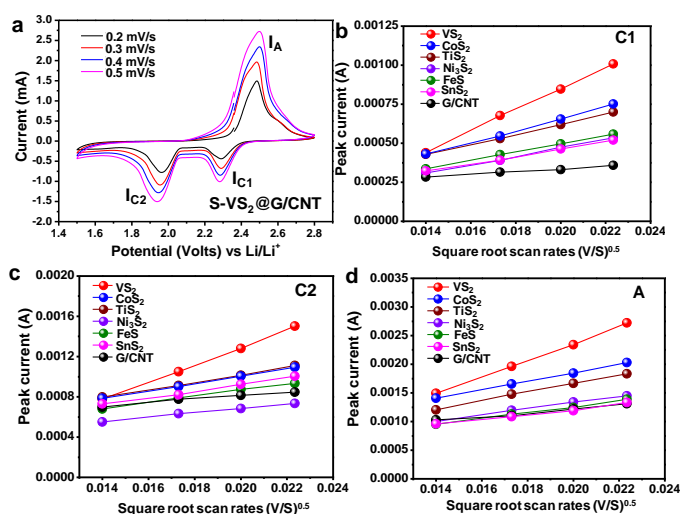


Figure 76. (a) Cyclic voltammetry (CV) curves of the $\text{S-VS}_2@\text{G/CNT}$ electrode at various scan rates. Plots of CV peak current for the (b) first cathodic reduction process (I_{C1} : $\text{S}_8 \rightarrow \text{Li}_2\text{S}_x$), (c) second cathodic reduction process ($\text{Li}_2\text{S}_x \rightarrow \text{Li}_2\text{S}_2/\text{Li}_2\text{S}$), and (d) anodic oxidation process ($\text{Li}_2\text{S}_2/\text{Li}_2\text{S} \rightarrow \text{S}_8$) versus the square root of the scan rates.

Task 8.7 – Addressing Internal “Shuttle” Effect: Electrolyte Design and Cathode Morphology Evolution in Lithium–Sulfur Batteries (Perla Balbuena, Texas A&M University)

Project Objective. The project objective is to overcome the Li-metal anode deterioration issues through advanced Li-anode protection/stabilization strategies including (i) *in situ* chemical formation of a protective passivation layer and (ii) alleviation of the “aggressiveness” of the environment at the anode by minimizing the polysulfide shuttle with advanced cathode structure design.

Project Impact. Through formulation of alternative electrolyte chemistries as well as design, fabrication, and test of improved cathode architectures, it is expected that this project will deliver Li/S cells operating for 500 cycles at efficiency greater than 80%.

Approach. A mesoscale model including different realizations of electrode mesoporous structures generated based on a stochastic reconstruction method will allow virtual screening of the cathode microstructural features and the corresponding effects on electronic/ionic conductivity and morphological evolution. Interfacial reactions at the anode due to the presence of polysulfide species will be characterized with *ab initio* methods. For the cathode interfacial reactions, data and detailed structural and energetic information obtained from atomistic-level studies will be used in a mesoscopic-level analysis. A novel sonochemical fabrication method is expected to generate controlled cathode mesoporous structures that will be tested along with new electrolyte formulations based on the knowledge gained from the mesoscale and atomistic modeling efforts.

Out-Year Goals. By determining reasons for successes or failures of specific electrolyte chemistries, and assessing relative effects of composite cathode microstructure and internal shuttle chemistry versus that of electrolyte chemistry on cell performance, expected results are : (1) develop an improved understanding of the Li/S chemistry and ways to control it; (2) develop electrolyte formulations able to stabilize the Li anode; (3) develop new composite cathode microstructures with enhanced cathode performance; and (4) develop a Li/S cell operating for 500 cycles at an efficiency greater than 80%.

Collaborations. This is a collaborative work combining first-principles modeling (Perla Balbuena, TAMU), mesoscopic level modeling (Partha Mukherjee, TAMU), and synthesis, fabrication, and test of Li/S materials and cells (Vilas Pol, Purdue University).

Milestones

1. Complete coin cell testing of various C/S electrodes. (December 2015 – Complete)
2. Using electrochemical and transport modeling, gain an understanding of the mesoscopic interfacial reactions. (March 2016 – Complete)
3. Complete evaluation of deposition-induced stress and mechanical interplay. (June 2016 – Complete)
4. Determination of SEI nucleation and growth at the PS/Li anode interface. *Go/No-Go*: Determine reasons for electrolyte failure or success. (September 2016 – Complete)

Progress Report

SEI nucleation and growth at the PS/Li interface. A detailed AIMD study of the reactions at the surface of Li metal has shown buildup of the various species due to the long-chain polysulfide migration from cathode to anode. These simulations demonstrated the rapid formation of Li_2S on the Li metal surface and its dependence on the exposed crystallographic surface. In the presence of an oxidant such as LiNO_3 , the most likely products would be sulfates and sulfites. However, the PS species continue forming Li_2S even when a sulfate film starts to cover the anode surface, at least up to a certain thickness that would avoid electron transfer. This work also

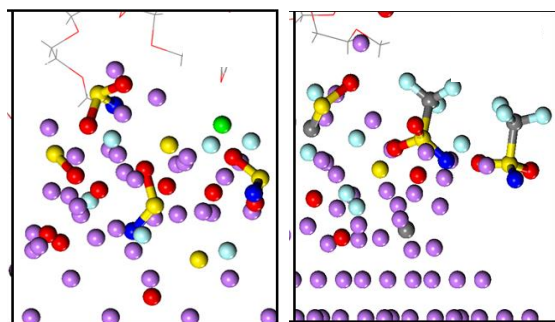


Figure 77: Solid electrolyte interphase layer formation illustrating fast decomposition of salt at a 4M concentration. Left: LiFSI; Right: LiTFSI.

investigated the effect of higher molar concentration of salts, and specifically, the differences between LiFSI and LiTFSI on the possible SEI formed. Figure 77 illustrates that while decomposition of LiFSI is almost complete (leading to LiF as main product and many SO_2 anion radicals that also attach to the surface), LiTFSI results also in LiF but also yields much larger residual species that could lead to polymeric components.

In collaboration with a PNNL group, the results of this team's simulations are being used to analyze XPS results and identify SEI products on Li anodes due to PS shuttle effects. A manuscript is being prepared.

Reasons for electrolyte failure or success. DFT and AIMD simulations were conducted to characterize the behavior of the electrolyte mixtures, ion association and transport, and reduction of the species as a function of the number of electrons in the system, representing applied voltage. Various solvents (with variable solvation power) and salts have been investigated, and the team is currently summarizing the results. In addition, new simulations are being conducted to characterize the discharge reactions in a larger system containing solid S and C in contact with the electrolyte phase. These simulations have already shown formation of long-chain PS species; now the focus is on the first plateau of the discharge curve, where the long-chain PS species are reduced to shorter chain and on the analysis of the deposition of the insoluble products on the C surfaces.

Understanding the effect of sulfur loading and LiCl salt in the Li-S Cathode. Sulfur lithiation leads to 80% volume expansion. Therefore, if the cathode porosity is not enough, this may lead to partial pore blockage and increased electrolyte phase transport resistance and cell shut down. A mesoscopic model is used to understand sulfur loading and cathode porosity effects on pore blockage and cell inefficiency. Also, it was theoretically predicted that LiCl salt as an electrolyte additive may improve the Li-S cathode performance. First-principles simulations demonstrate that the negatively charged Li vacancy (V_{Li}^-) is the major charge carrier in solid Li_2S precipitation. The Cl^- ion can be incorporated into Li_2S during discharge, which can increase the concentration of V_{Li}^- and thus lead to a significant decrease in electrical resistivity. The density of states of Cl^- -incorporated Li_2S illustrate that the valence band of the Cl^- -incorporated are not completely occupied. Hence, the hole polaron can also serve as a charge carrier when V_{Li}^- is exhausted out.

Autogenic synthesis of graphene-sulfur composites. A novel autogenic process to synthesize carbon-sulfur composites is demonstrated. This process allows pressurized and vaporized sulfur to homogeneously penetrate the microstructure of the surrounding C substrate, allowing greater electrochemical contact of S and C due to homogeneous deposition of vaporized S during the cooling process. The autogenic loading of S is sensitive to the heating profile (that is, the time allowed for phase transformation between melting, vaporization, and deposition). Two heating profiles were used: (1) melting-focused, and (2) vaporizing focused. The difference in the two profiles is carried out to determine the effect of vaporization versus melting time for sulfur penetration of the carbon matrix. Electrochemical experiments have been carried out to test the new composites.

Patents/Publications/Presentations

Publications

- Liu, Z., and D. Hubble, P. B. Balbuena, and P. P. Mukherjee. “Adsorption of Insoluble Polysulfides Li_2S_x ($x = 1, 2$) on Li_2S Surfaces.” *Phys. Chem. Chem. Phys.* 17 (2015): 9032-9039.
- Camacho-Forero, Luis E., and Taylor W. Smith, Samuel Bertolini, and Perla B. Balbuena. “Reactivity at the Lithium-Metal Anode Surface of Lithium-Sulfur Batteries.” *J. Phys. Chem. C* 119, no. 48 (2015): 26828-26839.
- Tsai, C. S. J., and A. D. Dysart, J. H. Beltz, and V. G. Pol. “Identification and Mitigation of Generated Solid By-Products during Advanced Electrode Materials Processing.” *Environ. Sci. Technol.* 50, no. 5 (2016): 2627-2634.
- Dysart, Arthur A., and Juan C. Burgos, Aashutosh Mistry, Chien-Fan Chen, Zhixiao Liu, Perla B. Balbuena, Partha P. Mukherjee, and Vilas G. Pol. “Towards Next Generation Lithium-Sulfur Batteries: Non-Conventional Carbon Compartments/Sulfur Electrodes and Multi-Scale Analysis.” *J. Electrochem. Soc.* 163, no. 5 (2016): A730-741.
- Liu, Zhixiao, and Samuel Bertolini, Partha Mukherjee, and Perla B. Balbuena. “ Li_2S Film Formation on Lithium Anode Surface of Li-S batteries.” *ACS Appl. Mat. & Interfaces* 8, no. 7 (2016): 4700-4708.
- Kamphaus, Ethan, and Perla B. Balbuena. “Long-Chain Polysulfide Retention at the Cathode of Li-S Batteries.” *J. Phys. Chem. C* 120, no. 8 (2016): 4296-4305.
- Liu, Zhixiao, and Perla B. Balbuena, and Partha P. Mukherjee. “Evaluating Silicene as a Potential Cathode Host to Immobilize Polysulfides in Lithium-Sulfur Batteries.” *J. Coord. Chem.* In press.
- Barai, P., and A. Mistry and P. P. Mukherjee. “Poromechanical Effect in the Lithium-Sulfur Battery Cathode.” *Extreme Mechanics Letters* (2016). doi: 10.1016/j.eml.2016.05.007.

Presentation

- BMR Program Review Meeting, LBNL, Berkeley, California (January 22, 2016): “Addressing Internal ‘Shuttle’ Effect: Electrolyte Design and Cathode Morphology Evolution in Li-S Batteries; DE-EE-0006832”; P. B. Balbuena.

Task 8.8 – Mechanistic Investigation for the Rechargeable Lithium–Sulfur Batteries (Deyang Qu, University of Wisconsin Milwaukee; Xiao-Qing Yang, BNL)

Project Objective. The primary objectives are to conduct focused fundamental research on the mechanism for Li-S batteries, investigate the kinetics of the sulfur redox reaction, develop electrolyte and additives to increase the solubility of Li_2S , and optimize the sulfur electrode design. In this objective, special attention will be paid to the investigation of highly soluble polysulfide species including both ions and radicals, and the potential chemical equilibrium among them. Through such investigation, the detail pathway for polysulfide shuttle will be better understood, and alleviation of the obstacle will be explored.

Project Impact. Rechargeable Li-S battery is a potential candidate to meet the demand of high-energy density for the next generation rechargeable Li battery. Through the fundamental mechanistic investigation, the mechanism of Li-S batteries can be better understood, which will lead to the material design and battery engineering to materialize the potential of Li-S chemistry. Li-S batteries could enable competitive market entry of EVs by reducing the cost and extending the driving distance per charge.

One-Year Goals. The project has the following goals: (1) complete development of an analytical method for the quantitative and qualitative determination of all polysulfide ions in nonaqueous electrolytes, and (2) complete the initial design of an *in situ* electrochemical study for the sulfur reduction reaction.

Collaborations. The principal investigator is the Johnson Controls Endowed Chair Professor; the University of Wisconsin Milwaukee and BNL team has close collaboration with Johnson Controls scientists and engineers. The collaboration enables the team to validate the outcomes of fundamental research in pilot-scale cells. This team has been working closely with top scientists on new material synthesis at ANL, LBNL, and PNNL, with U.S. industrial collaborators at General Motors, Duracell, and Johnson Controls, as well as international collaborators in Japan and South Korea. These collaborations will be strengthened and expanded to give this project a vision both on today's state-of-the-art technology and on tomorrow's technology in development, with feedback from the material designer and synthesizers upstream as well as from the industrial end users downstream.

Milestones

1. Complete literature review and feasibility study of the methods for polysulfide determination. (December 2015 – Complete)
2. Complete development of the essay to determine all polysulfide ions. (March 2016 – Complete)
3. Complete design qualification for an *in situ* electrochemical high-performance liquid chromatography MS (HPLC-MS) cell for Li-S investigation. (June 2016 – Complete)
4. Complete identification of polysulfide ions formed from elemental sulfur. (September 2016 – Complete)

Progress Report

This quarter, the reliable HPLC-MS analytical technique developed previously was applied to investigate the chemical and electrochemical reactions of elemental sulfur and polysulfide ions in the Li-S battery electrolytes. The interactions of the sulfur species with Li anode and various electrolytes were studied.

Various commonly used electrolytes for Li-S batteries were studied using HPLC with a derivatization method. Unfortunately, none of them were found very suitable for Li-S batteries, as either (1) the sulfur dissolve destroys the SEI layer and reacts with the Li, such as in LiTFS/DME, LiTFSi/DME, LiTFSi/DME/DOL, or (2) the salts react with polysulfide ions, for example, LiDFOB/DME and LiBOB/DME. As an example, the sulfur dissolve in the most commonly used electrolyte (LiTFSi/DME/DOL) in Li-S

batteries was exposed to Li for 8 days, and the solution was then derivatized and analyzed by chromatogram; the elemental sulfur was found reduced to polysulfide ions of various lengths. In another example, LiBOB/DME electrolyte was found reacting with polysulfide ions, even though it remained stable with *elemental sulfur* and Li metal. The results are shown in Figures 78 and 79, respectively.

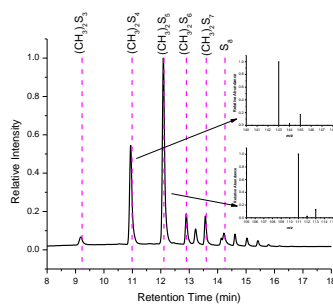


Figure 78. The chromatogram of LiTFSi/DME/DOL electrolyte with Li metal for 8 days then derivatized by methyl triflate. The inset spectra are the corresponding mass spectrometry spectra for $(\text{CH}_3)_2\text{S}_4$ and $(\text{CH}_3)_2\text{S}_5$.

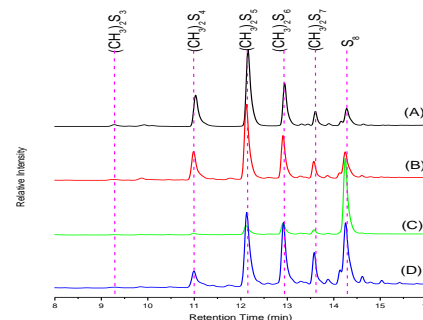


Figure 79. 0.1 M LiTFS/DME electrolytes: original polysulfide mixture (a); mixed with LiTFS (20 mM) (b); mixed with LiBOB (20 mM) (c); and mixed with LiDFOB (20 mM) (d). All samples were first derivatized by methyl triflate before high-performance liquid chromatography analysis.

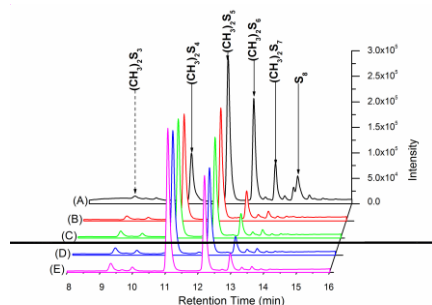


Figure 80. Chromatograms of derivatized polysulfide mixtures: original polysulfide mixture (a), polysulfide mixture with Li metal for 1 hour (b), polysulfide mixture with Li metal for 4 hours (c), polysulfide mixture with Li metal for 24 hours (d), and polysulfide mixture with Li metal for 96 hours (e).

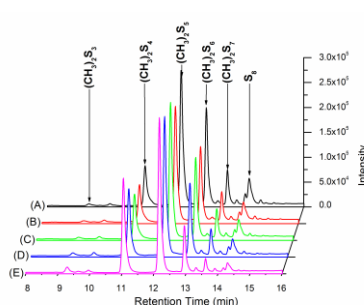


Figure 81. Chromatograms of derivatized polysulfide mixtures: original polysulfide and LiNO_3 mixture (a), polysulfide and LiNO_3 mixture with Li metal for 1 hour (b), polysulfide and LiNO_3 mixture with Li metal for 4 hours (c), polysulfide and LiNO_3 mixture with Li metal for 24 hours (d), and polysulfide and LiNO_3 mixture with Li metal for 96 hours (e).

intensities for $(\text{CH}_3)_2\text{S}_6$ and $(\text{CH}_3)_2\text{S}_7$ indicated the consumption of S_6^{2-} and S_7^{2-} in the mixture by lithium metal. Figure 81 shows the similar test, but with the addition of LiNO_3 in the electrolyte. The results show that LiNO_3 can significantly slow down interaction between polysulfides with Li metal, but cannot stop the reaction.

The reaction between polysulfides and a lithium anode in a Li-S battery was also examined by the HPLC method. The results demonstrated that the polysulfide species with six sulfur atoms or more were reactive with lithium metal. Although the reaction can be greatly inhibited by the addition of LiNO_3 in the electrolyte, LiNO_3 cannot form a stable protection layer on Li anode to prevent the reaction during storage. Figure 80 shows the reaction of polysulfide ions with metallic Li in a Li-S battery electrolyte without LiNO_3 . The dramatically decreased peak

Patents/Publications/Presentations

Publication

- Zheng, Dong, and Xiao-Qing Yang, and Deyang Qu. “Reaction between Lithium Anode and Polysulfide Ions in a Lithium-Sulphur Battery.” *Chem Sus Chem* 9 (2016): 2348-2350.

Task 8.9 – Statically and Dynamically Stable Lithium–Sulfur Batteries (Arumugam Manthiram, U Texas Austin)

Project Objective. The project objective is to develop statically and dynamically stable Li-S batteries by integrating polysulfide-filter-coated separators with a protected Li-metal anode through additives or a modified Li_2S cathode with little or no charge barrier during first charge. The project includes demonstration of electrochemically stable cells with sulfur capacities of $> 1,000 \text{ mA h g}^{-1}$ and cycle life in excess of 500 cycles (dynamic stability) along with positive storage properties (static stability) at $> 70 \text{ wt\%}$ sulfur content and $\sim 5 \text{ mg cm}^{-2}$ loading that will make the Li-S technology superior to the present-day Li-ion technology in terms of cost and cell performance.

Project Impact. The combination of polysulfide-filter-coated separator, Li-metal-protection additives, and Li_2S cathode modifications offers a viable approach to overcome the persistent problems of Li-S batteries. This project is systematically integrating the basic science understanding gained in its laboratory of these three aspects to develop the Li-S technology as the next-generation power source for EVs. The project targets demonstrating cells with sulfur capacities of over $1,000 \text{ mA h g}^{-1}$ and cycle life in excess of 500 cycles along with good storage properties at high sulfur content and loading that will make the Li-S technology superior to the present-day Li-ion technology in terms of cost and cell performance.

Approach. Electrochemical stability of the Li-S cells is improved by three complementary approaches. (i) The first approach focuses on the establishment of an electrochemically stable cathode environment by employing PS-filter-coated separators. The PS-filter coatings aim to suppress the severe polysulfide diffusion and improve the redox capability of the Li-S cells with high-sulfur loadings. The study includes an understanding of the materials characteristics, fabrication parameters, electrochemical properties, and battery performance of the PS-filter-coated separators. (ii) The second approach focuses on electrode engineering from two aspects. First, the investigation of a Li-metal anode with coating- and additive-supporting approaches is aimed at improving the safety of Li-S cells. Second, the research on activated- Li_2S cathode with little or no charge-barrier will promote the performance and safety of the C- Li_2S cells. (iii) The integration of approaches (i) and (ii) would create statically and dynamically stable Li-S batteries for EVs.

Out-Year Goals. The overall goal is to develop statically and dynamically stable Li-S batteries with custom cathode and stabilized anode active materials. In addition to developing a high-performance battery system, a fundamental understanding of the structure-configuration-performance relationships will be established. Specifically, optimization of the electrochemical and engineering parameters of polysulfide-filter-coated separators aims at comprehensively investigating different coating materials and their corresponding coating techniques for realizing various high-performance custom separators. The developed polysulfide-filter-coated separators can be coupled with pure sulfur cathodes and allow them to attain high sulfur loading and content. Multifunctional polysulfide-filter-coated separators, high-loading sulfur cathodes, stabilized-Li-metal anodes, activated- Li_2S cathodes, and novel approaches on the cell design and optimization are anticipated to provide an in-depth understanding of the full-cell battery chemistry and to realize statically and dynamically stable Li-S batteries for EVs.

Collaborations. This project collaborates with ORNL.

Milestones

1. Database of coating materials and polysulfide-filter coatings established. (December 2015 – Complete)
2. Database of fabrication parameters and S-filter-coated separators established. (March 16 – Complete)
3. Low-capacity fade rate and self-discharge testing completed. (June 2016 – Complete)
4. *Go/No-Go*: Lightweight design and electrochemical stability demonstrated. (September 2016 – Complete)

Progress Report

This quarter, the group has demonstrated the enhanced dynamic and static electrochemical performances of lithium-sulfur batteries by analyzing the cells fabricated with various polysulfide-filter (PS-filter)-coated separators. Benefiting from the database built in the first and second quarters, the PS-filter coatings effectively suppress the capacity fade during dynamic cell cycling and the severe self-discharge behavior during static cell resting. Thus, this quarter the group has successfully passed the *Go/No-Go* milestone 4.

The dynamic electrochemical stability has been examined with various PS-filter-coated separators coupled with pure sulfur cathodes that had a high sulfur loading of $> 3.4 \text{ mg cm}^{-2}$ and a high sulfur content of 70 wt.% (Figure 82). The optimized PS-filter-coated separators investigated had three different PS-filter coatings: (i) spherical-carbon-single wall carbon nanotube (SWCNT) coating, (ii) layer-by-layer (LBL) CNF coating, and (iii) LBL CNT coating. Figure 82a-b shows that the cells with the spherical-carbon-SWCNT-coated separators and the LBL CNF-coated separators display the targeted discharge capacity ($1,000 \text{ mA h g}^{-1}$) and areal capacity (4.0 mA h cm^{-2}). Moreover, they both exhibit long-term cycle stability for 500 cycles with a low dynamic capacity-fade rate of only $< 0.12\%$ per cycle. By transferring the LBL technique to CNTs, the resulting LBL CNT coatings with a high conductivity weigh as low as 0.04 mg cm^{-2} . Benefiting from the conductive CNT coatings and their excellent polysulfide-retention capability, the cells fabricated with the light-weight LBL CNT-coated separators are able to operate well at high rates (C/5 and C/2) with excellent dynamic battery performance, high electrochemical utilization, and stable cyclability for 300 cycles (Figure 82c-d).

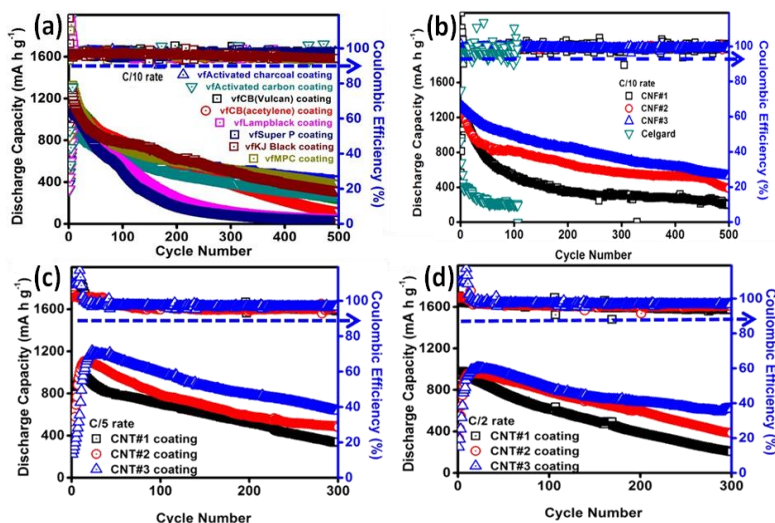


Figure 82. Dynamic cycling performances of the cells fabricated with the (a) spherical-carbon single-wall carbon nanotube (SWCNT)-coated separators, (b) layer by layer carbon nanofiber (LBL CNF)-coated separators, and (c-d) layer by layer carbon nanotube (LBL CNT)-coated separators.

Furthermore, the cells fabricated with the spherical-carbon-SWCNT-coated separators and the LBL CNF-coated separators exhibit low self-discharge and retain high charge-storage capacities after resting for 60 and 120 days, as seen in Figure 83. The static capacity-retention rate and capacity-fade rate of the cells with the spherical-carbon-SWCNT-coated separators are, respectively, 73% and 0.4% per day for a 60-day rest period. The LBL CNF-coated separators demonstrate a static capacity-retention rate of 63% and a low static capacity-fade rate of 0.3% per day after resting for 120 days, which is one of the longest self-discharge analyses reported so far.

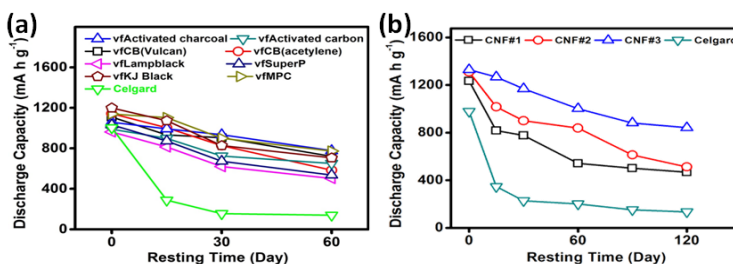


Figure 83. Static resting performances of the cells fabricated with the (a) spherical-carbon single-wall carbon nanotube (SWCNT)-coated separators and (b) layer by layer carbon nanofiber (LBL CNT)-coated separators.

Patents/Publications/Presentations

Publications

- Chung, S.-H., and C.-H. Chang, and A. Manthiram. “A Core–Shell Electrode for Dynamically and Statically Stable Li–S Battery Chemistry.” *Energy & Environmental Science* 9 (2016): 3188–3200.
- Chung, S.-H., and C.-H. Chang, and A. Manthiram. “Hierarchical Sulfur Electrodes as a Testing Platform for Understanding the High–loading Capability of Li–S Batteries.” *Journal of Power Sources* (in press).
- Luo, L., and S.-H. Chung, and A. Manthiram. “Trifunctional Multi–walled Carbon Nanotubes/ Polyethylene Glycol (MWCNT/PEG) –coated Separator through a Layer–by–Layer Coating Strategy for High–Energy Li–S Batteries.” *Journal of Materials Chemistry A* (in review).
- Chang, C.-H., and S.-H. Chung, and A. Manthiram. “Highly Flexible, Freestanding Tandem Sulfur Cathodes for Foldable Li–S Batteries with High Areal Capacity.” *Advanced Functional Materials* (in review).

Presentations

- Indian Institute of Technology Madras, Chennai, India (August 16, 2016): “Materials for Electrochemical Energy Conversion and Storage Technologies”; A. Manthiram. Invited.
- 4th International Workshop on Nanotechnology, Renewable Energy, and Sustainability, Xi’an Jiaotong University, Xi’an, China (September 19, 2016): “Electrical Energy Storage: Next Generation Battery Chemistries”; A. Manthiram. Invited keynote talk.
- Hanyang University, Seoul, South Korea (September 21, 2016): “New Battery Chemistries Enabled by Solid-Electrolyte Separators”; A. Manthiram. Invited.

TASK 9 – LITHIUM–AIR BATTERIES

Summary and Highlights

High-density energy storage systems are critical for EVs required by the EV Everywhere Grand Challenge. Conventional Li-ion batteries still cannot fully satisfy the ever-increasing needs because of their limited energy density, high cost, and safety concerns. As an alternative, the rechargeable Li-O₂ battery has the potential to be used for long-range EVs. The practical energy density of a Li-O₂ battery is expected to be ~ 800 Wh kg⁻¹. The advantages of Li-O₂ batteries come from their open structure; that is, they can absorb the active cathode material (oxygen) from the surrounding environment instead of carrying it within the batteries. However, the open structure of Li-O₂ batteries also leads to several disadvantages. The energy density of Li-O₂ batteries will be much lower if oxygen has to be provided by an onboard container. Although significant progress has been made in recent years on the fundamental properties of Li-O₂ batteries, the research in this field is still in an early stage, and many barriers must be overcome before practical applications. The main barriers include:

- Instability of electrolytes. Superoxide species generated during discharge or O₂ reduction process is highly reactive with electrolyte and other components in the battery. Electrolyte decomposition during charge or O₂ evolution process is also significant due to high over-potentials.
- Instability of air electrode (dominated by carbonaceous materials) and other battery components (such as separators and binders) during charge/discharge processes in an O-rich environment.
- Limited cyclability of the battery associated with instability of the electrolyte and other components of the batteries.
- Low energy efficiency associated with large over-potential and poor cyclability of Li-O₂ batteries.
- Low power rate capability due to electrode blocking by the reaction products.
- Absence of a low-cost, high-efficiency oxygen supply system (such as oxygen selective membrane).

The main goal of the PNNL Task is to provide a better understanding on the fundamental reaction mechanisms of Li-O₂ batteries and identify the required components (especially electrolytes and electrodes) for stable operation of Li-O₂ batteries. The PNNL researchers will investigate stable electrolytes and oxygen evolution reaction (OER) catalysts to reduce the charging overvoltage of Li-O₂ batteries and improve their cycling stability. New electrolytes will be combined with stable air electrodes to ensure their stability during Li-O₂ reaction. Considering the difficulties in maintaining the stability of conventional liquid electrolyte, the Liox team will explore the use of a nonvolatile, inorganic molten salt comprising nitrate anions and operating Li-O₂ cells at elevated temperature (> 80°C). It is expected that these Li-O₂ cells will have a long cycle life, low over potential, and improved robustness under ambient air compared to current Li-air batteries. At ANL, new cathode materials and electrolytes for Li-air batteries will be developed for Li-O₂ batteries with long cycle life, high capacity, and high efficiency. The state-of-the-art characterization techniques and computational methodologies will be used to understand the charge and discharge chemistries. The University of Massachusetts/BNL team will investigate the root causes of the major obstacles of the air cathode in the Li-air batteries. Special attention will be paid to optimizing high surface carbon material used in the gas diffusion electrode, catalysts, electrolyte, and additives stable in Li-air system and with capability to dissolve Li oxide and peroxide. Success of this project will establish a solid foundation for further development of Li-O₂ batteries toward practical applications for long-range EVs. The fundamental understanding and breakthrough in Li-O₂ batteries may also provide insight on improving the performance of Li-S batteries and other energy storage systems based on chemical conversion processes.

Highlight. The PNNL group demonstrated a non-carbon based air electrode based on boron carbide (B₄C), which exhibits much better cycling stability than those of TiC electrode reported before.

Task 9.1 – Rechargeable Lithium–Air Batteries (Ji-Guang Zhang and Wu Xu, PNNL)

Project Objective. The project objective is to develop stable electrolyte and air electrode to reduce the charging overvoltage and improve the cycling stability of rechargeable lithium-oxygen (Li-O₂) batteries. New air electrode will be synthesized to improve the capacity and cycling stability of Li-O₂ batteries. New electrolytes will be investigated to ensure their stability during Li-O₂ reaction.

Project Impact. Li-air batteries have a theoretical specific energy that is more than five times that of state-of-the-art Li-ion batteries and are potential candidates for use in next-generation, long-range EVs. Unfortunately, the poor cycling stability and low Coulombic efficiency of Li-air batteries have prevented practical application to date. This work will explore a new electrolyte and electrode that could lead to long cyclability and high Coulombic efficiency in Li-air batteries that can be used in the next-generation EVs required by the EV Everywhere Grand Challenge.

Out-Year Goals. The long-term goal of the proposed work is to enable rechargeable Li-air batteries with a specific energy of 800 Wh/kg at cell level, 1000 deep-discharge cycles, improved abuse tolerance, and less than 20% capacity fade over a 10-year period to accelerate commercialization of long-range EVs.

Collaborations. This project engages in collaboration with the following:

- Chunmei Ben (NREL) – Metal oxide coated glassy carbon electrode
- Chongmin Wang (PNNL) – Characterization of cycled air electrodes by TEM/SEM

Milestones

1. Synthesize and characterize the modified solvent and the TM oxide catalyst coated carbon material. (December 2015 – Complete)
2. Identify a modified carbon air electrode that is stable in a Li-O₂ battery by using conventional glyme solvent. (June 2016 – Complete)
3. Demonstrate stable operation of Li-O₂ battery by employing the new electrolyte and modified air electrode. (September 2016 – Complete)

Progress Report

This quarter, boron carbide (B_4C) was systematically investigated as a non-carbon based oxygen electrode material in comparison with TiC and CNTs for aprotic Li- O_2 batteries. The cycling performance data shown in Figure 84a demonstrate that B_4C is much more stable than CNTs and TiC based air electrodes. The XRD results in Figure 84b also show that B_4C nanoparticles are stable after 250 cycles and nearly no residues of Li_2O_2 and Li_2CO_3 are left on the electrode surface. The SEM image (not shown here) of the B_4C air electrode after 250 cycles exhibits nearly the same porous structure of the pristine electrode, indicating good stability of the optimized B_4C /PTFE air electrodes. The XPS analysis on the cycled B_4C air electrode also shows no generation of B-O species. These results clearly demonstrate that B_4C is a very promising alternative oxygen electrode material for aprotic Li- O_2 batteries.

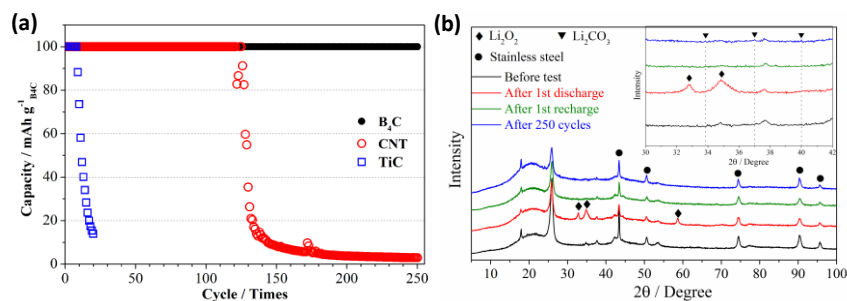


Figure 84. (a) Cycling performance of Li- O_2 cells with B_4C , TiC and carbon nanotubes (CNT)-based air electrodes under 100 mAh g⁻¹ at 0.1 mA cm⁻² within the voltage range of 2.0~4.7 V. (b) X-ray diffraction of B_4C electrode before test, after the first discharge, after the first recharge, and after 250 cycles.

The electrochemical properties of B_4C based oxygen electrode was further improved by decorating B_4C surface by ultrafine iridium particles (Ir/ B_4C) nanocomposites. The systematic investigations on charging the Li_2CO_3 preloaded Ir/ B_4C electrode in an ether-based electrolyte via electrochemical performance, XRD, and XPS demonstrate that Ir/ B_4C electrode can decompose Li_2CO_3 with an efficiency close to 100% at below 4.37 V. In contrast, the bare B_4C without Ir electrocatalyst can only decompose 4.7% of preloaded Li_2CO_3 . A Li- O_2 battery using the Ir/ B_4C electrode shows more highly enhanced cycling stability than that using

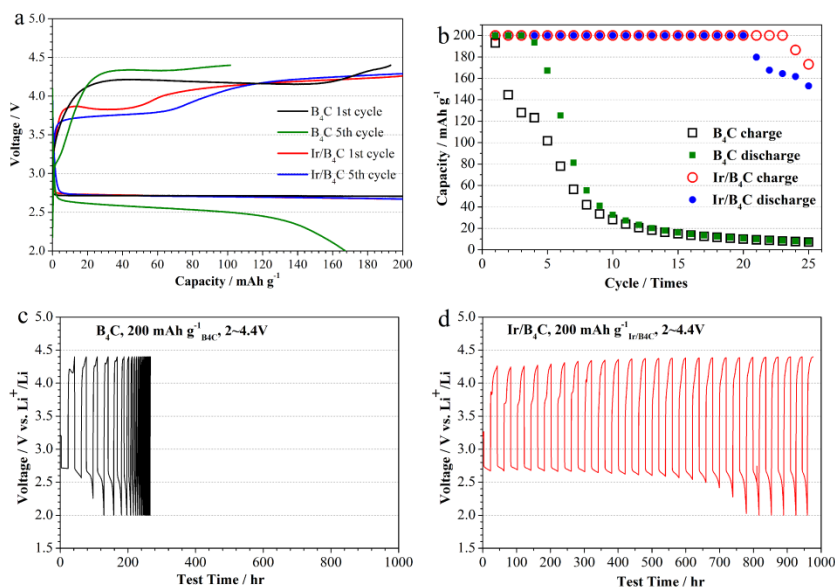


Figure 85. Discharge/charge voltage profiles (a), capacity versus cycle number (b) and cycle curves (c: B_4C cell, d: Ir/ B_4C cell) of Li- O_2 cells using B_4C and Ir/ B_4C oxygen electrodes under 200 mAh g⁻¹ at 10 mA g⁻¹ within the voltage range of 2.0 ~ 4.4 V.

the bare B_4C electrode (Figure 85). The SEM images (not shown here) show that Ir/ B_4C electrode can largely eliminate the formation and accumulation of side reaction products. The decomposition mechanism of Li_2CO_3 in the presence of Ir/ B_4C electrocatalyst has been further investigated. These results clearly demonstrate that Ir/ B_4C is an effective oxygen electrode material to completely decompose Li_2CO_3 at relatively low charge voltages and is of significant importance in improving the cycling performance of aprotic Li- O_2 batteries.

Patents/Publications/Presentations

Publications

- Liu, B., and P. Yan, W. Xu,* J. Zheng, Y. He, L. Luo, M. E. Bowden, C.-M. Wang,* and J.-G. Zhang.* “Electrochemically Formed Ultrafine Metal Oxide Nanocatalysts for High-Performance Lithium-Oxygen Batteries.” *Nano Lett.* (2016), in press. doi: 10.1021/acs.nanolett.6b01556.
- Song, S., and W. Xu,* R. Cao, L. Luo, M. H. Engelhard, M. E. Bowden, B. Liu, L. Estevez, C.-M. Wang, and J.-G. Zhang.* “B₄C as a Stable Non-Carbon Based Oxygen Electrode Material for Lithium-Oxygen Batteries.” Submitted for publication.

Presentations

- 9th Symposium on Energy Storage Beyond Lithium-Ion, Richland, Washington (May 24-26, 2016): “Optimization of Concentrated DMSO-Based Electrolytes for Stable Cycling of Li-O₂ Batteries”; B. Liu, W. Xu, P. Yan, M. H. Engelhard, X. Sun, D. Mei, S. T. Kim, J. Cho, C.-M. Wang, and J.-G. Zhang. Poster.
- 9th Symposium on Energy Storage Beyond Lithium-Ion, Richland, Washington (May 24-26, 2016): “B₄C as a Stable and Non-Carbon Based Oxygen Electrode Material for Aprotic Lithium-Oxygen Batteries”; S. Song, W. Xu, R. Cao, L. Luo, M. H. Engelhard, M. E. Bowden, B. Liu, L. Estevez, C.-M. Wang, and J.-G. Zhang.* Poster.
- 18th International Meeting on Lithium Batteries, Chicago, Illinois (June 19-24, 2016): “B₄C as a Stable and Non-Carbon Based Oxygen Electrode Material for Aprotic Lithium-Oxygen Batteries”; S. Song, W. Xu, R. Cao, L. Luo, M. H. Engelhard, M. E. Bowden, B. Liu, L. Estevez, C.-M. Wang, and J.-G. Zhang.* Poster.

Task 9.2 – Efficient Rechargeable Li/O₂ Batteries Utilizing Stable Inorganic Molten Salt Electrolytes (Vincent Giordani, Liox)

Project Objective. The project objective is to develop high specific energy, rechargeable Li-air batteries having lower overpotential and improved robustness under ambient air compared to current Li-air batteries. The technical approach involves replacing traditional organic and aqueous electrolytes with a nonvolatile, inorganic molten salt comprising nitrate anions and operating the cell at elevated temperature (> 80°C). The research methodology includes powerful *in situ* spectroscopic techniques coupled to electrochemical measurements (for example, electrochemical MS) designed to provide quantitative information about the nature of chemical and electrochemical reactions occurring in the air electrode.

Project Impact. If successful, this project will solve particularly intractable problems relating to air electrode efficiency, stability, and tolerance to the ambient environment. Furthermore, these solutions may translate into reduced complexity in the design of a Li-air stack and system, which in turn may improve prospects for use of Li-air batteries in EVs. Additionally, the project will provide materials and technical concepts relevant for developing other medium temperature molten salt Li battery systems of high specific energy, which may also have attractive features for EVs.

Out-Year Goals. The long-term goal is to develop Li-air batteries comprising inorganic molten salt electrolytes and protected lithium anodes that demonstrate high (> 500 Wh/kg) specific energy and efficient cyclability in ambient air. By the end of the project, it is anticipated that problems hindering use of both the Li anode and air electrode will be overcome due to materials advances and strategies enabled within the intermediate (> 80°C) operating temperature range of the system under development.

Collaborations. This project engages in collaboration with the following:

- Bryan McCloskey (LBNL): Analysis of air electrode and electrolyte
- Julia Greer (Caltech): Design of air electrode materials and structures

Milestones

1. Quantify e^-/O_2 and oxygen evolution reaction / oxygen reduction reaction (OER/ORR) ratio for metals and metal alloys in half cells under pure O₂. (December 2015 – Complete)
2. Determine the kinetics and mechanisms of electrochemical nitrate reduction in the presence of O₂, H₂O, and CO₂. (March 2016 – Complete)
3. Synthesize electronically conductive ceramics and cermets. (March 2016 – Complete)
4. Quantify e^-/O_2 and OER/ORR ratio for electronically conductive ceramics and cermets in half cells under pure O₂. (June 2016 – Complete)
5. *Go/No Go*: Demonstrate $e^-/\text{O}_2=2$ and OER/ORR ratio=1, +/- 5% and correcting for the effect of Li₂O₂ crossover. (June 2016 – Complete)
6. Demonstrate Li₂O yield=1, $e^-/\text{O}_2=4$ and OER/ORR ratio=1, +/- 5%. (September 2016 – Complete)
7. Demonstrate discharge specific power and power density ≥ 800 W/kg and ≥ 1600 W/L, respectively, based on air electrode mass and volume. (September 2016 – Complete)
8. Demonstrate solid electrolytes that are stable to molten nitrate electrolytes over a temperature range of 100°C to 150°C for 6 months or greater. (September 2016 – Complete)

Progress Report

This quarter, the formation of Li_2O ($4e^-$ per O_2 reaction) as discharge product in Li/O_2 cells comprising the molten nitrate electrolyte and operating at 150°C was investigated. Cells using different cathode materials, namely carbon black, IrO_2 , Pt, and Ni nanoparticles, were discharged at $0.1 \text{ mA}/\text{cm}^2$ under O_2 gas. Discharge voltage cutoff was set to 2.6 V versus Li^+/Li to avoid electrolyte (NO_3^-) reduction. Each cathode was then recovered from the cell and analyzed by XRD. No evidence for Li_2O was observed. Lithium peroxide remains the dominant discharge product in these cells. Next, the project investigated the rate capability of Li/O_2 cells comprising a lithium anode, a molten nitrate electrolyte, and a Super P carbon:PTFE air cathode. Typical air electrode mass and volume was 4 mg (carbon + binder) and $7.8 \times 10^{-3} \text{ cm}^3$ (1 cm diameter electrode, 100 microns thick), respectively. Potential step experiments were performed to measure the maximum attainable current (and associated peak power) for both the discharge and the charge process. Figure 86a shows cell discharge and charge current variation with time, using a 2.72 V constant discharge voltage and a 2.92 V constant charge voltage, respectively ($\pm 100 \text{ mV}$ overpotential based on $E_{\text{eq.}(\text{Li}_2\text{O}_2)} = 2.82 \text{ V}$). Discharge specific power was found to be ca. $2400 \text{ W}/\text{kg}$ with discharge power density being ca. $1200 \text{ W}/\text{L}$, respectively, based on air electrode mass and volume.

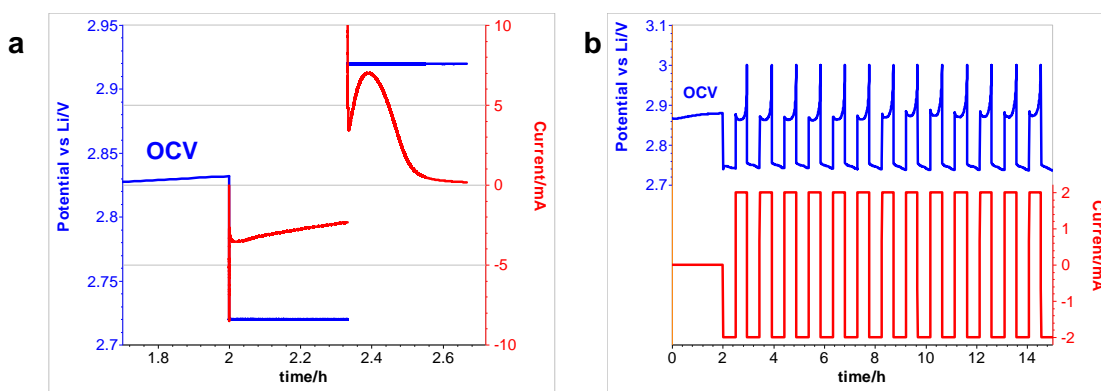


Figure 86. (a) Cell discharge/charge current variation with time (2.72 V constant discharge voltage/2.92 V constant charge voltage), under O_2 gas, at 150°C . (b). Li/O_2 cell galvanostatic cycling in $\text{LiNO}_3\text{-KNO}_3$ at 150°C under O_2 at 2 mA constant current (500 mA/g carbon or $2.5 \text{ mA}/\text{cm}^2$ current density).

Of note, fairly high peak currents can be achieved during charge, consistent with fast kinetics for Li_2O_2 oxidation in the molten nitrate electrolyte. The project also investigated the chemical stability of ceramic electrolytes towards molten nitrate salts at 150°C for an extended period of time (1-6 months). Different solid electrolyte samples were kept in contact with 1 g of melt at 150°C in a Swagelok cell, and XRD was recorded once a month to monitor any change in the crystal structure, indicative of chemical reaction(s) with molten $\text{LiNO}_3\text{-KNO}_3$. Figure 87 displays XRD patterns of solid electrolyte material at different aging times. One can clearly observe a peak shift that indicates possible cation swapping and change in the crystal lattice parameters. Additional materials are being prepared, and more testing is under way to fully evaluate their stability in the molten salt electrolyte.

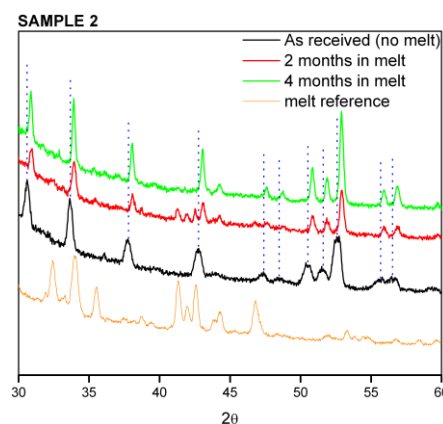


Figure 87. X-ray diffraction analysis of a ceramic electrolyte aged in $\text{LiNO}_3\text{-KNO}_3$ eutectic at 150°C .

Patents/Publications/Presentations

Presentation

- 18th International Meeting on Lithium Batteries, Chicago, Illinois (June 2016): “Intermediate Temperature Molten Salt Lithium Batteries, New Chemistries and Beyond”; V. Giordani.

Task 9.3 – Lithium–Air Batteries (Khalil Amine, ANL)

Project Objective. This project will develop new cathode materials and electrolytes for Li-air batteries for long cycle life, high capacity, and high efficiency. The goal is to obtain critical insight that will provide information on the charge and discharge processes in Li-air batteries to enable new advances to be made in their performance. This will be done using state-of-the-art characterization techniques combined with state-of-the-art computational methodologies to understand and design new materials and electrolytes for Li-air batteries.

Project Impact. The instability of current nonaqueous electrolytes and degradation of cathode materials limits the performance of Li-air batteries. The project impact will be to develop new electrolytes and cathode materials that are stable and can increase cycle life and improve efficiency of Li-air batteries.

Approach. The project is using a joint theoretical/experimental approach for design and discovery of new cathode and electrolyte materials that act synergistically to reduce charge overpotentials and increase cycle life. Synthesis methods, in combination with design principles developed from computations, are used to make new cathode architectures. Computational studies are used to help understand decomposition mechanisms of electrolytes and how to design electrolytes with improved stability. The new cathodes and electrolytes are tested in Li-O₂ cells. Characterization along with theory is used to understand the performance of the materials used in the cell and make improved materials.

Out-Year Goals. The out-year goals are to find catalysts that promote discharge product morphologies that reduce charge potentials and find electrolytes for long cycle life through testing and design.

Collaborations. This project engages in collaboration with Professor Amin Salehi (University of Illinois-Chicago), Professor Yang-Kook Sun (Hanyang University), Professor Yiyang Wu (Ohio State University), and Dr. Dengyun Zhai (China).

Milestones

1. Development of new cathode materials based on Pd nanoparticles and ZnO coated carbon that can improve efficiency of Li-O₂ batteries through control of morphology and oxygen evolution catalysis. (December 2015 – Complete)
2. Investigations of mixed K/Li salts and salt concentration on the performance of Li-O₂ batteries with goal of increasing cycle life. (March 2016 – Complete)
3. Computational studies of electrolyte stability with respect to superoxide species and salt concentrations for understanding and guiding experiment. (June 2016 – Complete)
4. Investigation of use of electrolytes to control the lithium superoxide content of discharge products of Li-O₂ batteries to help improve efficiency and cycling. (September 2016 – Complete)

Progress Report

The stability of lithium superoxide was investigated for the Li-O₂ battery based on rGO with added Ir nanoparticles. This Li-O₂ cell resulted in the formation and stabilization of lithium superoxide as a discharge product. Evidence for the presence of lithium superoxide came from numerous experimental techniques. The stability of the lithium superoxide in the tetraglyme (TEG)/LiTFSI electrolyte used in the cell was investigated using Raman spectroscopy. The cathode was harvested and packed under Ar in a gas tight Raman cell with some electrolyte remaining on the cathode. The spectra are taken with a laser sampling spot of ~1 μm in diameter and with the microscope kept at the same area as close as possible under microscope. The Raman spectra of the discharge product of the Ir-rGO cathode in Figure 88 shows the presence of a 1123 cm^{-1} peak, consistent with the range of values that have been observed for superoxide stretching frequencies. It is also consistent with the Raman peak of 1156 cm^{-1} observed for NaO₂. There is also a peak at 1505 cm^{-1} that has recently been attributed to the strong interaction between LiO₂ and graphitic carbon surface. The broad peak below ~1000 cm^{-1} is due to the electrolyte.

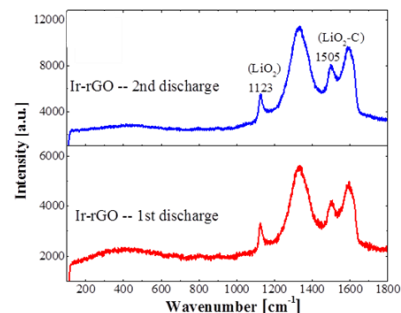


Figure 88. Raman spectra of the Ir-rGO cathode after first and second discharge in the Li-O₂ cell.

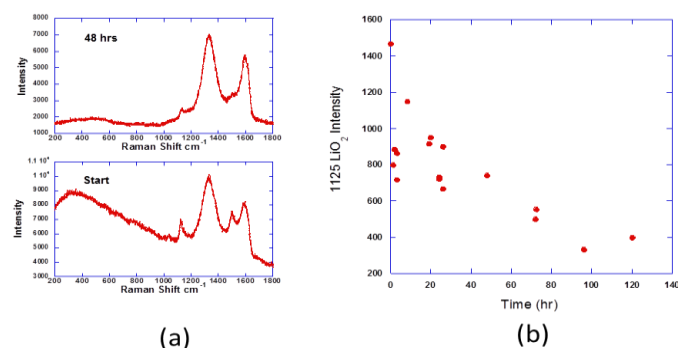


Figure 89. Raman spectra of the Ir-rGO cathode after discharge in the Li-O₂ cell as a function of time to investigate stability.

suggests a gradual decay of the lithium superoxide to lithium peroxide and oxygen due to disproportionation.

EPR measurements were further used to identify the presence of LiO₂ shown in Figure 90 in the initial discharge product of the cell using the Ir-rGO cathode. To maximize the amount of LiO₂, the Li-O₂ cell was discharged to 3000 mAh/g. The sample was collected right after discharge and packed under Ar in a sealed EPR tube. Figure 90 reveals a new peak at 3193 G due to LiO₂ that is not present in the cathode without the discharge product. There is no EPR experimental data for orthorhombic LiO₂, so the project calculated EPR parameters, which are qualitatively consistent with the experimental position. Thus, experimental results from both EPR and Raman have confirmed the presence of LiO₂ in the Li-O₂ cell based on the cathode material using Ir-rGO and its stability in the presence of the tetraglyme (TEG)/LiTFSI electrolyte.

For the stability studies, the cell is taped to the microscope stage to minimize any movement of the sample when it is left for 140 hours to track the Raman peaks decay with time. The spectra are taken with a similar laser sampling spot (~1 μm in diameter) with the microscope kept at the same area as close as possible under microscope. The results are shown in Figure 89. The scatter in the spectra may be due to the effect of vibrations on the focus of the laser beam. The Raman spectra measured as a function of time exhibit a decreasing intensity of the peak at 1123 cm^{-1} . This is also consistent with the HE-XRD results and

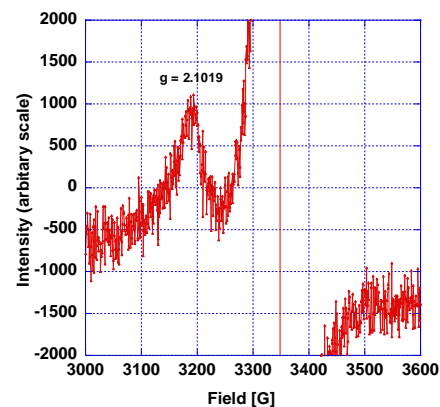


Figure 90. Raman spectra of the Ir-rGO cathode after first and second discharge in the Li-O₂ cell.

Patents/Publications/Presentations

Patent

- Lithium-air batteries having ether based electrolytes; K. Amine, L. A. Curtiss, J. Lu, K. C. Lau, and Y.-K Sun; Patent No. 8,968,941.

Publication

- Luo, X., and J. Lu, E. Sohm, L. Ma, T. Wu, J. G. Wen, D. Qiu, Y. Xu, Y. Ren, D. J. Miller, and K. Amine. “Uniformly Dispersed FeO_x Atomic Clusters by Pulsed Arc Plasma Deposition: An Efficient Electrocatalyst for Improving the Performance of Li-O₂ Battery.” *Nano Research* 9 (2016): 1913.

Presentation

- Cluster Surface Interactions Workshop, ANL, Chicago, Illinois (June 1-3, 2016): “Subnanometer Metal Clusters as Electrocatalysts in Li-O₂ Batteries”; L. A. Curtiss.

TASK 10 – SODIUM-ION BATTERIES

Summary and Highlights

To meet the challenges of powering the PHEV, the next generation of rechargeable battery systems with higher energy and power density, lower cost, better safety characteristics, and longer calendar and cycle life (beyond Li-ion batteries, which represent today's state-of-the-art technology) must be developed. Recently, Na-ion battery systems have attracted increasing attention due to the more abundant and less expensive nature of the sodium resource. The issue is not insufficient lithium on a global scale, but what fraction can be used in an economically effective manner. Most untapped lithium reserves occur in remote or politically sensitive areas. Scale-up will require a long lead time, involve heavy capital investment in mining, and may require the extraction and processing of lower quality resources, which could drive extraction costs higher. Currently, high costs remain a critical barrier to the widespread scale-up of battery energy storage. Recent computational studies on voltage, stability, and diffusion barriers of Na-ion and Li-ion materials indicate that Na-ion systems can be competitive with Li-ion systems.

The primary barriers and limitations of current state-of-the-art of Na-ion systems are as follows:

- Building a sodium battery requires redesigning battery technology to accommodate the chemical reactivity and larger size of sodium ions.
- Lithium batteries pack more energy than sodium batteries per unit mass. Therefore, for sodium batteries to reach energy densities similar to lithium batteries, the positive electrodes in the sodium battery need to hold more ions.
- Since Na-ion batteries are an emerging technology, new materials to enable sodium electrochemistry and the discovery of new redox couples along with the diagnostic studies of these new materials and redox couples are quite important.
- In sodium electrochemical systems, the greatest technical hurdles to overcome are the lack of high-performance electrode and electrolyte materials that are easy to synthesize, safe, and non-toxic, with long calendar and cycling life and low cost.
- Furthermore, fundamental scientific questions need to be elucidated, including (1) the difference in transport and kinetic behaviors between sodium and lithium in analogous electrodes; (2) sodium insertion/extraction mechanism; (3) SEI layer on the electrodes from different electrolyte systems; and (4) charge transfer in the electrolyte–electrode interface and Na⁺ ion transport through the SEI layer.

This task will use synchrotron-based *in situ* X-ray techniques and other diagnostic tools to evaluate new materials and redox couples, to explore fundamental understanding of the mechanisms governing the performance of these materials, and provide guidance for new material developments. This task will also be focused on developing advanced diagnostic characterization techniques to investigate these issues, providing solutions and guidance for the problems. The synchrotron based *in situ* X-ray techniques (XRD and hard and soft XAS) will be combined with other imaging and spectroscopic tools such as HR-TEM, MS, and TXM.

Task 10.1 – Exploratory Studies of Novel Sodium–Ion Battery Systems (Xiao-Qing Yang and Xiqian Yu, Brookhaven National Laboratory)

Project Objective. The primary objective is to develop new advanced *in situ* material characterization techniques and to apply these techniques to explore the potentials, challenges, and feasibility of new rechargeable battery systems beyond the Li-ion batteries, namely the Na-ion battery systems for PHEVs. To meet the challenges of powering the PHEV, new rechargeable battery systems with high energy and power density, low cost, good abuse tolerance, and long calendar and cycle life must be developed. This project will use synchrotron-based *in situ* X-ray diagnostic tools developed at BNL to evaluate the new materials and redox couples, exploring the fundamental understanding of the mechanisms governing the performance of these materials.

Project Impact. The VTO Multi Year Program Plan describes the goals for battery: “Specifically, lower-cost, abuse-tolerant batteries with higher energy density, higher power, better low-temperature operation, and longer lifetimes are needed for the development of the next-generation of HEVs, PHEVs, and EVs.” If this project succeeds, the knowledge gained from diagnostic studies and collaborations with U.S. industries and international research institutions will help U.S. industries develop new materials and processes for a new generation of rechargeable battery systems beyond Li-ion batteries, such as Na-ion battery systems, in their efforts to reach these VTO goals.

Approach. This project will use synchrotron-based *in situ* X-ray diagnostic tools developed at BNL to evaluate the new materials and redox couples to enable a fundamental understanding of the mechanisms governing the performance of these materials and to provide guidance for new material and new technology development regarding Na-ion battery systems.

Out-Year Goals. Complete the *in situ* XRD and absorption studies of tunnel structured $\text{Na}_{0.66}[\text{Mn}_{0.66}\text{Ti}_{0.34}]\text{O}_2$ with high capacity and $\text{Na}(\text{NiCoFeTi})_{1/4}\text{O}_2$ with high rate and long cycle life capability as cathode materials for Na-ion batteries during charge-discharge cycling.

Collaborations. The BNL team has been working closely with top scientists on new material synthesis at ANL, LBNL, and PNNL, with U.S. industrial collaborators at General Motors and Johnson Controls, and with international collaborators.

Milestones

1. Complete the synchrotron-based *in situ* XRD studies of tunnel structured $\text{Na}_{0.44}[\text{Mn}_{0.44}\text{Ti}_{0.56}]\text{O}_2$ as cathode material for Na-ion batteries during charge-discharge **cycling**. (December 2015 – Complete)
2. Complete *in situ* XRD of the $\text{Na}_{0.66}[\text{Mn}_{0.66}\text{Ti}_{0.34}]\text{O}_2$ high-capacity cathode material for Na-ion half-cell during discharge/charge cycling in a voltage range between 1.5 V and 3.9 V. (March 2016 – Complete)
3. Complete the synchrotron based XANES studies of $\text{Na}(\text{NiCoFeTi})_{1/4}\text{O}_2$ at Ni, Co, Fe, and Ti K-edge as cathode material for Na-ion batteries during charge-discharge cycling. (June 2016 – Complete)
4. Complete the synchrotron based *in situ* XRD studies of $\text{Na}(\text{NiCoFeTi})_{1/4}\text{O}_2$ as cathode material for Na-ion batteries during charge-discharge cycling. (September 2016 – Completes)

Progress Report

This quarter, the FY 2016 fourth milestones were completed. BNL has been focused on the X-ray absorption studies of a novel single phase quaternary O3-type layer-structured transition metal oxide $\text{Na}(\text{NiCoFeTi})_{1/4}\text{O}_2$ (O3-NCFT) synthesized by a simple solid-state reaction as a new cathode material for sodium-ion batteries. The local structures and valence state changes of Ni, Co, Fe, and Ti of the O3-NCFT during charge and discharge were studied using *ex situ* XAS at the Ni, Co, Fe, and Ti K-edge. Figure 91a/c/e/g shows the Ni, Co, Fe, and Ti K-edge XANES spectra during the charge process, respectively. The charge/discharge curve and corresponding states where the XAS scans were taken are shown in the right panel of Figure 91. For the Ni K-edge (Figure 91a), a rigid shift of the white line to high energy is observed, indicating the oxidation of Ni ions during Na extraction. The absorption edge at the end of the charged state is quite similar to the reference compound LiNiO_2 , indicating the valence state of Ni in NCFT after 0.5 Na extracted is 3^+ . For Co and Fe (Figure 91c/e), small shifts of the edge position to higher energy are observed. Compared with the metal oxide reference spectrum, it can be estimated that the valence states of Co and Fe after charge are between 3^+ and 4^+ . For Ti (Figure 91g), the energy position of K-edge does not shift, but with little shape change. It is reasonable because the valence state of Ti is 4^+ in the pristine NCFT. During the discharge process (Figure 91b/d/f/h), all of the XANES spectrum for Ni, Co, Fe and Ti undergo opposite evolutions.

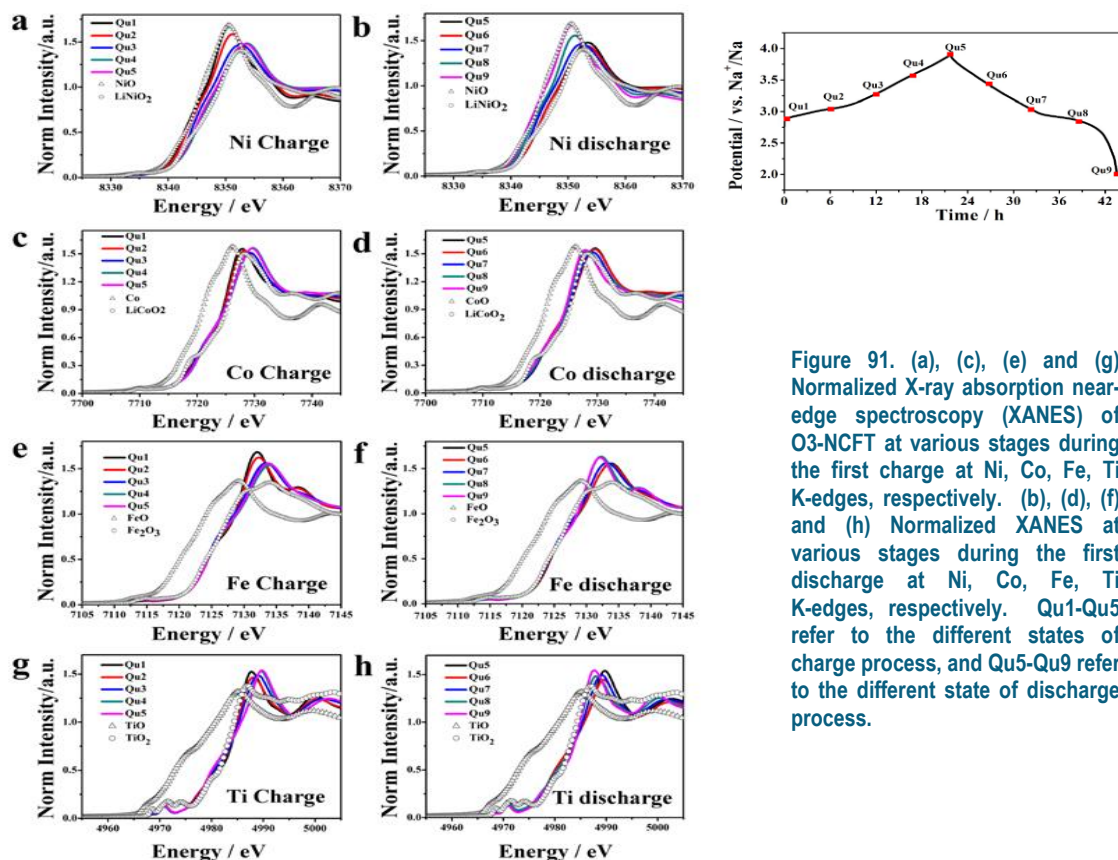


Figure 91. (a), (c), (e) and (g) Normalized X-ray absorption near-edge spectroscopy (XANES) of O3-NCFT at various stages during the first charge at Ni, Co, Fe, Ti K-edges, respectively. (b), (d), (f) and (h) Normalized XANES at various stages during the first discharge at Ni, Co, Fe, Ti K-edges, respectively. Qu1-Qu5 refer to the different states of charge process, and Qu5-Qu9 refer to the different state of discharge process.

Patents/Publications/Presentations

Publication

- Liu, Jue, and Liang Yin, Lijun Wu, Jianming Bai, Seong-Min Bak, Xiqian Yu, Yimei Zhu, Xiao-Qing Yang, and Peter G. Khalifah. “Quantification of Honeycomb Number-Type Stacking Faults: Application to $\text{Na}_3\text{Ni}_2\text{BiO}_6$ Cathodes for Na-Ion Batteries.” *Inorg. Chem.* 55, no. 17 (2016): 8478–8492. doi: 10.1021/acs.inorgchem.6b01078 (publication date, August 17, 2016).

Presentation

- Seminar at Energy Sciences Institute, Yale University, New Haven, Connecticut (September 14, 2016): “Using Synchrotron Based *In Situ* X-ray Diffraction and Absorption and TXM Techniques to Study the New Electrode Materials for Next Generation of Batteries”; Enyuan Hu, Xiao-Qing Yang*, Xiqian Yu, Yongning Zhou, Seong-Min Bak, Hung-sui Lee, Zhaoxiang Wang, and Yijin Liu. Invited.